IN VITRO TOXICOLOGICAL STUDY OF PARTICULATE MATTER AND THE RELATIONSHIPS WITH PHYSICOCHEMICAL PROPERTIES OF PARTICLES

by

Umme Salma Akhtar

A thesis submitted in conformity with the requirements
for the degree of Doctor of Philosophy

Department of Chemical Engineering and Applied Chemistry
University of Toronto

In vitro toxicological study of particulate matter and the relationships with physicochemical characteristics of particles

Umme Salma Akhtar

Doctor of Philosophy Degree

Department of Chemical Engineering and Applied Chemistry

University of Toronto

2015

Abstract

Numerous epidemiological and toxicological studies have reported substantial evidence linking airborne particulate matter (PM) exposure to adverse health effects. PM-initiated oxidative stress at the cellular level is considered a potential mechanism contributing the pathogenesis of cardiopulmonary diseases. However, there remain major gaps in knowledge about the relationship between toxicity and the physicochemical properties of PM. The main objective of this study was to investigate the effects of different source-related and size-fractionated ambient PM on cellular responses to identify relevant physicochemical properties (e.g., size, composition, and redox activity) of particles that could be responsible for the effects. Another objective was to evaluate whether progressive oxidative stress-induced cellular responses (i.e., activation of antioxidant defence at lower level of oxidative stress, followed by inflammatory response, and ultimately cell death as the stress level increases) represent a potential biological mechanism affecting cells in all size fractions. For this purpose, different source-related Standard Reference Materials (industrial, urban, and diesel PM), and size-fractionated ambient coarse, fine, and ultrafine PM (collected from Toronto, Canada) were tested. A549 cells were exposed to different

PM doses for certain duration. After exposure, the cells were analyzed for different biological responses and the responses were then compared with available physicochemical properties of the PM.

This study demonstrated that exposure to PM can initiate mass-dependent antioxidant, proinflammatory, and cytotoxic responses. Among the different source and size-related PM, transition metal-enriched industrial and coarse PM exhibited the greatest cytotoxic effect, whereas organic compound-enriched ultrafine PM caused significant induction of antioxidant defence. Correlation analyses with chemical constituents suggested transition metals and organic compounds were associated with the observed biological responses. However, the observed biological responses could not be explained by particle size or composition alone. Both of these properties should be considered when explaining the observed PM toxicity. This study also showed that ultrafine PM initiated the hypothesized progressive biological responses, whereas different biological pathways might be involved in coarse and fine PM. Overall, this study demonstrated that the cellular responses varied substantially after *in vitro* exposure to PM from different sources and ultrafine PM could be as potent as coarse and fine PM.

Acknowledgements

I would like to express my sincere gratitude to my supervisors Dr. Greg J. Evans and Dr. Jeremy A. Scott for their continuous support throughout the entire period of the study. Dr. Evans's guidance and motivation have helped me to continue looking for new research ideas. Dr. Scott's shared his knowledge which has helped me immensely in developing my understanding about toxicological studies. I would like to thank my PhD committee members, Dr. Chung-Wai Chow and Dr. Edgar Acosta, for providing encouragement and constructive suggestions.

I would like to thank Dr. Nivedita Khanna and Xiaomin Wang for teaching me cell culture techniques and sharing their knowledge with me. Thanks to Dr. Michelle North and Hajera Amatullah for helping me with different molecular biology analysis techniques. I would also like to thank all my lab mates from SOCAAR lab; especially Dr. Cheol-Heon Jeong, Dr. Neeraj Rastogi, Dr. Krystal Godri Pollitt, Dr. Maygan McGuire, Kelly Sabaliauskas, Natalia Mykhaylova, Naomi Zimmerman, and Josephine Cooper for helping me with research questions and experiments. I also thank Dr. Mike Fila for sharing his ideas with me. Thanks to Applied Research Associates, Inc. (Albuquerque, NM, USA) for free access to MPPD V2.0 2002-2009.

I would like to thank the funding agencies for supporting the study: Natural Sciences and Engineering Research Council of Canada (NSERC), Canadian Institutes of Health Research (CIHR), Canada Foundation for Innovation (CFI), and Ontario Research Fund (ORF). I would also like to thank the funding organizations for awarding me with Ontario Graduate Scholarship (OGS), Queen Elizabeth II/Richard Quittenton Scholarship, McAllister Graduate Fellowship, and Edward Jarvis Tyrell Fellowship during my study.

I would like to thank my family and friends for their continual support throughout my life. My mother and sisters have always been my inspiration. Words are not enough to describe how my husband has always helped me. Without him, my dream would have never come true. My little Zubi has also tried her best to help me with reading journals and typing the thesis sometimes. Finally and above all, I would like to thank my father who always dreamt big for me. Today he is not here to see my achievements, but I am sure he will know about it.

Contents

List of Figures

List of Tables

Preface

This thesis is comprised of a series of manuscripts that have been published or are in preparation for submission to be published in peer-reviewed scientific journals. Therefore, repetition of introductory and experimental details was inevitable. U.S. Akhtar was the primary author in all manuscripts under the guidance of Drs. G.J. Evans and J.A. Scott. The specific contributions of co-authors are detailed below. Copyright clearances were obtained from respective publishers for the published works.

Chapter 1: Introduction

Contributions: U.S. Akhtar wrote the contents of this chapter and Drs. G.J. Evans and J.A. Scott provided editorial comments.

Chapter 2: *In vivo* and *in vitro* assessment of particulate matter toxicology

Published in: Urban Airborne Particulate Matter: Origin, Chemistry, Fate and Health Impacts. Springer Berlin Heidelberg, 2011, 427-449, doi: 10.1007/978-3-642-12278-1.

Author list: U.S. Akhtar, J.A. Scott, A. Chu, and G.J. Evans

Contributions: U.S. Akhtar was the primary author of the manuscript. A. Chu did literature review for biological mechanism of particle toxicity on cardiovascular system and wrote a related passage. Drs. G.J. Evans and J.A. Scott provided guidance on the structure and editorial comments.

Chapter 3: Cytotoxic and proinflammatory effects of ambient and source-related particulate matter in relation to the production of reactive oxygen species (ROS) and cytokine adsorption by particles

Published in: Inhalation Toxicology, 2010; 22(S2), 37-47, doi:10.3109/08958378.2010.518377.

Author list: U.S. Akhtar, R.D. McWhinney, N. Rastogi, J. Abbatt, G.J. Evans, and J.A. Scott

Contributions: Dr. R.D. McWhinney developed redox activity analysis method and conducted the experiments. Dr. N. Rastogi analyzed the samples for chemical composition. Both also contributed to the manuscript by providing results and related discussion. Dr. J. Abbatt provided editorial comments on the manuscript. U.S. Akhtar was responsible for the overall design of the study and for executing the *in vitro* experiments. She took the lead in analyzing the data and writing the manuscript. The study was executed under the supervision of Drs. G.J. Evans and J.A. Scott, who provided guidance at all stages and editorial comments.

Chapter 4: The combined effects of physicochemical properties of size-fractionated ambient particulate matter on *in vitro* toxicity in A549 human lung epithelial cells

Published in: Toxicology Reports, 2014, 1, 145-156, doi: 10.1016/j.toxrep.2014.05.002.

Author list: U.S. Akhtar, R.D. McWhinney, N. Rastogi, B. Urch, C.W. Chow, G.J. Evans, and J.A. Scott

Contributions: Dr. N. Rastogi collected the ambient particle samples and conducted the chemical characterization of the samples. Dr. R.D. McWhinney conducted redox activity analysis of the samples. Both also contributed to the manuscript by providing results and related discussion. Drs. B. Urch and C.W. Chow provided editorial comments on the manuscript. U.S. Akhtar was responsible for the overall design of the study, executing the *in vitro* experiments, analyzing data, and writing the manuscript. The study was executed under the supervision of Drs. G.J. Evans and J.A. Scott, who provided guidance at all stages and editorial comments.

Chapter 5: Conclusions and recommendations

Contributions: U.S. Akhtar wrote the contents of this chapter and Drs. G.J. Evans and J.A. Scott provided editorial comments.

Appendix A: Supplemental Materials of Chapter 3

Contributions: same as Chapter 3

Appendix B: Supplemental Materials of Chapter 4

Contributions: same as Chapter 4

Appendix C: Particle deposition and clearance mechanisms and computational modeling of particle deposition in the respiratory tract

Contributions: U.S. Akhtar did literature review of papers and performed the MPPD model simulations. U.S. Akhtar wrote the chapter under the supervision by Dr. .J. Evans, who provided guidance on the structure and editorial comments.

Appendix D: Assessment of a new air-liquid interface exposure device Sized Aerosol *in Vitro* Exposure System (SAIVES) for toxicology study of particulate matter

Contributions: Dr. N. Rastogi developed the exposure system. U.S. Akhtar was responsible for testing the deposition efficiency of the system. U.S. Akhtar also wrote the report and Drs. G.J. Evans, J.A. Scott, and Dr. N. Rastogi provided editorial comments.

Appendix E: A. Chu obtained the images using the facilities at Department of Materials Science & Engineering, University of Toronto.

Chapter 1
Introduction

1. Background

Air pollution is caused by the introduction of chemical, physical or biological agents into the air that could be harmful to humans, animals or plants. Air pollution has recently been classified as carcinogenic to humans (Group 1) by the World Health Organization (WHO), International Agency for Research on Cancer (IARC, 2013). Outdoor air pollution is a mixture of different pollutants, which include the criteria air pollutants, particulate matter (PM), carbon monoxide (CO), ozone (O_3), nitrogen dioxide (NO_2), and sulfur dioxide (SO_2) (United States Environmental Protection Agency (USEPA), 2012). There are also many hazardous air pollutants, including benzene, dioxin, asbestos, toluene, and metals, such as cadmium, mercury, chromium, and lead compounds. These pollutants are associated with serious health effects, such as cancer, reproductive effects, birth defects, and adverse environmental effects. Some of these pollutants are already listed as carcinogenic or potential carcinogenic agents by IARC (e.g. polycyclic aromatic hydrocarbons, PAHs (Group 2A/2B/3), benzene (1), asbestos (1), radon (1), carbon black (2B), and formaldehyde (1)) (IARC, 2013).

Ambient PM has recently been classified as a Group 1 carcinogenic agent (IARC, 2013). This classification was decided based on the weight of evidence of carcinogenicity in humans from epidemiological and experimental studies and the understanding of mechanisms leading to lung carcinogenicity (Loomis et al., 2013). Studies conducted in different cities across the globe, among non-smokers or adjusting for smoking habits, have reported consistent relationships between ambient PM concentration and lung cancer incidence or mortality (Beeson et al., 1998; Laden et al., 2006; Pope et al., 2002; Raaschou-Nielsen et al., 2013; Turner et al., 2011). A recent study, based on 545 U.S. counties from 2000 to 2007, reported that a decrease of 10 $\mu g/m^3$ in fine PM concentration was associated with an increase in mean life expectancy of 4.2 months (standard deviation: 1.9 months) (Correia et al., 2013). Several animal studies have reported significant increases in the incidence of lung tumors in animals (rats and mice) after chronic

whole body exposure to tobacco smoke (Hutt et al., 2005), diesel emission (Heinrich et al., 1995), and urban air pollution (Reymao et al., 1997). In addition to carcinogenicity, exposure to ambient PM has also been associated with increased mortality and morbidity due to cardiovascular diseases; and hospital admissions for aggravation of respiratory diseases, such as chronic obstructive pulmonary diseases (COPD), asthma, and other effects (**Table 1.1**). Susceptible population such as children, older adults, and persons with preexisting respiratory or cardiovascular diseases are at increased risk of suffering from the adverse effects of PM (Goldberg et al., 2006; Halonen et al., 2009; Long et al., 1998; Sacks et al., 2011).

Table 1.1: Possible effects of PM on human respiratory and cardiovascular systems

System	Possible Effects	References
Respiratory system	Cough, wheezing, chest tightness, and shortness of breath in susceptible group	Long et al., 1998
	Hospital admissions for asthma, bronchitis, pneumonia, and COPD	Peng et al., 2008; Zanobetti et al., 2000
	Deficit in lung growth in children	Gauderman et al., 2004
	Development in childhood asthma	Clark et al., 2010
	Increased lung cancer mortality	Pope et al., 2002; Laden et al., 2006
	Increased mortality	Pope et al., 2002; Ostro et al., 2010
Cardio-vascular system	Hospital admissions and emergency department visits for treatment of cardiovascular diseases	Atkinson et al., 2010; Peng et al., 2008; Zanobetti et al., 2000
	Reduced heart rate variability	Gold et al., 2000
	Ischemic heart disease	Peters et al., 2001
	Heart failure	Pope et al., 2008
	Cerebrovascular disease	Miller et al., 2007
	Cardiac arrhythmia/arrest	Peters et al., 2000
	Mortality due to ischemic heart disease, heart failure, and cardiac arrest	Pope et al., 2004

Currently PM exposure is monitored and regulated in terms of its mass concentration. However, mass concentration as a dose metric is not adequate in explaining the biological responses observed. Accumulating evidence is suggesting that particle-associated biological responses are related to other physicochemical properties such as size, composition, and/or surface area. All these properties vary widely depending on the sources of the particles. For example, particles from agricultural processes and mining operations are often bigger in size, whereas emissions from vehicles consist of numerous small-sized particles. PM from traffic-sources is composed of different organic compounds and metals, whereas PM from other sources can be enriched in crustal materials and ionic compounds (USEPA, 2004). Although only a few epidemiological studies connecting health effects with PM source have been conducted to date, there is emerging evidence that PM from combustion and traffic sources correlate positively with increased mortality and cardiopulmonary diseases (Gehring et al., 2010; Laden et al., 2000; Mar et al., 2000). *In vivo* and *in vitro* studies have also found that PM from urban and industrial sources were highly toxic and induced inflammatory effects after exposure (Seagrave et al., 2006; Duvall et al., 2008; Bonetta et al., 2009). Therefore, source-related PM toxicity studies with detailed physicochemical characterization of the PM are essential to understand the source-specific health effects.

For measurement and regulatory purposes, particles less than 10 μm in aerodynamic diameter (AD) are divided into three size fractions: PM_{10} (AD <10 μm), $PM_{2.5}$ (AD <2.5 μm) and ultrafine (UF) (AD <0.1 μm) (USEPA, 2004). PM_{10} is further divided as coarse (AD 2.5 to 10 μm) and fine (AD <2.5 μm) PM. In North America and Europe, fine PM is most commonly monitored; occasionally, coarse PM is also monitored. Most of the long term epidemiological studies reporting correlations between ambient PM and cardiopulmonary morbidity and mortality are based on fine PM concentration data. Due to the limited monitoring of UF particles, there is little epidemiological evidence upon which to assess the toxic potential of UF particles. However, there is emerging evidence that UF particles might be equally or more toxic than coarse and fine PM (Gilmour et al., 2007; Li et al., 2003b; Stoelzel et al., 2007). It has been suggested that the UF particle fraction within fine particles may be responsible for the observed effects on morbidity and mortality (Delfino et al., 2005). While the relative contribution of UF to the total PM mass is low, in terms of number concentration UF particles constitutes much or most of the

total PM concentration. Therefore, comparative investigations of size-fractionated PM are important for understanding the role of particle size and the potential toxicity of UF particles. There also remain major knowledge gaps regarding the relationship between toxicity and other physicochemical properties, such as surface area, number concentration, and particle composition. While the particles may be composed of many chemicals and constituents, including inorganic ions, metallic compounds, elemental carbon, organic compounds, and crustal compounds (USEPA, 2004), the constituents responsible for the observed toxic effects remain largely unknown. Size-fractionated investigations based upon detailed chemical composition data have been limited to date.

2. Research hypotheses, questions, and objectives

The overall hypotheses of this thesis were that particle exposure would induce differential dose-dependent toxicological effects on the cells (i.e., antioxidant defence, proinflammatory changes, and ultimately cell death) for different size-fractionated PM and that these cellular responses would vary depending on the diverse physicochemical properties of the different source-related and size-fractionated PM; higher toxicity was expected for transition metal and organic compound enriched particles. These hypotheses were examined through *in vitro* studies designed to achieve the following objectives:

1. Assess the variability in biological responses in relation to the physicochemical properties of PM, such as mass, size, and composition, and their redox activity.

2. Compare the biological/toxicological effects within different source-related and size-fractionated particles.

3. Provide a preliminary development and evaluation of a field deployable cell exposure device, Sized Aerosol *in Vitro* Exposure System (SAIVES).

This design of the study sought to improve the current state of knowledge of PM toxicity by answering the following research questions:

- What is the current understanding of the biological mechanisms underlying PM associated adverse health effects?

- To what extent are biological responses related to the physicochemical properties of PM beyond mass (e.g., size, composition, etc.)?
  - Among the chemical components commonly found in PM, are some significantly more toxic?
  - Are the toxicities associated with different PM size fractions due to the differences in the size or composition of these particles?

- Are any differences associated with different physicochemical properties suggestive of different biological mechanisms?

Chapter 2

In vivo and *in vitro* assessment of particulate matter toxicology

Umme S. Akhtar, Jeremy A. Scott, Amanda Chu, Greg J. Evans

Urban Airborne Particulate Matter: Origin, Chemistry, Fate and Health Impacts
Springer Verlag Berlin Heidelberg, 2011, 427-449, doi: 10.1007/978-3-642-12278-1

Abstract

Exposure to ambient particulate matter (PM) can have profound adverse effects on human health. Epidemiology studies have revealed associations between ambient PM and health effects ranging from increased hospital admissions to increased mortality rate. Factors such as particle size, surface area, and composition appear to influence how the body reacts to the inhaled PM. *In vivo* studies using humans and animals have provided insight into the toxicity of different types of PM, in terms of lung and vascular functions as well as inflammatory and oxidative stress markers. *In vitro* studies using human cells are allowing elucidation of pathophysiological mechanisms underlying observed *in vivo* effects. The most common pathway proposed for respiratory effects is the production of reactive oxygen species (ROS) causing oxidative stress in mammalian cells. Cardiovascular effects may also be caused by release of proinflammatory and prooxidant mediators from the lungs, but autonomic imbalance and translocation of PM to systemic circulation are also postulated as potential mechanisms.

1. Introduction

Air pollution is a major threat to human health worldwide. According to a World Health Organization report (WHO, 2006), more than two million premature deaths can be attributed each year to air pollution. In Canada, premature deaths associated with chronic exposure to air pollution are expected to rise 83% between 2008 and 2031 and estimated economic costs of air pollution will be over $250 billion by 2031 (Canadian Medical Association (CMA), 2008). Adverse health effects associated with air pollution may be caused by both gaseous (nitrogen oxides, sulfur oxides, ozone, etc.) and particulate pollutants. Epidemiological studies have found

consistent correlations between all-cause or cause-specific (respiratory and cardiovascular) mortality and inhalation of particulate matter (PM), even at low and moderate ambient PM concentrations (Brook et al., 2003; Katsouyanni et al., 2003; Schwartz, 1994). These correlations suggest that PM air pollution is responsible for about 0.8 million premature deaths and 6.4 million years of life lost globally (Cohen et al., 2005). Though emission of gaseous pollutants has decreased significantly over the last few decades because of the implementation of stringent regulations and better emission control technologies, PM concentrations have decreased at a slower rate. This is due to the simultaneous increase in combustion-based energy use, such as the increase in motor vehicles worldwide, specifically in urban areas (Valavanidis et al., 2008). The physicochemical properties of PM, specifically size-distribution and composition, have also changed with time (Valavanidis et al., 2008). In recent years, PM air pollution has been the subject of a multitude of epidemiological and toxicological studies because of its intense effects on human health and economy.

Ambient PM is a complex mixture of gaseous, solid, and liquid substances with variations in size, composition, and origin (Brook et al., 2003; Mazzarella et al., 2007; Sioutas et al., 2005). PM is generally classified by size as this determines the transport and removal rate of PM in the air. In terms of health effects, PM size determines the deposition site of PM within the respiratory tract (USEPA, 2004). Particles with an aerodynamic diameter (AD) less than 10 μm are considered as the respirable fraction; those larger than 10 μm are removed in the nasal passages. For measurement and regulatory purposes, PM less than 10 μm AD are divided into three major fractions: PM_{10} (AD <10 μm), $PM_{2.5}$ (AD <2.5 μm) and ultrafine (UF) (AD <0.1 μm) (USEPA 2004). PM_{10} is further divided as coarse (AD 2.5 to 10 μm) and fine (AD <2.5 μm) PM. The physicochemical properties of PM, such as size-distribution and composition, largely depend on the source. While fine and UF particles are predominantly produced by combustion processes, coarse particles are generated mainly by mechanical processes. Fine and UF particles consist primarily of inorganic ions, hydrocarbons, and metals, whereas coarse particles consist of crustal materials, such as sea salt, abrasion products, and bioaerosol (Kok et al., 2006; Squadrito et al., 2001). Numerous epidemiological studies have found significant associations between PM exposure and adverse health effects, specifically in respiratory and cardiovascular systems. Associations ranged from increased hospital admissions and emergency department visits for

treatment of respiratory and cardiovascular diseases to increased lung cancer and cardiovascular diseases mortality. These effects were quite severe in the elderly and in populations with pre-existing cardiopulmonary diseases (Goldberg et al., 2000; Zanobetti and Schwartz, 2005). Variable levels of significance of PM-associated health effects have been reported in different studies. The main reason for such variation among the studies is the difference in geographic location. Thus, it is important to recognize the regional variability of PM sources, composition, population exposure, and potential susceptible populations (USEPA, 2004).

Several epidemiological studies have examined the health effects of size fractionated PM (PM_{10}, $PM_{2.5}$, and $PM_{10-2.5}$). These studies suggested that, of the different size fractions, $PM_{2.5}$ was most significantly associated with mortality (Brook et al., 2003; Fairley, 1999). While chronic exposure has been associated with increased atherosclerosis (Kuenzli et al., 2005), short term exposure to $PM_{2.5}$, for as little as two hours, may elevate the risk of acute cardiovascular events (Peters et al., 2001). Although only a few epidemiological studies on UF particles have been published to date, there is emerging evidence that they also contribute significantly to adverse health effects (Peters et al., 1997; Sioutas et al., 2005). It has been postulated that UF particles may actually be the pollutant underlying the morbidity and mortality that have been associated with $PM_{2.5}$ (Delfino et al., 2005). Preliminary results have found a positive correlation between UF particles and increased mortality and morbidity for respiratory and cardiovascular effects in susceptible populations (Politis et al., 2008). However, considerable further investigation of UF-particle exposure-related health effects is required. While standards for PM_{10} and $PM_{2.5}$ have already been established in North America, an ambient standard for UF particles has yet to be established. In recent years, epidemiological studies have focused more toward investigating the health impacts of different size-fractionated PM, including UF particles.

As increased rates of mortality and morbidity have been observed for both short- and long-term exposures to PM at ambient levels, the general consensus is that PM concentrations should be decreased as much as is reasonably achievable. In a study of the reductions in $PM_{2.5}$ concentrations in 51 US cities over the last two decades, Pope et al., (2009) found that a decrease of 10 $\mu g/m^3$ in the fine PM concentration was associated with an increased average life expectancy of seven months. However, these observations have primarily been through

epidemiological associations. A parallel knowledge of PM toxicity is essential in order to develop scientifically established standards and health policies regarding ambient PM concentration. Considerable progress has been made toward understanding the pathophysiological mechanisms of PM-induced adverse health effects over the last decade. This chapter describes our current understanding of PM induced respiratory and cardiovascular diseases with the different methodologies used to evaluate PM toxicity.

2. Importance of physiochemical properties of PM

The physical and chemical characteristics of inhaled particles can have a profound effect on the nature and degree of the toxic effects of PM. Particle size is one of the most important factors determining the deposition site and consequent clearance in the respiratory tract- the smaller the particles, the deeper the deposition site in the respiratory tract, the slower the clearance rate, and the higher the probability of particle-cell interactions. Of all the PM fractions, deposition of UF particles is of great interest as these particles could remain in the pulmonary tissue, and their retention may cause lung damage (Politis et al., 2008). UF particles may also cross the lung epithelium barrier and translocate into the systematic circulation (Brook, 2008). This translocation may contribute to acute manifestation of cardiovascular diseases (Nemmar et al., 2004), as well as neurological alterations (Calderon-Garciduenas et al., 2004). Nemmar et al., (2002) also demonstrated that inhaled UF carbon particles can pass rapidly into the systemic circulation. Studies have observed translocation of inhaled UF particles to the brain in rats (Oberdörster et al., 2004); however, no studies have confirmed translocation of ambient UF particles to extra pulmonary organs (i.e., the liver and brain) in the human body (Möller et al., 2008). Experimental studies have observed higher pulmonary responses, such as indications of inflammation, for UF particles compared to fine particles (Duvall et al., 2008; Li et al., 2003b). Findings from recent studies suggest that, along with size other physical properties of UF particles (i.e., higher total surface area and number concentration per unit mass) may also contribute significantly toward the observed response (Oberdörster, 2001; Wittmaack, 2007).

In addition to the physical characteristics, accumulating evidence suggests that particle composition is also responsible for particle-associated adverse health effects. While ambient

particles may be composed of thousands of chemicals and constituents, including inorganic ions, metallic compounds, elemental carbon, organic compounds, and crustal compounds (Hetland et al., 2004; USEPA, 2004), the components responsible for the observed toxic effects remain largely unknown. The effects on human health could be related to a single PM component or to a possible synergistic interaction of multiple components. Based on experimental studies, it has been proposed that transition metals and organic compounds are primarily responsible for inducing oxidative stress within lung cells. Oxidative stress was positively correlated with high organic carbon and polycyclic aromatic hydrocarbons (PAHs) content of PM (Li et al., 2003b, 2002, & 2000). Oxidative stress-mediated cytokine production could be metal dependent, as transition metals (e.g. iron, vanadium, nickel, lead) may catalyze free radical production in the lung cells (Carter et al., 1997). Several studies have also revealed that the presence of endotoxins on particle surfaces may initiate inflammatory response in the cells (Becker et al., 2003; Hetland et al., 2004). Therefore, different physicochemical PM properties, including size, surface area, number, and composition, can play a significant role in initiating PM induced health effects. Nonetheless, no single physical or chemical characteristic has been identified that could explain most of the health effects observed.

3. Toxicological investigations of particulate matter

Although epidemiological studies provide extensive evidence of PM-associated health effects, there are some limitations. Primarily, it is difficult to demonstrate causality and to also eliminate the confounding effects of other pollutants through epidemiology alone (Devlin et al., 2005). Thus, toxicology studies are essential to complement epidemiological findings and can provide insight into the pathophysiological mechanism(s) underlying the adverse health effects that are observed in epidemiological studies. Evidence of toxicity from toxicology studies is also essential for establishing guidelines (WHO, 2006). Two approaches are most commonly used to study of PM toxicity: *in vivo*-controlled human and animal exposure studies, and *in vitro*-exposure of cells to PM. Although both of these approaches have well defined strengths and limitations, each approach provides a needed contribution to understanding the impact of PM on human health. Recent *in vivo* and *in vitro* studies have mainly focused on determining the pathophysiological mechanisms of PM-induced health effects, the PM characteristics (i.e., size,

surface area, chemical composition, etc.) responsible for the observed effects, and the susceptible subgroups that are at increased risk of adverse health effects due to PM exposure (Duffin et al., 2002; Gilmour et al., 2007., Happo et al., 2010; Hetland et al., 2001; Horemans et al., 2012; Huang et al., 2011; Londahl et al., 2012; Perrone et al., 2013; Steenhof et al., 2011).

3.1 *In vivo* studies

3.1.1 Human exposure studies

Controlled human exposure studies are essential to establish the health consequences of PM exposures. These studies are typically designed to study inhalation of size-defined PM under highly controlled conditions that will allow the characterization of exposure-response relationships. Since humans are exposed to the pollutant of interest, specifically size-fractionated PM, causality can be established easily and the confounding effects of other pollutants can be minimized (Devlin et al., 2005). Another advantage of such clinical studies is the ability to select subjects with a known clinical status (i.e., healthy vs. a specific disease, typically cardiovascular or pulmonary disease) and observe the pathophysiological responses of interest. However, controlled human exposures have some limitations (Utell and Frampton, 2000). For both practical and ethical reasons, clinical studies are restricted to exposure concentrations and durations that will only elicit transient responses in human subjects. These studies involve a small number of sample subjects, which excludes susceptible populations at higher risk. Chronic exposure or high PM concentration related health effects are not attainable by the clinical studies. These experiments are also very costly to perform.

3.1.1.1 Subjects

For PM exposure studies, subjects are typically classified by age, gender, smoking habit, residence locations, and physical conditions such as lung function and cardiovascular status, etc. Healthy subjects are non-smokers who have no history of chronic respiratory and cardiovascular diseases, and are further characterized by the absence of allergies, chronic medical conditions or chronic medications, and airways that are not hyper-responsive, as assessed by inhalation challenge tests (Beckett et al., 2005; Brook et al., 2009; Dubowsky et al., 2006; Gong et al.,

2005). Susceptible individuals are more vulnerable to PM than healthy subjects, thus clinical studies of susceptible groups along with healthy subjects are of great interest to policy makers developing national ambient standards. These standards are usually designed to protect susceptible groups (Utell and Frampton, 2000). The choice of susceptible population depends on the outcomes of the research interests. Generally, elderly persons, individuals with previous history of asthma, COPD, and cardiovascular disease are considered as susceptible populations for PM exposure studies (Dubowsky et al., 2006; Gong et al., 2003; Mills et al., 2008). Depending upon the design of the study, comparisons of health-outcomes can be made with healthy controls, or subjects can act as their own controls when exposed to PM and filtered air over multiple sessions (Urch et al., 2005).

3.1.1.2 Exposure conditions

Clinical PM exposure studies are typically conducted in environmentally controlled chambers up to 20 m^3 (e.g., 4.5 × 2.5 ×1.5 m in LWH) in volume. These studies employ different exposure methods, such as full-body, mouth-only, nose-only, and mouth-nose inhalation exposures (USEPA, 2004). Full-body exposure is the most realistic approach as it mimics the typical environmental exposure conditions that are experienced daily. For ethical reasons, exposure protocols are designed to elicit transient, clinically insignificant (i.e., safe) effects with minimally invasive measurement techniques to assess outcomes (Utell and Frampton, 2000). Subjects are exposed to higher PM concentrations that would not typically be observed for ambient concentrations in most regions. The major consideration for using high concentration is that in real life human are exposed to ambient PM chronically (i.e., years); however, the clinical studies are conducted acutely (i.e., hours). Thus, a high concentration exposure may induce effects similar to chronic exposure. It is also assumed that exposure of healthy subjects to relatively high concentrations may reconcile for the compromised tissue/organ functions of susceptible individuals contributing to the observed health effects in epidemiological studies (USEPA, 2004). Exposure concentrations can also be selected based on findings from animal exposure studies (Beckett et al., 2005). Most exposures are conducted over a 2 h duration period, which may include intermittent or continuous exercise to induce oral breathing and increase ventilation. From the exposure perspective, the augmented oral breathing and ventilation reduces the fraction

of PM loss in the nasopharyngeal region and consequently enhance the PM dose that reaches the lower respiratory tract (Utell and Frampton, 2000; WHO, 2006). Some studies allow the subjects to perform tasks while monitoring and characterizing the ambient PM concentrations. These tasks can include: outdoor running (Rundell et al., 2007) or going for a day trip (Dubowsky et al., 2006). These exposures better match conditions that may be encountered on a daily basis, but also include many confounding factors.

Concentrated ambient particle system (CAPS) is a new technology that has been developed to allow ambient particles to be concentrated in real time by factors of 25 or more (Sioutas et al., 1995). CAPS chambers are typically smaller in size (3-5 m^3 in volume) and mimic the ambient conditions in a particular geographical area. Variations in particulate composition between cities can affect the impact of the findings (Mills et al., 2008). Furthermore, exposure concentrations can vary from day to day depending on ambient levels of PM from which the air is taken, as well as the concentrating factor of the instrument used. Exposure concentrations in CAPS can range from relatively low levels to concentrations much higher (23 $\mu g/m^3$ to 311 $\mu g/m^3$) than those commonly found in polluted cities (USEPA, 2004). In the CAPS, PM can be separated from other atmospheric gaseous pollutants that facilitate the study of PM induced effects individually, among others. Current technology allows exposure to all PM size-fractions including coarse, fine, and UF particles (Gong et al., 2005; Graff et al., 2009; Mills et al., 2008). CAPS for human exposure studies are still rare with two facilities in the US and one in Canada at the Southern Ontario Centre for Atmospheric Aerosol Research (SOCAAR) located at the Gage Occupational and Environmental Health Unit, within the University of Toronto's Faculty of Medicine (SOCAAR, 2007). Several clinical studies have used diesel engine exhaust and smoking machines as model anthropogenic pollutants (Peretz et al., 2008; Weiss et al., 1999). Model particles with specific physical and chemical characteristics are used in some exposure studies which allow the investigation of the appropriate dose metrics (i.e.; size, surface area, composition, etc.) responsible for the observed effects (Beckett et al., 2005).

3.1.1.3 Endpoints

As would be expected from the above description of the human exposure studies, the respiratory

and cardiovascular outcomes assessed in human clinical studies are determined based on scientific and practical considerations. Results from epidemiologic studies and/or animal exposure studies work as guidelines for selecting outcome measures. In most of the respiratory response studies, a symptom questionnaire is prepared and results are recorded as a score with a standardized grading system. The most commonly used pulmonary function test (PFT) is the spirometry test, which measures the breathing pattern. Typically evaluated breathing parameters in spirometry are the forced vital capacity (FVC), forced expiratory volume in 1 sec (FEV_1), maximal mid-expiratory flow (MMEF), and peak expiratory flow (PEF) (Ghio et al., 2000; Gong et al., 2005 & 2003; Utell and Frampton, 2000). These outcomes are easy to perform and are generally reproducible within subjects. Arterial oxygen saturation (SpO_2), an indication of the amount of oxygen bound to hemoglobin, can be measured continually by pulse oximetry (Gong et al., 2005 & 2003). To collect cells and epithelial lining fluid of the lower respiratory tract in humans, sputum induction is often used (Beckett et al., 2005; Gong et al., 2005 & 2003). Fiberoptic bronchoscopy is another analytical method that allows more invasive collection of samples from the respiratory tract for further analysis (Utell and Frampton, 2000). A number of techniques have been developed based on fiberoptic bronchoscopy, which allows sampling of fluids and cells from the lower respiratory tract. Bronchoalveolar lavage (BAL) samples the epithelial lining fluid and cells of the distant airways. Other techniques developed using fiberoptic bronchoscopy are bronchial brushing (to collect airway epithelial cells and tissue), and endobronchial (to collect bronchial epithelium cells) or transbronchial (to collect alveolar tissue and distal bronchial epithelium) biopsy. Fiberoptic bronchoscopy has also been used for the intrabronchial instillation of PM in human subjects at definite locations in the lung (Ghio and Devlin, 2001). Analysis of the collected cells and fluid can provide a useful measure of airway inflammation. Measurement of nitric oxide in exhaled air is another useful tool to detect lung inflammation (Adamkiewicz et al., 2004; Delfino et al., 2006).

Vascular function is measured in a variety of ways. The most basic tests that can be performed non-invasively during exposures are: blood pressure (BP), heart rate (HR), and heart rate variability (HRV) (Beckett et al., 2005; Brook et al., 2009; Gong et al., 2003; Urch et al., 2005). Furthermore, brachial artery diameter (BAD), flow-mediated dilatation (FMD), nitroglycerin-mediated dilatation (NMD), and arterial compliance can also be measured in subjects (Brook et

al., 2009 & 2002; Rundell et al., 2007). To examine the effect of PM on vasomotor function, vasodilatation can be induced using intravascular infusions of bradykinin, acetylcholine, sodium nitroprusside, and verapamil, and measuring the forearm blood flow (Mills et al., 2007; Törnqvist et al., 2007). Electrocardiograms can also be used to determine any increases in ischemic burden (Brook et al., 2009; Mills et al., 2007). Finally, blood tests can be used to determine fibrinolytic function as an indicator of blood viscosity (Mills et al., 2007; Törnqvist et al., 2007). Blood, sputum, cells, and fluids of the respiratory tract are collected after exposure and are analyzed for complete blood cell count (Brook et al., 2009), different markers of oxidative stress and systemic inflammation, such as leukocytes, polymorphonuclear neutrophils (PMN), cytokines, and platelets (Ghio et al., 2000; Graff et al., 2009; Mills et al., 2008), serum C-reactive protein (Brook et al., 2009; Dubowsky et al., 2006; Mills et al., 2008), and alterations in gene expression (Dubowsky et al., 2006; Törnqvist et al., 2007).

3.1.2 Animal exposure studies

To compensate for the limitations described previously, animal exposure studies are commonly used to assess causality and potential biological mechanisms at higher PM concentrations and under chronic exposure conditions (Devlin et al., 2005). Animal exposure studies are relatively inexpensive to perform when compared to clinical studies; however, one major limitation of animal exposure studies is that they require the appropriate extrapolation of doses and biological responses from animals to human. Thus, the similarities and differences between laboratory animal species and humans in regards to the anatomy of the respiratory tracts and cardiovascular system, life span, diet, exercise, genetic variability, and biological and physiological response must be recognized before extrapolation of these findings can be made possible (McClellan 2000; Valentine and Kennedy 2008).

3.1.2.1 Subjects

The most commonly used animals in PM exposure studies are rodents, including rats, mice, guinea pigs, and hamsters. Rodents have been used extensively in inhalation toxicology studies, and hence a large amount of information is available on the physiological responses of rodents (Valentine and Kennedy, 2008). These animals are generally used as inbred strains, thus

reducing the genetic heterogeneity compared with human subjects; and whole litters can be treated similarly, allowing siblings to act as controls for exposures. Therefore, there is a lesser degree of variability in the responses in animal models. Rodents are most commonly used for studying chronic toxicity and carcinogenesis effects as they have a relatively short lifespan as compared to humans (Valentine and Kennedy, 2008). As more adverse responses have been observed in populations with a pre-existing history of respiratory and cardiovascular disease, specific animal models can be used to study the effects of PM that are observed in susceptible populations, including acute and chronic airways inflammation, representative of obstructive and restrictive lung disease, surgically-induced ischemic heart disease or myocardial infarction, or mice that are genetically predisposed toward hyperlipidemia (Maier et al., 2008; Saldiva et al., 2002; Suwa et al., 2002). PM exposure studies have also been conducted on dogs with an induced coronary artery occlusion to investigate exacerbation of myocardial ischemia during coronary artery occlusion due to PM exposure (Bartoli et al., 2009; Wellenius et al., 2003).

3.1.2.2 Exposure condition

Animals are exposed to PM using the same exposure routes (i.e., full-body, nose-only, and/or mouth-only) as the clinical studies described above. In the nose-only exposure system, animals are restrained in a small chamber and allowed to inhale though an exposure hole. While restraint can induce stress, thus affecting the heart rate (Narciso et al., 2003); blood pressure (Vincent et al., 2001), and gene expression in the lung (Thomson et al., 2009) in the exposed animals, this approach allows for increased certainty in terms of the actual exposures delivered. In contrast, a full-body exposure chamber provides a more realistic approach of PM inhalation, but can be complicated if the animals are allowed to roam (i.e., free-range). Exposure durations in full-body chambers may last from five to six hours for animals (Araujo et al., 2008; Dormans et al., 1999; Saldiva et al., 2002) compared with only one to two hours for humans. Daily exposures can be allowed to continue for several weeks to develop subchronic (Carter et al., 2006) and chronic (Mauad et al., 2008) exposure models. Along with inhalation experiments, intrapharyngeal or intratracheal instillation of collected PM, via the nose or trachea, have also been applied to animal exposure models. Instillation studies allow delivery of a higher dose directly to the lung

(Suwa et al., 2002; Ulrich et al., 2002; USEPA, 2004), and also allow exposure to known concentrations of well-characterized PM suspended in an aqueous medium (Suwa et al., 2002).

3.1.2.3 Endpoints

Many of the endpoints examined for animals are the same as those for humans. These include clinical signs of pulmonary function and responsiveness to contractile agonists (i.e., methacholine or histamine); vascular function tests such as HRV, ST-segment elevation, and frequency of arrhythmias before and after exposure; and, BAL analysis (Carter et al., 2006; Saldiva et al., 2002; Ulrich et al., 2002; Wellenius et al., 2003). PM concentration relative to body weight or organ weight (post-exposure) can also be measured to determine PM deposition in the organ (Dormans et al., 1999). Furthermore, because experimental animals are often euthanized at the end of the experiment, the end-points can be more invasive and allow for a greater dissection of tissue-specific mechanisms. Histopathological changes of the lung, heart, and other organs (i.e., liver, kidney, spleen, etc.) can also be assessed following PM exposures (Araujo et al., 2008; Saldiva et al., 2002; Suwa et al., 2002). Blood samples can also be collected to assess the effect of PM on different hematological parameters, such as hemoglobin, differential white blood cell count (WBC), clinical chemistry (i.e., pH, total protein, albumin, etc.) (Dormans et al., 1999). In dog models, a hydraulic balloon occluder is implanted in dogs around a coronary artery to facilitate particulate exposure. Factors such as myocardial blood flow, arrhythmia incidence or acute myocardial ischemia are measured during forced occlusions that usually occur after PM exposure (Bartoli et al., 2009; Wellenius et al., 2003).

3.2 *In vitro* studies

As the next logical step in the reductionist approach, *in vitro* studies have the potential to describe the underlying cellular and molecular mechanisms, while *in vivo* studies can provide interpretation of the underlying pathophysiological mechanisms (Devlin et al., 2005). *In vitro* studies allow interactions between specific cell lines of interest and PM in ways that are not feasible with *in vivo* studies. A major advantage of *in vitro* models is that cellular and subcellular functions (i.e., cell growth and cell-to-cell interactions) and the molecular pathways can be studied in a more detailed manner (Rothen-Rutishauser et al., 2008). Another advantage of *in*

vitro studies using human cells over animal models is that uncertainty regarding extrapolation from animal to human models can be minimized. Human cells cultured by following standardized cell culture practices are considered to yield high reproducible results (Rothen-Rutishauser et al., 2008). However, one drawback of *in vitro* studies is that the cells may not respond as they would when they are in the body, particularly in regards to immortalized cell lines. These cells do not interact with the multiple cell types in the tissues and are not supported by endogenous nutrients or other paracrine factors (Maier et al., 2008). Nonetheless, results obtained from *in vitro* studies exposing PM to human cell lines generally concur with the findings obtained in the human clinical studies (Devlin et al., 2005). Thus, *in vitro* models of human cells with appropriate growth and exposure techniques can advance the research while reducing the use of animal models for PM toxicity studies (Bakand et al., 2006).

3.2.1 Exposure techniques

In vitro exposure of cells to PM requires special exposure apparatus that allows close contact between the cells and the test compounds for significant exposure durations (Aufderheide, 2005). A number of methods have been developed to date- the simplest, least expensive, and most widely used of these methods is to collect PM on filters. Once collected, the PM is resuspended in a liquid medium and the suspension is added to the cells. The cellular responses can then be investigated in detail (Becker et al., 2003; Hetland et al., 2004; Mazzarella et al., 2007). However, there are major limitations with this method, including changes in PM fractions and chemical characteristics during the sample collection, extraction, and resuspension. For example, the composition of collected PM may change due to loss of volatile organic compounds and the size distribution of PM can also be altered by agglomeration of small particles (Bruijne et al., 2009). Thus, particles are added to the cells as a suspension in culture medium which differs substantially from the actual deposition of airborne particles onto cells. The quantity (i.e., mass or number) of particles that actually interacts with the cells cannot be determined (Maier et al., 2008). Alternatively, impingers have also been used to collect PM directly in a liquid medium; however, the composition and surface characteristics of PM are changed whenever it is transferred into a liquid media (Bruijne et al., 2009). Compared to the above-mentioned methods, exposure of cells at the air liquid interface (ALI) is the most realistic method. Using the ALI

system, the apical surface of the epithelial cell monolayer is exposed to PM while the basolateral surface of the cells is fed with the medium through the porous membrane (Aufderheide, 2005) (**Figure 2.1**). In this process, the PM characteristics remain unchanged prior to deposition. The Navicyte Horizontal Diffusion Chamber (Harvard Apparatus, USA) is one such system. It is designed to expose cells to the atmosphere while media is supplied through a porous membrane. The exposure chamber is mounted on a heated block at 37°C (Bakand et al., 2006). Aufderheide (2005) developed a new *in vitro* exposure system- the Cultex® (Hanover, Germany), based on the ALI cell culture approach. This system has been used successfully for *in vitro* investigations of gaseous compounds (Ritter et al., 2001), cigarette smoke (Fukano et al., 2006), and automobile exhaust (Knebel et al., 2002); however, it has not been used for ambient PM. A recent advance in the field of *in vitro* study of PM exposure is the use of the electrostatic precipitator (ESP). Electrostatic precipitation is usually used in PM collection and monitoring, and has recently been adapted for direct exposure of airway epithelial cells to PM (Bruijne et al., 2009). With this method, PM carried in the sample flow is charged and then subjected to a convergent electrostatic field. PM drifts across the flow and deposits on a collection plate at the bottom of the instrument (Bruijne et al., 2009). In the case of *in vitro* investigations of cell exposure to PM, the PM collection plate is replaced with a cell containing well/plate. This method overcomes the modification of PM characteristics caused by collection in media and provides higher collection efficiency.

Cells are typically exposed to ambient PM (PM_{10}, $PM_{2.5}$, UF), diesel exhaust particles (DEP), or cigarette smoke using these exposure systems (Fukano et al., 2006; Hetland et al., 2004; Li et al., 2002; Mazzarella et al., 2007). Some studies have used well-characterized Standard Reference Materials (SRMs) from the National Institutes of Standards and Technology (NIST, 2009) and engineered nanoparticles, such as zinc oxide, titanium dioxide, in liquid medium (Baulig et al., 2003; Boland et al., 1999; Gurr et al., 2005; Hatzis et al., 2006; Lu et al., 2009; Sawyer et al., 2010). Although standard or engineered materials are not true ambient PM, the materials are representative of ambient PM. These materials also elicit similar responses in cells to the ambient PM. The majority of the *in vitro* studies use PM exposure doses in the range of 10 to 1000 µg/mL (PM mass/volume of the suspension solutions) which are equivalent to 2.1-210 $\mu g/cm^2$ (PM mass/surface area of the culture plate; for a 6 well plate). Exposure duration ranges

from 2 to 72 h across the studies (Mitschik et al., 2008). Although it is speculated that PM doses used in the *in vitro* studies are higher than real life exposure concentrations, several studies have showed that these concentrations are somewhat relevant to real life scenarios (Li et al. 2003a; Gangwal et al., 2011; Risom et al., 2005). Several *in vitro* studies have reported significant biological responses at the PM dose as low as 10 µg/ml (~2.1µg/cm^2) for exposure duration of 4 to 24 h (Li et al., 2002; Ramgolam et al., 2008; Steenhof et al., 2011). Therefore, PM doses ranging from 10 to 1000 µg/mL for exposure duration of 4 or 24 h were used in this thesis for PM exposure experiments.

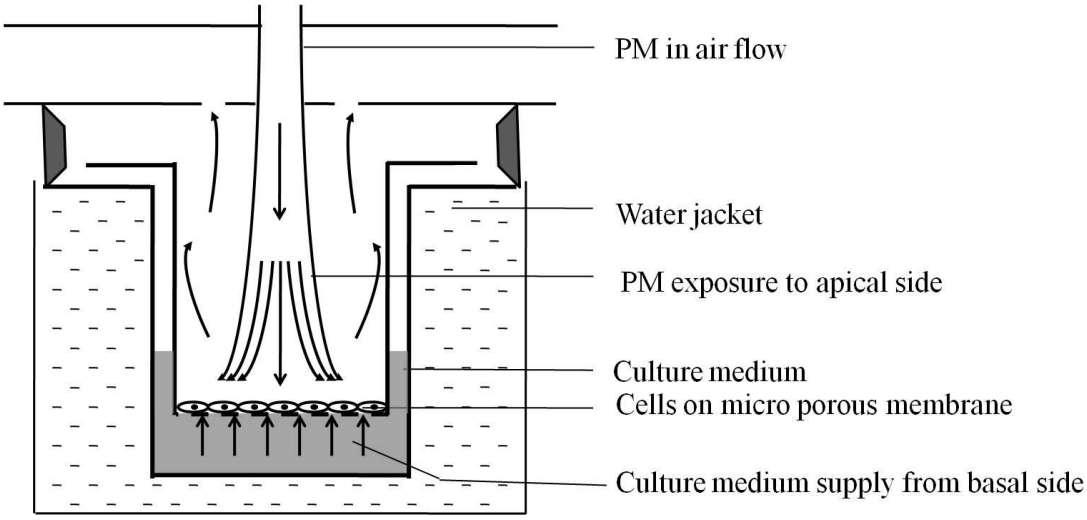

Figure 2.1: Air-liquid interface cell exposure system.

3.2.2 Cell lines

In vitro studies have been conducted using a range of human and animal cells to examine the effects of PM exposure. In this chapter, attention has been focused on human derived cells only. The cells may be collected from freshly isolated tissues (primary cells) or may be generated from a continuous cell line (Rothen-Rutishauser et al., 2008). The application of primary cells has some limitations, including the lack of availability from healthy persons, limited numbers of cells from each isolation, and inter-donor variation. In contrast, transformed cells are homogenous and more stable, and thus allow reproducibility. However, these cells are not supported by endogenous nutrients or other paracrine factors and exhibit little phenotypic

differentiation (Rothen-Rutishauser et al., 2008). The most studied transformed cell lines are: airway epithelial cell lines- Calu-3, 16HEB14o-, BEAS-2B, alveolar epithelial cell line- A549, and a macrophage cell line- THP-1 (Mitschik et al., 2008; Rothen-Rutishauser et al., 2008). Most *in vitro* studies using PM investigate the effect on the lung cells, as it represents the first line of defence to the outside environment and has the greatest surface area for exposures. However, certain studies have examined the exposure effects of PM on the circulatory system, focusing primarily on pulmonary artery endothelial cells (Bai et al., 2001; Karoly et al., 2007). A triple co-culture *in vitro* model of the human airway barrier has been developed by growing human blood monocytes derived macrophages and dendritic cells on the apical and the basal sides of A549 cells to study the interaction of particles with a complex cell culture system (Rothen-Rutishauser et al., 2005). Translocation of particles (AD 1 μm) was observed between the cells, although the dendritic cells were not exposed directly to the particles. This complex model is more realistic and better characterizes particle uptake and translocation, and allows cell-to-cell communication upon particle exposure. Though, more investigation is required in order to recognize the pathway(s) of interplay between different cell types.

3.2.3 Endpoints

Several endpoints can be studied *in vitro*, including PM translocation into the cells, cytotoxicity, induction of oxidative stress, inflammation, DNA damage, and apoptosis, specifically in human pulmonary epithelial cells and pulmonary artery endothelial cells (Bai et al., 2001; Li et al., 2003b, 2002, & 2000; Karoly et al., 2007; Mazzarella et al., 2007). **Table 2.1** summarizes findings from several *in vitro* studies focusing mainly on oxidative stress, inflammation, and the cytotoxic effects of PM. Upregulation of antioxidant enzymes and proinflammatory cytokines are considered as markers of oxidative stress and the inflammatory response in human cells. Among the antioxidant enzymes, glutathione (GSH), superoxide dismutases (SOD), and heme oxygenase (HMOX-1) have been measured in several studies (Hatzis et al., 2006; Lauer et al., 2009; Li et al., 2003b & 2002). The decrease in GSH/glutathione disulfide (GSSG) ratio was measured by glutathione assay as an indicator of oxidative stress. Inflammation can be investigated by determining upregulation of proinflammatory cytokines, such as interleukins (IL-6, IL-8), tumor necrosis factor (TNF-α), macrophage inflammatory protein (MIP); and

chemokines, such as monocyte chemotactic protein (MCP)-1, granulocyte macrophage colony stimulating factor (GM-CSF) (Becker et al., 2005 & 2003; Boland et al., 1999; Carter et al. 1997; Fujii et al., 2001; Hetland et al., 2001; Ramgolam et al., 2008, Watterson et al., 2007). Expression profiling of genes responsive to oxidative stress and inflammation can be analyzed based on mRNA or protein synthesis, using reverse-transcription polymerase chain reaction (RTPCR)/RNase Protection Assay (RPA), and Western blotting/Enzyme-Linked Immunosorbent Assays (ELISA), respectively (Hetland et al., 2004; Li et al., 2002; Mazzarella et al., 2007). Cell viability is generally determined using colorimetric assays such as the MTT (Microculture Tetrazolium) (Watterson et al., 2007) and WST (Water-soluble Tetrazolium Salt) assays (Bai et al., 2001), and/or staining test, such as trypan blue exclusion (Boland et al., 1999; Fujii et al., 2001) and propidium iodide (PI) test (Hetland et al., 2004). In the colorimetric assays, the tetrazolium salts MTT and WST are reduced to formazan only by metabolically active cells, which can be quantified by spectrophotometric means. In the staining tests, viable cells with an intact membrane exclude certain dyes, such as trypan blue and PI, whereas dead cells take up the dye. The numbers of viable cells can then be counted using a microscope or a flow cytometer for trypan blue or PI tests, respectively.

4. Biological mechanisms of toxicity

Several pathophysiological mechanism pathways have been proposed to explain PM induced adverse health effects. Oxidative stress is the most investigated mechanism relating to PM exposure and incidence of different cardiopulmonary diseases (Li et al., 2008; Valavanidis et al., 2008). PM mediated oxidative stress may arise from a number of sources; the largest of which is reactive oxygen species (ROS) such as hydrogen peroxide (H_2O_2), superoxide ($O_2^{\cdot -}$) radical, hydroxyl ($OH^{\cdot}$) radical, etc. These species are either present on the PM surface, generated by components within the PM, or generated through the biological response. Squadrito et al., (2001) showed that fine PM may contain large quantities of free radicals (10^{16} to 10^{17} unpaired spins/g). The presence of soluble transition metals, such as iron, copper, chromium, and vanadium, or organic compounds, such as quinones, on PM surfaces can induce ROS generation in biological systems (Squadrito et al., 2001). Furthermore, ROS can also be generated from activated immune cells during particle-elicited inflammation (Schins and Hei, 2007). It is not yet known to

what degree each mechanism contributes to overall PM-induced generation of ROS. Excessive generation of ROS may overwhelm the antioxidant defence system of the human body resulting in oxidative stress. This leads to the activation of a number of redox-sensitive signaling cascades that can be injurious to the cell, tissue, organ, and ultimately, to the organism as a whole (Li et al., 2003a).

4.1 Respiratory system

Li et al., (2008) proposed a three phase hierarchical cellular oxidative stress model that provides a mechanistic platform to understand how PM elicits adverse health effects in the respiratory system (**Figure 2.2**). Initially, at low levels of oxidative stress, protective effects are induced by transcription factors, such as nuclear factor erythroid-2 (Nrf-2), to reduce biological damage as it activates more than 200 protective antioxidant and detoxification enzymes. Collectively, these enzymes are known as phase 2 enzymes that act in a coordinated manner to protect the lungs from oxidant damage. For example, while SOD catalyzes O_2^- dismutation to H_2O_2, catalase (CAT) and glutathione peroxidase (GPx) prevent formation of the hydroxyl radical ($OH^{\cdot}$) from H_2O_2 and detoxify H_2O_2 to non-toxic products (oxygen and water) (Quinlan et al., 1994). If this protective antioxidant response fails to provide protection against ROS generation, increasing ROS production can generate a proinflammatory response. Oxidative stress activates the mitogen-activated protein kinase (MAPK) and nuclear factor kappa beta (NF-κB) signaling cascades. MAPK controls the synthesis of activator protein (AP)-1, regulating gene expression related to inflammation, and other important functions, including cell proliferation or death. These signaling cascades are responsible for the expression of cytokines, chemokines, and adhesion molecules, which cause inflammation in the lungs. Finally, at toxic levels of oxidative stress, apoptosis and necrosis can occur. Perturbation of mitochondrial permeability transition pores can release proapoptotic factors such as cytochrome c and induce apoptosis of the lung cells. Continuous exposure to PM can result in chronic pulmonary inflammation and eventually cause and/or aggravate impairment of lung development and lung diseases, including COPD, cystic fibrosis, and asthma (Kok et al., 2006). Chronic inflammation can ultimately cause lung fibrosis and epithelial cell hyperplasia, potentially resulting in lung tumors and cancer (Oberdörster, 1996).

Table 2.1: Summary of *in vitro* studies using different human cell lines

Reference	Cell Type	PM type	Exposure Conditions	Endpoints	Findings
Di Pietro et al., 2009	A549	Oil fly ash (collected from power plant)	Serial dilution of original sample 1, 2, 4, 6, 8, 14, and 24 h	Cell viability, intracellular ROS production, DNA damage, lipid peroxidation assessment, and determine the cellular compartments responsible for ROS production and lipid peroxidation	A dose- and time-dependent relation found between metal content of oil fly ash and ROS generation. ROS generation significantly correlated with DNA damage. In the absence of the morphological damage, cytoplasmic compartment generated intracellular ROS. Lipid peroxidation is dose and metal type dependent.
Mazzarella et al., 2007	A549	Diesel exhaust $PM_{1.0}$	100, 200, 400 µg/ml 24, 48, 72 h	Immunocytochemistry, intracytoplasmic cytokines assessment and ELISA for IL-6 and IL-8	Cell wall alternation, PM internalization, cytoplasmic vacuolization and dose dependent increase in IL-6 and IL-8 observed.
Karoly et al., 2007	Human pulmonary artery endothelial cells (HPAEC)	UF or vehicle exhaust	100µg/ml UF or vehicle for 4 h	Quantitative-PCR for selected genes, Western blot analysis for tissue factor (F3) regulation	Coagulation marker up-regulation, expression of HMOX-1, IL-6 and IL-8 with UF PM exposure.

Reference	Cell Type	PM type	Exposure Condition	Endpoints	Findings
Fukano et al., 2006	A549	Whole cigarette smoke CULTEX	About 50-500 µg/vessel	Cell viability and RT-PCR for HMOX-1	No significant change in cell viability. Dose dependant HMOX-1 expression observed for both whole smoke and gas/vapor phase.
Hetland et al., 2004	A549	Coarse, fine, UF, and Mineral rich PM_{10}	0, 200, 400, 600, 800, 1000 µg/ml 40 h	Cell viability, ELISA for IL-6 and IL-8, apoptosis	Increasing in IL-6, IL-8 observed upto 600 µg/ml, but decreased at higher conc. due to toxicity. Similar potency for cytokine induction for coarse, fine and UF.
Becker et al., 2003	Primary alveolar macrophage	Coarse, fine, UF	50 µg/ml 18 to 20 h	ELISAs for IL-6, TNFα, MCP-1, and MIP-1α, phagocytosis, expression of phagocyte receptor	Cytokine induction order: coarse > fine > UF. Presence of microbial products in coarse fraction caused higher cytokine induction.
Li et al., 2002	THP-1	DEP	10, 25, 50, 100, 200 µg/ml 16, 18 h	Western blotting for HMOX-1, manganese-SOD and c-Jun N-terminal kinase cascade (JNK), GSH/GSSG ratio, apoptosis	HMOX-1 expression at low oxidative stress, proceeds to JNK activation and IL-8 secretion at intermediary level, and cellular toxicity observed at higher oxidative stress level.

Reference	Cell Type	PM type	Exposure Condition	Endpoints	Findings
Bai et al., 2001	HPAEC	Diesel exhaust particles	15µg/ml for 1.5 or 24 h, 30 µg/ml for 2 or 24 h	Cell viability of confluent and subconfluent cells using WST-8 assay	Decrease in cell viability with 15µg/ml in subconfluent, 30 µg/ml subconfluent and some confluent.
Fuiji et al., 2001	Primary human bronchial epithelial cells	PM_{10}	10, 100, 500 µg/ml 2, 8, 24 hr	Rnase and ELISA for leukemia inhibitory factor (LIF), GM-CSF, IL-1 and IL-8	mRNA levels of LIF, GM-CSF, IL-1 and IL-8 increased in dose-dependent manner between 100 and 500 µg/ml.
Boland et al., 1999	16HBE14o-	SRM 1650 DEP	0-20 $\mu g/cm^2$ 6, 12, 24 hr	Cytotoxicity, phagocytosis, ELISA for IL-8, GM-CSF, and IL-1 β	DEP underwent phagocytosis by epithelial cells and translocated through the cell. A time-dependent increase in IL-8, GM-CSF, and IL-1β observed.

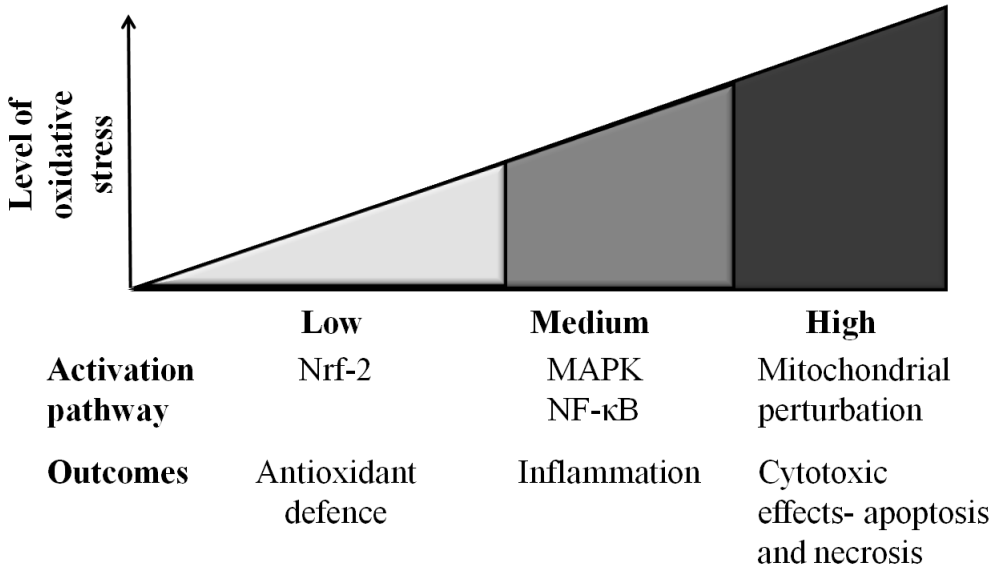

Figure 2.2: Hierarchical cellular oxidative stress model (adapted from Li et al., 2008).

4.2 Cardiovascular system

Although it is clear that PM has a profound effect on cardiovascular health, the mechanisms underlying this process are still unclear. Three mechanisms have been proposed linking PM and CV effects: 1) irritation of the pulmonary system leading to systemic release of proinflammatory or prooxidative mediators; 2) autonomic imbalance leading to sympathetic nervous system activation or parasympathetic nervous system withdrawal; and 3) direct transfer of nanoparticles to the circulatory system through the alveoli (Brook, 2008; Nemmar et al., 2002). The cardiovascular consequences of PM exposures are likely caused by more than one pathway occurring simultaneously. The first pathway- release of proinflammatory and prooxidative mediators is supported by the results of human exposures. Several studies have observed increases in leukocytes, platelets, PMN, and cytokines (i.e., IL-6 and TNF-α) in peripheral blood (Dubowsky et al., 2006; Mills et al., 2008; Törnqvist et al., 2007) with exposure to dilute diesel PM. Similarly, increased levels of 8-isoprostane in exhaled breath when exposed to CAP suggest oxidation of tissue phospholipids (Mills et al., 2008). The second pathway- autonomic imbalance is also supported by current research. HRV, a marker of autonomic tone, has been shown to be affected by PM (Brook et al., 2004; Fakhri et al., 2009; Gold et al., 2000). Short-term reduced low-frequency HRV has been associated with sudden death in patients with chronic heart failure

(La Rovere et al., 2003). Furthermore, the deposition of PM on pulmonary nerve endings may cause an imbalance in autonomic control of the heart, leading to decreased HRV. The decreased HRV, in turn, raises the possibility of sudden death in sufferers of chronic heart failure (Karoly et al., 2007). The third proposed pathway remains controversial. Attempts to prove translocation of (^{99m}Tc)– labelled carbon nanoparticles (Technegas) from the lungs to the circulatory system have had mixed results (Nemmar et al., 2002). Despite the controversy, the implications of translocation of nanoparticles would be incalculable, given that UF particles have the highest number concentration of all PM. Chan and his group (University of Toronto, Canada) are currently working on quantifying nanoparticles such as carbon and gold nanoparticles in excised organs, after in vivo dosing for many innovative applications in diagnostics (Fischer et al., 2007). It is hypothesized that low-to- moderate grade inflammation induced by chronic PM exposure may initiate and accelerate atherosclerosis. Acute exposure to high concentrations of PM may cause vasoconstriction leading to myocardial infarction (Peters et al., 2001) or other ischemic events (Dominici et al., 2006).

5. Conclusions

Knowledge generated through epidemiological, *in vivo* and *in vitro* studies has allowed substantial progress in recent years in our understanding of the pathophysiological mechanisms underlying PM-induced adverse health effects. There is a mounting body of evidence indicating that human exposure to ambient PM at concentrations typical of urban areas can cause serious health problems. The respiratory and cardiovascular systems have been identified as the primary targets of inhaled PM. Both *in vivo* and *in vitro* toxicology studies have identified oxidative stress-initiated inflammation as one of the major pathways of induced respiratory and cardiovascular diseases. Although the assessment of PM toxicity has been studied extensively, knowledge gaps still remain. Most of the *in vivo* and *in vitro* studies have observed biological responses at very high PM concentrations; however, epidemiological studies have found increased mortality even at relatively low ambient PM concentrations. The mechanisms responsible for the increased health risks associated with these low PM concentrations have not yet been identified in toxicological investigations. There is also no clear consensus on a unique

physicochemical characteristic of PM that could explain the observed biological responses. More rigorous animal exposure studies which investigate the pathophysiological consequences of well characterized PM exposures are required to identify the effects of both acute and chronic PM exposure in both healthy and diseased models. Further investigation is also required to develop an optimal *in vitro* exposure system to determine which properties of PM may be causing the biological effects and to define the mechanisms underlying these biological effects observed *in vivo*. New findings obtained from both *in vivo* and *in vitro* studies will allow regulatory agencies to develop better air quality standards in order to reduce health risks to both in the general public and susceptible individuals.

Chapter 3

Cytotoxic and proinflammatory effects of ambient and source-related particulate matter in relation to the production of reactive oxygen species (ROS) and cytokine adsorption by particles

Umme S. Akhtar, Robert D. McWhinney, Neeraj Rastogi, Jonathan Abbatt, Greg J. Evans, Jeremy A. Scott

Inhalation Toxicology, 2010, 22(S2): 37–47, doi:10.3109/08958378.2010.518377

Abstract

The composition of airborne particulate matter (PM) varies widely depending on its source, and recent studies have suggested that particle-associated adverse health effects are related to particle composition. The objective of this study was to compare the biological/toxicological effects of different source-related PM. Specifically, we investigated the biological/toxicological effects of Standard Reference Materials (SRMs): non-ferrous dust (PD-1, industrial), urban PM (UPM, SRM1648a), and diesel PM (DPM, SRM2975), and ambient $PM_{2.5}$ (PM with an aerodynamic diameter <2.5 μm) collected at an urban site (Toronto, Canada). The dithiothreitol assay was used to measure the redox activity of the particles. Human alveolar epithelial cells (A549) were exposed to a range of concentrations (10-1000 μg/ml) of total PM, and the respective water-soluble and insoluble fractions, for 24 h. Biological responses were then evaluated in terms of cytotoxicity and interleukin (IL-8) release, and compared with the PM composition and redox activity. We demonstrated that transition metal-enriched PD-1 exhibited the greatest cytotoxic effect (LD_{50} values of 100-400 μg/ml vs. >1000 μg/ml for the SRM1648a, SRM2975, and ambient $PM_{2.5}$). Similarly, the PM-induced release of IL-8 was greatest for PD-1 (~6-9 ng/ml vs. ~1.5-3 ng/ml for others). These endpoints were more responsive to metals compared with secondary inorganic ions and organic compounds. Interestingly, we demonstrated a high degree of adsorption of IL-8 to the various SRMs and ambient $PM_{2.5}$, and subsequently derived a new correction method to aid in interpretation of these data. These characteristics likely impart

differential effects toward the toxic and immune effects of PM.

1. Introduction

The World Health Organization (WHO, 2006) has defined air pollution as a continuous threat to human health that is associated with more than two million premature deaths each year. According to a Canadian Medical Association report (CMA, 2008), air pollution in Canada will result in a cumulative loss of almost 800,000 lives and an economic cost of $250 billion by 2031. Ambient air often contains a complex mixture of pollutants and elucidation of the relative contributions of different agents to these impacts remains unresolved. However, epidemiological studies have found a consistent direct relationship between increased ambient particulate matter (PM) mass concentration and cardiopulmonary morbidity and mortality (Brook et al., 2003; Dockery et al., 1993; Laden et al., 2000; Pope et al., 2002). Animal and human experimental studies have also found that exposure to high PM concentration can cause aggravation of respiratory and cardiovascular diseases (Mills et al., 2008; Saldiva et al., 2002; Urch et al., 2005).

Epidemiological, *in vivo*, and *in vitro* studies have contributed substantially to our understanding of the pathophysiological mechanisms of PM-induced adverse health effects. Recent studies have proposed oxidative stress-induced inflammation as one of the major pathways of PM-induced respiratory diseases (Li et al., 2003a, 2008). PM-mediated oxidative stress is mainly caused by reactive oxygen species (ROS), such as hydrogen peroxide (H_2O_2), superoxide ($^{\cdot}O_2^-$), and hydroxyl radical ($OH^{\cdot}$). ROS may be generated by free radicals present on particle surfaces, by the chemical reaction of specific PM constituents (Li et al., 2003a; Squadrito et al., 2001), or through PM-mediated activation of mitochondria or NAD(P)H-oxidase enzymes and immune cells (Schins and Hei, 2007). Intracellular and extracellular production of ROS can activate a number of redox-sensitive signaling cascades that could, in turn, induce inflammatory responses (Kelly, 2003; Li et al., 2008 & 2003a). The inflammatory response is involved through upregulation of various signaling molecules, such as cytokines, chemokines, and adhesion molecules, in the lung. Interleukin-8 (IL-8) is a proinflammatory chemokine that is produced by pulmonary epithelial cells and macrophages (Kunkel et al., 1991). Thus, the nature and degree of

oxidative stress induced by particulate air pollution can depend upon the chemical reactivity of the PM and the responses that they induce in specific cell populations.

Accumulating evidence suggests that PM-associated adverse health effects are related to particle composition. Limited epidemiological, *in vivo,* and *in vitro s*tudies have found that specific constituents of PM, such as transition metals (Fe, Cu, Ni, and V), play important roles in eliciting pulmonary responses (Frampton et al., 1999; Ghio, 2004; Huang et al., 2004; Laden et al., 2000). *In vitro* investigations also suggest that particle-associated organic compounds can initiate such effects after PM exposure (Boland et al., 2001 &1999; Gualtieri et al., 2009; Ramgolam et al., 2009). Epidemiological studies have not been able to establish any definitive association between the effects of organic compounds and health (Schwarze et al., 2006). Studies measuring intracellular or extracellular ROS production capacity of PM have shown that the redox activity of PM is associated with redox-active metals (e.g., Fe, Cu, Cr, and Zn), and organic compounds, especially polycyclic aromatic compounds (PACs) (Becker et al., 2005; Cho et al., 2005; DiStefano et al., 2009; Li et al., 2003b; Ntziachristos et al., 2007). Based on these experimental findings, it has been proposed that transition metals and PACs are primarily responsible for inducing oxidative stress and inflammation within the lung through of ROS. Transition metal ions present on PM surfaces can produce ROS or catalyze the formation of $OH^{\cdot}$ from H_2O_2 through Fenton (reaction of transition metals with $^{\cdot}O_2^-$) and Haber-Weiss (reaction between $^{\cdot}O_2^-$ and H_2O_2) reactions (Li et al., 2008). PACs, such as quinones and hydroquinones, can produce $O_2^{\cdot -}$ that acts as a catalyst for both Fenton and Haber-Weiss reactions (Balakrishna et al., 2009). In addition, polycyclic aromatic hydrocarbons (PAHs) can also be converted to quinones through biotransformation by cytochrome P450 and dihydrodiol dehydrogenase (Kelly, 2003). A number of *in vivo* and *in vitro* studies have also showed an association between biological effects and biological materials (such as endotoxins) adhered to the PM (Alexis et al., 2006; Becker et al., 2005; Camatini et al., 2012; Soukup and Becker, 2001; Steenhof et al., 2011; Wang et al., 2013).

Airborne PM is emitted from a number of anthropogenic sources, particularly from mobile and industrial sources. A study of five Canadian cities, recently showed that traffic contributes to 14-21% of the $PM_{2.5}$ mass with a further 10-15% coming from the oxidation of NO(g) emitted by vehicles (Jeong et al., 2011). Although a few epidemiological studies have connected health

effects with PM sources, there is emerging evidence that PM from combustion and traffic sources correlate positively with increased mortality and cardiopulmonary diseases. Birth cohort studies investigating the development of respiratory diseases have found an association between increased exposure to traffic-related $PM_{2.5}$ and the incidence of asthma, asthma symptoms, and upper respiratory infections (Brauer et al., 2002). In another study, a 10 $\mu g/m^3$ increase in $PM_{2.5}$ concentration from mobile-source emissions was associated with a 3.4% increase in daily mortality (Laden et al., 2000). Industrial emissions can also contribute to PM in urban areas. The study of five Canadian cities found that 5-15% of the $PM_{2.5}$ came from point sources, such as smelters, refineries, and cement kilns (Jeong et al., 2011). Even though these industrial sources contribute a smaller portion of the overall mass, industrial PM may contribute disproportionately to the health burden. A unique study conducted in Utah Valley demonstrated a reduction in hospital admission for respiratory diseases and daily mortality when a steel mill, which was the source of 50-70% of total PM_{10} (PM with an aerodynamic diameter <10 μm) in that valley, was closed for 13 months (1986-87) (Pope, 1991; Pope et al., 1992; Utah Bureau of Air Quality, 1990). An *in vitro* study comparing PM collected during the closure and reopening of the plant found that inflammatory responses were greater after the mill reopened (Frampton et al., 1999). Therefore, source-related PM toxicity studies are essential to understand source-specific health effects. Toxicological studies of PM collected from different sources will also guide the development of source-specific emission standards and risk management policies.

The objectives of this study were to compare the biological/toxicological effects of different source-related particles and to relate these to their composition and their capacity for ROS production. PM from industrial and diesel-operated mobile sources, and urban environments were used in this study. A549 cells were exposed to increasing PM concentrations followed by assessment of cell viability and proinflammatory response. Acellular ROS measurements were conducted to determine the redox activity of these particles. It was hypothesized that exposure of airway epithelial cells to PM would induce a proinflammatory response and adversely affect cell viability, in a manner that was dependent upon the chemical composition and the ROS production capacity of the PM. Additionally, acellular IL-8/PM exposure tests were conducted to calculate the factors necessary to correct factors for the adsorption of IL-8 to particles, with the

hypothesis that these correction factors would aid in the interpretation of the *in vitro* IL-8 release data. To the best of our knowledge, this was the first attempt to correct IL-8 concentration measured in alveolar epithelial cells after PM exposure.

2. Materials and methods

Please see the appended Data Supplement (Appendix A) for further description of the methods and results.

2.1 Chemicals

Cell culture medium Dulbecco's modified Eagle's medium (DMEM), penicillin-streptomycin, DL-dithiothreitol (98%), and 1, 2-napthoquinone were purchased from Sigma Aldrich (Oakville, ON, Canada). L-glutamine, trypsin, and phosphate buffer saline (PBS) were purchased from Invitrogen (Carlsbad, CA). Fetal bovine serum (FBS) was purchased from Wisent Inc. (St-Bruno, QC, Canada). MTT assay kits were purchased from American Type Culture Collection (ATCC) (Manassas, VA). The IL-8 enzyme-linked immunosorbent assay (ELISA) kits were purchased from Biolegend (San Diego, CA). Tris-HCl, tetrasodium EDTA, and trichloroacetic acid were purchased from Fisher Scientific (Whitby, ON, Canada), and 5, 5'-dithiobis (2-nitrobenzoic acid) were obtained from Alfa Aesar (Ward Hill, MA). Standard Reference Materials SRM1648a and SRM2975 were purchased from National Institute of Standards and Technology (Gaithersburg, MD). The non-ferrous dust sample (PD-1) was obtained from Canada Certre for Mineral and Energy Technology (Ottawa, ON, Canada).

2.2 Preparation of particle samples

The procedure for PM preparation is illustrated in **Figure 3.1**. SRM suspensions were prepared in cell culture medium at a PM concentration of 1000 µg/ml (mass/volume). The suspended particles were then sonicated for 30 min to avoid agglomeration. Water-soluble fractions were prepared by filtration of aliquots through a syringe filter (Acrodisc, 25 mm diameter, 0.2 µm porosity). Aliquots were centrifuged and washed three times with cell culture medium followed by resuspension in the same volume of the medium to isolate the insoluble fractions of the PM

suspensions. Ambient $PM_{2.5}$ collected on a Teflon® filter paper was recovered by sonicating the paper in 1 ml of cell culture medium for 30 min, similar to the procedure used by Ramgolam et al., (2008). Medium was then added to adjust the particle concentration to the final value of 1000 µg/ml. Particles were recovered directly in the medium to avoid the evaporation of extraction medium which could change the physiochemical properties of the PM and cells were exposed to the medium. As a control blank Teflon® filters were sonicated in cell culture medium. Experiments were performed within one hour of PM preparation to avoid variability in PM components in different fractions between replicates. Cells were exposed to the total PM suspensions, and the respective water-soluble and insoluble fractions at concentrations of 10 to 1000 µg/ml for 24 h. PM suspensions were prepared in serum-free and serum-containing (10% FBS) medium for cytotoxicity and proinflammatory assays, respectively. Filter extracts could not be checked for water-soluble and insoluble fractions as the collected mass was low.

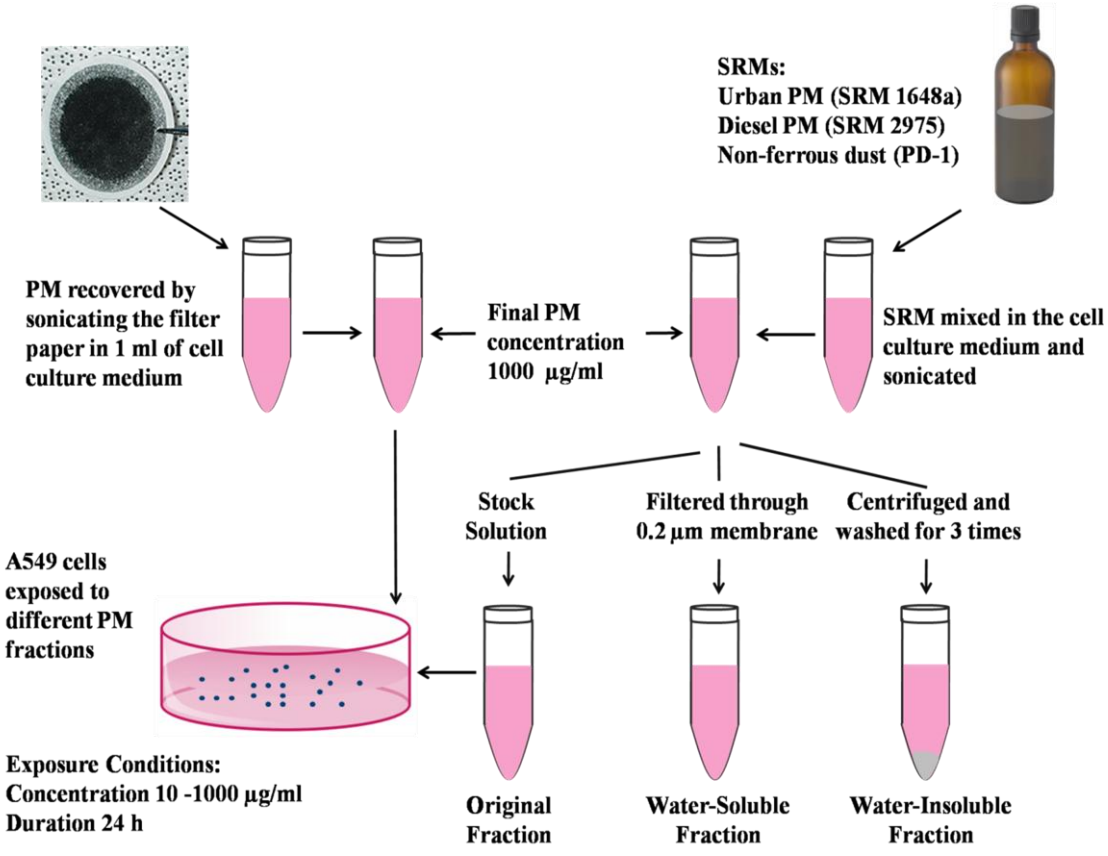

Figure 3.1: Experimental procedure for PM preparation and cell exposure.

2.3 Elemental analysis

For the analyses of water-soluble fractions of elements in the three SRMs, a known amount of each SRM (10 mg) was suspended in 5 mL of Milli-Q water (Millipore DQ-3, resistivity >18.3 MΩ) followed by ultrasonication (15 min, 3 times) and manual shaking. Subsequently, the solutions were filtered through a syringe filter (0.2 µm porosity) and acidified to pH <2 using trace metal grade HCl. These water-extracts were analyzed for 26 elements (Ag, Al, As, B, Ba, Be, Ca, Cd, Co, Cr, Cu, Fe, K, Mg, Mn, Mo, Na, Ni, Pb, Sb, Se, Si, Ti, Tl, V, Zn) using Inductively Coupled Plasma Atomic Emission Spectroscopy (ICP-AES, Perkin Elmer Optima 3700 DV) at the Analytical laboratory for Environmental Science Research and Training (ANALEST) facility of the University of Toronto.

2.4 Redox cycling activity of particles

The DTT assay used in this study was adapted from the procedure reported by Cho et al., (2005). Total PM suspensions were prepared in PBS (0.1 M, pH 7.4) at 1000 µg/ml PM concentration. Water-soluble and insoluble fractions were obtained following the same procedure described above. The stock solutions were subsequently diluted to a suitable concentration (approximately 100 µg/ml for SRM1648a and the Toronto-$PM_{2.5}$ samples, 60 µg/ml for the water-soluble extract of SRM2975, and 30 µg/ml for the insoluble and whole fractions of SRM2975) and mixed with DTT (1×10^{-4} M, 99% Sigma-Aldrich). At predetermined times during a 1 h period, 0.5 ml aliquots of the reaction mixture were quenched with 0.5 ml of a 10% w/w trichloroacetic acid solution. The quenched solution was mixed with 2 ml of 5, 5'-dithiobis (2-nitrobenzoic acid) (DTNB, 2×10^{-4} M, 99% Alfa Aesar) in a 0.4 M Tris buffer containing 20 mM EDTA at pH 8.9. The 2-nitro-5-thiobenzoate product was quantified using a Perkin Elmer Lambda 12 UV-Vis spectrophotometer using a wavelength of 412 nm. DTT activity was reported as nmol of DTT consumed per minute normalized to mass of PM in milligrams. The quality of the data was confirmed by performing the assay simultaneously on a solution of 97% 1, 2-napthoquinone.

2.5 Analyses of biological endpoints

Details of the cell culture procedure can be found in **Appendix A**. For cell viability and IL-8

concentration measurements, cells were exposed to PM in triplicate at each PM concentration, and were confirmed in two to three independent experiments for the SRMS. For the ambient PM, PM exposure was conducted in triplicate; however, the filter collected mass was not adequate for independent replication of experiments. Cell viability was determined using the MTT assay by following the manufacturer's instructions (Cat. No. 30-1010K, ATCC). The results were expressed as percentage of cell viability with respect to the relevant control. For IL-8 concentration measurement, cell supernatants from each individual well were collected after 24 h of PM exposure and centrifuged to remove any cell debris and remaining PM, and then frozen at -80°C for subsequent analysis. The IL-8 concentrations in the supernatants were measured in triplicate using an ELISA kit following the manufacturer's instructions (Cat. No. 431504, BioLegend).

2.6 Cytokine adsorption by particles in cell-free tests

As preliminary investigations demonstrated widespread variability between IL-8 releases in response to the SRMs, we tested whether the IL-8 released by cells into the medium was adsorbed by the particles (Kocbach et al., 2008; Seagrave, 2008). PM suspensions (10-1000 µg/ml) prepared in cell culture medium with 10% FBS were incubated with standard IL-8 (2 ng/mL) for 24 h. Adsorption tests were conducted for the three SRMs and one filter sample for Toronto-$PM_{2.5}$ (F-1). After exposure, the supernatants were analyzed for the remaining IL-8 concentration by ELISA. As for the cellular IL-8 release experiments, both the PM exposure and ELISA analyses were performed in triplicate and in two independent experiments for the SRMs. Based on the remaining IL-8 concentration measurements, correction factors (CFs) were derived for each particle type to relate the surface-bound and solution IL-8 concentrations (described in Supplemental materials and methods, **Appendix A**).

2.7 Statistical analyses

Statistical analyses were performed using GraphPad Prism 4.0c (La Jolla, CA, USA) and MINITAB 14 (State College, PA, USA). The minimum number of replicates for all treatments was three. All experiments were repeated in at least two independent experiments for each of the

SRMs. All results are reported as the mean ± SEM. Statistical differences between experimental groups were tested by one-way analysis of variance (ANOVA) followed by Tukey post-test for comparison with control. Spearman rank correlation (ρ) test was used to determine the relationships between different variables. Two-way ANOVA was used to investigate the effect of IL-8 adsorption on *in vitro* IL-8 measurements, for different PM concentrations. If the effect was significant, t-test was conducted to determine the statistical difference between the corrected and original IL-8 data at individual PM concentrations. Statistical differences were considered significant when $p < 0.05$.

3. Results

3.1 Elemental composition of the SRMs

The elemental composition of the SRMs can be found in the Data Supplement (**Tables A.1 & A.2**). The water-soluble elemental concentrations measured for the three SRMs are shown in **Table 3.1**. PD-1 contained significant amounts of water-soluble metals (Cd, Zn) even though many of the key metals (e.g., Cu, Pb, Fe) related to ROS production were mostly present in their insoluble forms. SRM1648a had high water-soluble concentrations for many crustal elements (e.g., Ca, K, Mg, Na) and transition metals (e.g., Cu). However, Cu concentration in the water-soluble fraction of PD-1 were still higher compared to that of SRM1648a (Cu = 2,230 µg/g for PD-1 vs. Cu = 140 µg/g for SRM1648a). Based on **Table 3.1** and Supplemental **Table A.1**, the water-soluble fractions of PD-1 and SRM 1648a comprised approximately 14% and 19% of the total fractions, respectively. SRM2975 was mostly water-insoluble and thus the concentrations of most of the elements were below the detection limit.

3.2 Redox cycling activity of particles

The DTT assay was successfully applied to SRM1648a, SRM2975, and Toronto-$PM_{2.5}$ (both F-1 and F-2); analysis of PD-1 was inconclusive. The DTT consumption rate was the highest for total SRM2975, which was 8-fold greater than that for SRM1648a (**Figure 3.2**). Interestingly, for both SRMs, the redox-activity of the total fraction was reflective of the sum of the activities of both the water-soluble and insoluble fractions. The redox activity of ambient PM was similar (F-

1) or ~2-fold higher (F-2) than the standard UPM (SRM1648a), likely due to differences in composition on different days. The water-soluble fraction of SRM1648a contributed to 82%, whereas the water-insoluble fraction of SRM2975 contributed to 85% of the total activity.

Table 3.1: Water-soluble concentrations (µg/g) of major metals measured by ICP-AES (percentage of total concentration of respective metals are presented in parenthesis)

Metal	Non-ferrous dust (PD-1)	Urban PM (SRM1648a)	Diesel PM (SRM2975)
Ca	2100	45300 (78)	165
Cd	2100 (75)	29 (39)	BDL
Cu	2230 (3)	140 (23)	3
Fe	BDL	44 (0.01)	BDL
K	111	3410 (32)	BDL
Mg	443	2430 (30)	190
Mn	123	283 (36)	BDL
Na	106	1610 (38)	BDL
Ni	BDL	5 (6)	BDL
Pb	1050 (4)	BDL	BDL
Si	BDL	29 (0.02)	BDL
Zn	87800 (24)	2940 (61)	252

BDL- below detection limit

3.3 Effect of SRMs and ambient Toronto-$PM_{2.5}$ on cell viability

Figure 3.3 shows the cytotoxicity profile of different source-related PM, as determined using the MTT assay. Of the SRMs, all fractions of PD-1 (total, water-soluble, and insoluble) were more toxic than the other two SRMs or the Toronto-$PM_{2.5}$ (PD-1 > SRM1648a > SRM2975 > Toronto $PM_{2.5}$). For PD-1, a statistically significant decrease with respect to the control was observed starting at a PM concentration of 10 µg/ml, and almost 100% of the cells were dead at a dose of 400 µg/ml (**Figure 3.3A**). The lowest cell viabilities for total SRM1648a and SRM2975 (45%

and 58%, respectively) were observed at the highest PM dose (1000 µg/ml; **Figure 3.3 B & C**).

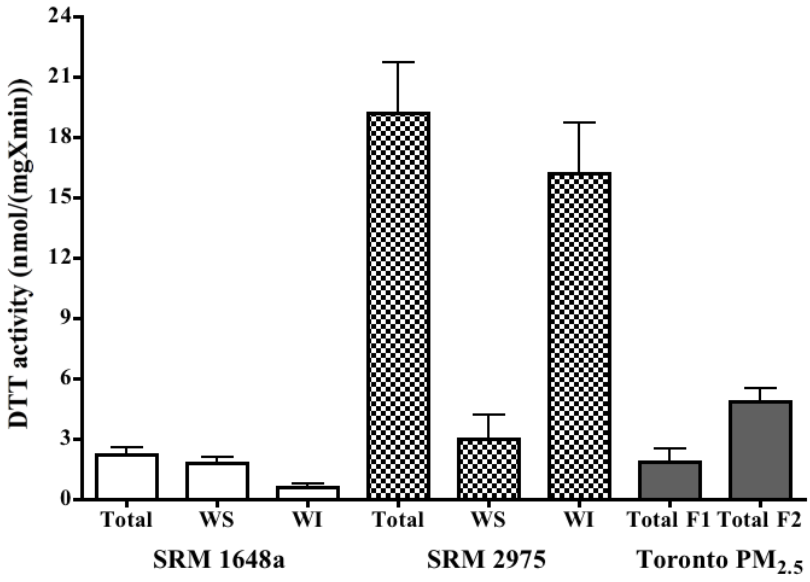

Figure 3.2: Redox activity of SRM1648a, SRM2975, and Toronto-$PM_{2.5}$ (F-1 and F-2) measured using DTT Assay. The activity was high for SRM2975, which was enriched in organic compounds. The capacity of Toronto-$PM_{2.5}$ was comparable to the urban PM standard. The redox activity of the water-soluble and insoluble fractions summed up to the activity of the total fraction. The data are reported as the mean ± SEM (n = 3). WS- water-soluble, WI- water-insoluble.

For all three SRMs, the toxicity profiles of the water-insoluble fractions followed that of the total suspensions. No significant toxic response was observed after exposure to the water-soluble fractions of SRM1648a and SRM2975, whereas the water-soluble fraction of PD-1 remained cytotoxic. These findings suggest that the insoluble fraction of the particles play an important role on the cytotoxic response of mammalian cells. For ambient filter sample, the control blank Teflon® filters showed no cytotoxic effects for 24 h exposure. A progressive decrease in cell viability was observed with increasing concentrations of Toronto-$PM_{2.5}$ (**Figure 3.3D**). These Toronto-$PM_{2.5}$ samples exhibited a cytotoxicity trend similar to the UPM standard (SRM1648a) but were generally less toxic. The lowest cell viabilities of 60% and 72% were observed at 1000 µg/ml of F-1 and F-2, compared with 45% for SRM1648a. **Table 3.2** presents the correlation

coefficients (ρ) of cell viability with the PM concentrations (μg/ml). Cell viability decreased significantly with increasing PM concentrations for total and water-insoluble fractions of all PM types (p <0.001). Cell viability also exhibited a significant negative association with the water-soluble fraction of PD-1 (p <0.0001), whereas the water-soluble fractions of SRM1648a and SRM2975 exhibited negative but non-significant associations (p >0.05).

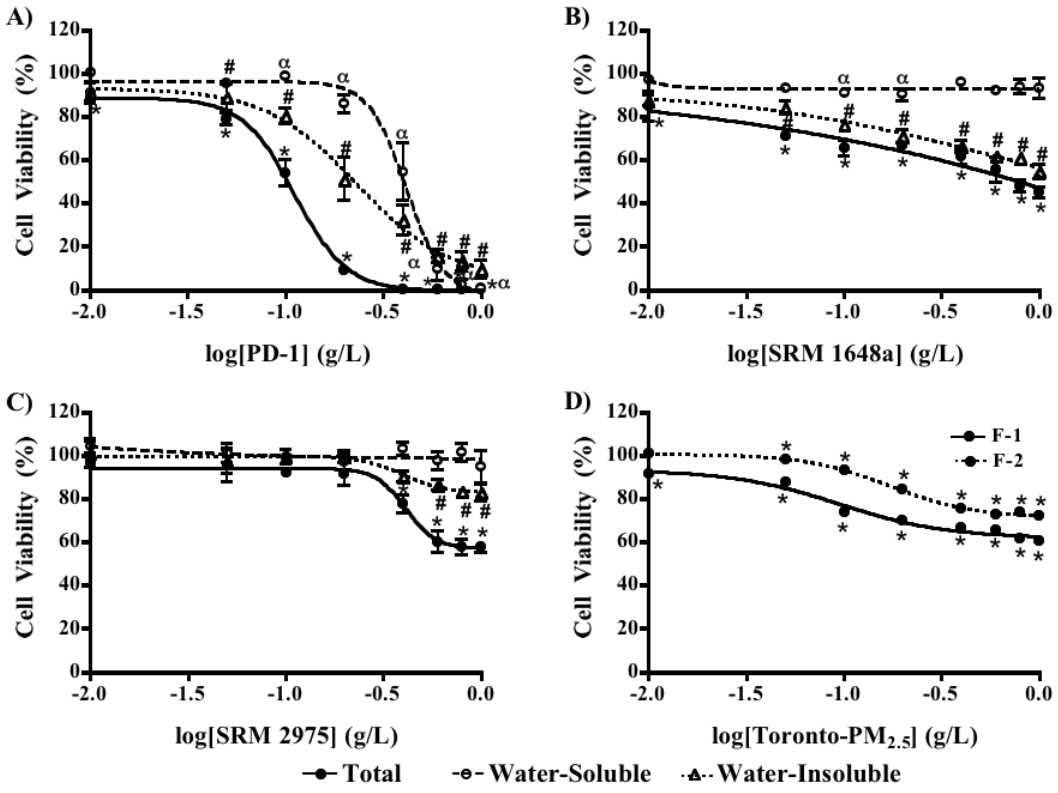

Figure 3.3: Cytotoxic response of different source-related PM measured using MTT assay. A) PD-1, B) SRM1648a, C) SRM2975, D) Toronto-$PM_{2.5}$. The results are presented as percentage of cell viability with respect to the relevant control. Three independent experiments were carried out in triplicate for SRMs, following the same experimental conditions. Cell viability data for water-soluble and insoluble fractions are plotted in terms of their representative total concentration. The data are reported as mean ± SEM (n = 3 for SRMs, n = 1 for Toronto-$PM_{2.5}$). Statistically significant difference from control (p <0.05): total- *, water-soluble- α, water-insoluble- #.

Table 3.2: Spearman's rank coefficients (ρ) between PM concentration (μg/ml) and biological responses

	Non-ferrous dust (PD-1)			Urban PM (SRM1648a)			Diesel PM (SRM2975)			Toronto-PM2.5	
	Total	WS	WI	Total	WS	WI	Total	WS	WI	F-1 Total	F-2 Total
Cell viability	-0.99$^{\#}$	-0.97$^{\#}$	-1$^{\#}$	-0.98$^{\#}$	-0.32	-1$^{\#}$	-1$^{\#}$	-0.4	-0.92$^{\alpha}$	-1$^{\#}$	-0.97$^{\#}$
IL-8 concentration	-0.03	-0.13	1$^{\#}$	0.77*	0.95$^{\#}$	0.83$^{\alpha}$	-0.68*	0.82$^{\alpha}$	-0.1	0.93$^{\alpha}$	1$^{\#\#}$
Increasing IL-8 concentration	1$^{\#}$	0.94$^{\#}$	1$^{\#}$	1$^{\#}$	0.98$^{\#}$	0.96$^{\#}$	1$^{\#}$	0.64	1$^{\#}$	1$^{\#}$	1$^{\#}$
Corrected IL-8 concentration				0.93$^{\alpha}$			0.62			0.96$^{\#}$	

WS- water-soluble, WI- water-insoluble, $p < 0.05$*****, $p < 0.01^{\alpha}$, $p < 0.0001^{\#}$

3.4 Proinflammatory response

IL-8 upregulation was observed at lower PM concentrations, with ~2-fold increases in IL-8 at PM concentrations as low as 10 µg/ml for all the PM samples. Similar to the cytotoxic effect, the proinflammatory response was the greatest for PD-1 (**Figure 3.4A**). The release of IL-8 increased progressively up to a PM concentration of 200 µg/ml (~11-fold higher than the control) and decreased significantly at PM concentrations >200 µg/ml. The IL-8 dose-response for the water-soluble fraction of PD-1 exhibited a similar trend. In contrast, a progressive increase was observed for the water-insoluble fraction of PD-1, despite the fact that cell viability was only 23% at the highest PM concentration. The reason for such an increase in IL-8 upregulation despite greatly reduced cell viability could not be identified.

The IL-8 induction potential for the total SRM1648a was greater than that of SRM2975 (**Figure 3.4B** & **C**); ~4-fold vs. ~2-fold increases for SRM1648a and SRM2975, respectively. For SRM2975, the IL-8 dose-response profile decreased significantly above a PM dose of 200 µg/ml even though the majority of the cells were still viable at these high levels (**Figure 3.3C**). The water-soluble fractions of SRM1648a and SRM2975 seemed to have little effect on IL-8 induction, similar to the cytotoxicity profile. The Toronto-$PM_{2.5}$ samples were less potent (~3-fold increase) than the UPM standard in inducing IL-8 (**Figure 3.4D**). The decrease in cell viability at high PM concentrations likely reduced the cytokine release induced by different fractions of the SRMs, especially for PD-1.

For the changes in IL-8 concentrations after exposure to PM, no consistent correlations were found with PM concentrations (**Table 3.2**). Strong positive correlations were found in some cases (total: SRM 1648a, Toronto-$PM_{2.5}$, water-soluble: SRM1648a, SRM2975, and water-insoluble: PD-1, SRM1648a). The poor and negative correlations for others were due to the observed decrease in IL-8 concentrations at higher PM concentrations. However, consideration of the IL-8 concentrations before this decline revealed strong positive associations between IL-8 upregulation and PM concentration for all (p <0.0001) except for the water-soluble fraction of SRM2975 (ρ = 0.643, p = 0.119).

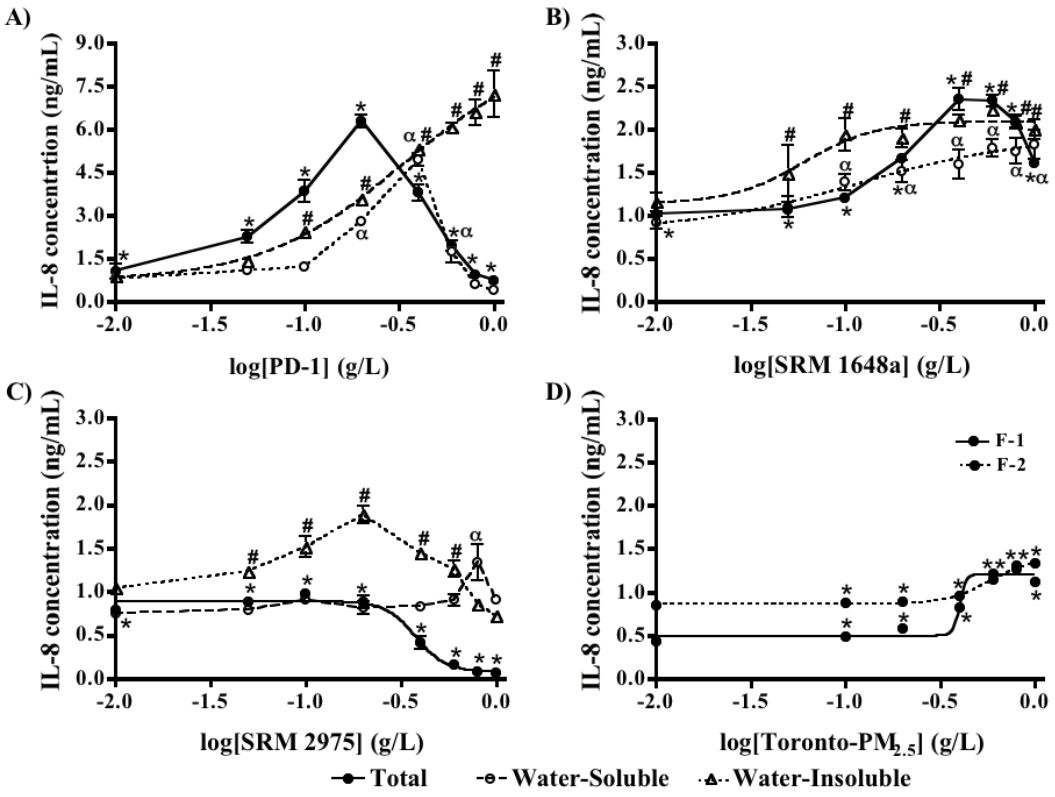

Figure 3.4: IL-8 induction by different source-related PM measured using ELISA assay. A) PD-1, B) SRM1648a, C) SRM2975, D) Toronto-$PM_{2.5}$. PM exposure experiments for cytokine detection were performed two times in triplicate following the same exposure conditions. IL-8 concentrations for water-soluble and insoluble fractions are plotted in terms of their representative total concentration. The data are reported as mean ± SEM (n = 6 for SRMs, n = 3 for Toronto-$PM_{2.5}$). Statistically significant differences from control (p <0.05): total- *, water-soluble- α, water-insoluble- #.

3.5 IL-8 adsorption by particles

Incubation of SRMs and Toronto-$PM_{2.5}$ with IL-8 standard in a cell-free system showed that particles with different physicochemical properties exhibited differential IL-8 adsorption capacities (**Figure 3.5**). The IL-8 adsorption was greatest for SRM2975 and decreased in the order: SRM2975 > SRM1648a > Toronto-$PM_{2.5}$ (F-1) > PD-1. As would be expected, adsorption of IL-8 also increased with increasing PM concentrations. For SRM1648a and SRM2975,

significant IL-8 adsorption was observed at PM concentrations as low as 50 µg/ml. The maximum degree of IL-8 adsorption was 87%, 73%, 56%, and 13% for SRM2975, SRM1648a, Toronto-$PM_{2.5}$, and PD-1, respectively. It has been shown that SRM2975, enriched in total carbon content, exhibited the highest IL-8 adsorption capacity, whereas this was the lowest with metal-enriched PD-1. In addition, SRM2975, with a higher specific surface area (91 m^2/g) compared to that of SRM1648 (29 m^2/g) (Medalia et al., 1983), adsorbed more IL-8. The SRM1648a used in this study was the same SRM that has been issued previously as SRM1648. Higher solubility of the PM would result in less adsorption as there would be no surface to adsorb to. Thus, the predominant insoluble content of SRM2975 was also expected to play an important role in IL-8 adsorption.

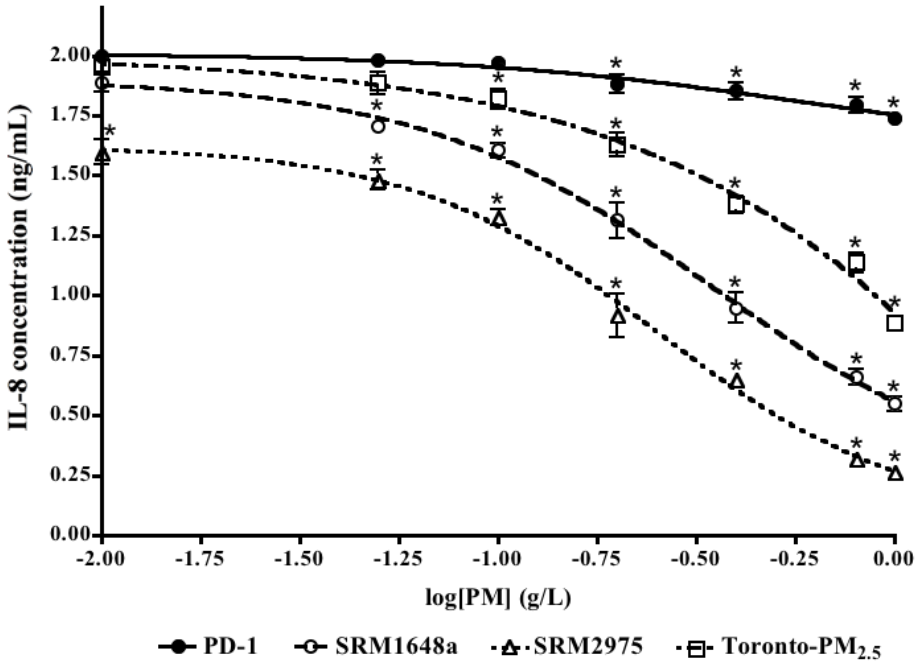

Figure 3.5: Determination of IL-8 adsorption by different particle types in an acellular PM exposure experiment. PM suspensions were prepared in cell culture medium with 10% FBS and incubated with 2 ng/ml of standard IL-8 for 24 h. The remaining IL-8 in the supernatants was analyzed by ELISA. The data are reported as mean ± SEM (n = 6) of duplicate experiments. Statistically significant differences from control (2 ng/ml of IL-8): $p < 0.05$*.

Based on the assumption of a linear isotherm model, partition coefficients (K) [pg IL-8/µg]/[pg IL-8/µl] were derived for each of the PM types: PD-1 = 0.2 µl/µg, SRM1648a = 3 µl/µg, SRM2975 = 6 µl/µg, and Toronto-$PM_{2.5}$ = 1 µl/µg. Correction factors derived from these values were applied to the IL-8 concentrations reported from the cellular PM exposure experiments (**Figure 3.4**). PD-1 did not adsorb significant amounts of IL-8 and hence no correction was necessary. For the other PM samples IL-8 adsorption could interfere significantly with the IL-8 measurements (SRM1648a: $p = 0.012$, SRM2975: $p = 0.004$, Toronto-$PM_{2.5}$: $p = 0.024$; **Figure 3.6**).

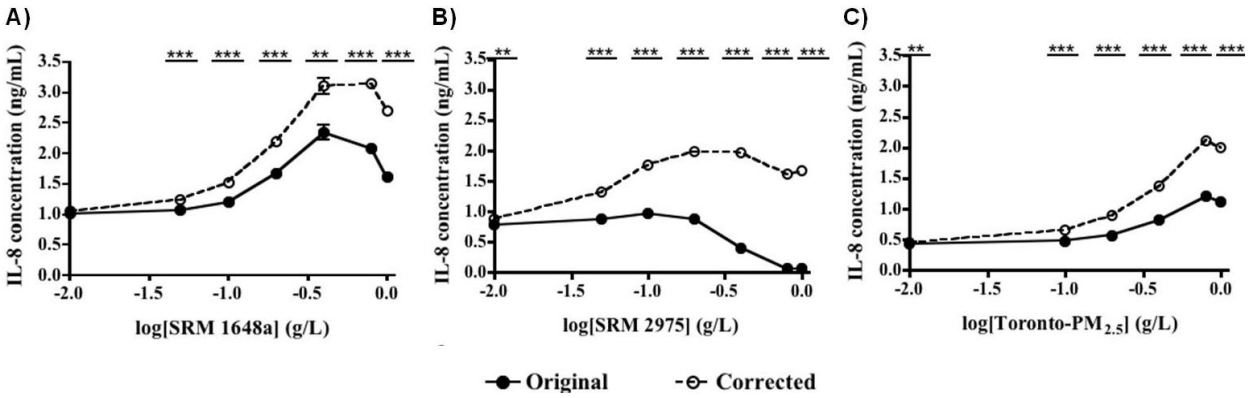

Figure 3.6: Correction of IL-8 concentrations measured in cellular PM exposure using respective correction factors. A) SRM1648a, B) SRM2975, C) Toronto-$PM_{2.5}$ (F-1). Correction factors equation: y = Kx, where y is the amount of IL-8 removed by unit mass of particles, x is the amount of the remaining IL-8, and K is the partition coefficient. K values: SRM1648a = 3 µl/µg, SRM2975 = 6 µl/µg, and Toronto- $PM_{2.5}$ = 1 µl/µg. Two-way ANOVA found significant differences between the original and corrected data (SRM1648a: $p = 0.012$, SRM2975: $p = 0.004$, Toronto-$PM_{2.5}$: $p = 0.024$). Results of t-tests at individual PM concentrations are shown: $p < 0.05$*, $p < 0.01$**, $p < 0.0001$***.

Applying this correction eliminated the decrease in IL-8 concentration observed for SRM2975 despite the higher cell viability (**Figure 3.6B**). The correlations between the corrected IL-8 concentrations and PM concentration for the total fractions of SRM1648a and Toronto-$PM_{2.5}$ (F-

1) were stronger compared to those for the original IL-8 data (ρ = 0.929-0.964, p <0.001-0.0001 vs. ρ = 0.767-0.929, p <0.02-0.001 for the corrected and uncorrected data, respectively; **Table 3.2**). However, even with the corrected data, the correlation between IL-8 and PM concentration for SRM2975 was still weak; although it was now positive (ρ = 0.619, p = 0.102 vs. ρ = -0.683, p = 0.042 for the corrected vs. uncorrected data, respectively).

4. Discussion

This study represents the first component of a long-term research program that seeks to identify the physicochemical properties of PM that are responsible for adverse health effects. Initially, three source-related SRMs with very different compositions (PD-1, SRM1648a, and SRM2975) were examined in order to evaluate differences in their toxicities and cytokine release. While PD-1 was mostly comprised of metals, such as Fe, Zn, and Cu, SRM1648a was enriched in crustal and secondary inorganic ions, such as SO_4^{2-} and NO_3^-, and SRM2975 had a high fraction of PAHs and other organic carbon compounds. We also investigated the effects of ambient $PM_{2.5}$ collected in Toronto on cytotoxicity and cytokine release. PD-1 exhibited the greatest cytotoxic effect (LD_{50}-values of 100-400 µg/ml vs. >1000 µg/ml for the SRM1648a, SRM2975, and ambient Toronto-$PM_{2.5}$). Similarly, the PM-induced release of IL-8 was greatest for PD-1 (~6-9 ng/ml vs. ~1.5-3 ng/ml for the SRM1648a, SRM2975, and ambient $PM_{2.5}$). Interestingly, we demonstrated a high degree of adsorption of the cytokine IL-8 to the various SRMs and ambient $PM_{2.5}$ and subsequently derived a correction factor to aid in interpretation of these data. These characteristics likely impart differential effects toward the toxic and immune effects of PM.

Investigation of SRMs offered several advantages over studying ambient samples alone. Firstly, the compositions of the SRMs had been well documented. Secondly, the homogeneity and mass abundance of SRMs compared to collected ambient samples increased the consistency in the measurement of the various biological endpoints and facilitated measurement of replicate samples, respectively. Furthermore, several studies have established that SRMs can be used as surrogates of urban/diesel PM (Boland et al., 2001; Hetland et al., 2004). Therefore, source-specific SRMs can be used along with direct samples of urban/diesel/industrial PM to determine the biological effects of PM. Use of SRMs also allowed comparison with the findings of other

toxicology studies. For example, Hetland et al., (2004) and Seagrave et al., (2004) examined the proinflammatory response of A549 cells to SRM1648 and SRM2975, respectively, and reported dose-response profiles similar to those reported herein. However, little or no cytotoxicity has been previously reported for SRM1648 and SRM2975 at the PM concentration range used in this study (10-1000 μg/ml). The reasons for this difference with other studies could be due to differences in cell lines, exposure conditions (i.e., PM concentration and duration) of the PM suspension, and analytical methods. For example, Seagrave et al., (2004) used lactate dehydrogenase (LDH) activity to investigate the toxicity, as compared to the MTT assay used in the present study. Hetland et al., (2004) used the same cell line (A549) and prepared SRM1648 suspension in serum-free medium, but added FBS 6 h after the exposure, which likely attenuated the toxic effects.

The influence of FBS on experimental results requires careful consideration. In the present cell viability investigation, serum-free cell culture medium was used as the cytotoxicity of PM was reduced in the presence of serum (appended as supplemental figure, **Figure A.2**). Some constituents of FBS, such as albumin, may act as metal chelators and would be expected to reduce the effects of PM if metals are present in the PM (Sánchez-Pérez et al., 2009). By contrast, the absence of serum in the cell culture medium resulted in a decrease in IL-8 release after exposure to PM (**Figure A.3**). Becker et al., (2003) showed that cytokine expression is dependent on the presence of lipopolysaccharide-binding proteins in serum. Thus, the presence or absence of serum in these experiments is dependent upon the end-points to be determined. In this study, the cytotoxicity and IL-8 data were not necessarily comparable as the cell culture medium was prepared with and without serum, respectively, for these two endpoints.

In terms of cytotoxicity, all PM samples elicited dose-dependent effects on cell viability. The largest reduction in cell viability was observed when the cells were exposed to PM collected from an industrial site. The high transition metal content of PD-1 (e.g., Fe, Cu, Zn) likely contributed to the observed toxic effect, as associations have been made between cytotoxic response and metal content (Fe, Zn, Cu, Pb, etc.) (Gualtieri et al., 2009; Hetland et al., 2004; Quinlan et al., 2002). The cytotoxic effects of specific metals (i.e., Zn, Cu, Ni, V, Fe) have been

studied *in vitro* and the respective toxic potencies have been differentiated (Riley et al., 2003). The order of toxicity based on LD_{50} was V > Zn > Cu > Ni > Fe. The DPM (SRM2975) exhibited less of an effect on cell viability, indicating that these particles, which are primarily comprised of elemental and organic carbon, were less toxic than the predominantly metal PD-1 particles. The cytotoxic responses observed for the standard and ambient urban PM samples SRM1648a and Toronto-$PM_{2.5,}$ were comparable with those reported for PM from other cities– Bilthoven, Netherlands (Hetland et al., 2004), Paris, France (Ramgolam et al., 2009), Milan, Italy (Gualtieri et al., 2009) for the given PM concentration range of 10-1000 µg/ml (equivalent to 3.12-312.5 µg/cm^2). Both the standard and ambient urban PM contained significant amounts of inorganic ions (i.e., SO_4^{2-}, NO_3^-). Unlike the metals, whether or not these inorganic ions play a direct role in eliciting the toxic effects remains to be determined. The limited epidemiological and experimental data available does not support any causal relationship between health effects and these inorganic ions (Reiss et al., 2007; Schlesinger, 2007). In this study, SRMs of greatly different composition were used, but the amount of matching PM composition data covering all the samples was limited. For example, no data were available for organic and inorganic contents of SRM1648a and SRM2795, respectively. Therefore, no conclusive correlations between specific chemical components and biological effects could be derived. Nonetheless, it can be suggested that cytotoxic and proinflammatory responses were more responsive to transition metals (e.g. Fe, Cu) compared to secondary inorganic ions (e.g., SO_4^{2-}, NO_3^-) and organic compounds, especially PAHs.

For the proinflammatory response, the order of cytokine release was similar but not identical to the cytotoxic response (PD-1 > SRM1648a > Toronto-$PM_{2.5}$ > SRM2975). At high PM concentrations, IL-8 release decreased, in contrast to the trends at low PM concentrations. Several other investigators have also reported decreased IL-8 release with increasing PM dose (Seagrave et al., 2004; Veranth et al., 2006). The attenuation of IL-8 release at high PM concentrations was found to be due in part to reduced cell viability and adsorption of IL-8 to the PM. Specifically; the present study showed that IL-8 was significantly adsorbed by PM, which led to underestimation of the actual IL-8 release. Greater adsorption of IL-8 was observed for particles with higher surface area and carbon content, mostly insoluble elemental carbon. This

finding was consistent with the previously reported preferential binding of IL-8 to carbonaceous particles (diesel and vehicle exhaust particles, wood smoke particles) compared to mineral-enriched particles (Kocbach et al., 2008; Seagrave et al., 2004). Adsorption by particles could potentially affect not only IL-8, but a wide range of proinflammatory cytokines, including IL-1β, IL-6, TNF-α, MCP-1, and IFN-γ, etc. (Kocbach et al., 2008; Seagrave et al., 2008), complicating or invalidating cytokine upregulation results. In this investigation, we developed a methodology to correct for this adsorption, based on partition coefficients derived from controlled IL-8 adsorption experiments. These corrections are quite significant and are considered essential for all investigations of cytokine release in the presence of PM.

Differential effects were observed when the cells were exposed to the water-soluble and insoluble fractions of the SRMs. It should be noted that the data for the water-soluble and insoluble fractions are plotted in terms of their respective total PM concentrations and thus do not represent the actual mass of PM present in these suspensions. In this study, the water-insoluble fractions were found to be more toxic than the soluble fractions for all three SRMs. The insoluble fractions included much of the metal content of the particles, which could explain the similarity in toxicity to the whole particles (**Table 3.1**). Other studies have also demonstrated that the insoluble fraction of particles has a much higher effect on IL-8 induction compared to the water-soluble fraction (Fujii et al., 2001; Huang et al., 2004). However, the water-soluble fraction was not completely benign. Indeed, the water-soluble fraction of PD-1, which contained high concentrations of Zn Pb, Cd, and Cu, exhibited greater cytotoxicity and proinflammatory responses than the insoluble fractions of the other two SRMs. Previous studies have suggested that the pulmonary response and cell injury effect of water-soluble fractions are related to the concentration of the soluble metal ions (Ghio et al., 1999; Knaapen et al., 2002). No significant toxicity or cytokine release was observed for the water-soluble fraction of SRM1648a suggesting that the common soluble PM constituents, i.e., SO_4^{2-}, NO_3^-, NH_4^+ and water- soluble organic carbon, may not influence these biological endpoints. An important limitation of this study is that the contribution of specific PM constituents such as metals and organic compounds cannot be studied because of the complex composition of the samples. In future, metal chelators (such as deferoxamine) and oxidation catalysts will be used to remove the metals and organic compounds

from the PM matrix to investigate the significance of these constituents.

The DTT assay used in this study represents an extracellular measurement of the redox activity of organic components in PM samples, particularly quinones; metal-related activity was not measured by this assay, as transition metals follow a different reaction pathway to generate hydroxyl radicals (Cho et al., 2005). Therefore, it should be emphasized that the DTT data was indicative of only one mechanism of ROS production potential of the particles and was not a measurement of total extracellular and intracellular ROS production. This might explain why the redox activity of organic-enriched SRM2975 was greatest, whereas the redox-activity of metal-enriched PD-1 could not be determined in this study. This might also clarify the observed poor concordance between the biological effects and redox activity, although it was hypothesized that the effects would be dependent upon the redox activity of PM. For example, the order of cytotoxic and proinflammatory responses for water-soluble and insoluble fractions of SRM1648a (water-insoluble > soluble) was not consistent with the order of the redox activity (water-soluble > insoluble). **Table 3.1** indicates that most of the metal elements of SRM 1648a are present in the water-insoluble fraction. Therefore, the redox potential of these metal contents of the insoluble fraction was not measured by the DTT assay.

As anticipated, the redox activity was greater for organic-enriched SRM2975 among other PM and the order of redox activity for SRM2975 was total > water-insoluble > water-soluble. The water-insoluble fraction contributed to about 85% of the total DTT based redox activity. These results were consistent with another study that showed about 90% of redox activity of DPM was due to insoluble particles (Shinyashiki et al., 2009). The SRM2975 trends could be explained in several ways: firstly, components within black carbon could possess redox active functional groups, such as humic-like substances, within the DEP (Shinyashiki et al., 2009). Secondly, since quinones are similar to PAHs, they could become strongly adsorbed to black carbon within the particles, such that they would not be easily extracted by water, but were still accessible when the DTT assay was applied to either the total extract or the insoluble fraction.

5. Conclusions

This study demonstrated that the cytotoxic and proinflammatory responses of human alveolar epithelial cells varied substantially after *in vitro* exposure to PM from different sources. PM collected from a smelter facility was found to be highly toxic, supporting the importance of toxicological studies of PM collected from specific industrial operations. Metal-enriched PM (PD-1) was more toxic and induced a greater proinflammatory response compared with the inorganic ions-enriched SRM1648a and ambient $PM_{2.5}$, and organic-enriched SRM2975. The cytotoxicity and proinflammatory responses of Toronto-$PM_{2.5}$ and urban PM standard were similar. PM mass concentration was found to have an inhibitory effect on cell viability and augmented IL-8 release. In this study, insoluble constituents of particles played a dominant role in inducing both cytotoxic and proinflammatory effects. Lastly, this study identified that IL-8 adsorption by particles resulted in underestimation of IL-8 levels and would lead to misinterpretation of outcomes from *in vitro* studies. From these findings we suggest that cytokine concentrations measured in cellular PM exposure experiments should be corrected using appropriate partition coefficients derived from cytokine adsorption experiments using individual PM samples.

Chapter 4

The combined effects of physicochemical properties of size-fractionated ambient particulate matter on *in vitro* toxicity in A549 human lung epithelial cells

Umme S. Akhtar, Robert D. McWhinney, Neeraj Rastogi, Bruce Urch, Chung-Wai Chow, Greg J. Evans, Jeremy A. Scott

Toxicology Reports, 2014, 1, 145-156, doi: 10.1016/j.toxrep.2014.05.002

Abstract

Epidemiological and toxicological studies have suggested that the health effects associated with exposure to particulate matter (PM) are related to the different physicochemical properties of PM. These effects may occur through the initiation of differential cellular responses including: the induction of antioxidant defence, proinflammatory response, and ultimately cell death. The main objective of this study was to investigate the effects of size-fractionated ambient PM on epithelial cells in relation to their physicochemical properties. Concentrated ambient PM was collected on filters for three size fractions: coarse (aerodynamic diameter (AD), 2.5-10 μm), fine (0.15-2.5 μm), and quasi-ultrafine (<0.2 μm), near a busy street in Toronto, Ontario, Canada. Filters were extracted and analyzed for chemical composition and redox activity. Chemical analyses showed that the coarse, fine, and quasi-ultrafine particles were comprised primarily of metals, water-soluble species, and organic compounds, respectively. The highest redox activity was observed for fine PM. After exposure of alveolar epithelial cells A549 cells to PM (10-100 μg/ml) for 4 h, activation of antioxidant, proinflammatory and cytotoxic responses were assessed by determining the expression of heme oxygenase (HMOX-1, mRNA), interleukin-8 (IL-8, mRNA), and metabolic activity of the cells, respectively. All three size fractions induced mass-dependent antioxidant, proinflammatory, and cytotoxic responses to different degrees. Quasi-ultrafine PM caused significant induction of HMOX-1 at the lowest exposure dose. Correlation

analyses with chemical components suggested that the biological responses correlated mainly with transition metals and organic compounds for coarse and fine PM and with organic compounds for quasi-ultrafine PM. Overall, the observed biological responses appeared to be related to the combined effects of size and chemical composition and thus both of these physicochemical properties should be considered when explaining PM toxicity.

1. Introduction

Among the common ambient air pollutants, epidemiological studies have identified that exposures to particulate matter (PM) correlate most consistently with pulmonary and cardiovascular morbidity and mortality (Dockery et al., 1993; Gauderman et al., 2004; Katsouyanni et al., 2001; Pope et al., 1995). While ambient PM range from 0.001 to 100 μm in AD (Brook et al., 2003), particles larger than 10 μm AD are generally trapped in the nasal passages (International Commission on Radiological Protection (ICRP), 1994). Based on size, PM smaller than 10 μm AD is divided into three fractions: PM_{10} (AD <10 μm), $PM_{2.5}$ (AD <2.5 μm) and ultrafine (UF) (AD <0.1 μm) (USEPA, 2004). PM_{10} is further divided into coarse (AD 2.5 to 10 μm) and fine (AD <2.5 μm) PM (USEPA, 2004). The fate of inhaled particles depends on their size, which determines their site of deposition in the lung, which in turn influences their rate of clearance. While larger particles are primarily deposited in the extrathoracic and thoracic regions, smaller particles (<1 μm) deposit deep in the lung, particularly in the alveolar region (ICRP, 1994). Of further concern, ultrafine particles also have the potential to cross the lung alveolar-capillary border and gain access to the circulation (Brook, 2008; Nemmar et al., 2002), which can have serious implications in terms of systemic toxicity and cardiovascular disease. Several studies have reported translocation of ultrafine particles to secondary target organs, including the liver, spleen, heart, and brain in rats (Oberdörster et al., 2004; Semmler et al., 2004). However, to date, translocation of particles has only been observed in spleens and livers of coalmine workers after long-term exposure to very high doses (LeFevre et al., 1982). While exposure standards for PM_{10} and $PM_{2.5}$ have already been established in North America, an ambient standard for ultrafine particles has yet to be established.

Recent studies have suggested that the presence of excessive reactive oxygen species (ROS), i.e., hydrogen peroxide (H_2O_2), superoxide ($O_2^{\cdot-}$), and hydroxyl radical ($OH^{\cdot}$) in PM, may lead to oxidative stress in the pulmonary system (Li et al., 2003a). ROS can be generated from soluble transition metals (Cu, Cr, Fe, etc.) or organic compounds (OCs), i.e., polycyclic aromatic hydrocarbons (PAHs), that are present on the surface of particles (Squadrito et al., 2001; Verma et al., 2010). Li et al., (2003a & 2002) proposed that oxidative stress may initiate a specific sequence of cellular responses. At lower levels of oxidative stress, antioxidant enzymes are activated in order to protect the lung. If this antioxidant response of the cell fails to provide protection against the generation of ROS, an inflammatory response may be induced to attract inflammatory cells to the site of "injury". Finally, at toxic levels, cell death occurs through both apoptosis and necrosis (Li et al., 2003a & 2002; Li et al., 1997; Xiao et al., 2003). Thus, the progressive increase in the severity of the response to PM suggests a hierarchical dose-effect relationship, whereby the activation of antioxidant mechanisms precedes inflammatory responses and in turn ultimately cell death. Long-term exposure to PM resulting in chronic pulmonary inflammation may also impair lung development, and increase the risk of developing pulmonary diseases, including asthma and chronic obstructive pulmonary diseases (Gauderman et al., 2004; Gehring et al., 2010; Schikowski et al., 2005).

An intensive, collaborative, multidisciplinary field campaign 'Health Effects of Aerosols in Toronto (HEAT)' was conducted in Toronto in 2010. The main objectives of this campaign were to: 1) characterize the physicochemical properties of Toronto's size-fractionated concentrated ambient PM (Rastogi et al., 2012); 2) measure different cellular responses (i.e., antioxidant defence, proinflammatory changes, and cytotoxicity) of airway epithelial cells to PM; 3) identify relationships between the physicochemical characteristics of the PM and the cellular responses; and 4) assess the differential effects of different PM size fractions on both pulmonary and cardiovascular functions (Amatullah et al., 2012). We hypothesized that particle exposure would induce dose-dependent differential toxicological effects (i.e., antioxidant defence, inflammatory changes, and ultimately cell death) on the cells and that these cellular responses would vary depending on the diverse physicochemical properties of the different size-fractionated PM.

2. Materials and methods

2.1 Collection of ambient particles

Concentrated ambient PM was collected using the high volume ambient particulate concentrator system located at the Gage Occupational and Environmental Health Unit, University of Toronto, which is located on a busy downtown street. The concentrator facility consists of three Concentrated Ambient Particle Systems (CAPS) that fractionate and concentrate ambient PM in the coarse (2.5 < AD < 10 μm), fine (1.5 < AD < 2.5 μm), or quasi-ultrafine (AD < 0.2 μm) size ranges. On average, coarse, fine, and quasi-ultrafine particles were concentrated (by mass) by factors of ~103, 36, and 28, respectively. We have previously reported a detailed description of the effectiveness of these three systems (McWhinney et al., 2012; Rastogi et al., 2012).

Size-fractionated PM was collected on filters on weekdays during the winter of 2010 (February 19 to March 19). Samples were simultaneously collected over 4 to 8 h on 47 mm quartz (Whatman, USA), 47 mm Teflon (Pall Gelman, USA), and 37 mm Teflon filters (Pall Gelman, USA) for chemical characterization, determination of redox activity, and *in vitro* analyses, respectively. The number of filters used for this study was 7 for coarse, 6 for fine, and 8 for quasi-ultrafine PM. All filters were weighed gravimetrically before and after sampling to measure the total collected PM mass. To prevent photo-degradation and evaporation loss, the filter samples were then sealed and kept in the dark at -20°C until further analyses. Information regarding the PM collection times and collected mass is described in **Supplemental Table B.1** (**Appendix B**). The filters were extracted using cell culture medium, as described previously (Akhtar et al., 2010). The extraction efficiency varied from 65% to 90% for the three different particle sizes. Extraction efficiency was the highest for fine particles with the highest water-soluble fraction.

During the study period, the number concentrations of the size-distributed ultrafine particles (diameter: 10-800 nm) were also measured online using a Scanning Mobility Particle Sizer (SMPS) (Model 3080, TSI) (**Supplemental Figure B.1A**). The particle surface area was calculated from the number concentration data, assuming the particles were spherical (**Supplemental Figure B.1B**). Particle-bound polycyclic aromatic hydrocarbons (p-PAHs)

concentrations were determined using a Photoelectric Aerosol Sensor (PAS, Model PAS2000CE, EcoChem Analytics) (**Supplemental Figure B.2**).

2.2 Chemicals and assay kits

Dulbecco's modified Eagle's medium (DMEM), penicillin-streptomycin, DL-dithiothreitol (DTT, 98%) and 1, 2-naphthoquinone were obtained from Sigma Aldrich (Oakville, ON, Canada). L-Glutamine, 0.05% trypsin, and superscript II reverse transcriptase kits were obtained from Invitrogen (Carlsbad, CA, USA). Fetal bovine serum (FBS) and phosphate buffer saline (PBS) were obtained from Wisent Inc. (St-Bruno, QC, Canada). Tris-HCl, tetrasodium EDTA and trichloroacetic acid were obtained from Fisher Scientific (Whitby, ON, Canada), and 5, 5'-dithio-bis (2-nitrobenzoic acid) was obtained from Alfa Aesar (Ward Hill, MA, USA). The MTT assay was performed using a kit from the American Type Culture Collection (ATCC) (Manassas, VA, USA). RNA extraction kits and TaqMan master mix were obtained from Qiagen® (Germantown**,** MD, USA) and Applied Biosystems® (Life Technologies Inc., Burlington, ON), respectively. Plasmids and primers for HMOX-1 and IL-8 were obtained from OriGene (Rockville, MD, USA) and Integrated DNA Technologies Inc. (Coralville, IA, USA), respectively.

2.3 Cell culture and particle exposure

A549 cells (American Type Culture Collection, Rockville, MD, USA), a cell line of human adenocarcinomatous cells derived from lung cancer that exhibits characteristics of alveolar epithelial cells, were used in this study (Giard et al., 1973). Cell culture and *in vitro* PM exposures were performed, as described previously (Akhtar et al., 2010) with several modifications. Cells were seeded at 2.5×10^5 cells/ml in 96-well plates for the MTT assay and at 1×10^6 cells/ml in 6-well plates for real-time polymerase chain reaction (RT-PCR). PM suspensions were prepared in cell culture medium containing 10% FBS and were added to the cells at final concentrations of 10, 50, and 100 µg/ml (mass/volume) for 4 h along with appropriate media-treated controls. The exposure duration was selected based on the expression of IL-8 (protein) in our previous study (Akhtar et al., 2010). Cells were exposed to PM isolated from each filter in triplicate at each PM concentration.

2.4 PM chemical characterization

For chemical speciation, the quartz filters were cut into three pieces: two quarters and one half portions. One quarter portion was used for the analyses of acid-soluble elements. From the half portion, 1.7 cm diameter punches were taken for elemental carbon (EC) and organic carbon (OC) analyses using a Sunset EC-OC analyzer, according to the National Institute of Occupational Health and Safety (NIOSH) 5040 protocol (Birch and Cary, 1996). The mass of the OC fractions was converted to the organic mass (OM) by multiplying by a factor of 1.4 to account for the mass of oxygen in addition to the OC mass. The fractions of OM measured at various temperatures (310, 475, 615, and 870˚C) were named as OM-1, OM-2, OM-3, and OM-4, respectively, representing their volatility order. The remaining filter portion was extracted with deionized water (Millipore DQ-3, resistivity >18.3 MΩ) for analysis of water-soluble cations, including amines, anions, metals, and organic carbon (WSOC). Acid and water-soluble extracts were analyzed for 26 elements (Ag, Al, As, B, Ba, Be, Ca, Cd, Co, Cr, Cu, Fe, K, Mg, Mn, Mo, Na, Ni, Pb, Sb, Se, Si, Ti, Tl, V, and Zn) using Inductively Coupled Plasma Optical Emission Spectroscopy (ICP-OES, Perkin Elmer Optima 3700 DV) in the axial mode, at the Analytical Laboratory for Environmental Science Research and Training (ANALEST) facility of University of Toronto. Anions and cations in the size-fractionated PM sample water extracts were measured by Ion Chromatography (Dionex ICS-2000). WSOC was measured using a Total Carbon Analyzer system (Shimadzu TOC-$V_{CPH/CPN}$) equipped with an 8-port sampler. The DTT assay was used to measure the redox activity of the PM samples, as previously described (Akhtar et al., 2010). Redox activity was expressed as the rate of DTT consumption per minute normalized to the quantity of PM used.

2.5 Analyses of biological endpoints

In this study, heme oxygenase (HMOX-1) was selected as the biomarker of induction of antioxidant enzymes. HMOX-1 is known to be highly responsive to oxidative stress and plays a protective role by producing the antioxidant bilirubin through the degradation of heme. To evaluate the proinflammatory response to PM, IL-8 expression was measured at both the mRNA and protein levels. The results for IL-8 (protein) are presented in Supplemental Materials

(**Appendix B, Section S.1**). IL-8 acts as a chemoattractant factor and is a ubiquitous early response marker of inflammation in many cell types. Following 4 h-exposure of cells to PM, cell lysates and supernatants were collected from each well. Total RNA was extracted from cell lysates using a RNeasy mini kit according to the manufacturer's instructions (Cat. No. 74104, Qiagen) and was quantified using a Nanodrop-1000 system (Thermo Scientific). First strand cDNA was synthesized from 1 µg of mRNA for each sample using SuperScript® II Reverse Transcriptase (Invitrogen™). Expression of HMOX-1 and IL-8 mRNA was quantified using an Applied Biosystems 7900HT Fast Real-Time PCR System. The copy number of the target gene was normalized to 18S RNA, as a housekeeping gene. The primers and probe sets for HMOX-1, IL-8, and 18S are reported in **Table 1**. MTT assays were performed as described previously (Akhtar et al., 2010). All assays were conducted in triplicate.

Table 4.1: Primers and probes used for real-time RT-PCR

Gene Target	Forward Primer	Reverse Primer	Probe
HMOX-1	5'-TCAGGCAGAGGGT GATAGAAG-3'	5'-TTGGTGTCATGGGT CAGC-3'	5'-TGGATGTTGAGCA GGAACGCAGT-3'
IL-8	5'-ATACTCCAAACCT TTCCACCC-3'	5'-TCTGCACCCAGTTT TCCTTG-3'	5'-CCACACTGCGCCA ACACAGAAA-3'
18S	5'-GGACATCTAAGGG CATCACAG-3'	5'-GAGACTCTGGCAT GCTAACTAG-3'	5'-TGCTCAATCTCGG GTGGCTGAA-3'

2.6 Statistical analyses

Statistical analyses were performed using GraphPad Prism 4.0c (La Jolla, CA, USA). All biological response results are reported as the mean ± standard error of the mean (SEM) and relative to controls. Non-parametric statistical analyses were used because the data were not normally distributed. Kruskal-Wallis one-way analysis of variance with post-hoc Dunn's multiple comparison test were used to compare the redox-activities of different sized PM and to

determine the difference in biological responses between controls and different PM concentrations. Two-way ANOVA was used to investigate the effects of size and concentration on the biological endpoints. Biological response data for all three size fractions were also plotted on the same graph with elemental concentration to test for the effect of size on the responses. Spearman correlations (ρ) were used to assess the strength of relationships between composition and biological responses. Correlation tests were also used to examine the relationship between quasi-ultrafine particle number concentration and surface area (4 h averaged data) and biological responses. Statistical differences were considered significant at $p < 0.05$.

3. Results

3.1 PM characterization

Each of the PM size fractions exhibited distinct chemical compositions (**Figure 4.1**). The metal concentrations (including water-soluble metals) were the highest in the coarse fraction (22%), whereas quasi-ultrafine PM was dominated by OM (53%). On average, water-soluble components (ions, amines, and OC) comprised 59% of the fine PM, compared with 41% and 28% in the ultrafine and coarse PM, respectively. Among the water-soluble compounds, a significant contribution of anions (i.e., NO_3^-, SO_4^{2+}, $C_2O_4^{2-}$, PO_4^{3-}, Cl^-) was observed for both fine and coarse PM (**Supplemental Figure B.3**). While ultrafine PM was comprised of the highest proportion of amines (38%) and OC (24%), coarse PM contained the highest proportion of water-soluble metals (17%). In ultrafine PM, trimethyl amine (TMA) contributed about 41% of the total amine concentration. Detailed information regarding the chemical compositions are provided in **Supplemental Tables B.2, B.3, and B.4**.

3.2 Redox activity measurement

The ROS generation potential of the collected coarse, fine, and ultrafine PM samples was analyzed using the DTT assay. This assay demonstrated that each of the PM size fractions exhibited measureable redox activity (**Figure 4.2**). The activity was higher for fine and quasi-ultrafine particles compared with coarse PM ($p < 0.05$).

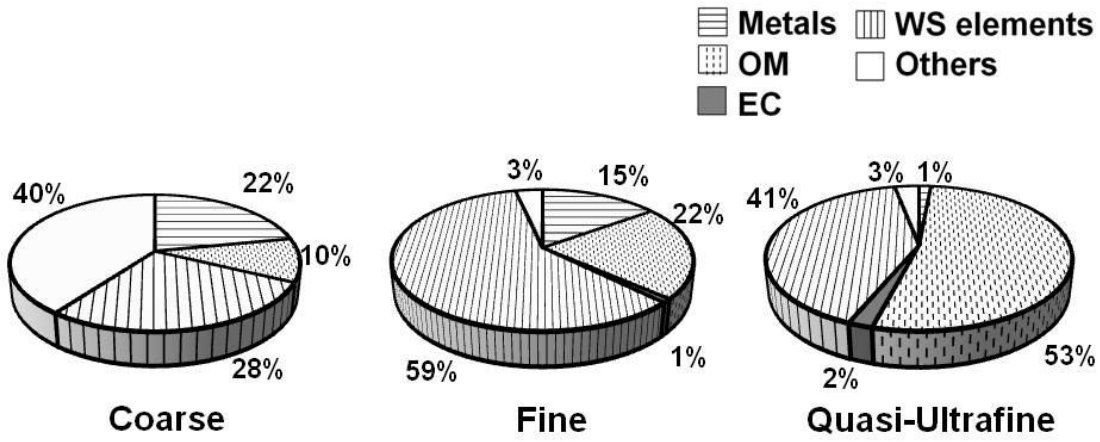

Figure 4.1: Average chemical composition of concentrated ambient coarse, fine, and quasi-ultrafine PM collected from Toronto (EC = elemental carbon, OM = organic mass, WS = water-soluble elements (anions, cations, amines, organic carbon OC)).

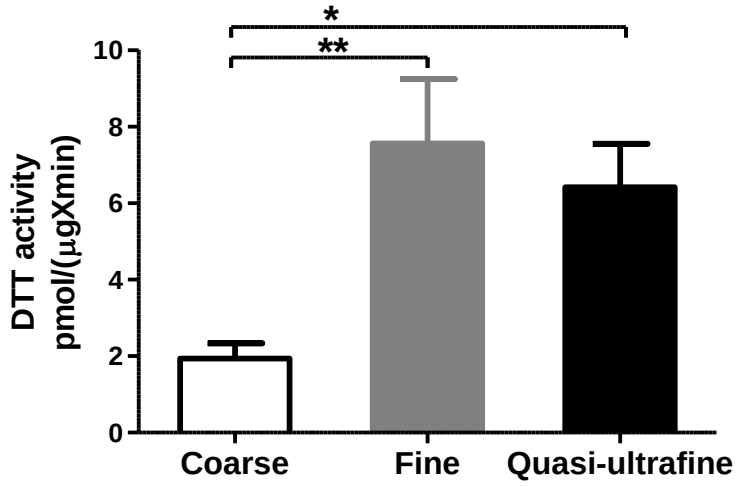

Figure 4.2: Redox activity of coarse, fine, and quasi-ultrafine PM, as measured by the DTT assay. Data are expressed as the mean ± SEM (*n* = 7, 6, and 8 for coarse, fine, and quasi-ultrafine, respectively). Kruskal-Wallis test followed by Dunn's multiple comparison test showed that redox activity for fine and quasi-ultrafine PM were significantly higher than coarse PM (* $p < 0.05$, ** $p < 0.01$).

3.3 Effect of different size-fractionated PM on biological endpoints

3.3.1 Activation of antioxidant defence

HMOX-1 mRNA expression increased in a dose-dependent manner in response to all three size fractions (**Figure 4.3A**). Significant induction of HMOX-1 expression was observed as compared to controls at 10 µg/ml for ultrafine PM and at 50 µg/ml for the other size fractions. At exposure levels of 100 µg/ml, the order of response was coarse ≥ ultrafine > fine. HMOX-1 expression was significantly lower for fine PM compared with both coarse ($p<0.05$ by two-way ANOVA) and ultrafine PM ($p <0.001$), but was similar between the coarse and ultrafine PM.

3.3.2 Activation of the proinflammatory response

Significant induction of IL-8 (mRNA) expression was observed as compared with controls at 50 µg/ml for ultrafine PM and at 100 µg/ml for the other size fractions (**Figure 4.3B**). At exposure levels of 100 µg/ml, the order of response was ultrafine = fine > coarse. IL-8 expression was significantly lower for coarse PM compared with both fine ($p <0.01$) and ultrafine PM ($p <0.001$), but was similar between the fine and ultrafine PM.

3.3.3 Cell viability

The cytotoxicity profiles for coarse, fine, and ultrafine PM were determined using the MTT assay (**Figure 4.3C**). Similar to the antioxidant and proinflammatory responses, a PM concentration-dependent decrease in cell viability was observed. For coarse and fine PM, a statistically significant decrease was observed starting at PM mass concentrations of 50 µg/ml, whereas significant cytotoxicity for ultrafine PM was observed at 100 µg/ml. At 100 µg/ml, cell viability decreased to 70%, 84%, and 87% for coarse, fine, and ultrafine particles respectively. Two-way ANOVA analyses showed that the coarse PM were more cytotoxic than fine and ultrafine PM ($p <0.001$).

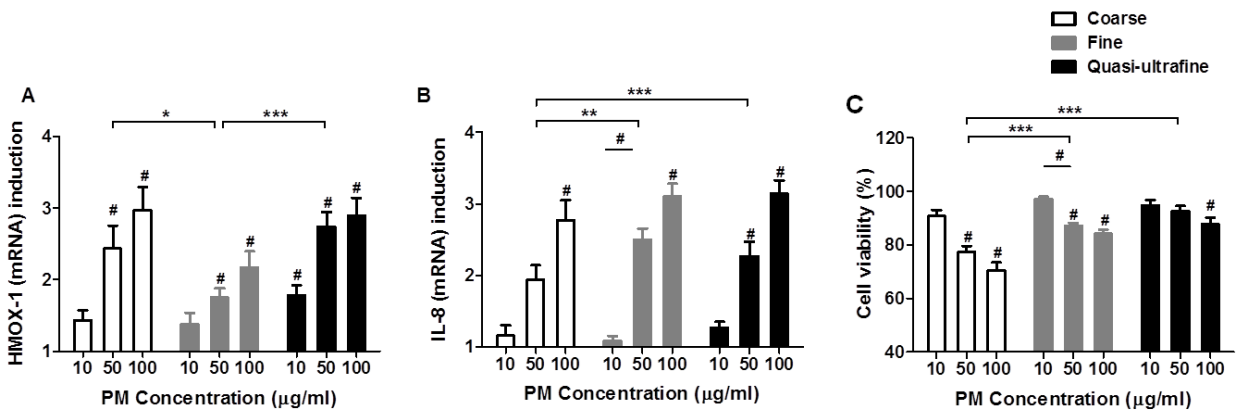

Figure 4.3: Effect of different size-fractionated ambient PM on different biological endpoints. A549 cells were exposed to coarse, fine, and ultrafine PM at mass concentrations of 10, 50, and 100 μg/ml (mass/volume) for 4 h. (A) HMOX-1 (mRNA), (B) IL-8 (mRNA), and (C) cytotoxic responses. HMOX-1 and IL-8 expressions are presented as fold change and cytotoxic responses are presented as the percentage of cell viability relative to controls. The data are presented as mean ± SEM (n=21, 18, and 24 for coarse, fine, and ultrafine, respectively, for HMOX-1 and IL-8 expression, n = 7 for coarse, 6 for fine, and 8 for ultrafine for cytotoxicity). Statistically significant differences from control and in between concentrations # ($p < 0.05$) and between sizes of PM *, **, *** $p < 0.05$, 0.01, 0.001, respectively).

3.4 Linear regression and correlation analyses

Scatter plots of selected chemical constituents with biological endpoints were used to examine whether the differences in the responses were due to the mass concentrations of different elements vs. particle size (**Figures 4.4, 4.5, and 4.6)**. If the responses were governed by mass concentration alone, all data for the three PM size fractions would be expected to be fit along the same regression line. Three distinct and independent linear regression lines were observed for most of the elements, indicating that for the same elemental mass concentration, the responses were different between the different PM sizes. The slopes of the biological response vs. total PM mass concentration and the different PM constituent masses were also determined for the different size fractions (**Supplemental Tables B.5**). Among the 17 elements, the slopes of the dose-response relationships were significantly different among the sizes for 4 (HMOX-1), 15

(IL-8 mRNA), and 12 (cell viability) elements. Greater slope values were generally observed for metals in ultrafine PM and for OM for coarse PM. Although metal and OC concentrations were lower in ultrafine and coarse PM, respectively, the high slope values indicated that small increments of these PM constituents could have greater influence on the biological responses. Slope values were higher for Cr, Ti, and OM across all size fractions and biological endpoints than for total PM mass, suggesting that these two metals and OM impose comparatively greater effects compared to other chemical elements.

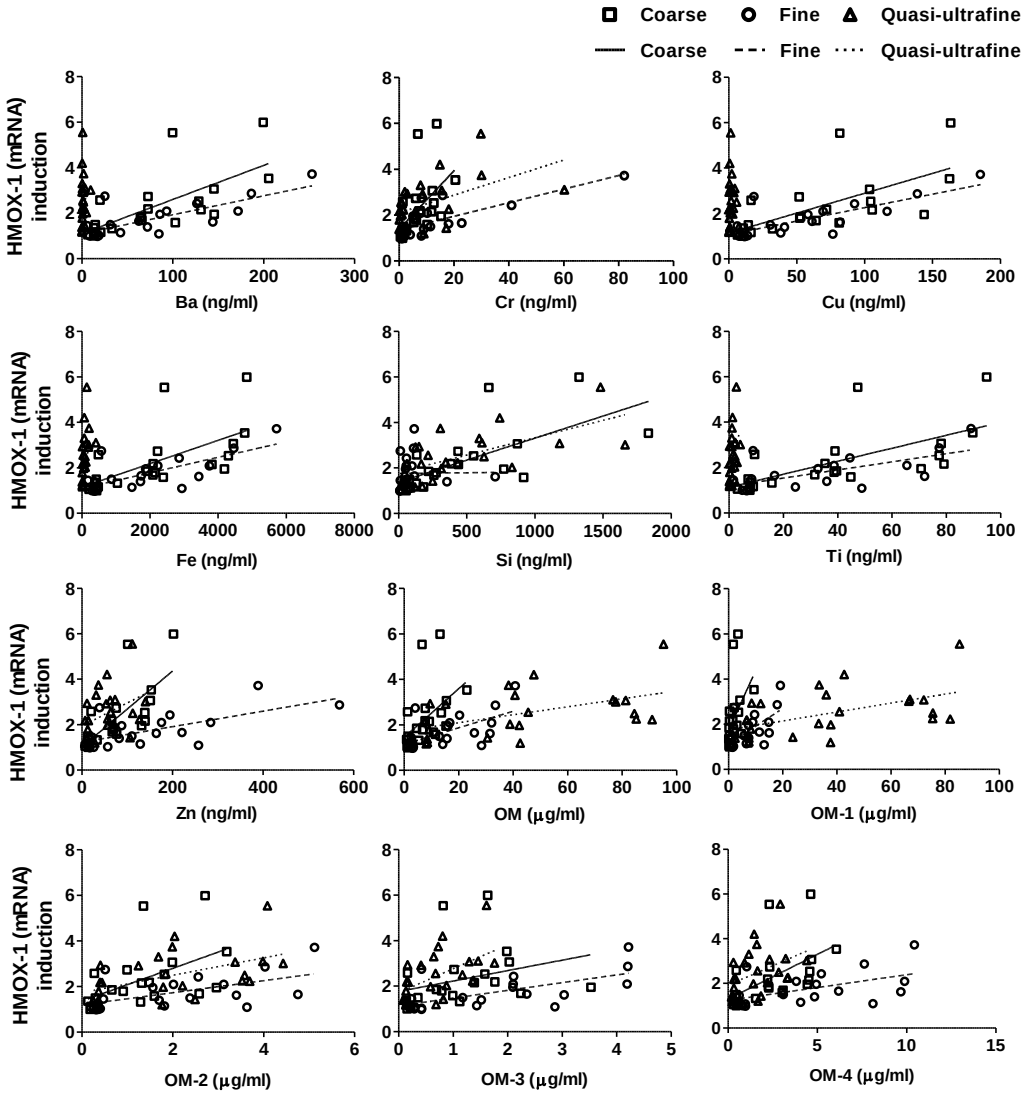

Figure 4.4: Scatter plots of selected chemical elements vs. HMOX-1 upregulation for coarse, fine, and quasi-ultrafine PM.

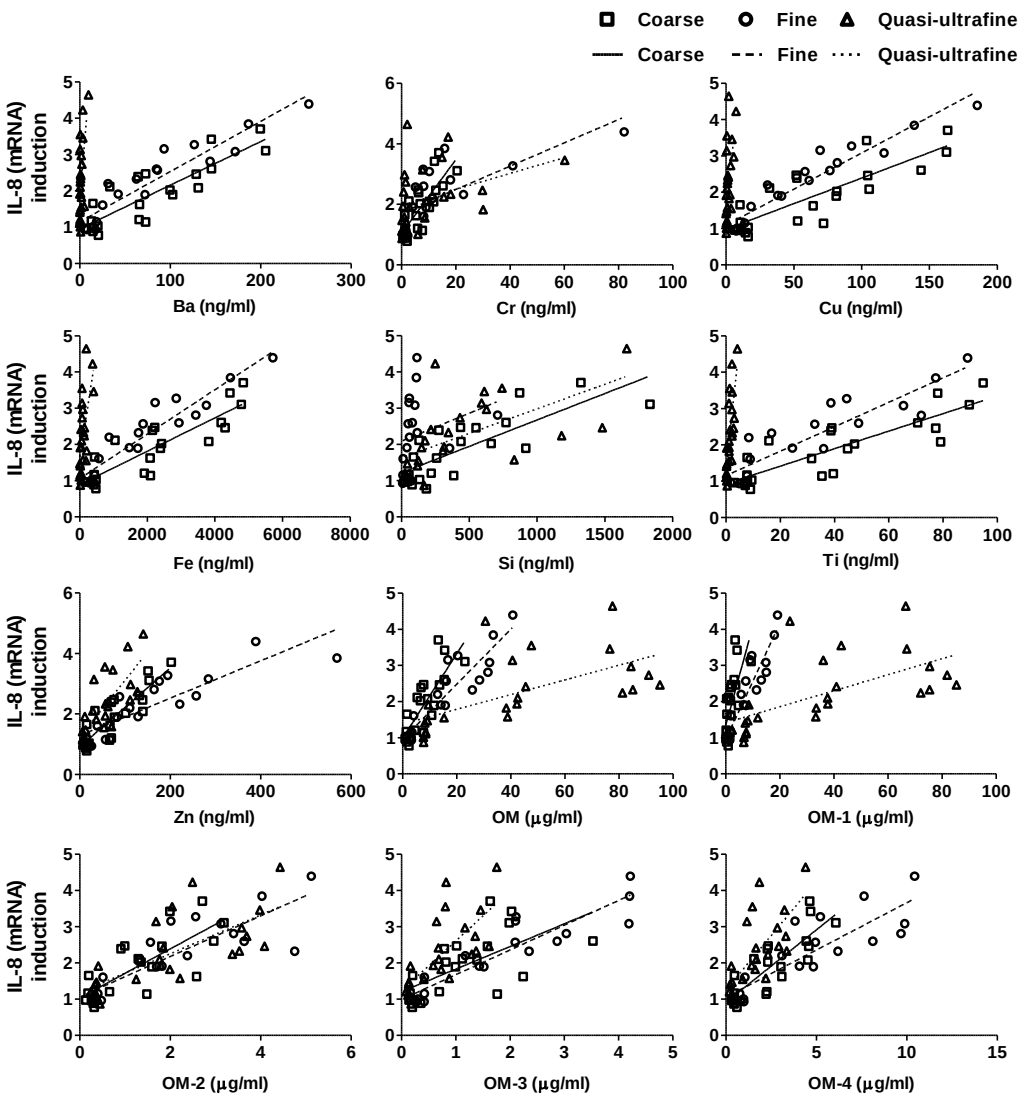

Figure 4.5: Scatter plots of selected chemical elements with IL-8 (mRNA) upregulation for coarse, fine, and quasi-ultrafine PM.

The Spearman correlation coefficients (ρ) for the biological endpoints with different chemical constituents, redox activity, and between the other biological endpoints are reported in **Supplemental Tables B.6, 7, 8, and 9**. All the correlation values mentioned hereafter were statistically significant ($p < 0.05$). In the coarse size range, all three biological endpoints (HMOX-1 and IL-8 (mRNA) positively and cell viability negatively) correlated with total Al, Ba, Ca, Cr, Cu, Fe, Mg, Mn, Na, Si, Ti, Zn, and OC fractions. For fine PM, Ba, Cr, Cu, Fe, Mg, Mn, Ti, Zn,

and OC fractions correlated positively with HMOX-1 and IL-8 (mRNA) and inversely with cell viability.

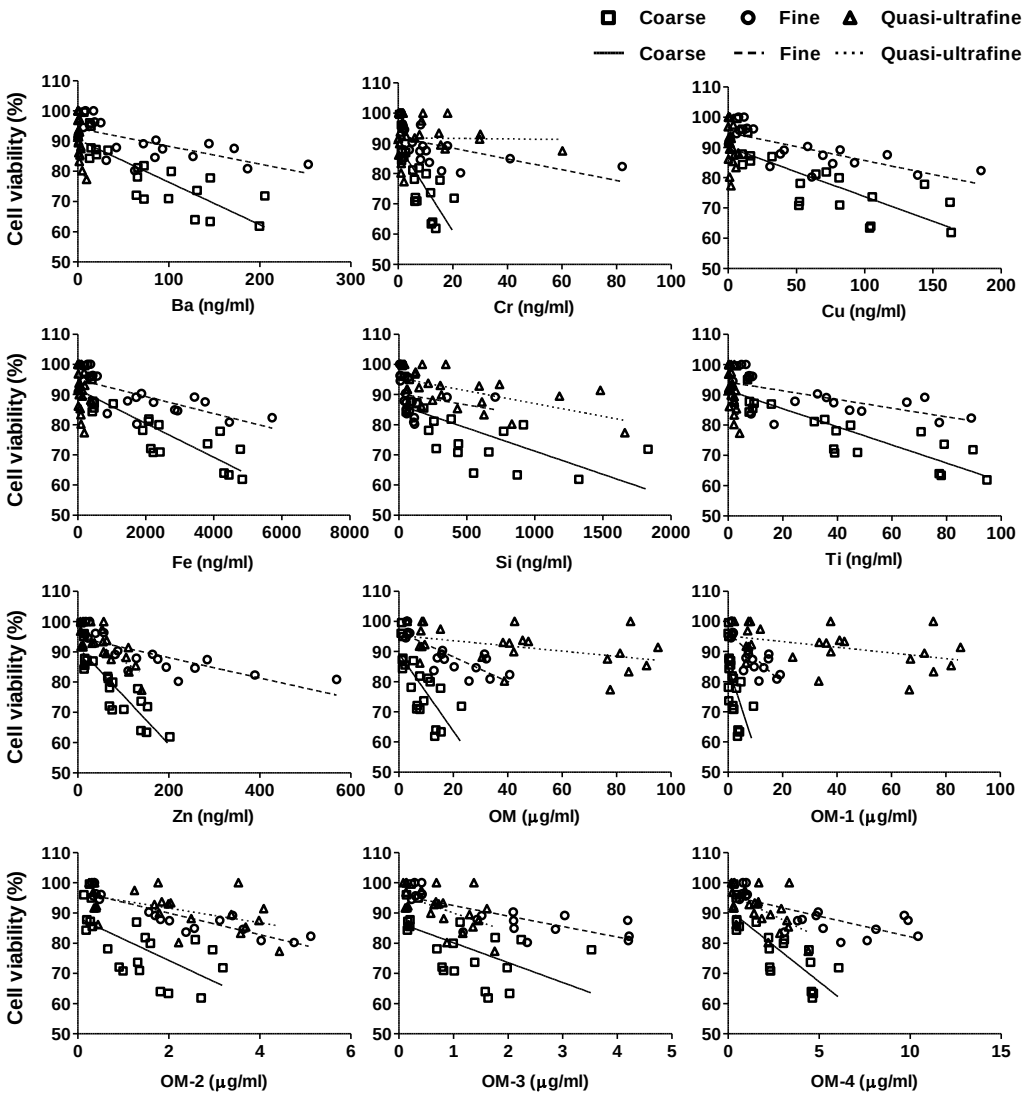

Figure 4.6: Scatter plots of selected chemical elements with cell viability for coarse, fine, and quasi-ultrafine PM.

For ultrafine PM, total Mn, Na, Si, Ti, Zn, and OC fractions correlated positively with the upregulation of HMOX-1 and IL-8 (mRNA), and inversely with cell viability. Redox activities correlated with all biological responses (inversely with cell viability) for all size fractions. For ultrafine particles, all the biological responses were also correlated with trimethyl amine (TMA) and dimethyl amine (DME) (**Supplemental Table B.7**). No significant correlations were found

between number concentration, surface area, and biological responses for ultrafine PM; except for cell viability, which correlated positively with particle number concentration (**Supplemental Table B.8**). Among the biological responses, IL-8 expression consistently correlated inversely with cell viability in all size fractions (**Supplemental Table B.9**).

4. Discussion

This *in vitro* study investigated the antioxidant, proinflammatory, and cytotoxic effects of coarse, fine, and quasi-ultrafine PM collected in Toronto, Ontario, Canada. Size-dependant cellular responses were observed after exposure to PM. All the size fractions exhibited differential biological effects with respect to oxidative stress and inflammatory responses, and cell death. Coarse PM exhibited higher cytotoxic responses than fine and ultrafine PM, whereas quasi-ultrafine PM-induced antioxidant and inflammatory responses were as high as coarse and fine PM, respectively. Based on the correlations of the chemical elements with biological endpoints, and the inter-correlations among the elements, it appeared that the observed responses for all size fractions were associated with traffic-related sources (exhaust and non-exhaust). The sampling site was located next to a busy road with ~20,000 automobiles/weekday. At this site, 25% to 51% of the $PM_{2.5}$ mass comes from local sources and the main local source is vehicular traffic (Jeong et al., 2011).

4.1 Redox activity and biological responses

Since urban ultrafine particles are associated with traffic emissions, they are generally high in organic matter and contain higher mass loadings of PAHs than coarse or fine particles (Cho et al., 2005; Fine et al., 2004). Quinone species are highly active redox-cycling catalysts (Squadrito et al., 2001) and are present in gasoline and diesel engine exhaust particles (Jakober et al., 2007). Quinones may be generated during the oxidation of PAHs associated with exhaust particles (Sasaki et al., 1997; Wang et al., 2007). The DTT assay used in this study is particularly reactive to organic species, specifically to quinones. This assay measures quinone-catalyzed production of $O_2^{\cdot-}$ by the transfer of electrons from DTT to oxygen (Kumagai et al., 2002). Semi-continuous measurement of p-PAHs during the HEAT campaign showed that ultrafine PM had higher

concentrations of p-PAHs than coarse and fine PM, in both ambient and concentrated PM samples (**Supplemental Figure B.2**). Therefore, it was expected that ultrafine particles enriched with PAHs would exhibit greater redox activity than fine and coarse particles (Cho et al., 2005; Ntziachristos et al., 2007, Rossner et al., 2010). However, in this study fine PM was found to be more redox active than ultrafine and coarse PM. HMOX-1 is a sensitive biomarker of oxidative stress and its expression would thus be expected to be related to the redox potential of the particles. The increased expression of HMOX-1 following exposure to coarse and ultrafine particles compared with fine PM also suggested that the DTT assay did not comprehensively measure the redox potential of the coarse and ultrafine particles. The lack of an association between HMOX-1 expression and the redox activity, as measured by the DTT assay, could be due to two reasons. Firstly, there is evidence suggesting that aqueous chemistry within the CAPS can promote adsorption of condensable vapors, which likely adds a large amount of OM to the concentrated ultrafine particles (McWhinney et al., 2012). For example, the abundance of amine compounds in these samples was much higher than that typical of urban ultrafine PM; concentrations of amine containing particles are usually quite low, but short-term exposure spikes do occur in cities around the world. The addition of these amine compounds and other OM may have skewed the observed redox activities, since these are expressed per unit PM mass. Thus, if the condensable material deposited on the particles exhibited lower redox activity than the original particles it would decrease the DTT activity per unit mass observed for the ultrafine particles. Secondly, the contribution of transition metals in coarse particles, i.e., Fe and Cu, to the redox activity could not be determined by this assay, as these metals catalyze ROS production following a different reaction pathway (Fenton reaction, metals reduce H_2O_2 producing $OH^{\cdot}$) (Halliwell and Gutteridge, 1999). Thus, this approach did not allow us to differentiate between metal and organic-based redox activity, and could limit the interpretation of these findings.

4.2 Differential responses for different sized PM

Dose-dependent increases in HMOX-1 and IL-8 expression and decreases in cell viability were observed in this study for all three PM size fractions. However, only the ultrafine particle data supported the differential cellular responses proposed by Li et al., (2002). Significant activation

of the antioxidant defence response, i.e., upregulation of HMOX-1, was observed at a lower ultrafine PM concentration (10 µg/ml), whereas proinflammatory response (IL-8) and cell death were induced at 50 and 100 µg/ml particle mass concentrations, respectively. This finding was consistent with other studies using diesel exhaust particles (size <1 µm) that have shown that cytoprotective pathways are induced at relatively low levels of oxidative stress and that cellular apoptosis or necrosis occurs at a higher level of oxidative stress (Li et al., 2002; Xiao et al., 2003). Li et al., (2002) suggested that the hierarchical oxidative stress model was governed by the OC content of particles, especially PAHs. The ultrafine samples collected in Toronto were also highly enriched in PAHs compared with coarse and fine PM. By contrast, for coarse PM, while cytotoxic effects were observed at the lowest PM dose (10 µg/ml), significant upregulation of HMOX-1 was not observed until a higher dose was reached. Thus, the results for the coarse PM were inconsistent with the hierarchical oxidative stress model proposed by Li et al., (2002) and hence this model is likely not applicable for all particle sizes.

More generally, it appears that the cells were responding differently when exposed to the coarse vs. quasi-ultrafine PM. The possibility exists that metals, different water-soluble or organic species, and endotoxins could trigger different or a combination of biological pathways leading to different responses. For example, several studies have also suggested that the presence of endotoxins on the particle surface may initiate inflammatory responses in the cells, particularly for larger particles (Camatini et al., 2012; Mantecca et al., 2010; Steenhof et al., 2011; Steerenberg et al., 2006; Wang et al., 2013). A recent study from our group measured the endotoxin levels in concentrated coarse (293 EU/mg) PM at this site, and found that human exposure to these concentrations was associated with inflammatory responses (Behbod et al., 2013). The possibility that particles of differing size or composition may elicit alternate or additional biological pathways further complicates interpretation.

4.3 Effects of different physicochemical properties

Exposure to specific components within the different size fractions showed different degrees of responses (**Figures 4.4-4.6**). If size has no impact on the biological responses, then similar responses should have been observed following exposure to the equivalent mass concentrations

of the components of different size fractions. Thus, the different linear regression lines for the different components indicated that the observed responses were not caused by total or component mass alone; initial particle size may also play a role in inducing the response.

Similarly, the variability in our observed responses cannot be explained based on size alone; otherwise the order of response for different sizes would be expected to always be the same across studies. *In vitro* studies conducting spatial and temporal PM toxicity studies have not reported any consistent relationships between biological responses and PM sizes (Camatini et al., 2012; Duvall et al., 2008; Laurer et al., 2009; Perrone et al., 2013; Seagrave et al., 2006). It is likely that the differences in composition within different PM size-fractions played an important role on the observed responses. Higher slope values for transition metals (Cr and Ti) and OM compared with total PM mass and other chemical elements suggested their stronger influence on the observed responses, as hypothesized. The relative abundance of transition metals in coarse PM might be related to the observed cytotoxic effects (Moon and Becker, 1999), whereas ultrafine PM with higher OCs could induce greater activation of inflammatory response (Li et al., 2010).

A third important physical property that can play an important role in the extent of PM toxicity is particle surface area, particularly in the case of the smaller particles. Several studies have suggested that the surface area of particles is the critical determinant of their biological effects and should be used as a dose metric when comparing particle-induced effects (Duffin et al., 2002; Hetland et al., 2001; Oberdörster, 2001; Wittmaack, 2007). Depending on the size of the particles, equal masses of PM could be comprised of quite different numbers of particles, which would lead to significant differences in surface area. For monodispersed particles with unit density, only one particle/cm^3 with a diameter of 2.5 μm would constitute a mass concentration of 10 μg/m^3 compared with the same mass concentration of particles 20 nm in diameter would comprise about 2.4 million particles/cm^3 with 100 times more surface area (Oberdörster, 1995). In this study of size-fractionated particles, all experiments were conducted based on an equal mass exposure. Thus, the quasi-ultrafine particles were comprised of the greatest number of particles and total surface area for a given mass. Given the differential responses to the three size fractions, it would not be appropriate to assume that the observed biological effects could be

fully described by a single property, i.e., size or surface area. It is most likely that the observed biological effects were the combined effect of mass, size, surface area, and chemical composition. Furthermore, correlation coefficients calculated between surface area and biological responses did not support this hypothesis; suggesting that the complexity of the cellular responses is much greater than originally hypothesized.

4.4 Potential emission sources related to the biological responses

The correlation analyses between chemical elements and biological responses helped to determine the toxicological contribution of different constituents toward the biological endpoints for the different particle sizes. For coarse and fine particles, HMOX-1 expression and cell viability correlated significantly with transitional metals (Cr, Cu, Fe, and Ti) and OC fractions, whereas for ultrafine particles, correlations were found mainly with the OC fractions. IL-8 mRNA upregulation was affected by both transition metals and OC for all size fractions. Correlation analyses among elements also helped to identify potential PM sources responsible for the observed effects (**Supplemental Tables B.10, 11, and 12**). For coarse and fine particles, Ba, Cr, Cu, Fe, Mn, Si, Ti, and Zn were significantly inter-correlated, indicating that the elements might be coming from similar sources. As the study site is located next to a busy street, potential sources for these metals could be traffic exhaust and non-exhaust emission sources, i.e., brake and tire wear (Thorpe and Harrison, 2008). Contaminated road dust and roadside soils could also contribute to the metal concentrations (Rehbein et al., 2012). Further, these metals have all been found to exhibit diurnal and weekday/weekend patterns at this site, similar to other traffic-related pollutants. OC, which correlated significantly with Fe, Mn, and Ti for both coarse and fine particles, could also be produced by the same traffic sources (Thorpe and Harrison, 2008). In the ultrafine size range, higher EC and OC concentrations were observed in the morning and afternoon, respectively, indicating that the primary emission (in the morning) and secondary particle formation (in the afternoon) could be the sources of ultrafine in that location (Ahlm et al., 2012). The particle size distribution of the ambient air (maximum number concentrations for 10–30 nm particles) also suggested that primary emissions from vehicles were a major source of ultrafine particles (Rastogi et al., 2012).

4.5 Limitations of the study

There are several limitations to this study. Firstly, filter extracts were used for the cell exposure experiments. The filter extraction methodology used in this study emphasizes the mass/composition-related responses rather than those associated with the particle number or surface area, as the filter collection/extraction process was presumed to not conserve the original number concentration, size distribution or surface area properties of the particles. Secondly, particles were added to the cells as a suspension in culture medium, which differs substantially from the actual deposition of airborne particles onto the respiratory cell surface. The quantity (i.e., mass or number) of particles that actually interacts with the cells could, therefore, not be determined. Thus, it is not surprising that the relationships between the physicochemical properties (number concentration, surface area, and chemical composition) and biological responses were significant when considering composition alone. Thirdly, particles for the chemical analysis and biological tests were collected on different filters and were extracted in different media. Therefore, the particle extraction efficiency could be different among the filters used. Fourthly, the concentrating process for the ultrafine PM causes a shift in the size distribution for small particles (20-40 nm) (Rastogi et al., 2012). Composition of the ultrafine particles was also altered by the addition of excess OM during the condensation process (McWhinney et al., 2012). These factors could have led to a reduction in the redox activity of ultrafine particles. Furthermore, as noted above, the method of assessment of redox activity did not allow the differentiation between metal and organic-based redox activity. Finally, the biological responses observed in the A549 cell line limits the interpretation of these findings to whole organism exposures. Future studies using primary cells will be helpful to confirm and translate these findings into higher models (i.e., whole animal/human exposures).

5. Conclusions

This *in vitro* study investigated the comparative biological effects of size-fractionated ambient PM on human alveolar epithelial cells. This study demonstrated that exposure to ambient PM can initiate mass-dependent antioxidant, proinflammatory, and cytotoxic responses. The biological

responses correlated strongly with transition metals and OC fractions for the coarse and fine particles, and with OC fractions for the quasi-ultrafine particles. For all three size fractions, traffic-related emissions appeared to trigger the biological responses. However, the biological responses did not correlate consistently with any specific particle size fraction. These observations indicate that these responses are dependent upon physicochemical properties, such as size and composition, and that these yield complex patterns that preclude making simple generalizations. It appears that the observed biological responses were caused by the combined effects of different physicochemical properties of the particles. Therefore, it is important to consider the combined influences of these physicochemical properties when explaining PM toxicity.

Chapter 5
Conclusions and Recommendations

1. Conclusions

In vitro methods are commonly used for toxicological investigations. These studies are simpler, faster, and cheaper than *in vivo* studies. *In vitro* studies allow the investigation of the role of specific sources and components of PM on toxicity and specific biological pathways of interest. Numerous *in vitro* studies have been conducted to date, in order to better understand the observed biological responses and the underlying mechanisms of the responses. However, no single study has investigated the differential effects of size-fractioned ambient PM on oxidative stress-induced biological responses. This series of *in vitro* studies is the first to investigate the extent of the responses for PM with different size distributions, chemical compositions, and redox activities.

The thesis focused on the comparative toxicological investigation of different source-related and size-fractioned PM. The objective of these experiments was to compare the toxicological effects of the particles in relation to their size, composition, and redox activity to identify responsible physicochemical properties causing the effects. A human adenocarcinomatous cell line A549 which exhibits some characteristics of alveolar epithelial cells were exposed to PM in this study. Determination of toxicity profile of ultrafine particles was one of the main objectives of this study. Ultrafine particles deposits mainly in the distal region of the lung. A549 cell line was chosen to represent the region. Therefore, the biological responses observed in this study will better represent the responses observed in the alveolar region. For the source-related study (Chapter 3), Standard Reference Material (SRM) samples from different sources were used. Industrial source-related PM (collected from an industrial smelter and diesel-powered forklift exhaust) were chosen to study occupational exposure hazards, whereas the investigation of urban PM highlighted the toxicity of ambient PM to which we are exposed day-to-day. The diverse chemical composition of the particles was also considered when selecting the sources. Transition metal enriched (i.e., Fe and Cu) PM collected from the smelter facility showed the highest

toxicity and proinflammatory responses compared with other sources, which highlighted the importance of further toxicological investigations of PM collected from specific sources. However, there were some limitations in this study. Relevant chemical composition data was only partially available for these SRMs. Therefore, correlation analyses between the biological responses and chemical composition could not be determined. In addition, the average particle size of the SRMs, especially the non-ferrous dust (PD-1) and urban PM (SRM 1648a) samples, was larger than the inhalable size range (>10 μm) (**Appendix Figure E.1**). This study highlighted the importance of an *in vitro* investigation of inhalable PM (<10 μm) with detailed physicochemical characterization of the particles.

Toronto is the largest city in Canada where the annual peak (98th percentile) 24 h fine PM concentration in 2011 ranged from 18.4 to 23.6 $\mu g/m^3$ at different monitoring stations; below Canada's new 24 h air quality standard for fine PM of 28 $\mu g/m^3$ (Environment Canada, 2013). Transboundary air pollution, traffic, biomass burning, and road dusts are major sources of fine PM in Toronto (Jeong et al., 2011). Previously, a number of animal and human exposure studies have been conducted in Toronto (North et al., 2013; Penton et al., 2013; Urch et al., 2010 & 2005). However, these studies focused mainly on the toxicity of coarse or fine PM and no detailed chemical characterization was conducted to compare with the biological responses. An intensive field campaign study 'Health Effects of Aerosols in Toronto (HEAT)' was conducted focusing on the characterization of the physicochemical properties and toxicity of the size-fractionated ambient PM. The comparative toxicity of different sized PM was determined by both *in vivo* (Amatullah et al., 2012) and *in vitro* (Chapter 4) studies. The particle concentrator facility used in this study was also characterized in details during the campaign (McWhinney et al., 2012; Rastogi et al., 2012).

For the size-fractionated PM exposure, dose-dependent antioxidant, proinflammatory, and cytotoxic responses were observed among all sizes. Although it was hypothesized that particle exposure would induce dose-dependent differential toxicological effects on the cells (i.e., antioxidant defence, proinflammatory response, and ultimately cell death), exposure to the different size fractions showed different degrees of responses (**Figure 4.3**). A shorter duration (4 h) was chosen for this study to observe the biological responses at an earlier time point and also

to compare the findings with that of the *in vivo* study conducted during HEAT campaign (Amatullah et al., 2012). Quasi-ultrafine PM caused significant induction of HMOX-1 at the lowest exposure dose (10 µg/ml), whereas coarse particles caused the highest cytoxicity at that dose. Only ultrafine PM, which was enriched in PAHs (**Figure B.2**), exhibited the differential cellular responses as hypothesized. This was consistent with the findings of a previous study (Li et al., 2002) that also suggested that the hierarchical oxidative stress model is governed by the OC content of particles. Coarse and fine PM enriched in metals, different water-soluble species, and biological agents like endotoxin, could have triggered different biological pathways. However, identification of these pathways was not within the scope of this study.

The correlation analyses between different physicochemical properties and biological responses helped to determine the importance of different properties toward the biological endpoints. For similar mass exposure of different components, the biological responses were different for different sized PM indicating the role size played (**Figures 4.4–4.6**). However, the variability observed in the biological responses could not be explained based on size alone. In addition to size, chemical composition and related redox activity of the particles played major roles toward toxicity. Among other components, the endpoints correlated significantly with transitional metals (Cr, Cu, Fe, and Ti) and OC fractions for coarse and fine particles, whereas correlations were found mainly with the OC fractions for ultrafine particles. Higher slope values for transition metals (Cr and Ti) and OC compared with total PM mass and other chemical elements suggested their stronger influence on the observed responses. Although the redox activity measured by DTT assay could not measure the full redox potential of the particles, all these components are known to be related to higher redox potentiality.

The physicochemical properties of the particles are dependent variables. For an equal mass concentration, the surface area of ultrafine particles would be significantly higher than that of coarse and fine PM (depending on the number concentration). Some chemical constituents are prevalently found in specific PM size fractions, e.g., crustal metals are mostly abundant in coarse PM. Particle size is an important factor in determining the deposition location and clearance rates of particles in the lung. Particle-cell interaction and particle internalization in the cells also depend on particle size. Furthermore, the redox potential of the particles depends on particle

composition. In addition, particles with high surface area and redox-active constituents on their surface may lead to higher surface reactivity. Given the complexity of these relationships, the observed biological responses are better explained by considering different physical properties, such as, mass, size, related properties (i.e., surface area), chemical composition, and redox activity. However, in this study the results could only be explained using mass, size, chemical composition, and redox activity due to limited available data.

The findings from the *in vivo* study conducted during the HEAT campaign reported exposure to coarse PM resulted in significant changes in respiratory airways resistance and hyperresponsiveness in healthy mice, whereas ultrafine particles caused no significant effect on the pulmonary function (Amatullah et al., 2012). Coarse PM exposure also resulted in significant increases of the total number of cells and macrophages in the BAL samples compared with fine and ultrafine exposures. Similar to the *in vitro* study, HMOX-1 (mRNA) concentration in lung tissues were also measured and no significant differences were observed after PM exposure compared with filter air exposure and in between sizes (not published, **Supplemental Figure B.6**). Therefore, the findings from the *in vitro* study were not in full agreement with that of the *in vivo* study. The differences in the findings exemplify the difficulty in interpreting and comparing the results between *in vivo* and *in vitro* studies. Previous studies have also reported little correlations between *in vivo* and *in vitro* findings (Becher et al., 2001; Sayes et al., 2007; Seagrave et al., 2005). Several factors could contribute to the differences in the *in vivo* and *in vitro* observations. This *in vitro* study used a human (transformed) cell line, whereas healthy mice were exposed to PM through nasal inhalation in the *in vivo* study. A single cell line may responds differently than the collected cells of the lung would do. Most of the pulmonary endpoints used in these studies were also not comparable to each other. The actual PM dose reaching the lung surface and the cell line could also not be determined. The lowest *in vitro* PM dose (10 µg/ml ~ 2.1 µg/cm^2) at which significant biological responses were observed was approximately 1000 times higher than the *in vivo* PM dose the mice could have experience in the alveolar region for particle exposure to 300 µg/m^3 for 4 h. Therefore, the differences in the species, single cell line versus whole lung exposure, lack of comparative biological endpoints, and uncertain dose concentration could lead to the discrepancies. However, *in vitro* studies

remain to be an important tool in determining useful information about dose-response relationships and biological pathways.

This study also identified that IL-8 (protein) adsorption by particles resulted in underestimation of IL-8 levels that could lead to misinterpretation of the outcomes from *in vitro* studies. It was suggested in Chapter 3 that cytokine concentrations measured in cellular PM exposure experiments should be corrected using appropriate partition coefficients derived from cytokine adsorption experiments specific to individual PM samples. A linear isotherm model was proposed to develop correction factors for each sample. The correcting method was further developed by another group (Herseth et al., 2013). During the HEAT study, IL-8 was measured at both the transcriptional (mRNA) and translational (protein) levels. Gene expression at the mRNA level is generally informative in the prediction of expected protein expression. Numerous studies have investigated the correlation between mRNA and protein expression levels in human cells/tissues. Findings from these studies have reported variable positive correlations between mRNA expression and protein levels suggesting that gene expression at the mRNA level is generally informative but not predictive of the protein level (Anderson and Seilhamer 1997; Guo et al., 2008; Shebl et al. 2010). In this thesis, differential effects on IL-8 mRNA and protein levels were observed for the different size-fractions (Chapter 4). The differences were the highest for quasi-ultrafine PM followed by fine and coarse PM. It has been reported that particles can interact with IL-8 protein produced by epithelial cells, thus impairing the quantification of IL-8 in biological samples (Chapter 3). Greater adsorption of IL-8 was observed for diesel particles with higher surface area and carbon content. Therefore, the greater variability between mRNA and protein levels observed for quasi-ultrafine particles could partly be attributed to the adsorption of IL-8 to the PM surface. The remaining differences could be due to the degradation of IL-8 mRNA prior to translation to protein. Quantification at the mRNA level measures the complete toxic potential of the particles at an earlier time point, whereas measurements at protein level identify the subsequent release of the marker that is likely to cause a biological effect. Thus, determination of both mRNA and protein levels are necessary and complementary for understanding the relevant biological pathways.

To compare the *in vitro* PM doses (µg/ml) used in this study with the real-life PM exposure concentrations, doses were converted to microgram of PM per unit of surface area (µg/cm^2) based on the PM dose (µg/ml), volume of the cell culture medium (ml) and the surface area of the cell culture plate (cm^2) (**Appendix C**). Multiple Path Particle Dosimetry (MPPD v 2.11, Albuquerque, NM, USA) model was used to estimate the duration required to experience PM dose of 2.5 µg/cm^2 for particle with diameter 0.1 µm. The dose has been reported to elicit significant biological responses *in vitro*. The durations were calculated for a healthy individual with higher particle deposition efficiency (1.4-fold higher than normal individual, due to variation in airway anatomy and breathing pattern) and an asthmatic individual (2-fold enhancement factor). Different exposure scenarios with very high PM concentrations (polluted city, cooking, workplace, and combination of all, PM concentration ranging from 540 to 5000 µg/m^3) and different levels of physical activity (i.e., resting to heavy exercise) were considered during the calculations. According to the simulation, it would take less than 32 h to experience such particle dose in the head region for most of the scenarios in a healthy person. The duration could range from 0.46 to 8.8 days in the tracheobronchial and 22.4 to 882 days in the alveolar regions. Particle deposition efficiency at the bifurcation points of the tracheobronchial region is expected to be 60-fold higher than the cylindrical airways in healthy individuals for the particle size (0.1 µm). Therefore, it would take less than 4 h for healthy and asthmatic individuals to experience 2.5 µg/cm^2 particle depositions at the bifurcation points when exposed to such high PM concentrations. Particle clearance rates are generally higher in the tracheobronchial region (>80% in 24 h) compared with the alveolar region (<1%). However, the cells at the bifurcation points may not be able to clear those particles within 4 h. Therefore, the *in vitro* doses (10 to 1000 µg/ml; equivalent to 2.1 to 210 µg/cm^2) used in this study are somewhat relevant to real life exposure scenarios for both healthy and asthmatic population.

The particle extraction and cell exposure methods used in this study could contribute to difficulties in the interpretation of the findings. There was the potential for alteration of the physiochemical properties of the particles during particle extraction from the filters and it was not possible to determine the actual PM dose interacting with the cells. Thus, exposure of cells to particles at the air liquid interface (ALI) is considered to be the preferred *in vitro* cell exposure

method for PM toxicity studies. At the ALI, the cells are directly exposed to PM without any alteration due to processing of the sample, and it is also possible to simultaneously characterize the particles online during the exposure. The performance of a preliminary field deployable cell exposure device, the Sized Aerosol *in Vitro* Exposure System (SAIVES), was evaluated in this thesis (**Appendix D**). An electrostatic precipitator was incorporated into the design of the device to increase particle deposition efficiency. At present, the deposition efficiency in the system ranges from 0.3 to 3.5%. With such low efficiency, it is not expected that cells would be exposed to sufficient ambient PM to elicit any biological responses within short exposure duration (e.g., 2 h). Based on the preliminary evaluation, several design modifications for the system were recommended to improve the deposition efficiency.

PM is a complex mixture of multiple components and each component may have multiple sources. Each source generates PM with different compositions. The size and other related physical properties (i.e., surface area and number concentration) of the particles also depend on the source. Furthermore, the effect of PM size is not independent of chemical composition as certain chemical constituents are prevalently found in specific PM size fractions. Therefore, it is difficult to identify and quantify the role of specific components or physical properties or sources in determining the associated health effects of PM. This thesis demonstrated that among the constituents, transition metals caused cytotoxicity and organic compounds caused activation of antioxidant and proinflammatory responses. These findings also suggested that the observed responses could be explained by relating PM composition, size, and related physical properties (i.e., surface area). PM composition also influenced the biological pathways causing the effects. Organic compounds were enriched in ultrafine PM and initiated the oxidative stress-mediated hierarchical biological response, whereas metals, different water-soluble species, and endotoxins in coarse and fine PM might have triggered different biological pathways. Findings of this study emphasized on the complexity of the toxicological pathways behind dose-response relationships. This thesis also demonstrated that the cellular responses varied substantially after *in vitro* exposure to PM from different sources. Thus, supporting the importance of toxicological studies of PM collected from specific industrial operations and traffic (exhaust and non-exhaust) related sources. The size-fractionated ambient PM study suggested that the toxic effects of ultrafine

particles could be as potent as coarse and fine PM. The knowledge generated from this study should help support the development of exposure standards for ambient ultrafine PM. Ultimately such standards and other environmental health policies will reduce particle pollution-related diseases and the associated costs. In conclusion, this thesis identified that the PM toxicity was caused by the combined effects of different physicochemical properties and the toxicological pathways of affecting the cells differed for different size fractions.

2. Recommendations

Several recommendations are suggested for future studies:

1) The DTT assay used in this study is an extracellular assay that was not able to determine the full redox potential of the particles. This assay mainly measures the redox activity of organic components in PM samples, particularly quinones. The redox potential of the metal constituents could not be directly measured by this assay. In addition to the DTT assay, measurement of the redox potential of transition metals is recommended, by following the rate of dihydroxybenzoate (DHBA) isomer formation from salicylate by hydroxyl radicals (procedure described in DiStefano et al., 2009). Hydroxyl radicals are produced following the Fenton reaction (Fe^{2+} + $H_2O_2 \rightarrow Fe^{3+}$ + $OH^{\cdot}$ + OH^{-}) by the transition metals present on the particle surface. The production of hydroxyl radicals can also be measured using electron paramagnetic resonance (EPR) (Shi et al., 2003).

2) It is also recommended that the redox potential of the particles should be examined using an intracellular assay, such as oxidant-sensing fluorescent probe 2', 7'-dichlorodihydrofluorescein diacetate (DCFH-DA). Findings from intracellular assay are expected to correlate well with the observed biological responses.

3) The role of ROS generation in eliciting oxidative stress-induced biological responses could also be determined by using free-radical scavengers, such as dimethylthiourea (DMTU); antioxidants, such as glutathione, *N*-acetylcysteine (NAC); or antioxidant enzymes, such as superoxide dismutase (SOD).

4) Pretreatment of particle extracts with metal chelators, i.e., diethylene triamine pentaacetic acid (DTPA) and deferoxamine (DEF), is recommended to remove the metals from the PM matrix to better understand the role of the metals toward toxicity. Similarly, the role of organic compounds toward toxicity can be determined by stripping the organic constituents by Soxhlet extraction.

5) Coarse PM generally contains biological material, such as pollen, and is enriched with bacteria-derived endotoxin. Analyses of coarse and fine PM collected from the same study site in Toronto have recently shown that both size fractions contain significant amounts of endotoxin. Endotoxin concentration has already been associated with inflammation in several *in vivo* and *in vitro* studies. Therefore, it is recommended to measure the endotoxin concentration of the collected PM, in addition to analyses of the chemical constituents.

6) The cell line (A549) used in this study is an immortalized human adenocarcinomatous cells derived from lung cancer that exhibits some of the characteristics of alveolar epithelial cells. Findings based on using the cell line differed from the *in vivo* condition. Future investigations using primary airway epithelial cell and/or co-culture of relevant cells will minimize this limitation.

7) IL-8 adsorption by particles may result in underestimation of IL-8 concentration leading to misinterpretation of the outcomes. To avoid this, it is suggested to correct cytokine concentrations by using appropriate correction factors derived from cytokine adsorption experiments using individual PM samples. However, derivation of the correction factors may not be always possible for all PM samples if the collected mass is low. Therefore, it is suggested to quantify IL-8 concentration at both mRNA and protein levels. The difference between mRNA and protein concentrations would be suggestive of the adsorption potency of the particles. Another approach would be to select a cytokine/chemokine that has negligible adsorption potency on particles such as IL-6 (Becker et al., 2003).

8) The IL-8 adsorption correction factor was developed for a single IL-8 dose only (2 ng/ml) which was directed towards correcting IL-8 upregulation levels observed in this study. The

model should be further developed for a wide range of IL-8 concentration levels to determine the saturation level of IL-8 adsorption on particles.

9) Direct particle exposure of cells at the ALI, along with simultaneous online characterization of particle properties (e.g., concentration and surface area) is recommended to minimize the alternation in particle properties during exposure.

10) For regulatory purposes, mass concentration is currently used as the basis for exposure standards for coarse and fine PM. The studies that comprise this thesis have shown that the toxicity of particles depends on the relative contribution of different chemical elements. For example, cytotoxic effects were the greatest for coarse and industrial particles, which were highly enriched in metal concentrations. However, it is not possible to establish a standard for each chemical component due to the complex composition of particles. Particles coming from different sources can be characterized according to their chemical composition. Based on the relative toxicity data of the different components, PM emission standards should be established for the major sources, which will ultimately lead to reductions of the concentrations of toxic components in the air.

Appendix A

Supplemental materials of Chapter 3

S.1 Sources of particles and elemental composition

Three different Standard Reference Materials (SRMs): non-ferrous dust (PD-1), urban PM (UPM, SRM 1648a), and diesel particulate matter (DPM, SRM 2975) were used in this study. PD-1 is a composite of dust samples collected from baghouses and an electrostatic-precipitator from the zinc and copper roaster stacks of the Hudson Bay Mining and Smelting Company Limited (Manitoba, Canada) (Canadian Certified Reference Materials Project (CCRMP), 2009). SRM 1648a was collected from an urban area (St Louis, MO, USA) in a baghouse over one-year from 1976–1977 (NIST, 2010a). SRM 2975 was collected from an industrial diesel-powered forklift using a special filtering system (NIST, 2010b).

Urban ambient fine PM ($PM_{2.5}$) were collected on Teflon filter papers with a nominal pore size of 2 μm (37 mm diameter, Pall Gelman, USA) using the Concentrated Ambient Particle Exposure Facility (CAPEF) located at the University of Toronto, Toronto, Canada. This sampling site is located downtown, next to a high traffic road (College St.). Receptor modeling has shown that on average ~25% to 50% of the $PM_{2.5}$ mass at this site comes from local sources and thus that regional sources are predominant (Jeong et al., 2011). Two filters: F-1- collected over a 1 week period in late fall (November, 2009) and F-2- collected in winter (February, 2010) were used in this study. The mass of the collected PM on filters was estimated by weighing the filters before and after sampling. The filters were then preserved in the darkness at -20°C for subsequent analyses.

The median diameters of the SRMs are 0.95 μm, 5.85 μm, and 19.4 μm for PD-1, SRM1648a, and SRM2975, respectively. Information regarding the elemental compositions of the three SRMs, from their certificates or literature, is presented in. Average PM speciation data for Toronto-$PM_{2.5}$, collected for 2004-2007 at the same site, are also presented in **Table A.1.** It should be noted that the Toronto-$PM_{2.5}$ sample used in the *in vitro* testing was collected over one day or more, ~1m above ground level, whereas the 2004-2007 data is an average for samples

collected on top of the three story building over four years. The highest concentrations of metals were observed in PD-1. The weight percentages of many metals relevant to ROS production were elevated: Zn- 36%, Fe- 12%, and Cu- 7.3%. The major inorganic elements in SRM 1648a were: SO_4^{2-} 15%, Si 12%, Fe 3.9%, and Al 3.4%. The total carbon content of SRM 2975 (65%) was higher than SRM 1648a (13%). Much of this carbon was elemental and the weight percentages of organic carbon were closer, 5% and 2.3%, in SRM 2975 and SRM 1648a, respectively. Abundant components in Toronto-$PM_{2.5}$ were SO_4^{2-} (24%), NO_3^- (19%), NH_4^+ (11%), elemental carbon (14%), and organic carbon (15%). A number of trace metal elements (Al, Ba, Ca, Cr, Fe, K, Mg, Mn, Na, Ni, Pb, Se Zn, V, Ti) were also measurable in Toronto-$PM_{2.5}$. **Table A.2** presents selective PAHs and nitro-PAHs elements in SRM 2975. Among the PAHs, chrysene, benzo[*b*]fluoranthene, indeno[1,2,3-*cd*]pyrene, benz[*a*]anthracene, dibenz[*a*,*h*]anthracene are classified as probable human carcinogens by United States Environmental Protection Agency (USEPA, 1993).

S.2 Cell culture

Human A549 alveolar epithelial cells (ATCC, Rockville, MD, USA) were used for the exposure experiments. Cells were grown in DMEM supplemented with 2 mM L-glutamine, 50 U/ml penicillin-streptomycin, and 10% heat inactivated FBS at 37°C supplied with 5% CO_2. Cells were seeded at a concentration of 2.5×10^5 cells/ml in 96-well plates. After 24 h, the medium was replaced with medium containing the PM. Cells exposed to cell culture medium only (no PM) were considered as control.

Table A.1: Chemical composition (µg/g) of different source-related PM

Chemical Component	Non-ferrous dust (PD-1)[a]	Urban PM (SRM 1648a)[a]	Diesel PM (SRM 2975)	Toronto-$PM_{2.5}$[b]
Al		34 300		2960
As	7700	115		
Ba		737		445
Br		502		126
Ca		58400		5530
C_{total}		127000	650000[d]	263000
$C_{elemental}$		105000	600000	108000
C_{org}		23000	50000	155000
Cd	2800	73.7		
Cl		4540		3800
Cr		402		493
Cu	70300	610		
Fe	122000	39200		6300
K		10600		4200
Mg		8130		1080
Mn		790		595
Na		4240		4730
Ni		82		221
Pb	27500	6550		273
Si	30500	128000		7930
Sr		215		54
Ti		4020		1190
V		127		753

Chemical Component	Non-ferrous dust (PD-1)[a]	Urban PM (SRM 1648a)[a]	Diesel PM (SRM 2975)	Toronto-$PM_{2.5}$[b]
Zn	359000	4800		1040
SO_4^{2-}	42700[c]	154200[c]		274000
NO_3^-		10700[c]		220000
NH_4^+		20100[c]		130000

[a]chemical composition of SRMs were collected from the analysis certificate provided by CAMNET or by NIST, [b]average ambient fine PM speciation data for 2004 to 2007 (Jeong et al., 2011), [c]Tan et al., 2002, [d]Singh et al, 2004; blank indicated no data were available.

Table A.2: Selective polycyclic aromatic hydrocarbons (PAH) and nitro polycyclic aromatic hydrocarbons concentrations (µg/g) of SRM 2975 (NIST, 2010(b))

Chemical Component	Concentration (µg/g)	Chemical Component	Concentration (µg/g)
1-Nitropyrene	34.8	1,8-Dinitropyrene	3.10
Fluoranthene	26.6	9-Nitroanthracene	2.97
Phenanthrene	17	1,6-Dinitropyrene	2.36
Benzo[*b*]fluoranthene[a]	11.5	6-Nitrochrysene	2.22
Benzo[*ghi*]fluoranthene	10.2	2-Methylphenanthrene	2
Triphenylene	5.22	Indeno[1,2,3-*cd*]pyrene[a]	1.4
Chrysene[a]	4.56	Benz[*a*]anthracene[a]	0.32
3-Nitrofluoranthene	3.74	Dibena[*a*,*h*]anthracene[a]	0.52
7-Nitrobena[*a*]anthracene	3.46		

[a] probable human carcinogens (USEPA, 1993)

S.3 Cytokine adsorption by particles in cell-free tests

PM suspensions (10-1000 µg/ml) prepared in cell culture medium with 10% FBS were incubated with standard IL-8 (2000 pg/mL) for 24 h at 37°C with 5% CO_2. After exposure, the suspensions were centrifuged and the supernatants were analyzed for the remaining IL-8 concentration by ELISA. Based on the remaining IL-8 concentration measurements, correction factors (CFs) were derived for each particle type using a linear adsorption isotherm to relate the surface-bound and solution IL-8 concentrations. A partition coefficient (K) was calculated using the equation y = Kx, where x is the remaining IL-8 concentration in the medium, y is the amount of IL-8 removed per unit mass of particles. This determination of the partition coefficient only used IL-8 concentration data where the final IL-8 concentration was statistically different from the original value (2000 pg/ml) and the coefficient of variance of the measurements was less than 20%. The IL-8 release data from the *in vitro* assays for each particle was then estimated using these partition coefficients, by calculating the amount of IL-8 adsorbed by the particles from the measured IL-8 solution concentration. This adsorbed IL-8 was then added to the measured IL-8 in order to yield a corrected value. The accuracy of this correction method was evaluated by applying it to the IL-8 adsorption experiment data. It was found that 82-99.9% of the IL-8 could be accounted for using this approach (**Table A.3**).

Table A.3: Percentage of accuracy of the correction method for different PM type at difference PM concentrations

PM Concentration (µg/ml)	SRM 1648a	SRM 2975	Toronto-$PM_{2.5}$ (F-1)
10	97.69	93.28	99.90
50	93.85	96.37	98.91
100	96.21	93.88	99.87
200	91.92	99.09	97.77
400	85.28	89.34	96.57
800	86.04	93.17	97.59
1000	82.41	93.37	88.70

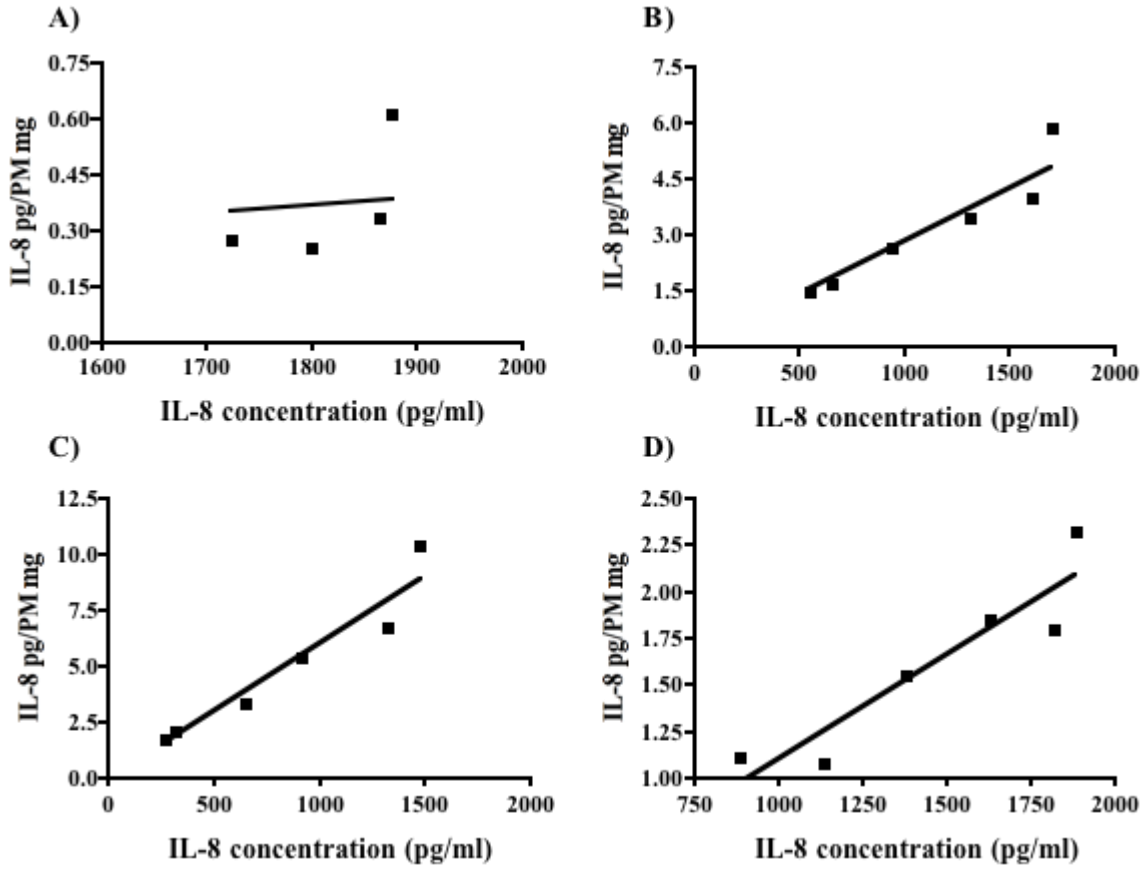

Figure A.1: Derivation of correction factors by applying acellular IL-8 adsorption tests. A) PD-1, B) SRM1648a, C) SRM2975, D) Toronto-$PM_{2.5}$. The partition coefficient K values: PD-1 = 0.2 µl/µg, SRM1648a = 3 µl/µg, SRM2975 = 6 µl/µg, and Toronto-$PM_{2.5}$ = 1 µl/µg.

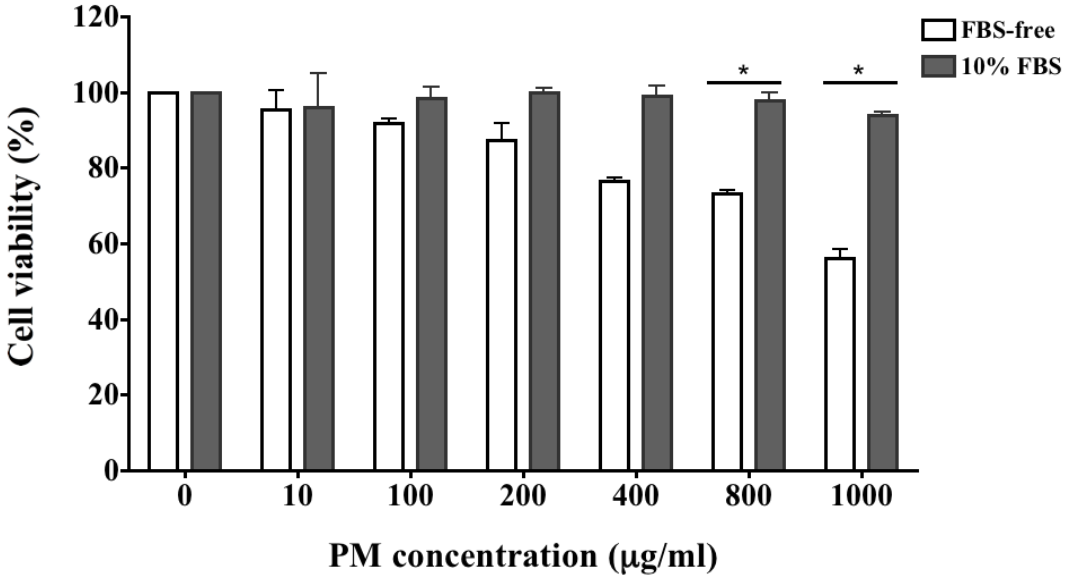

Figure A.2: Effect of presence and absence of serum protein on cell viability. SRM 1648a suspension was prepared in FBS-free and with 10% FBS in cell culture medium. Cells were exposed to the PM for 24 h and later analyzed for cell viability using MTT assay. The data are presented as mean ± SEM (n = 2) of duplicate experiments. Results from two-way ANOVA analyses showed that use of serum protein had significant effect on cytotoxic response of PM (p = 0.001). Significant difference between groups at different PM concentrations analyzed by t-test is shown: p <0.05*, p <0.01**, p <0.0001***.

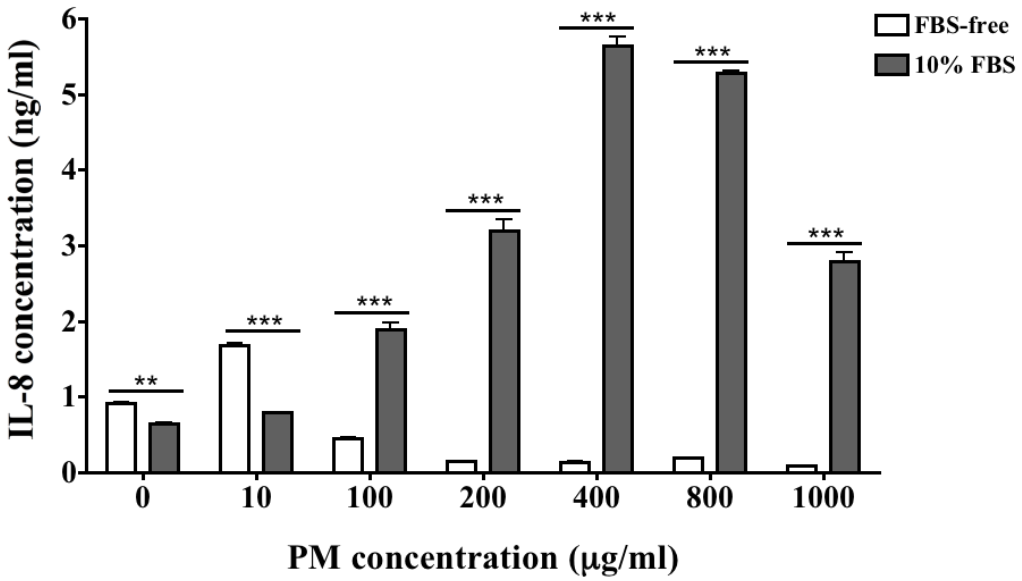

Figure A.3: Effect of presence and absence of serum protein on IL-8 induction. SRM 1648a suspension was prepared in FBS-free and with 10% FBS in cell culture medium. Cells were exposed to the PM for 24 h and later supernatants were collected and analyzed for IL-8 concentration ELISA kits. The data are presented as mean ± SEM (n = 6) of duplicate experiments. Absence of serum protein caused reduced induction of IL-8 concentration. Results from two-way ANOVA analyses showed that use of serum protein had significant effect on cytotoxic response of PM (p <0.0001). Significant difference between groups at different PM concentrations analyzed by t-test is shown: p <0.05*, p <0.01**, p <0.0001***.

Appendix B

Supplemental materials of Chapter 4

S.1 Analysis of IL-8 protein concentration

To evaluate the proinflammatory response to PM, IL-8 expression was also measured at the protein level along with transcriptional level (i.e., mRNA).

S.1.1 Methodology

Enzyme-linked immunosorbent assay (ELISA) kits were obtained from BioLegend (San Diego, CA, USA). Cells were seeded at 1×10^6 cells/ml in 6-well plates for ELISA. The collected supernatants were analyzed for IL-8 protein secretion using a commercially available ELISA kit. ELISA was performed as described previously (Akhtar et al., 2010).

S.1.2 Results

S.1.2.1 Effect of different size-fractionated PM on IL-8 protein expression

Induction of IL-8 was generally lower at the protein level than at the mRNA level for all size fractions, particularly at higher PM concentrations (**Supplemental Figure B.4**). At an equivalent mass-concentration of 100 μg/ml, the greatest difference was observed for ultrafine and fine (mRNA vs. protein: 3.1- vs. 1.3-fold) compared with coarse (2.8- vs. 1.5-fold) particles. The order of response at the mRNA level was different than that of at the protein level among the different size fractions. Specifically, IL-8 mRNA expression in response to the coarse particles was significantly lower than that following ultrafine and fine PM exposure (i.e., ultrafine = fine > coarse), whereas the protein concentrations followed the opposite trend (i.e., coarse > fine = ultrafine).

S.1.2.2 Linear regression and correlation analyses

Scatter plots of selected chemical constituents with IL-8 (protein) were plotted in Supplemental

Figure S.5. The slopes of the biological response vs. total PM mass concentration and the different PM constituent masses for IL-8 protein response was determined for the different size fractions (**Supplemental Tables B.5**). Among the 17 elements, the slopes of the dose-response relationships were significantly different among the sizes 2 elements. The Spearman correlation coefficients (ρ) of IL-8 protein expression with different chemical constituents, redox activity, and between the endpoints are reported in **Supplemental Tables B.6, 7, 8, and 9**. All the correlation values mentioned hereafter were statistically significant ($p < 0.05$). In the coarse size range, IL-8 (protein, p) positively correlated with total Ba, Cr, Cu, Fe, Si, Ti, Zn, OM, OM-1, 2, and 4. For fine PM, no correlations were observed for IL-8 (p). For ultrafine PM, total Si, Ti, Zn, OM, OM-1, 2, 3, and 4 correlated positively with the upregulation of IL-8 (p). Redox activities correlated with positively with IL-8 (p) for coarse and ultrafine PM.

S.1.3 Discussion

In this study, IL-8 was measured at both the transcriptional (mRNA) and translational (protein) levels. Gene expression at the mRNA level is generally informative in the prediction of expected protein expression. However, several studies have investigated the correlation between mRNA and protein expression levels in human cells/tissues. Findings from these studies have reported moderate and variable positive correlations suggesting that gene expression at the mRNA level is generally informative but not predictive of the protein level (Anderson and Seilhamer, 1997; Guo et al., 2008). Thus, determination of both mRNA and protein levels are necessary and complementary for understanding the relevant biological pathways. In our study, a differential effect in IL-8 mRNA and protein levels was observed for different size-fractions. The differences were highest for quasi-ultrafine PM followed by fine and coarse PM. In our previous study, we reported that particles can interact with IL-8 protein produced by epithelial cells, thus impairing most assays for quantification of IL-8 in biological samples (Akhtar et al., 2010). Greater adsorption of IL-8 was observed for diesel particles with higher surface area and carbon content. Therefore, the higher variability in mRNA and protein levels observed for quasi-ultrafine particles can partly be contributed to the adsorption of IL-8 to the PM surface.

Table B.1: Summary of PM sample collection (for *in vitro* analyses) during the HEAT Campaign

PM **size**	**Collection time**	**Sample ID**	**Mass (mg)**
Coarse	2/19/2010 9:00 – 17:00	C1	2.57
	2/22/2010 9:00 – 17:00	C2	1.75
	3/9/2010 13:00 – 17:00	C3	6.15
	3/10/2010 13:00 – 17:00	C4	4.3
	3/11/2010 9:00 – 13:00	C5	3.46
	3/12/2010 9:00 – 13:00	C6	1.24
	3/12/2010 13:00 – 17:00	C7	0.83
Fine	2/25/2010 9:00 – 17:00	F1	0.77
	3/2/2010 9:00 – 13:00	F2	0.66
	3/4/2010 9:00 – 13:00	F3	0.68
	3/4/2010 13:00 – 17:00	F4	0.95
	3/5/2010 9:00 – 13:00	F5	0.76
	3/5/2010 13:00 – 17:00	F6	0.77
Quasi-ultrafine	3/16/2010 9:00 – 13:00	UF1	1.88
	3/16/2010 13:00 – 17:00	UF2	1.37
	3/17/2010 9:00 – 13:00	UF3	1.90
	3/17/2010 13:00 – 17:00	UF4	1.78
	3/18/2010 9:00 – 13:00	UF5	1.90
	3/18/2010 13:00 – 17:00	UF6	1.51
	3/19/2010 9:00 – 13:00	UF7	0.97
	3/19/2010 13:00 – 17:00	UF8	1.80

Table B.2: Selected constituents of coarse (C), fine (F), and quasi-ultrafine (UF) PM (unit: metals ng/µg, EC and OMs%, µg/µg x 100)

Sample ID	Al	Ba	Ca	Cr	Cu	Fe	Mg	Mn	Na	Si	Ti	Zn	EC	OM	OM-1	OM-2	OM-3	OM-4
C1	6.4	0.66	60	0.054	0.64	21	10	0.44	54	2.6	0.32	0.67	0.13	11	1.9	2.6	2.2	3.1
C2	14	1.5	110	0.15	1.4	42	14	0.80	73	7.7	0.71	1.3	0.24	15	3.1	3.0	3.5	4.4
C3	18	1.3	131	0.12	1.1	38	20	0.93	26	4.4	0.79	1.4	0.19	9	0.32	1.3	1.4	4.5
C4	18	1.3	125	0.13	1.0	43	19	0.91	37	5.5	0.77	1.4	0.20	14	3.6	1.8	1.6	4.6
C5	17	1.5	104	0.12	1.0	44	15	0.90	29	8.7	0.78	1.5	0.20	16	4.2	2.0	2.0	4.7
C6	12	2.0	73	0.14	1.6	48	13	0.72	27	13	0.95	2.0	0.24	13	3.5	2.7	1.6	4.6
C7	12	2.1	64	0.21	1.6	48	12	0.71	30	18	0.90	1.5	0.26	23	9.3	3.2	2.0	6.1
F1	2.5	0.63	18	0.23	0.61	17	15	0.48	59	1.2	0.17	2.2	0.86	26	11	4.8	2.4	6.2
F2	8.7	2.5	70	0.82	1.9	57	12	1.3	50	1.1	0.89	3.9	1.6	41	19	5.1	4.2	10
F3	11	1.9	95	0.16	1.4	45	11	1.2	30	1.1	0.77	5.7	0.80	34	18	4.0	4.2	7.6
F4	6.5	0.85	48	0.082	0.77	29	5.7	1.5	12	0.79	0.49	2.6	0.75	28	13	3.6	2.9	8.1
F5	8.8	1.7	71	0.10	1.2	37	8.7	1.1	23	1.0	0.65	1.8	0.89	32	15	3.1	4.2	9.9
F6	10	1.4	71	0.18	0.82	34	9.2	1.5	25	7.1	0.72	1.6	0.84	32	15	3.4	3.0	9.7
UF1	0.16	0.016	1.7	0.011	0.058	0.90	0.12	0.082	0.58	6.3	0.022	1.1	3.1	84	75	3.6	1.2	2.8
UF2	0.33	0.023	3.2	0.015	0.034	0.74	0.70	0.068	4.7	4.3	0.030	1.3	1.7	91	82	3.7	1.4	3.3
UF3	0.29	0.033	0.94	0.17	0.074	3.8	0.15	0.13	1.1	2.5	0.022	1.1	3.4	31	24	2.5	0.8	1.8
UF4	0.10	0.035	0.81	0.60	0.044	4.1	0.12	0.21	1.3	6.1	0.023	0.73	1.9	77	67	4.0	1.5	3.2
UF5	0.057	0.007	0.89	0.16	0.011	1.3	0.18	0.082	1.7	12	0.022	0.62	3.0	81	72	3.4	1.3	2.3
UF6	0.11	0.008	1.6	0.30	0.014	1.4	0.25	0.082	3.6	15	0.028	1.1	1.6	95	85	4.1	1.6	2.9
UF7	0.24	0.10	1.9	0.021	0.021	1.9	0.22	0.16	4.0	17	0.042	1.4	2.6	78	67	4.4	1.8	4.4
UF8	0.13	0.007	0.85	0.18	0.011	1.1	0.052	0.052	0.78	3.4	0.023	0.57	1.4	85	75	3.5	1.4	3.4

Table B.3: Selected water-soluble elements of coarse (C), fine (F), and quasi-ultrafine (UF) PM

	Metals (ng/µg)								Ions (%)						
Sample ID	**Al**	**Ba**	**Ca**	**Cu**	**Fe**	**Mg**	**Si**	**Zn**	**Cl^-**	**NO_3^-**	**$SO_4^=$**	**$C_2O_4^=$**	**Na^+**	**NH_4^+**	**WSOC (%)**
C1	0.036	0.13	16	0.023	0.063	1.5	18	0.028	12	0.14	1.5	0.070	12	0.018	0.86
C2	0.12	0.30	38	0.080	0.092	2.3	23	0.042	15	3.0	4.0	0.088	12	0.028	0.051
C3	0.073	0.19	27	0.069	0.057	1.4	15	0.010	3.7	6.5	2.3	0.10	2.6	0.49	0.57
C4	0.074	0.21	35	0.080	0.057	2.1	11	0.016	4.4	11	2.9	0.093	4.9	0.85	0.54
C5	0.092	0.26	29	0.076	0.071	1.3	18	0.018	4.3	5.8	2.2	0.090	2.9	0.20	0.012
C6	0.21	0.80	49	0.49	0.24	5.0	8.2	0.12	3.4	22	7.2	0.26	4.4	2.5	0.033
C7	0.22	0.87	44	0.58	0.36	4.8	9.3	0.24	3.3	19	7.9	0.32	4.3	1.7	0.053
F1	0.14	0.33	16	0.27	0.29	12	1.2	0.91	16	14	19	0.48	3.4	6.3	6.1
F2	0.15	1.3	55	0.77	0.57	6.3	6.7	1.0	11	25	24	0.52	8.7	7.4	7.0
F3	0.31	0.66	61	0.35	0.68	3.1	20	0.49	5.3	5.7	9.2	0.26	4.3	0.80	7.0
F4	0.30	0.42	38	0.33	1.5	2.4	15	0.87	2.9	17	17	0.38	2.5	7.5	7.5
F5	0.27	0.63	43	0.38	0.47	3.1	14	0.41	5.6	47	18	0.35	3.5	5.8	3.5
F6	0.23	0.51	43	0.27	0.74	3.0	9.6	0.43	4.0	20	17	0.49	2.7	6.7	3.0
UF1	0.082	0.024	3.4	0.024	0.10	0.35	1.6	0.71	1.3	12	1.5	0.067	0.50	0.047	10
UF2	0.024	0.013	1.7	0.033	0.018	0.34	0.56	0.25	0.74	6.3	3.0	0.10	0.028	0.030	6.0
UF3	0.12	0.024	2.0	0.038	0.41	0.31	1.6	0.61	0.98	13	3.2	0.091	0.42	0.29	13
UF4	0.041	0.010	1.8	0.041	0.27	0.26	0.43	0.42	0.86	11	5.7	0.10	0.31	0.71	12
UF5	0.038	0.024	1.3	0.038	0.20	0.22	0.41	0.35	0.95	11	5.3	0.042	0.47	1.1	13
UF6	0.10	0.012	1.5	0.006	0.036	0.18	0.51	0.17	0.94	4.3	5.1	0.17	0.21	0.27	9.5
UF7	0.13	0.047	2.5	0.019	0.22	0.25	0.78	0.82	0.73	10	5.9	0.15	0.27	0.88	9.3
UF8	0.070	0.010	1.0	0.025	0.11	0.090	0.42	0.26	1.0	8.1	7.8	0.021	0.44	1.9	9.3

Table B.4: Different amine concentrations measured in ambient coarse (C), fine (F) and quasi-ultrafine (UF) PM (unit: $\mu g/m^3$)

Sample ID	Monomethyl amine (MMA)	Monoethyl amine (MEA)	Trimethyl amine (TMA)	Diethyl amine (DEA)	Triethyl amine (TEA)
C2	-	-	-	-	0.036
F3	-	-	-	0.099	-
F6	-	-	-	0.048	-
UF1	0.72	9.2	31	17	19
UF2	-	3.1	17	9.5	11
UF3	0.60	11	32	18	17
UF4	-	11	33	18	17
UF5	1.3	11	31	17	18
UF6	0.05	4.8	21	12	12
UF7	-	4.4	19	11	8.4
UF8	0.10	12	31	17	16

Table B.5: Dose-response slope values for different elements for coarse (C), fine (F) and quasi-ultrafine (UF) PM ((m)- mRNA, (p)- protein, CV- cell viability, significantly different slopes are indicated in bold, $p < 0.05$)

Elements	Size	HMOX-1	IL-8 (m)	IL-8 (p)	CV	Elements	Size	HMOX-1	IL-8 (m)	IL-8 (p)	CV
Total PM mass	C	0.017	0.018	0.003	-0.22	**Na**	C	1.2E-4	**2.4E-4**	2.8E-5	-0.003
	F	0.009	0.023	0.002	-0.14		F	2.6E-4	**4.5E-4**	1.0E-4	-0.003
	UF	0.012	0.021	0.003	-0.079		UF	0.004	**0.004**	0.001	-0.027
Al	C	0.001	**0.001**	2.1E-4	**-0.015**	**Si**	C	0.002	0.001	3.3E-4	-0.015
	F	0.001	**0.003**	3.2E-4	**-0.011**		F	6.3E-5	0.002	-1.2E-4	-0.007
	UF	0.009	**0.074**	0.005	**-0.35**		UF	0.002	0.001	2.0E-4	-0.008
Ba	C	0.015	**0.012**	0.003	**-0.14**	**Ti**	C	0.029	**0.024**	0.005	**-0.30**
	F	0.008	**0.014**	0.003	**-0.059**		F	0.018	**0.034**	0.006	**-0.14**
	UF	0.060	**0.29**	0.020	**-2.2**		UF	0.42	**0.72**	0.090	**-3.7**
Ca	C	1.1E-4	**1.4E-4**	2.5E-5	**-0.002**	**Zn**	C	**0.017**	**0.013**	0.003	**-0.16**
	F	1.6E-4	**3.2E-4**	4.3E-5	**-0.001**		F	**0.003**	**0.006**	0.001	**-0.034**
	UF	0.004	**0.008**	0.001	**-0.047**		UF	**0.010**	**0.019**	0.002	**-0.10**
Cr	C	**0.13**	**0.12**	0.023	**-1.4**	**OM**	C	**0.11**	**0.12**	**0.021**	**-1.3**
	F	**0.030**	**0.039**	0.013	**-0.18**		F	**0.036**	**0.076**	**0.012**	**-0.41**
	UF	**0.038**	**0.026**	0.007	**0.009**		UF	**0.018**	**0.020**	**0.004**	**-0.086**
Cu	C	0.018	**0.014**	0.003	**-0.16**	**OM-1**	C	**0.26**	**0.27**	**0.048**	**-2.8**
	F	0.012	**0.020**	0.004	**-0.092**		F	**0.078**	**0.16**	**0.025**	**-0.85**
	UF	0.021	**0.308**	0.026	**-1.4**		UF	**0.020**	**0.022**	**0.004**	**-0.094**

Elements	Size	HMOX-1	IL-8 (m)	IL-8 (p)	CV	Elements	Size	HMOX-1	IL-8 (m)	IL-8 (p)	CV
	C	0.001	**4.6E-4**	9.7E-5	**-0.006**		C	0.72	0.68	0.13	**-7.1**
Fe	F	3.4E-4	**0.001**	1.2E-4	**-0.003**	**OM-2**	F	0.26	0.56	0.090	**-3.6**
	UF	0.003	**0.006**	0.001	**-0.019**		UF	0.38	0.54	0.084	**-2.4**
	C	0.001	**0.001**	1.8E-4	-0.014		C	0.46	**0.62**	0.099	-6.6
Mg	F	0.001	**0.002**	3.2E-4	-0.013	**OM-3**	F	0.34	**0.68**	0.11	-3.5
	UF	0.018	**0.028**	0.004	-0.165		UF	1.1	**1.4**	0.29	-6.2
	C	0.020	**0.022**	0.004	**-0.29**		C	0.40	**0.40**	0.076	-4.8
Mn	F	0.006	**0.016**	0.001	**-0.081**	**OM-4**	F	0.11	**0.26**	0.037	-1.4
	UF	0.077	**0.14**	0.020	**-0.71**		UF	0.35	**0.60**	0.086	-2.9

Table B.6: Spearman correlation coefficients between selected elements and biological endpoints ((m)- mRNA, (p)- protein, CV- cell viability, significant correlations are indicated in bold, p <0.05)

Size	Endpoint	Acid Soluble metals												Organic mass					Redox Activity
		Al	Ba	Ca	Cr	Cu	Fe	Mg	Mn	Na	Si	Ti	Zn	OM	OM-1	OM-2	OM-3	OM-4	
Coarse	HMOX-1	**0.54**	**0.70**	**0.55**	**0.74**	**0.66**	**0.64**	**0.53**	**0.53**	**0.79**	**0.66**	**0.53**	**0.55**	**0.75**	**0.68**	**0.78**	**0.80**	**0.59**	**0.59**
	IL-8 (m)	**0.71**	**0.64**	**0.65**	**0.64**	**0.54**	**0.70**	**0.70**	**0.72**	**0.60**	**0.62**	**0.63**	**0.68**	**0.76**	**0.69**	**0.59**	**0.66**	**0.74**	**0.50**
	IL-8 (p)	0.41	**0.69**	0.39	**0.69**	**0.67**	**0.73**	0.41	0.42	0.31	**0.80**	**0.70**	**0.71**	**0.65**	**0.72**	**0.61**	0.36	**0.70**	**0.71**
	CV (-)	**-0.84**	**-0.84**	**-0.80**	**-0.84**	**-0.82**	**-0.92**	**-0.82**	**-0.84**	**-0.60**	**-0.86**	**-0.89**	**-0.91**	**-0.82**	**-0.73**	**-0.73**	**-0.64**	**-0.88**	**-0.77**
Fine	HMOX-1	0.36	**0.51**	0.34	**0.62**	**0.56**	**0.55**	**0.51**	**0.52**	0.46	0.34	**0.55**	**0.49**	**0.55**	**0.54**	**0.62**	**0.55**	**0.64**	**0.76**
	IL-8 (m)	**0.85**	**0.95**	**0.84**	**0.80**	**0.95**	**0.94**	**0.84**	**0.78**	**0.82**	**0.58**	**0.91**	**0.94**	**0.92**	**0.91**	**0.87**	**0.92**	**0.83**	**0.71**
	IL-8 (p)	0.22	0.02	0.21	-0.18	0.03	0.09	0.00	0.37	-0.08	0.15	0.08	0.01	0.10	0.09	0.07	0.10	0.27	0.18
	CV (-)	**-0.64**	**-0.68**	**-0.61**	**-0.81**	**-0.75**	**-0.72**	**-0.90**	**-0.63**	**-0.91**	**-0.69**	**-0.67**	**-0.87**	**-0.77**	**-0.77**	**-0.91**	**-0.77**	**-0.71**	**-0.76**
Quasi-ultrafine	HMOX-1	0.27	0.40	0.42	**0.54**	0.35	**0.57**	0.40	**0.57**	**0.64**	**0.67**	**0.57**	**0.48**	**0.56**	**0.58**	**0.60**	**0.60**	**0.46**	**0.62**
	IL-8 (m)	**0.70**	**0.53**	**0.57**	**0.46**	**0.61**	**0.65**	**0.80**	**0.71**	**0.76**	**0.76**	**0.80**	**0.79**	**0.78**	**0.78**	**0.80**	**0.78**	**0.75**	**0.71**
	IL-8 (p)	0.33	0.08	0.35	0.30	0.26	0.29	0.31	0.35	0.40	**0.47**	**0.54**	**0.45**	**0.62**	**0.63**	**0.49**	**0.51**	**0.51**	**0.52**
	CV (-)	-0.40	**-0.68**	**-0.57**	0.10	**-0.44**	-0.42	-0.38	**-0.62**	**-0.48**	**-0.63**	**-0.52**	**-0.65**	**-0.44**	**-0.50**	**-0.61**	**-0.54**	**-0.49**	**-0.45**

Table B.7: Spearman correlation coefficients between amines and biological endpoints for quasi-ultrafine particles (significant correlations are indicated in bold, p <0.05)

Endpoints	MMA	MEA	TMA	DEA	TEA
HMOX-1	0.17	0.38	**0.44**	**0.44**	0.40
IL-8 (m)	0.38	**0.69**	**0.72**	**0.72**	**0.73**
IL-8 (p)	**0.57**	**0.51**	**0.49**	**0.49**	**0.63**
CV	**-0.60**	-0.27	**-0.51**	**-0.51**	**-0.48**

(m)- mRNA, (p)- protein, CV- cell viability

Table B.8: Spearman correlation coefficients between particle number concentration and surface area with biological responses for quasi-ultrafine particles (significant correlations are indicated in bold, p <0.05)

	HMOX-1	IL-8 (m)	IL-8 (p)	CV
Number concentration	0.09	-0.62	-0.32	**0.78**
Surface area	-0.12	-0.52	-0.39	0.69

(m)- mRNA, (p)- protein, CV- cell viability

Table B.9: Spearman correlation coefficients between biological endpoints (significant correlations are indicated in bold, $p < 0.05$)

Size	Endpoint	HMOX-1	IL-8 (m)	IL-8 (p)
Coarse	**IL-8 (m)**	**0.55**		
	IL-8 (p)	0.28	0.34	
	CV	**-0.49**	**-0.67**	**-0.65**
Fine	**IL-8 (m)**	**0.56**		
	IL-8 (p)	0.05	-0.07	
	CV	**-0.50**	**-0.78**	0.00
Quasi-ultrafine	**IL-8 (m)**	**0.55**		
	IL-8 (p)	0.21	**0.63**	
	CV	-0.28	**-0.46**	-0.16

(m)- mRNA, (p)- protein, CV- cell viability

Table B.10: Spearman correlation coefficients between selected elements of concentrated coarse particles (significant correlations are indicated in bold, $p < 0.05$)

Element	Al	Ba	Ca	Cr	Cu	Fe	Mg	Mn	Na	Si	Ti	Zn	OM	OM-1	OM-2	OM-3
Ba	**0.844**															
Ca	**0.991**	**0.830**														
Cr	**0.858**	**0.979**	**0.847**													
Cu	**0.857**	**0.981**	**0.861**	**0.969**												
Fe	**0.860**	**0.973**	**0.832**	**0.964**	**0.956**											
Mg	**0.992**	**0.843**	**0.994**	**0.845**	**0.862**	**0.852**										
Mn	**0.999**	**0.842**	**0.992**	**0.852**	**0.856**	**0.858**	**0.996**									
Na	**0.736**	**0.762**	**0.762**	**0.791**	**0.766**	**0.726**	**0.762**	**0.739**								
Si	**0.752**	**0.966**	**0.726**	**0.949**	**0.932**	**0.965**	**0.744**	**0.749**	**0.666**							
Ti	**0.888**	**0.961**	**0.866**	**0.938**	**0.961**	**0.971**	**0.881**	**0.887**	**0.652**	**0.934**						
Zn	**0.879**	**0.964**	**0.853**	**0.935**	**0.952**	**0.983**	**0.875**	**0.881**	**0.664**	**0.945**	**0.995**					
OM	**0.823**	**0.940**	**0.809**	**0.939**	**0.896**	**0.930**	**0.835**	**0.827**	**0.857**	**0.917**	**0.870**	**0.895**				
OM-1	**0.539**	**0.769**	**0.503**	**0.781**	**0.699**	**0.810**	**0.543**	**0.543**	**0.692**	**0.844**	**0.682**	**0.730**	**0.879**			
OM-2	**0.726**	**0.927**	**0.738**	**0.910**	**0.914**	**0.886**	**0.753**	**0.731**	**0.895**	**0.888**	**0.829**	**0.845**	**0.945**	**0.827**		
OM-3	**0.748**	**0.838**	**0.761**	**0.819**	**0.813**	**0.786**	**0.777**	**0.752**	**0.958**	**0.747**	**0.721**	**0.742**	**0.900**	**0.716**	**0.938**	
OM-4	**0.873**	**0.949**	**0.853**	**0.922**	**0.925**	**0.964**	**0.888**	**0.881**	**0.761**	**0.925**	**0.945**	**0.965**	**0.960**	**0.808**	**0.897**	**0.825**

Table B.11: Spearman correlation coefficients between selected elements of concentrated fine particles (significant correlations are indicated in bold, $p < 0.05$)

Element	Al	Ba	Ca	Cr	Cu	Fe	Mg	Mn	Na	Si	Ti	Zn	OM	OM-1	OM-2	OM-3
Ba	**0.938**															
Ca	**0.998**	**0.934**														
Cr	**0.639**	**0.773**	**0.618**													
Cu	**0.917**	**0.983**	**0.913**	**0.812**												
Fe	**0.946**	**0.986**	**0.942**	**0.773**	**0.992**											
Mg	**0.754**	**0.808**	**0.736**	**0.917**	**0.849**	**0.833**										
Mn	**0.926**	**0.856**	**0.917**	**0.651**	**0.860**	**0.889**	**0.713**									
Na	**0.697**	**0.771**	**0.674**	**0.928**	**0.804**	**0.777**	**0.983**	**0.647**								
Si	**0.746**	**0.674**	**0.732**	**0.771**	**0.690**	**0.697**	**0.816**	**0.771**	**0.787**							
Ti	**0.955**	**0.975**	**0.953**	**0.754**	**0.971**	**0.983**	**0.781**	**0.926**	**0.728**	**0.715**						
Zn	**0.812**	**0.860**	**0.806**	**0.734**	**0.903**	**0.891**	**0.847**	**0.765**	**0.825**	**0.583**	**0.853**					
OM	**0.926**	**0.961**	**0.922**	**0.806**	**0.983**	**0.988**	**0.882**	**0.876**	**0.822**	**0.746**	**0.961**	**0.901**				
OM-1	**0.932**	**0.953**	**0.928**	**0.825**	**0.975**	**0.979**	**0.889**	**0.901**	**0.833**	**0.796**	**0.967**	**0.895**	**0.994**			
OM-2	**0.771**	**0.816**	**0.756**	**0.876**	**0.878**	**0.868**	**0.961**	**0.789**	**0.924**	**0.759**	**0.829**	**0.917**	**0.913**	**0.920**		
OM-3	**0.926**	**0.961**	**0.922**	**0.806**	**0.983**	**0.988**	**0.882**	**0.876**	**0.822**	**0.746**	**0.961**	**0.901**	**1.000**	**0.994**	**0.913**	
OM-4	**0.882**	**0.911**	**0.872**	**0.789**	**0.936**	**0.946**	**0.841**	**0.901**	**0.767**	**0.771**	**0.924**	**0.798**	**0.963**	**0.957**	**0.876**	**0.963**

Table B.12: Spearman correlation coefficients between selected elements of concentrated quasi-ultrafine particles (significant correlations are indicated in bold, $p < 0.05$)

Element	Al	Ba	Ca	Cr	Cu	Fe	Mg	Mn	Na	Si	Ti	Zn	OM	OM-1	OM-2	OM-3
Ba	**0.807**															
Ca	**0.917**	**0.750**														
Cr	0.166	0.223	0.116													
Cu	**0.843**	**0.806**	**0.748**	0.303												
Fe	**0.664**	**0.791**	**0.612**	**0.723**	**0.778**											
Mg	**0.801**	**0.681**	**0.897**	0.257	**0.647**	**0.613**										
Mn	**0.742**	**0.876**	**0.755**	**0.537**	**0.851**	**0.950**	**0.711**									
Na	**0.751**	**0.715**	**0.850**	0.321	**0.531**	**0.643**	**0.943**	**0.709**								
Si	**0.593**	**0.637**	**0.804**	0.371	**0.503**	**0.690**	**0.766**	**0.787**	**0.822**							
Ti	**0.823**	**0.773**	**0.880**	**0.465**	**0.676**	**0.786**	**0.860**	**0.846**	**0.903**	**0.854**						
Zn	**0.910**	**0.845**	**0.970**	0.230	**0.811**	**0.733**	**0.884**	**0.864**	**0.857**	**0.830**	**0.929**					
OM	**0.723**	**0.514**	**0.847**	0.386	**0.582**	**0.592**	**0.780**	**0.676**	**0.777**	**0.837**	**0.890**	**0.834**				
OM-1	**0.711**	**0.515**	**0.840**	0.389	**0.617**	**0.599**	**0.779**	**0.693**	**0.757**	**0.830**	**0.875**	**0.834**	**0.995**			
OM-2	**0.790**	**0.786**	**0.878**	**0.450**	**0.714**	**0.797**	**0.817**	**0.887**	**0.848**	**0.896**	**0.977**	**0.942**	**0.897**	**0.895**		
OM-3	**0.749**	**0.746**	**0.830**	**0.526**	**0.639**	**0.809**	**0.779**	**0.862**	**0.845**	**0.897**	**0.980**	**0.894**	**0.897**	**0.883**	**0.986**	
OM-4	**0.817**	**0.756**	**0.854**	**0.419**	**0.665**	**0.750**	**0.754**	**0.820**	**0.811**	**0.827**	**0.972**	**0.901**	**0.899**	**0.880**	**0.963**	**0.974**

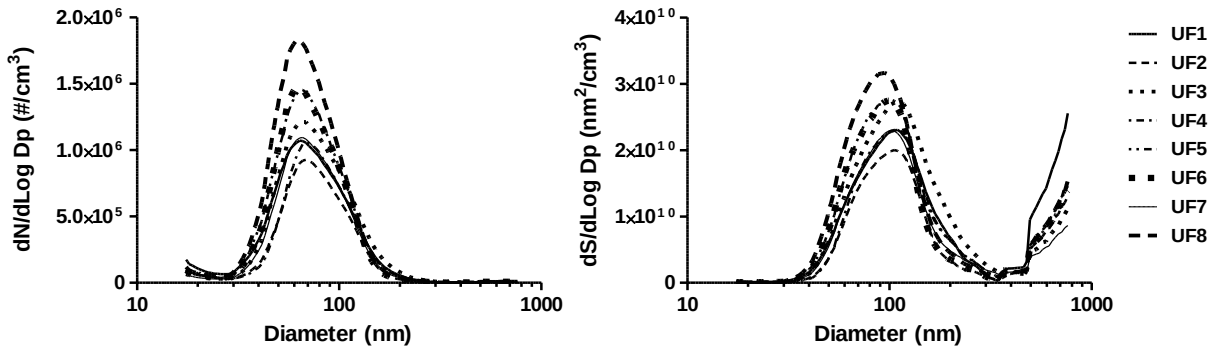

Figure B.1: Size distribution of time averaged A) number concentration (dN/dLogDp, #/cm^3) and B) surface area (dS/dLogDp, nm^2/cm^3) of concentrated ambient ultrafine particles (CAP) during the HEAT campaign.

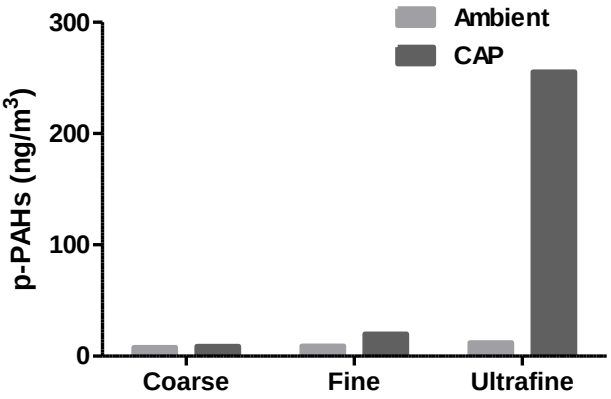

Figure B.2: Particle bound polycyclic aromatic hydrocarbons (p-PAHs) concentration of ambient and concentrated ambient particles (CAP) for different sized PM during the HEAT campaign.

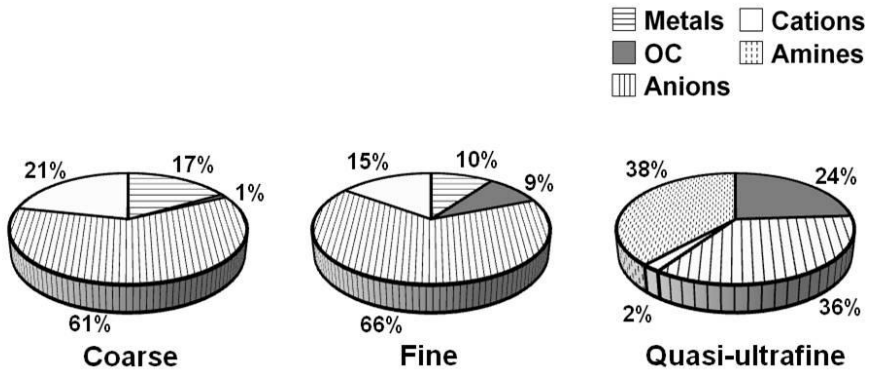

Figure B.3: Average contribution of water-soluble metals, anions, cations, amines, and organic carbon (OC) to total water-soluble elements of ambient coarse, fine, and quasi-ultrafine PM (anions = NO_3^-, SO_4^{2-}, $C_2O_4^-$, PO_4^{3-}, Cl^-; cations = Na^+, K^+, NH_4^+).

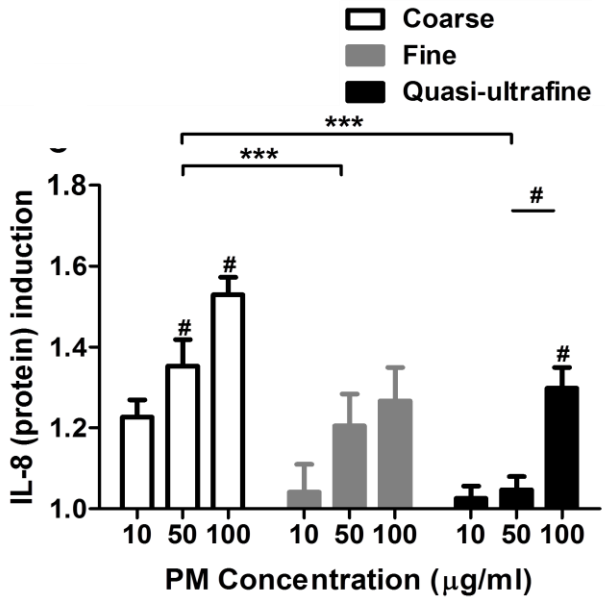

Figure B.4: Effect of different size-fractionated ambient PM on IL-8 protein expression. A549 cells were exposed to coarse, fine, and ultrafine PM at mass concentrations of 10, 50, and 100 μg/ml (mass/volume) for 4 h. IL-8 expressions are presented as fold change relative to controls. The data are presented as mean ± SEM (n = 21, 18, and 24 for coarse, fine, and ultrafine, respectively). Statistically significant differences from control and in between concentrations # ($p < 0.05$) and between sizes of PM *, **, *** $p < 0.05$, 0.01, 0.001, respectively).

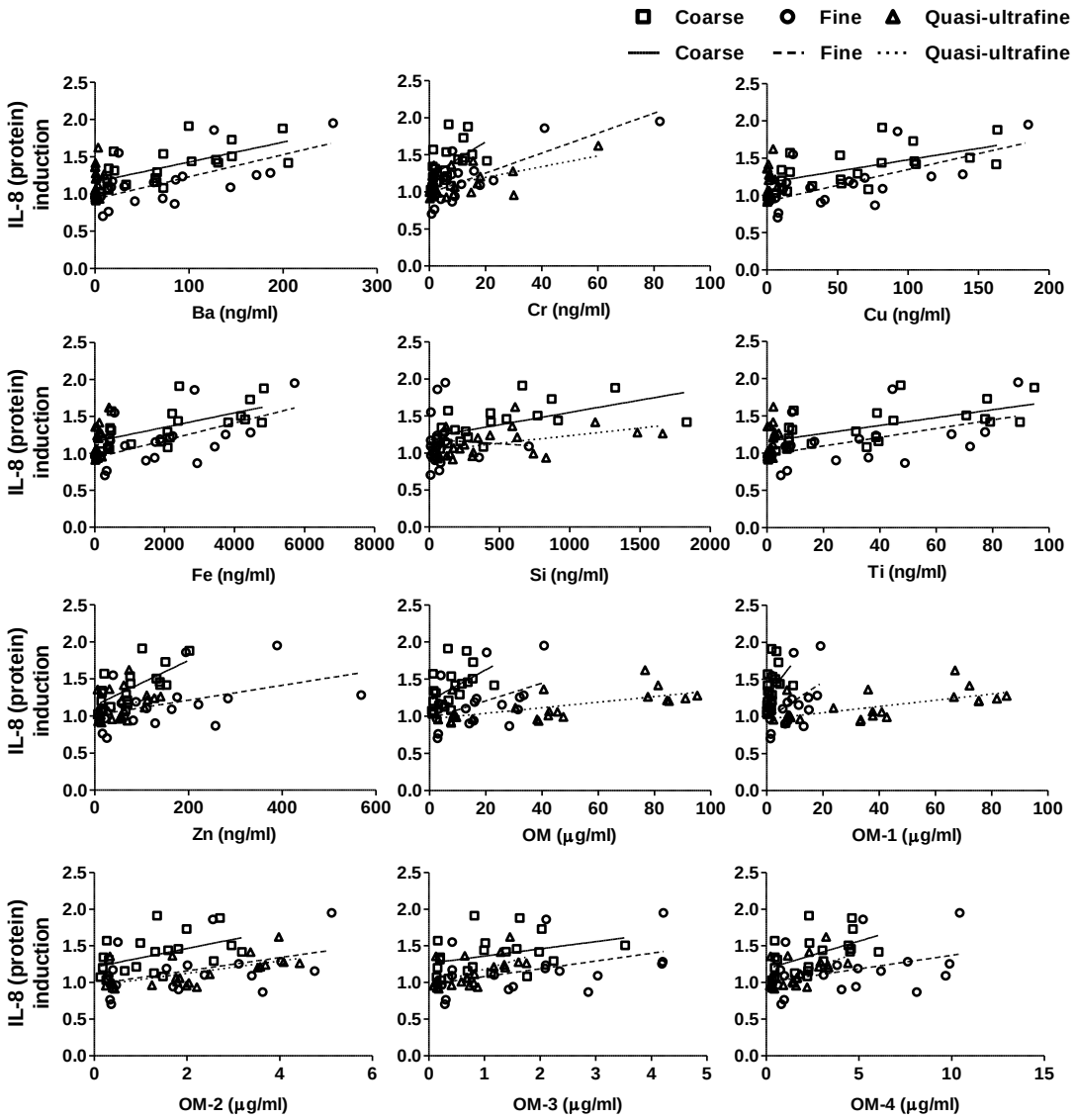

Figure B.5: Scatter plots of selected chemical elements with IL-8 (protein) for coarse, fine, and quasi-ultrafine PM.

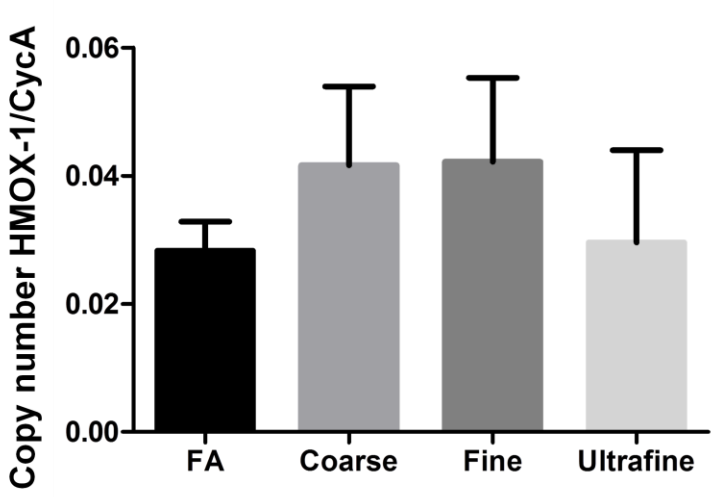

Figure B.6: HMOX-1 (mRNA) upregulation (normalized to CycA) in mice lung tissues after exposure to filter air (FA), coarse, fine, and quasi-ultrafine PM. The data are presented as mean ± SEM (n = 7 for FA and 10 for coarse, fine, and ultrafine).

Appendix C

Particle deposition and clearance mechanisms and computational modeling of particle deposition in the respiratory tract

1. Introduction

Human exposure to particulate matter (PM) occurs mostly via the respiratory tract during inhalation. Particles are transported with inspired air and a fraction of these particles is retained in the respiratory tract by deposition (Schulz et al., 2000). Deposited particles may instigate different respiratory diseases in human and the extent of such harmful effects depends on the clearance and/or translocation (into the blood or other organs) rates of the deposited particles. PM deposition and clearance strongly depends on the particle size, different physiological conditions, and structure of the respiratory tract (Schlesinger, 1995). Several computation models have been developed to predict the PM deposition fraction in the lung. In this chapter, the anatomical structure of the lung, particle deposition and clearance mechanisms, and different computational particle deposition models are briefly discussed.

2. Structure of the respiratory tract

Human respiratory tract is divided into three anatomical regions as illustrated in **Figure C.1**. These regions are distinctively different in their structure, airflow patterns, function, retention time, and sensitivity to deposited particles (ICRP, 1994; USEPA, 2004). The first region is extrathoracic (ET) region, also known as head airways or upper airways region. This region includes anterior nose, posterior nasal passage, larynx, pharynx, and mouth. ET region plays an important role in filtration and humidification of the inhaled air (ICRP, 1994). The second region is tracheobronchial region (TB); consisting of trachea, bronchi, and bronchioles (including terminal bronchioles). TB region is also called conducting airways region as the main function of this region is to transport air to and from the gas exchanging region of the lung. The last region is alveolar (A) or pulmonary region which includes respiratory bronchioles, alveolar ducts, alveolar

sacs, and alveoli. The main function of this region is to gas exchange between lung and blood (Hinds, 1999; USEPA, 2004).

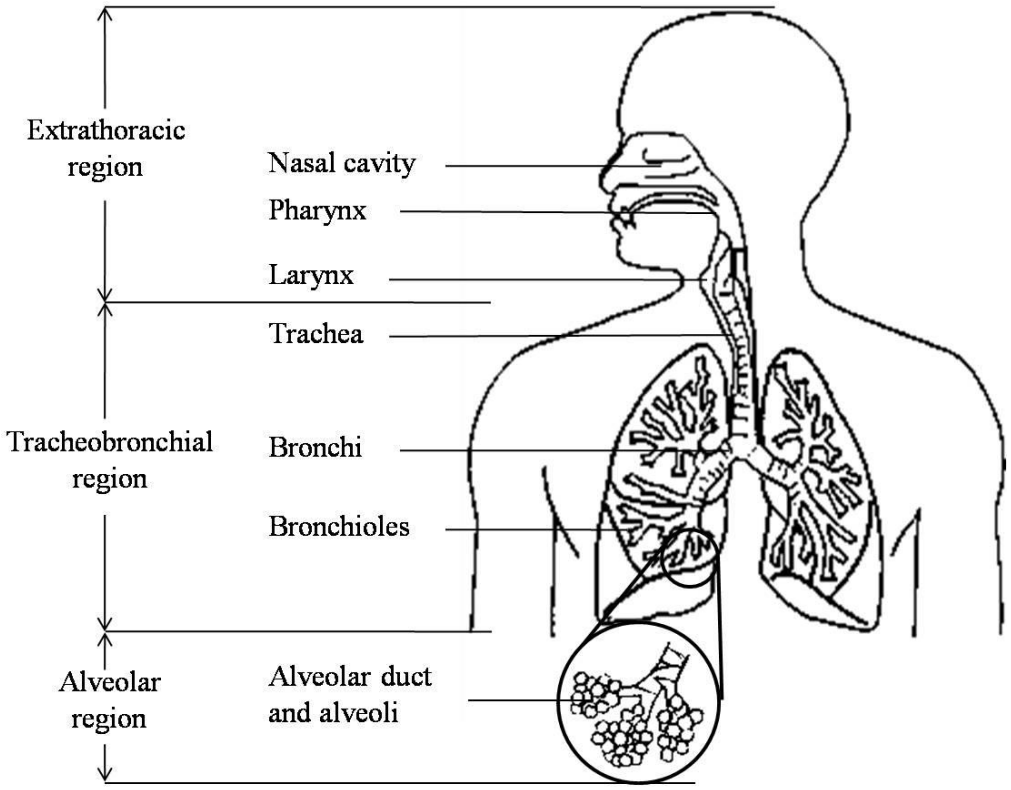

Figure C.1: Schematic diagram of human respiratory tract (adapted from ICRP, 1994).

For computational purposes, these three regions are divided into 23 generations (ICRP, 1994; Weibel, 1963). According to Weibel's symmetric lung morphometry model, every parent airway is divided into two identical branches with equal diameters and lengths and the dichotomous branching process continues from trachea down to alveolar sacs. Based on Murray's optimal branching law (Murray, 1926), the number of the identical airways is calculated as 2^n, where n is the generation number. Weibel proposed the following equations for airway internal diameter (d) and length (l) calculation.

For generations n = 0 to 3:

$$d = 1.8e^{-0.388n} \quad \ldots\ldots\ldots\ldots\ldots\ldots (1)$$

$$l = 12e^{-0.92n} \text{……(2)}$$

For generations *n* = 4 to 23:

$$d = 1.3e^{-0.293n+0.00624n^2} \text{……(3)}$$

$$l = 2.5e^{-0.17n} \text{……(4)}$$

Based on this model, different physical characteristics for different regions of the respiratory tract were calculated (**Table C.1**). The airways become narrower and shorter as proceeds down from trachea to alveoli. Total cross sectional area changes rapidly in the alveolar region due to large number of small airways. For inhalation at a steady rate, the velocity will gradually decrease along the airways with the increase in total airways cross sectional area as the air proceeds down toward alveoli. Therefore, the residence time of inhaled air will be higher in the alveolar sacs as compared to the trachea.

3. Particle deposition mechanisms in the lung

An airborne particle may deposits on the lung surface during its transit through the airways. Inhaled PM may deposits within the respiratory tract by the complex action of the five different mechanisms. The major three deposition mechanisms are sedimentation, diffusion, and inertial impaction. The other two minor mechanisms are interception and electrostatic precipitation (USEPA, 2004). The relative contribution of these mechanisms toward overall particle deposition depends largely on particle size and anatomical structure of the lung. The mechanisms are shown schematically in **Figure C.2**.

3.1 Sedimentation

Sedimentation occurs at a rate governed by the balance between the gravitational force and the viscous resistance of the air. As an upper limit the PM can achieve its terminal settling velocity (V_t). According to Stoke's law (USEPA, 1996)

$$(\pi/6)(\rho-\rho_{air})d_p^3 g = 3\pi\mu d_p V_t \text{ ……(5)}$$

where d_p is the particle diameter, ρ is the particle density, ρ_{air} is the air density, g is the

acceleration of gravity, and μ is the viscous resistance of the air.

Assuming the effect of ρ_{air} on the particle is minimal, V_t can be calculated as

$$V_t = \frac{d_p^2 \rho g K_s}{18\mu} \quad \ldots\ldots\ldots\ldots\ldots\ldots(6)$$

where K_s is the slip correction factor for particles with $d_p \leq 1\mu m$. By assuming the respiratory tract as randomly oriented cylindrical tubes, the deposition probability by sedimentation (P_S) in cylindrical airways is calculated as (Yeh and Schum, 1980):

$$P_S = 1\text{-}\exp\left[\frac{-2gK_s d_p^2 l \cos\varphi}{9\pi\mu d\bar{\upsilon}}\right] \quad \ldots\ldots\ldots\ldots\ldots\ldots(7)$$

where $\bar{\upsilon}$ is the mean flow velocity and φ is the inclination angle relative to gravity (φ = 0º for horizontal tube). Therefore, sedimentation of PM is common with increasing particle size (d_p >0.5 μm) and in the regions where air velocity is low and particle residence times are high, i.e., in the bronchiolar and alveolar regions. For sedimentation, the settling distance (S_s) can be defined as the terminal velocity multiplied by the residence time (Rostami, 2009).

$$S_S = V_t t \ldots\ldots\ldots\ldots\ldots\ldots(8)$$

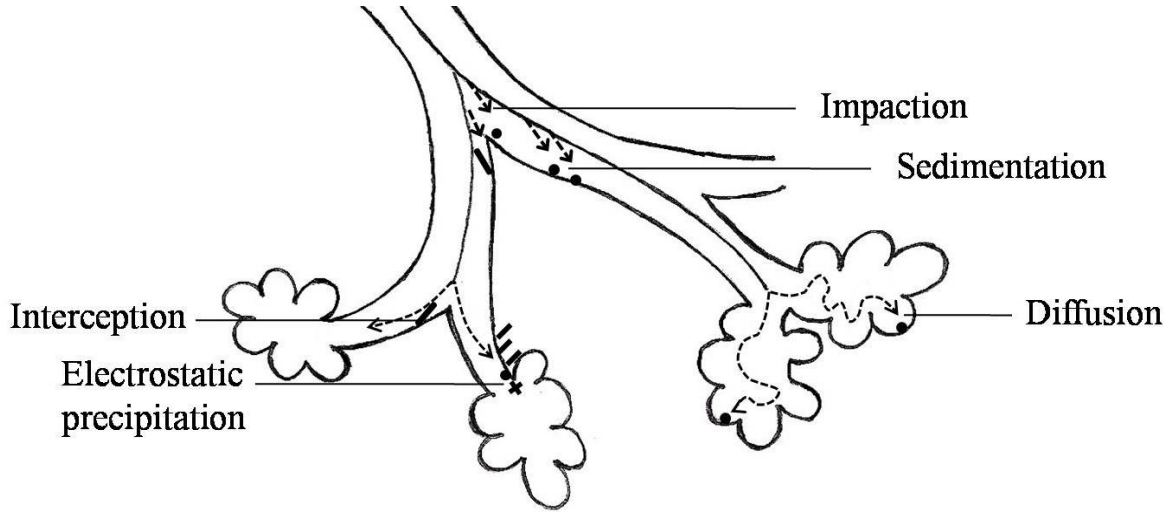

Figure C.2: Deposition mechanisms in the respiratory tract (adapted from McClellan, 2000).

Table C.1: Calculation of different physical characteristics for different regions of the respiratory tract

Airway segment	Generation number	Number of airways	Diameter (cm)	Length (cm)	Total cross-section (cm^2)	Volume (cm^3)	Residence time (ms)	Velocity (cm/s)
Trachea	0	1	1.8	12	2.5	31	244	49.1
Main bronchus	1	2	1.22	4.78	2.3	11	90	53.4
Bronchus	2	4	0.83	1.91	2.2	4	33	58.0
Bronchiolus	3	8	0.56	0.76	2.0	2	12	63.0
	4	16	0.44	1.27	2.5	3	25	50.3
	5	32	0.35	1.07	3.1	3	26	40.4
	6	64	0.28	0.90	4.0	4	29	31.6
	7	128	0.23	0.76	5.2	4	31	24.1
	8	256	0.19	0.64	6.9	4	36	18.0
	9	512	0.15	0.54	9.6	5	41	13.1
	10	$1.0x10^3$	0.13	0.46	13.5	6	49	9.3
	11	$2.0\ x10^3$	0.11	0.39	19.5	8	60	6.4
	12	$4.1\ x10^3$	0.09	0.33	28.9	9	75	4.3
	13	$8.2\ x10^3$	0.08	0.27	44.0	12	97	2.8
	14	$1.6\ x10^4$	0.07	0.23	68.6	16	127	1.8
	15	$3.3\ x10^4$	0.07	0.20	$1.1\ x10^2$	21	171	1.1

Airway segment	Generation number	Number of airways	Diameter (cm)	Length (cm)	Total cross-section (cm^2)	Volume (cm^3)	Residence time (ms)	Velocity (cm/s)
Terminal bronchiolus	16	6.6×10^4	0.06	0.16	1.8×10^2	30	237	0.70
Respiratory bronchiolus	17	1.3×10^5	0.05	0.14	3.0×10^2	42	336	0.41
	18	2.6×10^5	0.05	0.12	5.2×10^2	61	488	0.24
	19	5.2×10^5	0.05	0.10	9.2×10^2	91	727	0.14
Alveolar duct	20	1.0×10^6	0.04	0.08	1.7×10^3	139	1111	0.08
	21	2.1×10^6	0.04	0.07	3.1×10^3	218	1741	0.04
	22	4.2×10^6	0.04	0.06	5.9×10^3	350	2796	0.02
Alveolus	23	8.4×10^6	0.04	0.05	1.1×10^4	576	4604	0.01

Residence time = volume/minute ventilation rate.

Minute ventilation rate = tidal volume X breathing frequency = 625 ml × 12 #/min = 0.45 m^3/h

Tidal volume (625 ml) and breathing frequency (12/min) for an adult male at sleeping condition (ICRP, 1994)

3.2 Diffusion

Deposition by diffusion occurs due to collision of particles with air molecules following Brownian motion. This is the primary mode of deposition in the alveoli where air velocity is low and the residence time of the particles is longer. The mechanism is more prominent for submicrometre-sized particles (d_p <1 μm) as smaller particles have higher mobility and larger diffusion coefficient (Rostami, 2009; USEPA, 1996). The deposition probability by diffusion (P_D) in cylindrical airways can be calculated as (Yeh and Schum, 1980):

For laminar flow,

$$P_D = 1 - 0.819\, e^{-7.315x} - 0.0976\, e^{-44.61x} - 0.0325\, e^{-114x} - 0.0509\, e^{-79.31x^{2/3}} \quad \ldots\ \ldots (9)$$

where $x = \frac{2lD}{d^2\bar{\upsilon}}$ and D is diffusion coefficient of particles expressed by Stokes-Einstein equation as (USEPA, 1996):

$$D = \frac{kTK_s}{3\pi\mu d_p} \quad \ldots\ldots\ldots\ldots\ldots\ldots (10)$$

where k and T are the Boltzmann constant and absolute temperature, respectively.

For turbulent flow,

$$P_D = \frac{4\sqrt{Dt}}{d}\left(1 - \frac{4\sqrt{Dt}}{9d} + \ldots\ldots\right) \quad \ldots\ldots\ldots\ldots\ldots\ldots (11)$$

where t is the residence time in the airway determined by $l/\bar{\upsilon}$.

For diffusion mechanism, the diffusion length (S_D) can be calculated as (Rostami, 2009)

$$S_D = 2\sqrt{Dt} \quad \ldots\ldots\ldots\ldots\ldots\ldots (12)$$

3.3 Impaction

Impaction occurs when a particle fails to follow the airstream and contacts or impacts an airway surface (USEPA, 1996). It occurs due to particle inertia and resistance to change in the direction (Rostami, 2009). Therefore, impaction is generally observed where air velocities are higher and

airstream directional changes are abrupt, mainly in the upper respiratory tract and at or near airway branching points, for particles with a $d_p \geq 1$ μm. The likelihood of impaction increases with increasing mass (i.e. particle size and density). The deposition probability by impaction (P_I) is calculated as (USEPA, 1996)

$$P_I = 1-\frac{2}{\pi}\cos^{-1}(\theta.St) + \frac{1}{\pi}\sin\{2\cos^{-1}(\theta.St)\} \text{ for } \theta.St < 1 \quad \ldots\ldots\ldots\ldots\ldots\ldots(13)$$

$$P_I = 1 \text{ for } \theta.St \geq 1 \quad \ldots\ldots\ldots\ldots\ldots\ldots(14)$$

where θ is the bend angle or branching angle and St is the Stokes number expressed as $\frac{\rho d_p^2 K_s \bar{\upsilon}}{18\mu d}$.

Stopping distance (S_I) for impaction deposition, defined as the distance travelled by a particle before a considerable change in direction, can be calculated as

$$S_I = V_p \tau \quad \ldots\ldots\ldots\ldots\ldots\ldots(15)$$

where V_p is the particle initial velocity and τ is the relaxation time expressed as $\frac{\rho d_p^2 K_s}{18\mu}$.

3.4 Interception

Interception occurs when a particle is able to follow its gas streamline but comes into close physical contact with the airway surfaces for its unique shape and physical size (Rostami, 2009). This mechanism is dominant in the small airways for particles with elongated structure such as fibers. Fibers can conveniently follow the air streamline and reach the small airways. The possibility of deposition on fibers increases as their length approaches the diameters of small airways (USEPA, 1996). Equivalent mass diameter (d_{em}) for fibers can be calculated as (Asgharian and Yu, 1988)

$$d_{em} = d_f \beta^{\frac{1}{3}} \quad \ldots\ldots\ldots\ldots\ldots\ldots(16)$$

where d_f is the fiber diameter and β is its aspect ratio (length/diameter). Therefore, for a fiber with 100 μm length and 1 μm diameter, d_{em} would be 4.6 μm.

3.5 Electrostatic precipitation

Particles, naturally neutral, can acquire charges by collision with air molecules during their random thermal motion. These charged particles may be attracted to the airways surface because of the image charges induced by these particles on the surface or repulsive action of highly concentrated unipolar particles. The contribution of deposition by electrostatic precipitation to overall particle deposition is relatively negligible as compared to other mechanisms. This mechanism is also considered negligible for particles with d_p <0.01 μm as very few particles in these size range can carry enough charge (USEPA, 1996).

4. Factors affecting deposition of inhaled particles

In addition to particle size and anatomical structure of the lung, some biological factors also influence the particle deposition pattern in the respiratory tract. Some of these contributing factors are discussed in this section.

4.1 Physical activity

Typically air is inhaled through the nose during resting position. The route may change to oronasal or oral breathing in the case of nasal congestion or during excessive physical activity like running. During inhalation through nose, large particles are removed from the airstream by sedimentation and impaction on nasal hairs and at bends in the airflow path (ICRP, 1994). As the lung consists of three sequential regions (ET, TB, and A), more deposition in the upper respiratory tract would result in lower chance of deposition in the lower tract for those particles. Thus, the possibility of more particles reaching to the lower respiratory tract increases with the change of breathing route to oral or oronasal (ICRP, 1994). Increase in the physical activity level (from sleeping to heavy exercise) can cause higher tidal volume (V_T) and breathing frequency (f) in different age and sex groups (**Table C.2**) (ICRP, 1994). At a constant breathing frequency, for higher tidal volume inhaled particles travel deeper into the lung leading to higher deposition in the smaller conduction airways and pulmonary regions. However, the relationship with breathing frequency is not that straightforward. Increasing breathing frequency means increased air velocity and decreased residence time in the lung. Therefore, particle deposition by impaction

would increase due to higher air velocity rate. On the contrary, deposition by sedimentation and diffusion both would decrease because for lower residence time. Overall, the total particle deposition would depend on the relative influence of these two factors (V_T and f).

Table C.2: Breathing parameters for different physical activity levels (ICRP, 1994)

Parameters	Sleeping	Sitting (resting)	Light exercise	Heavy exercise
Male				
Tidal Volume, V_T (ml)	625	750	1250	1920
Breathing frequency, f (#/min)	12	12	20	26
Female				
Tidal Volume, V_T (ml)	444	464	992	1360
Breathing frequency, f (#/min)	12	14	21	33
Child (10 yr)				
Tidal Volume, V_T (ml)	304	333	583	752
Breathing frequency, f (#/min)	17	19	32	45

4.2 Age

The lung goes through developmental changes through childhood and into adolescence. Lung volume is smaller and airflow rate is higher in children as compared to adults (Murray, 1976). Thus, particle deposition pattern is expected to be different at different ages. Several studies have applied mathematical models to compare the total and regional depositions pattern of particles in children and adults. Phalen and Oldham (2001) and Musante and Martonen (1999) showed total fractional lung deposition was comparable and higher in children than adults, respectively. Both studies reported higher deposition pattern in the TB region in children. Similarly, limited experimental studies reported results ranging from no clear dependence of total deposition on age to slightly higher deposition in children than adults (Bennett and Zeman, 1998; Schiller-

Scotland et al., (1992). However, both experimental and theoretical studies have suggested that children would experience higher particle dose per lung surface area due to their smaller lung volumes as compared to that of adults.

4.3 Gender

Gender differences are observed in both neonatal lung development and physiology. Maturity in lung development is observed earlier in female than male fetuses. Surfactant production level is also higher in female fetuses which protect them from early development of respiratory distress syndrome (Fleisher et al., 1985). However, female lungs are smaller and weigh less in average than those of males at birth and continue to be that way into adolescence (Thurlbeck, 1982). The average size of female conducting airways is also smaller than those of adult males considering equivalent lung and body sizes (Martin et al., 1987). Thus, differences in PM deposition pattern are expected for males and females. Pritchard et al., (1986) suggested that due to differences in airway size, greater PM deposition occurs in the upper airways, and smaller deposition in the alveolar region, in females than males (for particle size range 2.5 to 7.5 μm). Kim and Hu (1998) showed a shift in maximum particle deposition from the peripheral to proximal regions with increasing particle size due to increased inertial impaction. However, localized particle deposition fraction was always higher for females for coarse particles. The smaller airways in females could contribute to additional deposition by impaction in the upper airways.

4.4 Airway obstruction

Chronic obstructive pulmonary disease (COPD) is one of the most common respiratory diseases (Buist et al., 2007) and is linked to PM exposure (Dockery et al., 1993; Hart et al., 2009; Sint et al., 2008). COPD is a long-term lung disease often combined by chronic bronchitis and emphysema**.** The lung of an individual with COPD suffers from different pathophysiological changes which cause alternations in both breathing pattern and lung morphology. COPD can cause airflow obstruction in the small conducting airways (<2 mm in diameter) due to chronic inflammation, loss of elasticity of the lung and destruction of the alveolar walls (Kirby et al., 2013; MacNee, 2006). COPD patients tend to breathe more frequently and more deeply than

health individuals resulting in higher f and V_T (Brown et al., 2002). Thus, COPD patients have higher ventilation rate (V_{min}) which is defined as the multiplication of tidal volume with breathing frequency. Several studies showed that COPD patients experienced higher deposited dose rate of inhaled fine (Bennett et al., 1997) and ultrafine particles (Brown et al., 2002; Löndahl et al., 2012) relative to healthy subjects, suggesting their susceptibility to PM exposure.

5. Particle clearance mechanisms in the lung

Particles that are deposited on the airway surface are either cleared from the respiratory tract or translocated to other pulmonary regions or to extrapulmonary organs. The clearance mechanisms and rates depend on the location of PM deposition and solubility of the particles. Poorly soluble particles deposited in the anterior nasal airways are cleared by sneezing, wiping, or blowing, whereas particles deposited in the oral passages are removed by coughing or by swallowing into the gastrointestinal tract (USEPA, 2004). In the nasal and oral passage, soluble particles may be absorbed to the epithelial cells via diffusion through the mucus layer and subsequently translocated into the bloodstream (USEPA, 2004). In the TB region, clearance of poorly soluble particles occurs mainly via mucociliary transport. The mucociliary escalator transports particle loaded mucus toward the oropharynx which it is eventually swallowed. Clearance may also occur in the TB regions through phagocytosis by resident airway macrophages (USEPA, 2004). Similar to the ET region, soluble particles are absorbed in the bloodstream through the mucus layer (USEPA, 2004). Several studies have showed that a considerable portion of the particles deposited in the TB region is cleared within 24 h and the remaining particles are cleared slowly (Camner et al., 1997; Falk et al., 1999). In the A region, clearance is slow due to the absence of mucociliary transport in this region. PM is cleared in this region mainly by phagocytosis by alveolar macrophages. Soluble particles deposited in the A region may be translocated rapidly to blood through absorption by the epithelial surface (USEPA, 2004).

6. Particle deposition models

Computational particle deposition models are important tool in predicting particle dosimetry for different exposure scenarios. A number of deposition models have been developed which differs in lung morphometry and mathematical modeling techniques. The models could be empirical, mechanistic or combination of both and focus on the whole lung or local deposition. The ICRP task group published a semi-empirical particle dosimetry model where empirical equations were derived based on both experimental data and theoretical calculations (ICRP, 1994). Although the initial purpose of the model was to calculate intake of airborne radionuclides for workers (Publication 30, ICRP, 1982), later the model calculations have been expanded to include general population for wide range of conditions (Publication 66, ICRP, 1994). The model now can be implemented for non-radioactive particle dosimetry for different gender, age, physical activity (sleeping to heavy exercise), monodisperse and polydisperse particles (0.005 to 100 μm), smoking habits and COPD lung conditions. In this model, ET and TB regions are subdivided into two more regions. ET is divided into the anterior nose (ET_1) and the posterior nasal passages, larynx, pharynx, and mouth (ET_2). TB is divided into the bronchial region (BB), consisting of the trachea and bronchi and the bronchiolar region (bb) consisting of the bronchioles and terminal bronchioles. These regions are considered as a series of filters through which particles pass through during inhalation and exhalation. Therefore, deposition in any region is affected by deposition in the preceding region. Deposition efficiency (η) on each filter is calculated as:

$$\eta = 1\text{-}e^{-aR^p} \quad \ldots\ldots\ldots\ldots\ldots\ldots(17)$$

where a and P are constants, and R is a function of particle size and volumetric flow rate (ICRP, 1994).

Particle deposition pattern in the different respiratory regions of an adult male (nasal breather engaged in sleeping condition) based on ICRP model data shows that particles with an AD >0.8 μm deposit mainly in the ET region (**Figure C.3**). Particle deposition was the lowest in the TB region for all size fractions. For UF particles (AD <0.1 μm), the deposition of particles is greater in the alveolar region. Higher deposition of ultrafine particles (smaller than 0.1 μm) in the alveolar region can be explained by the larger diffusion coefficient of particles in that region.

The coefficient decreases with increasing particle size leading to overall lower deposition (<40%) in the size range of 0.1 to 0.5 µm. After that, particle deposition increases in the ET region due to impaction mainly.

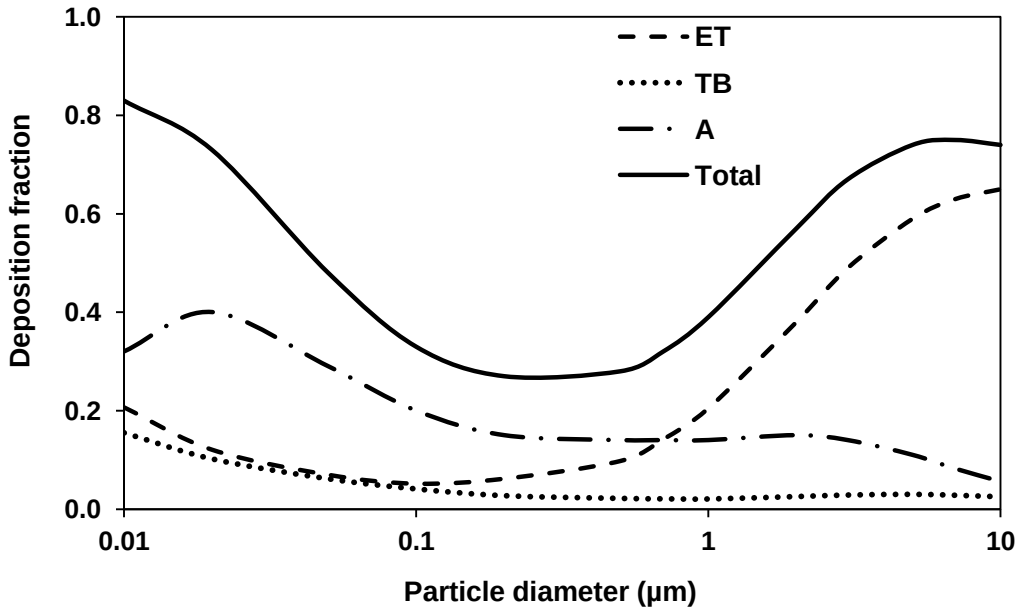

Figure C.3: Regional and total particle deposition fraction in the respiratory tract for an adult male (nasal breathing) using ICRP model.

Semi-empirical models are simple in calculation and require fewer assumptions about lung morphology as the models are based on actually measured deposition data in human volunteers. However, these models can only be applied to the particle sizes and volumetric flow rates covered in the underlying experiments. Particle deposition profile for different airway generations cannot be obtained using these models. In comparison, a deterministic single-path model offers options for calculating particle deposition in a specific airway generation. In a single-path model, it is considered that every parent airway is divided into two identical branches with identical geometrical parameters (length, diameter, branching and gravity angels) continuing from trachea to alveolar sacs (Weibel, 1963). Therefore, particles are expected to travel through the single pathway from the trachea to the alveolar sacs. For a given flow

conditions, deposition fractions are computed by applying analytical deposition equation. Considering that inhaled airflow is equally distributed among all airways, an identical particle deposition fraction is expected in each airway of a given generation (Yeh, 1980). Thus, the total deposition in a generation is obtained by multiplying the deposition fraction in an airway by the number of airways in that generation (Hoffman, 2009).

The single-path model is frequently used for its simplified respiratory structure. However, real human lungs are not symmetrical and have variable lung structure. Particle deposition dose in different regions depends on both the length of the total path traveled from inhalation to deposition site and the diameter and angels of the airways as well which differs among subjects. A symmetric single path model is unable to predict such variability. Several deterministic models have either modified the lung morphometry or introduced physical factors to overcome the limitation. Hofmann et al., (1989) used the Weibel's single-path model but introduced inter-subject variability in lung morphometric model by relating airway diameters and lengths with a person's age. Yeh and Schum (1980) measured detail geometrical dimensions of a human lung using a replica cast (Raabe et al., 1976) and used the dimensions to develop a five-lobe model (left upper lobe, LU; left lower lobe, LL; right upper lobe, RU; right middle lobe, RM; and right lower lobe, RL). Although the model followed the single-path model, asymmetric lobe structure with different number of airways were considered for theoretical calculations. In a stochastic lung structure model, the asymmetric nature of the lung is constructed based on the distributions of different morphometric parameters of lung (such as length, diameter, branching angle, and gravity angle) and correlations between these parameters as a function of airway generation (Koblinger and Hofmann, 1985). In this model, the pathway along which an inhaled particle travels is randomly selected using a Monte-Carlo method (Hofmann and Koblinger, 1990; Koblinger and Hofmann, 1990) and particle deposition probabilities are computed by deterministic equations proposed by Yeh and Schum (1980). The lung is considered as a Y bifurcation unit where a parent airway is divided into two random and asymmetrical daughter airways. Based on the distal lung volumes, it is randomly selected whether a particle travels through the major or minor airway. Therefore, the paths of inspired particles and the deposition fractions in the individual airways are different from each other. By simulating the random paths

of particles, a significant number of statistical means can be calculated for total, regional, and generational deposition (Hofmann and Koblinger, 1990; Koblinger and Hofmann, 1990 & 1985). The main advantage of a stochastic deposition model is that this model is based on a more realistic lung structure which considers both structural asymmetry and biological variability (Koblinger & Hofmann 1985).

Applied Research Associates, Inc. (ARA, Albuquerque, NM, USA) and The Hamner Institutes for Health Sciences (previously known as the Certre for Heath Research (CIIT), Research Triangle Park, NC, USA) in collaboration with the National Institute of Public Health and the Environment (RIVM) and the Ministry of Housing, Spatial Planning and the Environment, the Netherlands have developed the Multiple Path Particle Dosimetry (MPPD) model which calculates particle dosimetry for different lung models. This software offers open access to public for free upon online registration (MPPD V2.1, Albuquerque, NM, USA). The model can calculate particle dosimetry in both rat and human lungs. In this chapter, particle dosimetry was calculated for humans only. The model uses three different lung geometries for human: single or typical-path symmetric lung geometry (Yeh and Schum, 1980), 5-lobe limited asymmetric geometry (Yeh and Schum, 1980), and stochastic lung asymmetric geometry (Koblinger and Hofmann, 1985). The single-path model can calculate average regional depositions in head, TB, and A regions. It can also calculate average depositions per airway generation. The 5-lobe model also calculates average regional deposition per airway generation as well as lobar depositions. For the first two lung geometries, age-specific ten lung geometries were developed for ages between 3-months and 21-years-old. Thus, particle deposition calculation can be performed from infancy to adolescence. In the current version, this software allows the user to select different conditions for a number of parameters. Particle deposition profiles can be developed for a wide range of monodisperse and polydisperse particle sizes (0.001 to 100 μm). Variable particle concentration and density values can also be used. Different breathing scenarios (nasal, oral, and oronasal) can be selected depending on interest. Inhalability adjustment for smaller particle can also be specified. Variable breathing parameters (tidal volume (V_T), breathing frequency (f), inspiratory and pause fractions, functional residual capacity (FRC), and upper respiratory tract (URT) volume can also be defined by the user. In this study, the model was used to calculate

particle deposition in different regions of the lung for different lung geometries, ages, breathing routes and physical activities. Default model parameters used were (otherwise specified): FRC 3300 ml, URT 50 ml, V_T 625 ml, f 12/min, inspiratory fraction 0.5, pause fraction 0, particle size range 0.01 to 10 µm in diameter, particle concentration 10 µg/m^3, density 1 gm/cm^3.

Total and regional (head, tracheobronchial (TB), and alveolar (A) regions) particle deposition fractions were calculated for the three lung morphometries in an adult for sleeping breathing conditions (**Table C.2, Figure C.4**). Particle deposition profiles were the same for all three models for the head region. However, deposition profiles in the TB and A regions were different to some extent. Yeh/Schum symmetric and Yeh/Schum 5-lobe models predicted higher particle deposition than the other models for particles smaller than 0.1 µm in the TB and A regions, respectively.

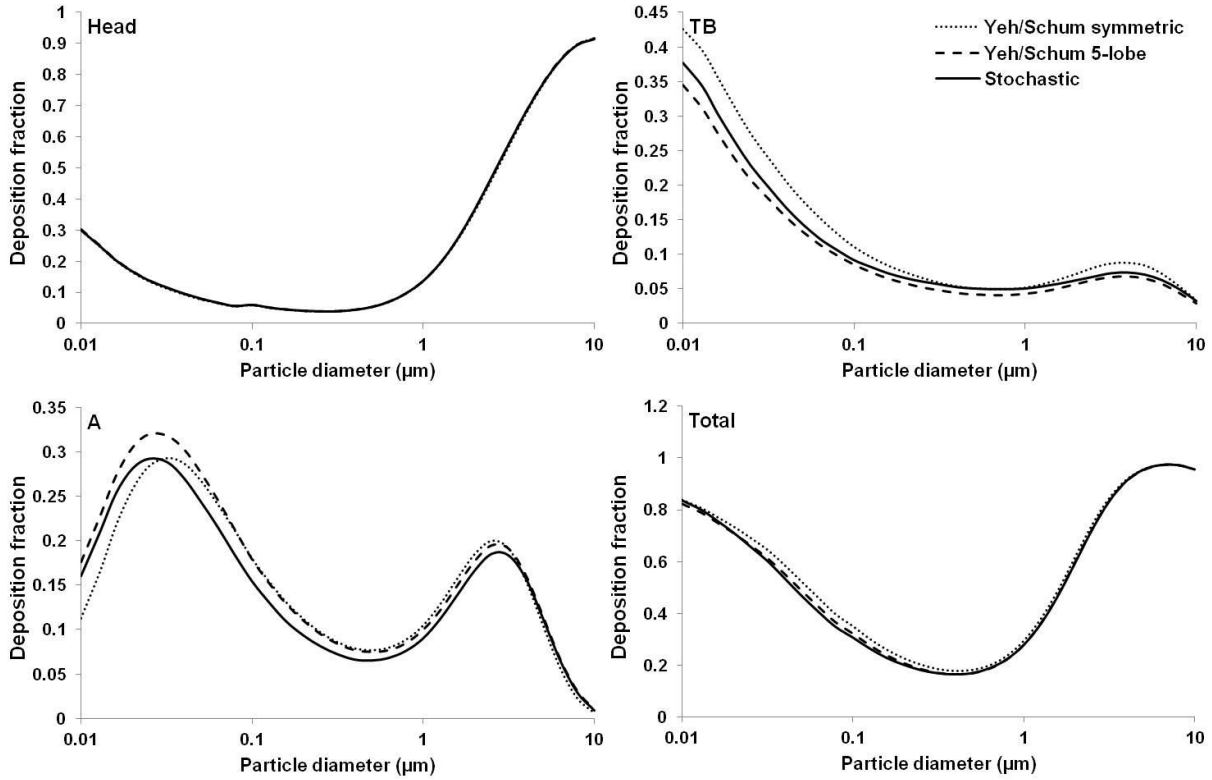

Figure C.4: Regional (head, tracheobronchial (TB), and alveolar (A) regions) and total particle deposition fraction in an adult for nasal breathing using different lung models.

Total particle deposition was slightly higher for the Yeh/Schum symmetric model than other models for particles <0.5 µm. Despite all the differences, the trends of the deposition pattern were similar for all models. When comparing with the ICRP model, the particle deposition profiles were similar, but the quantities were different. ICRP predicted lower particle deposition in the TB region, whereas calculated higher deposition in the A region, especially for UF particles. The total particle deposition profiles also resembles with deposition profiles determined by human exposure studies (Daigle et al., 2003; Löndahl et al., 2008; Rissler et al., 2012) in the human respiratory tract.

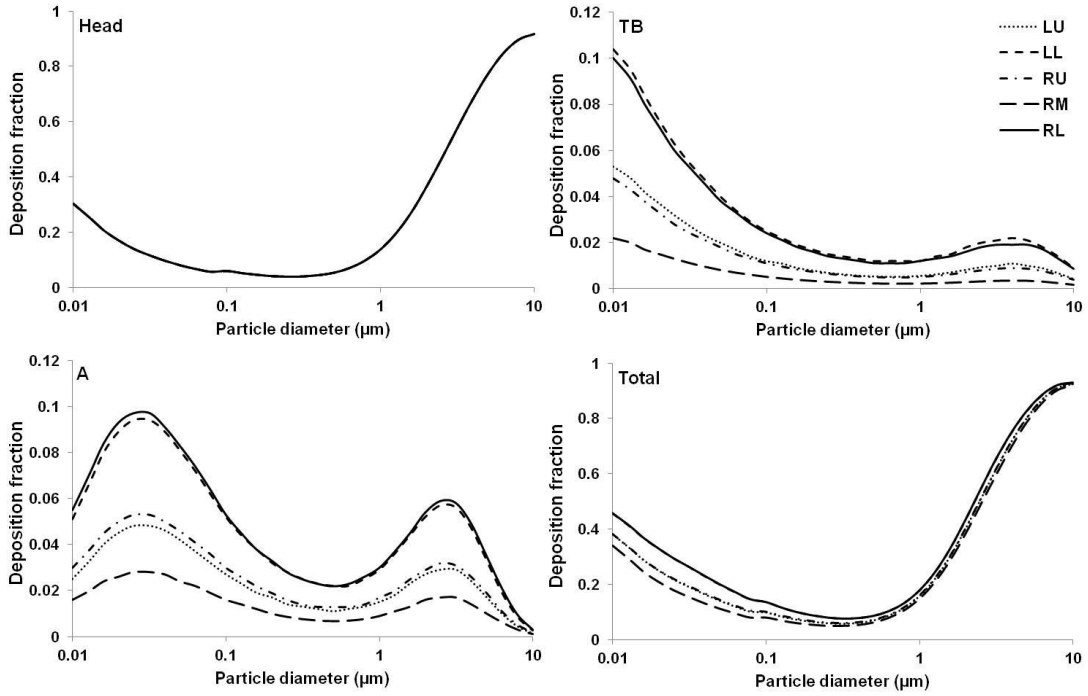

Figure C.5: Particle deposition fraction in different regions using Yeh-Schum 5-lobe model (left upper, LU; left lower, LL; right upper, RU; right middle, RM; and right lower, RL).

Calculation of lobar deposition using the 5-lobe model showed differential particle deposition in different lobes (**Figure C.5**). There was no difference in the head region as the structure for this region remained the same in all lobe models. For both TB and A regions, differences in lobar deposition were more pronounced for smaller particles (<0.1 µm). In these two regions, deposition fractions were almost the same for parallel lobes in the left and right lungs produced

almost identical results (LU-RU, LL-RL). Particle deposition was also higher in the lower lobes followed by the upper lobes and the right middle lobe.

Yeh/Schum 5-lobe model was used to calculate particle deposition fraction in different regions of lung from childhood to adolescence (3 months, 28 months, 9 yrs, and 21 yrs) (**Figure C.6**). Breathing parameters used by the MPPD model for different age groups are listed in **Table C.3**. There was no difference in particle deposition between 3 and 28 months old children. After that, difference was more pronounced with the increase in age. For larger particles (>2 μm), head deposition fractions in adult were larger than in children. In consequence, tracheobronchial and alveolar deposition fractions were larger for children than for adults for these particles. Ultrafine particle deposition was higher in children than adults for both regional and total deposition. For total deposition, deposition was higher in children than adults for particles upto 2 μm.

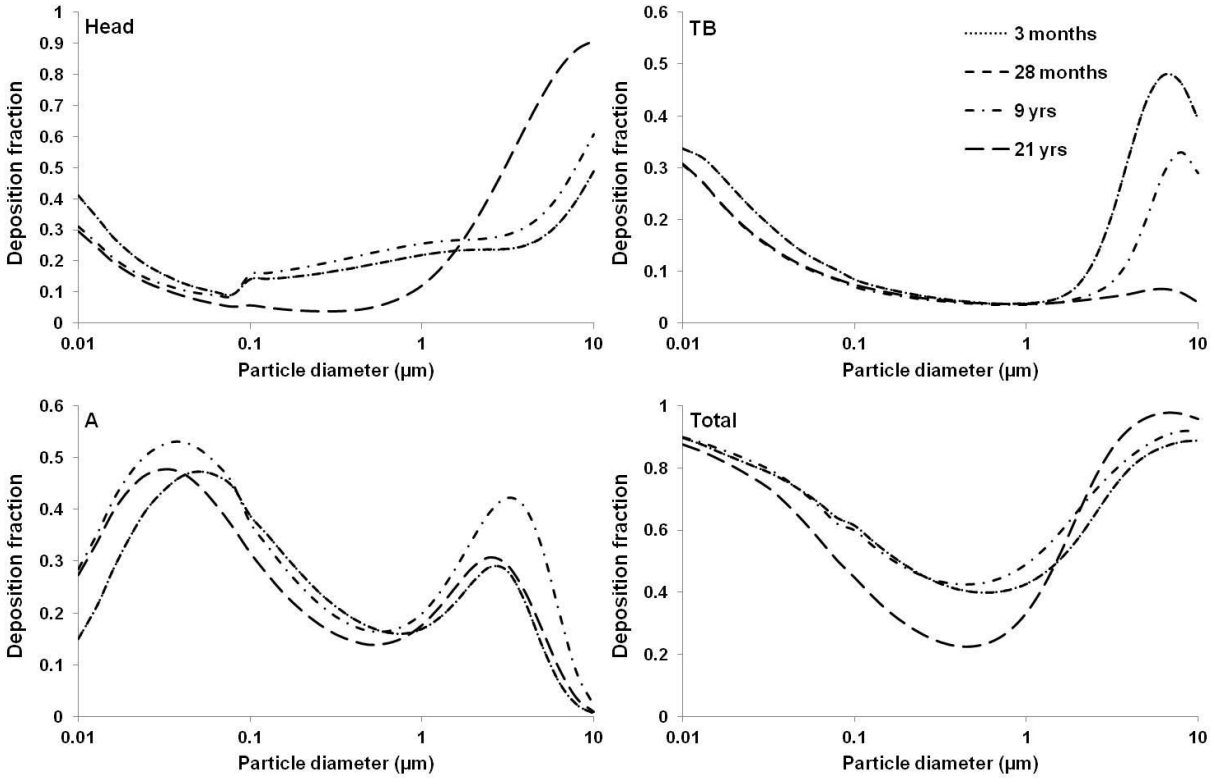

Figure C.6: Particle deposition fraction in different regions of the lung from childhood to adolescence for Yeh/Schum 5-lobe lung geometry using MPPD model.

PM deposition in adult male was also calculated using the Yeh/Schum 5-lobe model for different levels of physical activity (**Figure C.7**). It was assumed that breathing route would change with the level of activities. Nasal, oronasal, and oral breathing routes were considered for sleeping, light exercise, and heavy exercise, respectively. Breathing parameters (V_t and f) for different scenarios were collected from ICPR, 1994 (**Table C.2**). Particle deposition in the head was lower for light and heavy exercise conditions compared to resting condition. During oronasal and oral breathing, particle depositions in the nasal passage were expected to be lower or absent, respectively. Tracheobronchial deposition fractions for ultrafine particles decreased and increased for larger particles from rest to light and heavy exercise. Alveolar deposition was always higher for heavy exercise for both ultrafine and coarse particles indicating that with oral breathing more particles were able to reach deep in the lung. However, total particle deposition decreases from sleeping to heavy exercise condition as the particle residence time in the respiratory lung decreases with increasing physical activity level.

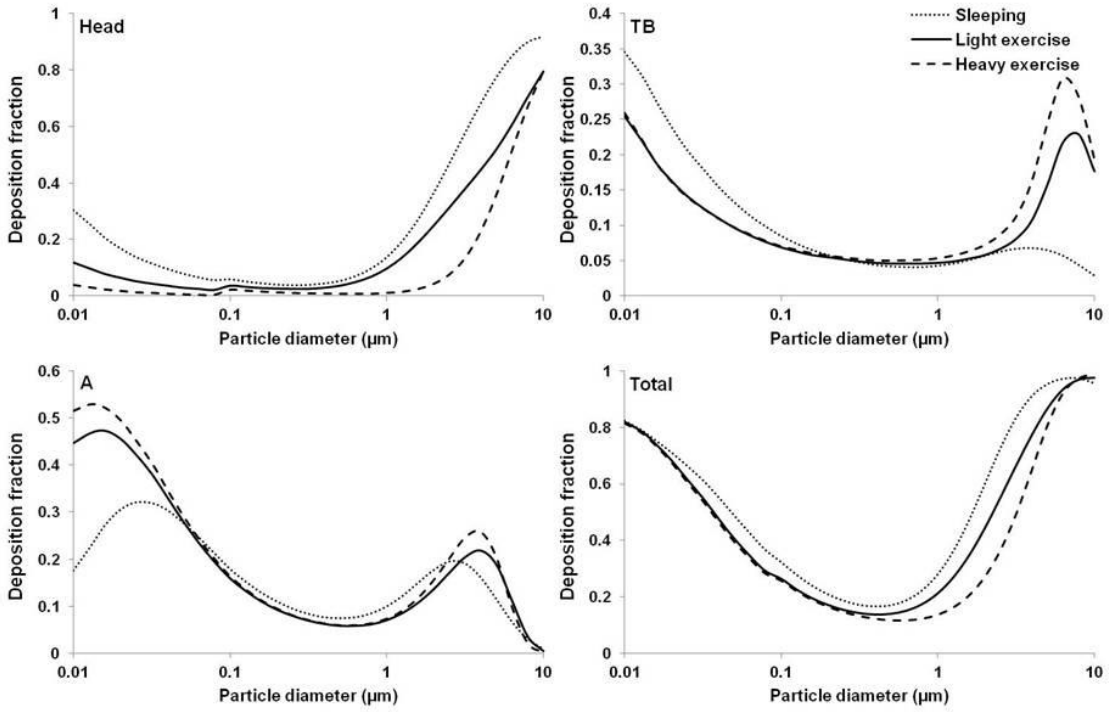

Figure C.7: Particle deposition fraction in different regions of the lung for different level of physical activity and breathing routes (sleeping: nasal, light exercise: oronasal, heavy exercise: oral) for Yeh/Schum 5-lobe lung geometry using MPPD model.

Table C.3: Breathing parameters for different age groups for particle deposition calculation of Yeh/Schum 5-lobe lung morphometry using MPPD model

Parameters	3 months	28 months	9 yrs	21 yrs
Functional residual capacity (FRC), ml	18	30.8	683	2123
Upper respiratory tract (URT), ml	2.45	7.9	22.4	42.3
Tidal volume (V_T), ml	30.4	100	296	477
Breathing frequency (f), #/min	39	26	17	14

7. Particle deposition in the respiratory tract

In our everyday life, we are exposed to different environments like indoor and outdoor. Particle concentration varies among different environments depending on the particle sources in that environment (**Table C.4**). Highly populated cities in developing countries can have PM_{10} concentration as high as 540 µg/m^3 (Alam et al., 2011), whereas particle concentration can reach up to 5000 µg/m^3 during cooking activities (Chao et al., 1998). We are also engaged in different level of activities such as resting and working. Particle mass deposition fraction in the lung and subsequent effects largely depend on the physical activity level (i.e., breathing pattern oral vs. nasal), exposure duration, particle size and concentration. The MPPD model was used to simulate particle mass deposition per surface area of the lung (µg/cm^2) for particles in the size range of 0.01 to 10 µm in different regions of the lung (head, tracheobronchial, and alveolar) for different exposure scenarios (e.g., cooking and working) with very high PM concentrations (**Figure C.8**) involving different level of physical activity level. Different exposure duration for different exposure scenarios were selected to reflect real life exposure conditions. Light physical activity level was chosen for cooking (2 h/day, 5000 µg/m^3), whereas heavy exercise level was chosen for occupational setting (8 h/day). For workplace, currently recommended upper limit for respirable dust concentration (5000 µg/m^3) by Occupational Safety and Health Administration (OSHA) was used. For living in a polluted city, resting conditions were considered for whole day exposure to 540 µg/m^3. Another scenario was considered where all three exposure scenarios were incorporated (2 h cooking, 8 h working, and resting for rest of the day). The breathing

parameters for different physical activity levels were used from **Table C.2**. Particle clearance rates were not considered during the calculation.

Table C.4: Example of high particulate matter concentration (μg/m^3) in different scenarios

Sites	Description	Sources	Size	PM conc.	Reference
Peshawar, Pakistan	An industrial city of steel industry, pharmaceuticals, food processing, firearms, etc.	Traffic emissions, re-suspended road dust, smoke, and emissions from heavy machinery.	PM_{10} $PM_{2.5}$	540 160	Alam et al., 2011
Hebei, China	City centre, near to construction site	Construction site, traffic sources	PM_{10}	232	Ni et al., 2013
Dongli, China	Suburban, industrial site	Oil refining, petrochemical facilities, iron and steel manufacturing, metal smelting, transportation, etc.	PM_{10}	212	Ni et al., 2013
Hatfield, UK	A tunnel with daily traffic volumes of ~48,500 during weekdays	Resuspension, diesel and petrol exhaust emissions, brake wear emissions and road surface wear	PM_{10} $PM_{2.5}$	117 68	Lawrence et al., 2013
Hong Kong	Indoor environment	Cooking	PM_{10}	5000	Chao et al., 1998
Iowa, USA	Poultry industry	Chickens' natural activities	PM_{10} $PM_{2.5}$	393 44	Li et al., 2011

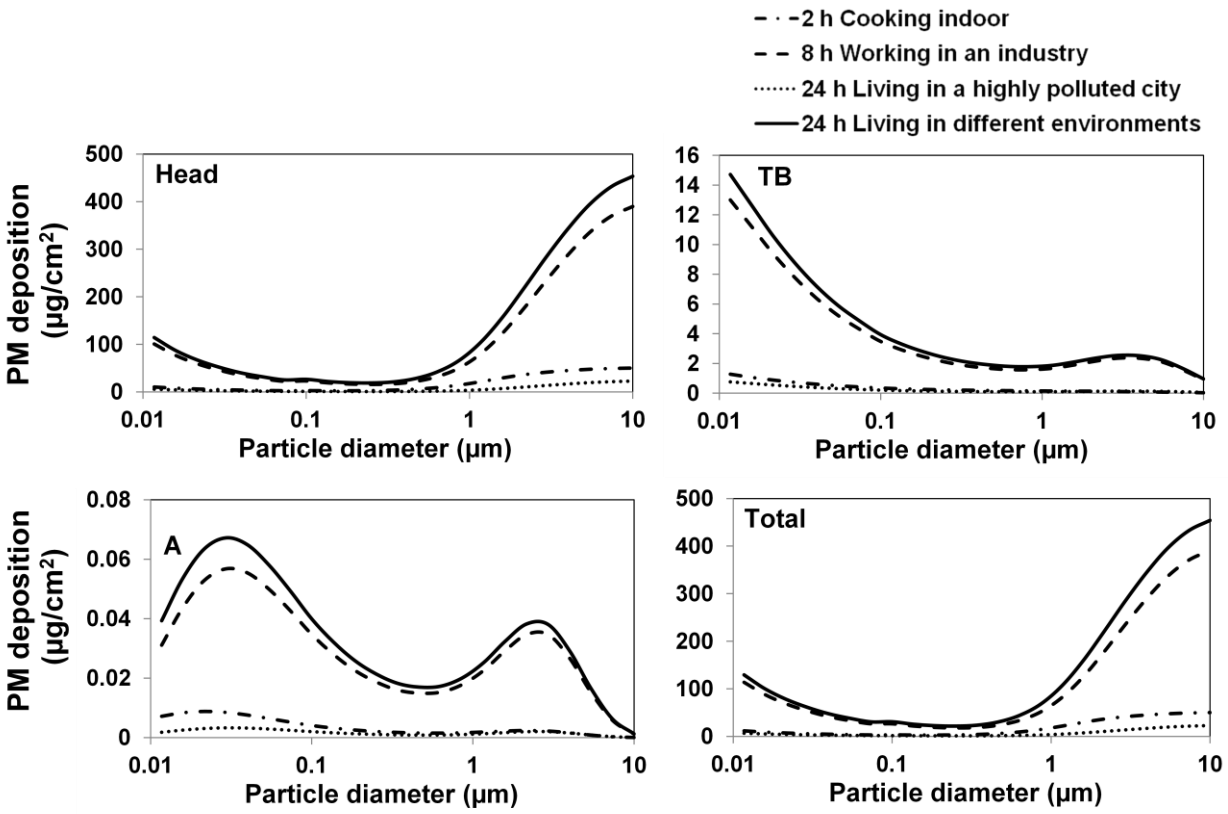

Figure C.8: Regional (head, tracheobronchial (TB), and alveolar (A) regions) and total particle deposition (µg/cm^2) in an adult exhibiting different level of physical activity in different exposure environments. Particle properties: particle size range 0.01 to 10 µm. Surface areas for head, TB and P regions are: 296, 3725, and 705,000 cm^2, respectively (ICRP, 1975).

Overall, particle deposition in terms of mass per surface area (µg/cm^2) was the highest for head region followed by tracheobronchial and alveolar regions (**Figure C.8**). The higher particle deposition in the head region is caused by the smaller surface area of that region, whereas larger surface area of alveolar region resulted in lower deposition (**Table C.1**). For the head region, deposition was higher for particles larger than 1 µm than other particle sizes. For both TB and A regions, deposition was dominant for particles smaller than 0.1 µm. Deposition for working 8 h in an industry caused the highest in all regions due to such high PM concentration and physical activity level. Although exposure duration during cooking activity was shorter than living in a highly polluted city (2 h vs. 24 h), deposition was higher in all three regions of the lung during

cooking than the other scenario because of higher PM concentration (5000 vs. 540 μg/m^3). The increased physical activity during cooking also caused higher deposition. Therefore, a person living in a highly polluted city (14 h) who is exposed to high PM concentration in workplace (8 h) and also cooks for 2 h a day is expected to experience very high PM mass deposition.

8. Relating *in vitro* doses with real life scenarios

It is normally speculated that PM doses used in experimental studies are higher than real life exposure concentration. PM concentration doses used in *in vitro* studies are typically expressed as PM mass/cell culture medium volume and range from 10 to 1000 μg/ml (Akhtar et al., 2010; Atkinson et al., 2010; Hetland et al., 2004; Huang et al., 2011; Jalava et al., 2009; Li et al., 2002; Mazzarella et al., 2007; Wang et al., 2013). Some studies already report the dose as PM mass per surface area (μg/cm^2) (Karlsson et al., 2004; Ramgolam et al.; 2008, Steenhof et al., 2011; Wessels et al., 2010). To obtain a common dose unit, *in vitro* PM doses expressed as mass/volume were converted to mass/surface area by incorporating three factors: PM dose (μg/ml), volume of the cell culture medium (ml), and surface area of the culture plate (cm^2). Comparable doses for 10-1000 μg/ml were calculated as 2.1-210 μg/cm^2 and 3.1-310 μg/cm^2 for 6 and 96 well plates, respectively. Several *in vitro* studies have reported significant biological responses at the PM dose as low as 10 μg/ml (equivalent to 2.1-3.1 μg/cm^2) for exposure duration from 4 to 24 h (Akhtar et al., 2014 & 2010; Li et al., 2002; Ramgolam et al., 2008; Steenhof et al., 2011).

There are different variables that may cause higher particle deposition in healthy and susceptible population. Intersubject variability in airway anatomy and breathing pattern may cause up to 40% variation in particle deposition in healthy people (Hussain et al., 2011). Enhanced deposition is also expected at airway branching zones relative to cylindrical airways in healthy individuals (Zhang and Papakadis, 2010). Computation modelling has showed that maximum local deposition enhancement factors at bronchial airway bifurcations for different particle sizes (1, 10, 20, 100, and 200 nm) ranged from 41 to 67 at 7.5 L/min flow rate (Balashazy and Hoffman, 2000). The deposition is expected to be even higher in patients with obstructive pulmonary diseases due to higher bronchial wall thickness and smaller lumen area in these

patients (Gupta et al., 2009; Kosciuch et al., 2013; Yilmaz et al., 2006; Zhang and Papakadis, 2010). Susceptible population such as asthma and COPD patients exhibit poor respiratory function (e.g., FEV_1) (Gong et al., 2003; Kirby et al., 2010; McCreanor et al., 2007; Svenningsen et al., 2014). Qualitative assessments of Computed Tomography (CT) scans in asthma and COPD patients also reported prevalence of bronchiectasis, damaged airways, and bronchial wall thickening (Gupta et al., 2009, Kirby et al., 2010; Svenningsen et al., 2014; Yilmaz et al., 2006). All these factors could lead to increased particle deposition and slower particle clearance in an individual with obstructive pulmonary diseases. In fact, a number of experimental studies have showed enhanced particle deposition in asthma and COPD patients with compared with healthy subjects (Bennett et al., 1997; Brown et al., 2002; Chalupa et al., 2004; Horemans et al., 2012; Kim and Kang, 1997; Löndahl et al., 2012).

Based on the MPPD simulations, the time interval required to achieve equivalent mass concentration of 2.5 μg/cm^2 (for particle size 0.1 μm) in different regions of the lung was determined for different exposure scenarios, in both healthy and susceptible person (**Table C.5**). For a healthy individual, deposition durations in all three regions were determined in an individual with higher deposition efficiency due to anatomical variations (1.4-fold than normal healthy individual). An enhancement factor of 60-fold was also used to determine enhanced particle deposition at the bifurcation points of the tracheobronchial region (calculated that for 0.1 μm particles). For an asthmatic individual, 2-fold deposition enhancement factor was applied for all conditions. Based on the simulation, it would take less than 32 h to experience such particle dose in the head region for most of the scenarios in a healthy person; the duration would be half for an asthmatic individual. The deposition duration could range from 0.46 to 8.8 days in the tracheobronchial and 22.4 to 882 days in the alveolar regions. However, it would take less than 4 h for healthy and asthmatic individuals to experience 2.5 μg/cm^2 particle dose at the bifurcation points when exposed to such high PM concentration. According to the model, particle clearance rates within 24 h of deposition are >80% and <1% in the TB and A regions, respectively. However, cells located at the bifurcation points might receive higher localized doses than other areas and the cells might not be able to clear those particles within 4 h. Therefore, healthy and high-risk asthmatic individuals living in a highly polluted city, cooking regularly, and

experiencing occupational exposure to high PM concentration could experience such level of particle deposition at some regions of the TB region in very short duration. Therefore, the exposure doses used in different *in vitro* studies are high but still relevant to real life exposure scenarios in some highly polluted cities and occupation settings.

Table C.5: Required exposure duration (day) to obtain particle mass deposition dose of 2.5 μg/cm^2 (particle size 0.1 μm) for different exposure scenarios in healthy and asthmatic individuals. Required duration for deposition at airway bifurcation points in the TB region are given in parenthesis.

Scenarios	Condition	Head	TB	A
Cooking indoor- 5 mg/m^3 (Chao et al., 1998), 2 h/day, Oronasal breathing light exercise	Healthy	0.65	5.10 (0.08)	442
	Susceptible	0.33	2.55 (0.04)	221
Working in an industry- 5 mg/m^3 (Li et al., 2011), 8 h/day, Oronasal breathing heavy exercise	Healthy	0.08	0.51 (0.01)	51.5
	Susceptible	0.04	0.26 (<0.01)	25.7
Highly polluted city- 540 mg/m^3 (Alam et al., 2011), 24 h Nasal breathing- sitting	Healthy	1.33	8.80 (0.15)	882
	Susceptible	0.66	4.40 (0.07)	441
24 h living in different environments (2 h/day cooking + 8 h working in a poultry + 14 h sitting in a highly polluted city)	Healthy	0.07	0.45 (0.01)	44.8
	Susceptible	0.03	0.23 (<0.01)	22.4

Factors considered for calculation: anatomical variations enhancing deposition efficiency (1.4-fold, Hussain et al., 2011); increased particle deposition at bifurcation points in the airway (60-fold, calculated that for 0.1 μm particles, Balashazy and Hoffman, 2000); and enhanced particle deposition rate in asthmatic airways (2-fold, Kim and Kang, 1997).

9. Conclusions

Particle deposition and clearance in the respiratory tract is a complex process which depends on particle size; structure of the respiratory tract; and several biological factors like age, gender, physical activity and existing respiratory conditions. Particle deposition efficiency in human lung from particle exposure studies can only be obtained for limited exposure conditions. Therefore, computations models are a great tool in predicting particle deposition profile for a wide range of exposure scenarios. A number of models have been developed based on measured or predicted lung morphometry which were able to predict regional and/or total particle deposition in the respiratory tract. These models are useful for obtaining average regional and overall deposition of particles in the lung. Deposition fractions calculated by MPPD model for different lung geometry (Yeh/Schum symmetric, Yeh/Schum 5-lobe, and stochastic) showed that deposition fractions in the head region and entire respiratory tracts were similar; however, were different in the tracheobronchial and alveolar regions. This could be due to the differences in the tracheobronchial and alveolar structure considered in the models. Although more detailed lung structures were included in the 5-lobe and stochastic models, simple typical lung model was also able to predict the particle deposition profile. Asymmetrical nature of five different lobes in the lung showed that particle deposition was not uniform in different lobes. Simulations were also conducted for different age and physical activity levels. Age-specific models have shown that ultrafine particle deposition was higher in children but rises in adults for larger particles. For different activity level, overall particle deposition decreases with increasing activity level due to increased minute ventilation rate. However, particles were able to reach deep in the lung as the breathing route changed from nasal to oral. Simulation results obtained using MPPD model showed that PM concentration doses used in *in vitro* studies are relevant to some real world exposure scenarios, for both healthy and susceptible population. Therefore, application of MPPD model will be helpful in determining more realistic *in vitro* doses. With a better understanding of lung morphology, airflow inside the respiratory tract, and particle deposition mechanisms and particle properties, these models are now able to predict particle deposition profiles without extensive human exposure studies. Results obtained from these models can be use for environmental and occupational exposure studies and for respiratory drug delivery purposes.

Appendix D

Assessment of a new air-liquid interface exposure device Sized Aerosol *in Vitro* Exposure System (SAIVES) for toxicology study of particulate matter

1. Introduction

The assessment of *in vitro* toxicological effects of particulate matter is a widely used technique. The current state of art of *in vitro* exposure methods has already been reviewed in Chapter 2. It was also shown in Chapter 4 that the conventional submerged method of *in vitro* techniques, i.e., collection of particles on filters and extraction followed by exposure to cells, lead to poor correlation between particle physicochemical properties (number and surface area) and biological responses. In addition, the actual particle dose to cells could not be confirmed in this method. Compared to the submerged method, exposure of cells at the air liquid interface (ALI) is the most realistic approach. ALI exposure has been limitedly used as an alternative approach for *in vitro* toxicological studies of gaseous and particle compounds. Both these methods have their respective advantages and disadvantages (**Table D.1**). Although ALI exposure technique requires complex design, this approach is considered as the closest to *in vivo* particle deposition. Several studies have showed that direct exposure recorded higher biological responses as compared to indirect exposure for the same mass concentration (Holder et al., 2008; Volckens et al., 2009). In the early design of ALI systems like Cultex® (Sibata, Japan) and Navicyte (Harvard Apparatus, USA), particle deposition was governed by gravitational and diffusive mechanisms from free flowing air. Due to very low particle deposition efficiency in these systems, particle generating system with very high loadings of PM such as smoking machine (Wolz et al., 2002), diesel exhaust (Holder et al., 2008) and laboratory scale tube furnace (Lestari et al., 2006) were used for exposure studies instead of ambient air. In the following designs electrical field was used to force deposition of charged particles on the cell surface to enhance particle deposition (Aufderheide et al., 2013; Bruijne et al., 2009, Savi et al., 2008, Sillanpää et al., 2008).

Table D.1: Summary of advantages and disadvantages of submerged exposure and air-liquid interface exposure of cell to particles

	Advantages	Disadvantages
Submerged exposure	• Simple technique • Regular cell culture device (plate, petri dish) and techniques can be used • No special experimental set-up is required as the exposed cells can be placed in a cell culture incubator (conditioned with 5% CO_2 and 95% relative humidity) • Experiments can be replicated	• Particles collection on different medias (filters, foams, etc.) are required • Particle extraction methods can alter the particle properties • Biological responses are related to mass dosimetry than other dosimetry related to surface area or number • Exact particle dose interacting with cells cannot be determined directly
Air-liquid interface exposure	• Better simulation of particle exposure • Allows exposure to PM with unaltered physicochemical properties • Precise dose determination is possible	• ALI requires additional design for particle generation and higher particle deposition, which could be complex • Special cell culture technique (on a Snapwell/Transwell) is required. • Particle exposure takes place outside of an incubator. Therefore, cell conditioning (with CO_2 and RH) is required.

2. Electrostatic precipitation

Electrostatic precipitation is a widely used method for particle removal from gaseous exhaust in an industrial setting. In an electrostatic precipitator (ESP), the particle collection process consists of two fundamental processes: i) particle charging and ii) particle collection (Parker, 2003). Particles are passed through an electric field where they receive electric charge. The same

electric field then causes the charged particles to drift away from the air/gaseous flow and deposit on a collection plate. The electric force can be significantly higher than the gravitational or inertial forces (Hinds, 1999). Therefore, application of electrostatic precipitation technique in a cell exposure device is expected to increase particle deposition efficiency. Both the charging and collection can take place in the same region which is called a single stage precipitator. In a two stage precipitator particle charging takes place in one section followed by another section where another electric filed is established for particle deposition (Oglesby and Nichols, 1978).

3. Ion production and particle charging

For particle charging in a precipitator, it is required to produce high concentrations of unipolar ions which will get attached to the particles. Corona discharge is a commonly used method for producing high concentrations of unipolar ions. In a corona discharge, a nonuniform electric field is established using a wire or needle as one electrode and a cylinder or plate as the other. The electric field is stronger near the wire and decreases rapidly with distance from the wire. When high discharge voltage is applied to the corona wire, free electrons are produced (**Figure D.1**). These electrons flee the electric field rapidly and collide with incoming air/gas molecules. The energy of the electrons is capable enough to knock out an electron from an air/gas molecule. Therefore, the air/gas molecule which is normally a good insulator becomes conductive by producing a positive ion and an electron. Each electron impacts another air/gas molecule resulting in large quantities of electrons and positive ions in the corona region (Oglesby and Nichols, 1978). If positive voltage is applied, the positive ions will move away from the wire to the other electrode creating a unipolar ion wind and the electrons will move rapidly to the wire. In case of negative voltage, the opposite will happen (Hinds, 1999). When particles in a gaseous stream are introduced in the ESP, these ions can collide with a particle and impart their charges to the particle. There are two mechanisms by which a particle can acquire charge: field charging and ion diffusion charging. Field charging is the result of ordered motions of ions governed by the electric field. The ions in the electric field travel along the field, collide with a particle present along the field line, and impart charge to the particle.

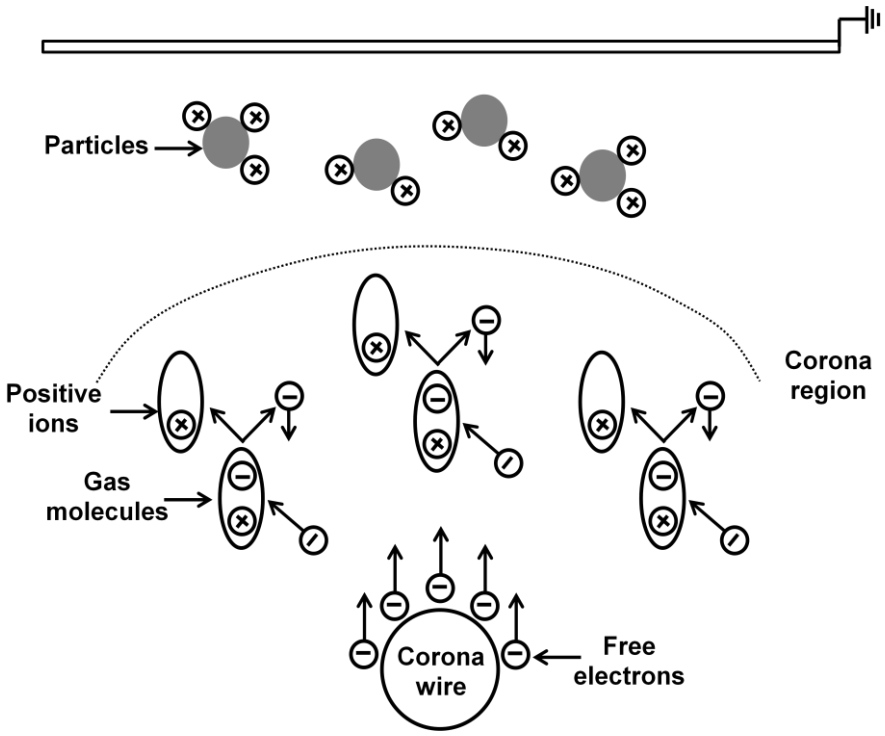

Figure D.1: The mechanism of corona discharge process. The corona wire is positively charged.

Initially, the ions converging on the particle result in distortion of the electric field lines. The degree of the distortion of the field lines depend on the relative permittivity of the particle material and the charge on the particle. As the particle continues to gain charge by colliding with ions, the particle charge (n) will continue to increase and create an electric field around the particle. Therefore, the particle will tend to repel the incoming ions (**Figure D.2**). The presence of the charge on the particle reduces the field strength and the number of field lines converging on the particle. Because of these changes, the rate of ions reaching the particle decreases as the particle becomes charged. Ultimately, the charge builds up to the point where no incoming field lines converge on the particle and no ions can reach the particle. At this maximum-charge condition, the particle is said to be at saturation charge (n_s). In diffusion charging, particles are charged by Brownian motion between the ions and the particles. The random motion is related to random thermal motion. No external electrical field is required for this mechanism and no saturation charge exists for the diffusion charging. This is due to the fact that the range of thermal velocities does not have an upper boundary limit.

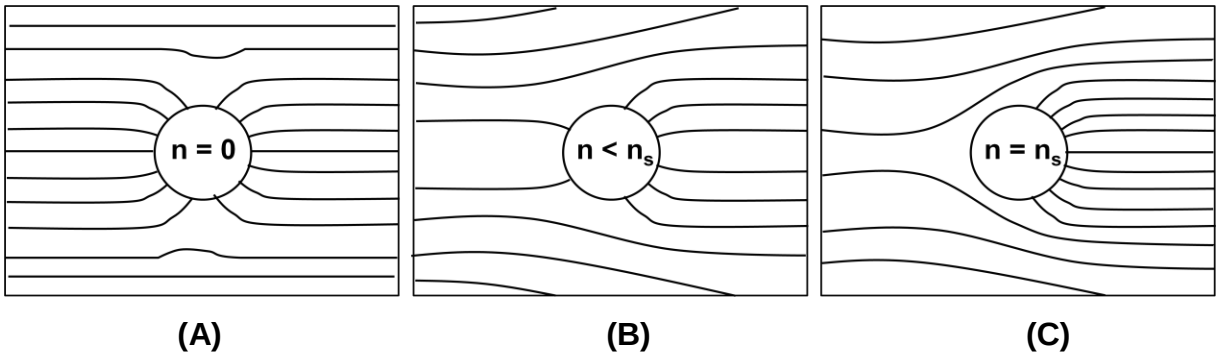

Figure D.2: Electric field lines for a particle in a uniform field experiencing field charging. (A) particle with no charge, (B) partially charged particle, (C) particle with saturation charge.

Both these mechanisms can occur at the same time to some extent. However, the relative contributions of these mechanisms depend on the particle size. Field charging contributes dominantly for larger particles (diameter >1 µm) as these particles have enough surface area for capturing gas ions. On the contrary, diffusion charging is the major contributor for smaller particles (diameter <0.1 µm) as diffusion coefficient is higher for particles with smaller diameter. For particles ranging between 0.1 to 1 µ m, both these mechanisms contribute and the relative contribution would depend on the particle diameter. Charge acquired by particles is proportional to the square of the diameter (d_p^2) in field charging and to the diameter (d_p) in diffusion charging (Hinds, 1999).

4. Sized-Aerosol *in Vitro* Exposure System (SAIVES)

An early prototype for a field deployable air liquid interface device, Sized Aerosol *In Vitro* Exposure System (SAIVES) was designed and developed at the SOCAAR lab (**Figure D.3**). The system is 34 X 14.5 X 5.5 (L X W X H) cm in dimension and weighs 4 kg. It consists of a two-stage ESP where the first stage functions as the charging zone (CZ) and the second stage works as the electrostatic precipitation zone (EPZ). For the CZ, a wire-plate configuration consisting of a thin copper wire and a rectangular aluminum (Al) plate was used with air flowing transverse to the wire. High positive voltage was applied to the copper wire to produce unipolar (positive) ions. As the wire is positively charged, the electrons move toward the wire and the positive ions

rapidly move toward the grounded electrode (Al plate). A positive corona was chosen over negative corona because positive corona produces ion across the entire wire length and the entire region around the wire is more stable (Hinds, 1999). Another concern regarding using a negative corona charger was that in the corona region enough energy could be present to produce ozone from oxygen and a negative corona can produce about 10 times as much ozone as a positive corona (Hinds, 1999). As the particles are introduced into the space between the wire and plate, the particles would undergo through field and diffusion charging to the same polarity as the wire.

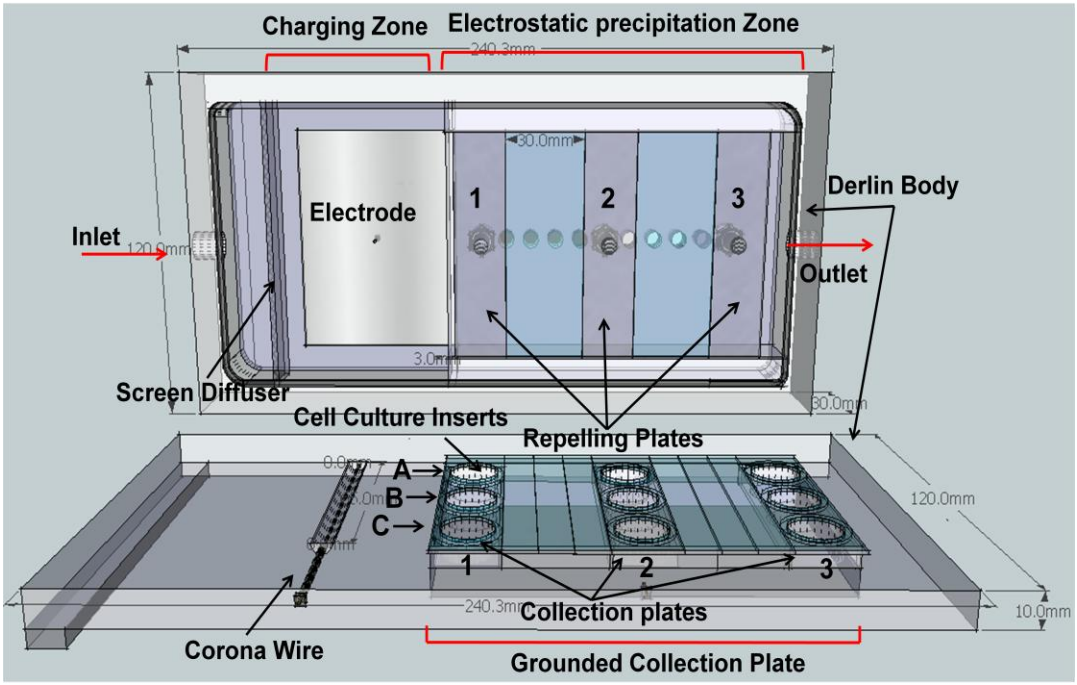

Figure D.3: Schematic diagram of SAIVES (in open position).

For the EPZ, a parallel-plate configuration was chosen where strong positive field were applied on the top plate and the base was grounded. In the EPZ, the charged particles are forced to drift toward the grounded collection plate by applying positive voltage at the repelling plates (**Figure D.4)**. Three aluminum electrodes were organized in parallel with an equal distance (4.5 cm) in between. Similar to the top, three collection plates were placed at the bottom for particle collection, aligned with the repelling plates. The position of the repelling and collection plates can be adjusted in horizontal direction as required. The purpose of having three adjustable

parallel plates was to achieve size segregated particle deposition across the length. It was expected that smaller particles would travel farther. Therefore, the plates can be arranged to capture size-fractionated deposition. The repelling plates could also be adjusted vertically. The strength of electrical field depends on the distance. Thus, the highest particle deposition could be accomplished by adjusting the vertical position of the plate. Positive field could be applied to individual or to all three repelling plates simultaneously. Each collection plate has three holes and each hole can hold a cell culture insert of 1.1 cm^2 (12 mm diameter, 0.4 µm pores, Snapwell™ inserts, Corning®, VWR International LLC., Mississauga, ON, Canada). Therefore, in total nine cell culture inserts can be placed in a single experiment. The purpose of the design was to maximize particle deposition in the holes where the cell culture inserts would be placed.

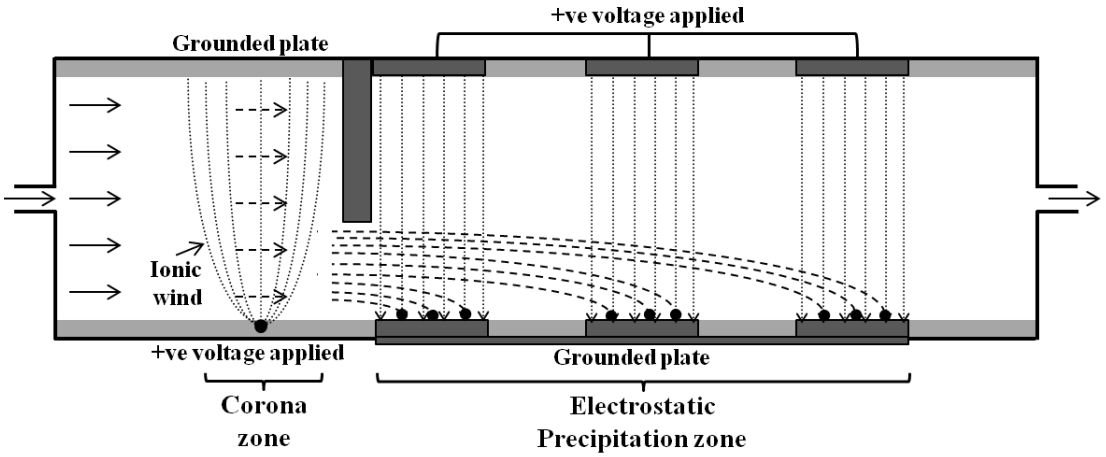

Figure D.4: Particle deposition profile in SAIVES.

4.1 Optimum setting for higher particle deposition

To operate the SAIVES efficiently, the optimum voltages to be applied at the CZ and EPZ for maximum particle deposition were determined at first. Ammonium sulfate ($(NH_4)_2SO_4$) particles with a size range of 6 to 300 nm were generated using an aerosol generator (Model 3076, TSI) and passed through the SAIVES. The number concentrations of the particles in different size bins were measured at the outlet using a Fast Mobility Particle Sizer (FMPS, Model 3091, TSI) (**Figure D.5**). Lower particle number concentration measured in FMPS indicated higher collection in SAIVES.

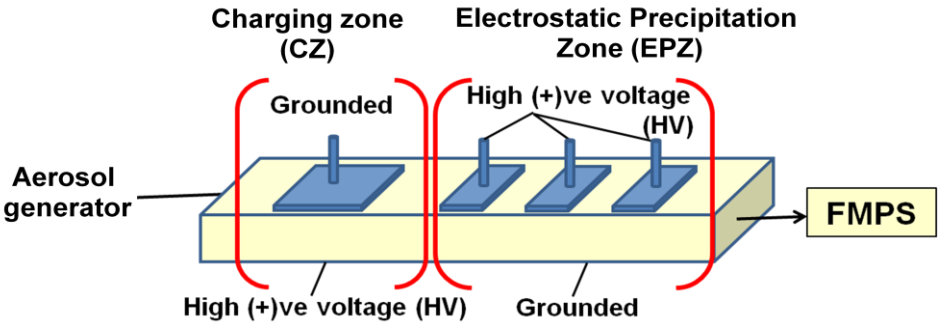

Figure D.5: Experimental set-up to determine the optimal operating conditions and collection efficiency of SAIVES.

First, positive voltage in the range of 1 to 6 KV was applied only to the charging zone to find optimum voltage for the highest particle deposition without any arcing in CZ. Similarly, positive voltage (1 - 6 KV) was applied to the EPZ for the best collection efficiency. For the CZ, the maximum particle deposition was observed at 6 KV (**Figure D.6A**); however, arcing was also observed at this voltage. Therefore, 5 KV was used as optimum voltage for CZ, and applied for the following experiments. Particle deposition was also maximum when 5 KV was applied to the EPZ (to all 3 plates simultaneously) (**Figure D.6B**). All these experiments were repeated three times and found to be consistent. Therefore, 5 KV was used for both CZ and EPZ for the rest of the experiments.

4.2 Collection efficiency of SAIVES

To determine the collection efficiency of SAIVES, several approaches were considered. First, the same setup as mentioned above was used to determine the efficiency. Particle number concentrations of ammonium sulfate in different size bins were determined for the following conditions: N_1: concentration measured before SAIVES; N_2: concentration measured after SAIVES, 5 KV to CZ only; and N_3: concentration measured after SAIVES, 5 KV to CZ and 5 KV to EPZ (all 3 plates simultaneously) (**Figure D.6A**). Particle concentrations were collected at least for 5 min for each condition and repeated for three times.

Particle collection efficiency (η_1) in SAIVES was calculated as:

$$\eta_1 = \frac{N_2 - N_3}{N_1} X100\% \ldots\ldots\ldots\ldots\ldots\ldots(1)$$

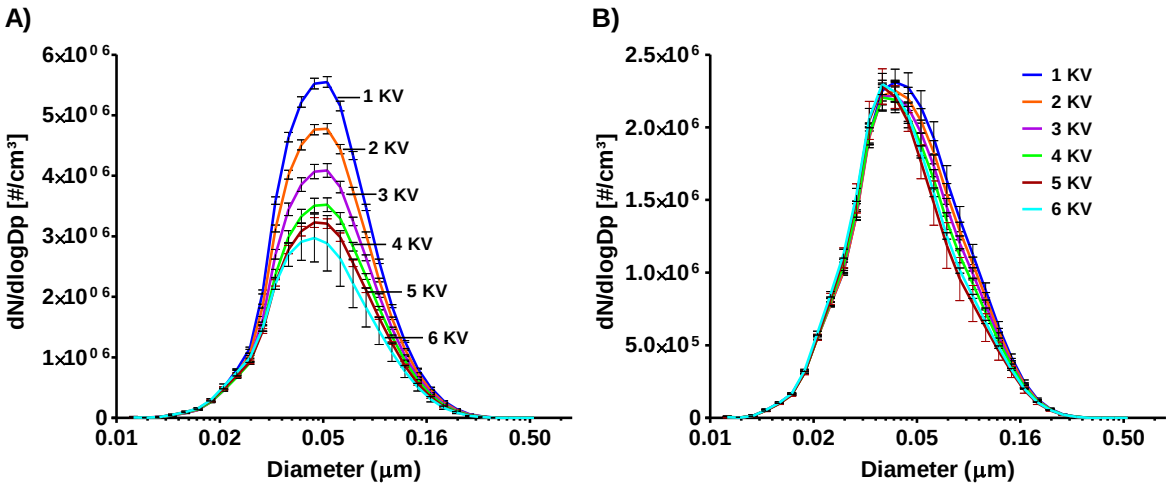

Figure D.6: Determining optimal operating conditions for SAIVES. A) Different voltage applied to the corona zone, B) constant voltage (5 KV) applied to the CZ and variable voltages were applied to the electrostatic precipitation zone (EPZ). Data is expressed as mean ± SD.

Although particle deposition was in between 30 to 40% for smaller particles (diameter <0.008 µm), particle deposition was absent for particle in the size range of 0.008 to 0.03 µm (**Figure D.7B**). Collection efficiency showed a step increase (0 to 40%) with increasing particle diameter, up to 0.1 µm and later reached equilibrium. Particle deposition efficiency in SAIVES was also checked in different ways using a fluorescence indicator (Zn_2SiO_4, with maximum particles present in the size range of 6 to 100 nm) (CAS No 68611-47-2, Sigma Aldrich, Oakville, ON, Canada). This indicator emits green light when illuminated with UV light (254 nm). 1 gm indicator was mixed in 500 ml of water to make stock solution and the same solution was used for the following experiments. The experiment was repeated four times. Initially the indicator was used to develop particle deposition profile following the same procedure described above. Particle deposition profile (**Figure D.8**) was mostly in agreement with the profile obtained using ammonium sulfate particles. Deposition was higher for particles smaller than 0.008 µm and was almost absent in the size range of 0.008 to 0.03 µm diameter. Collection efficiency showed a step

increase (upto 57%) with increasing particle diameter, up to 0.2 µm. However, instead of reaching equilibrium like before, efficiency continued to decrease for particles greater than 0.2 µm.

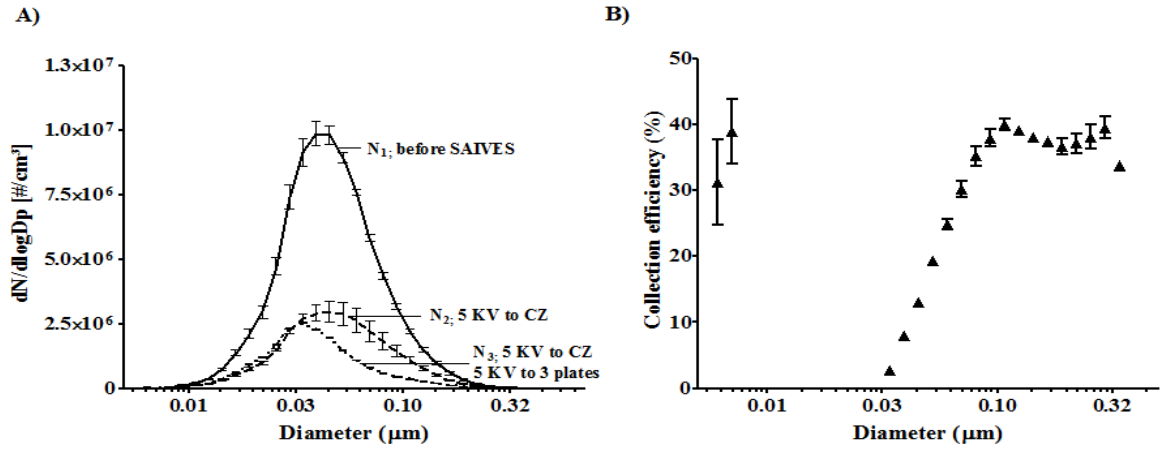

Figure D.7: A) PM number concentration measured by FMPS for different conditions. B) Collection efficiency of SAIVES at the optimum operating conditions: 5 KV to CZ and 5 KV to ESZ. Data is expressed as mean ± SD (n = 3).

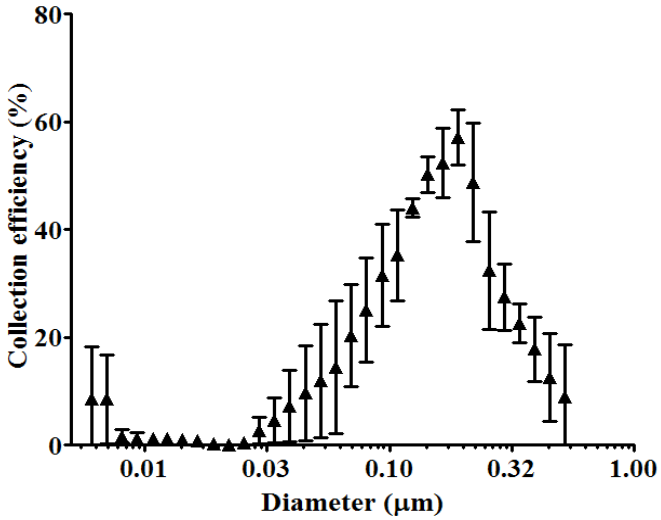

Figure D.8: Collection efficiency of SAIVES using a fluorescence indicator. Data presented as mean ± SD.

Particle deposition efficiency calculated using the difference between condition N_2 and N_3 should indicate the particle amount that was deposited on the collection plates. However, from these experiments it cannot be confirmed whether the particles actually deposited on the collection plates and exactly how much of those particles deposited in the desired location, i.e., in the holes where cell culture inserts will be placed. To determine the actual particle deposition profile, the same experiments were performed using the fluorescence indicator for 4 h. After the experiment, SAIVES was placed under the UV light of a biological safety unit (Model 1385, Thermo Fisher Scientific Inc., Mississauga, ON, Canada) and images were taken. Particle deposition was comparatively uniform inside the system when no charge was applied (**Figure D.9A**). After applying charge to CZ and EPZ, particle path flow was altered and significant amount of particles were deposited on the top plate, especially on the wall that separated the CZ and EPZ (**Figure D.9B**). Therefore, the actual particle deposition on the collection plates may not be as high as 40 and 57% as determined before (**Figure D.7B** and **Figure D.8**).

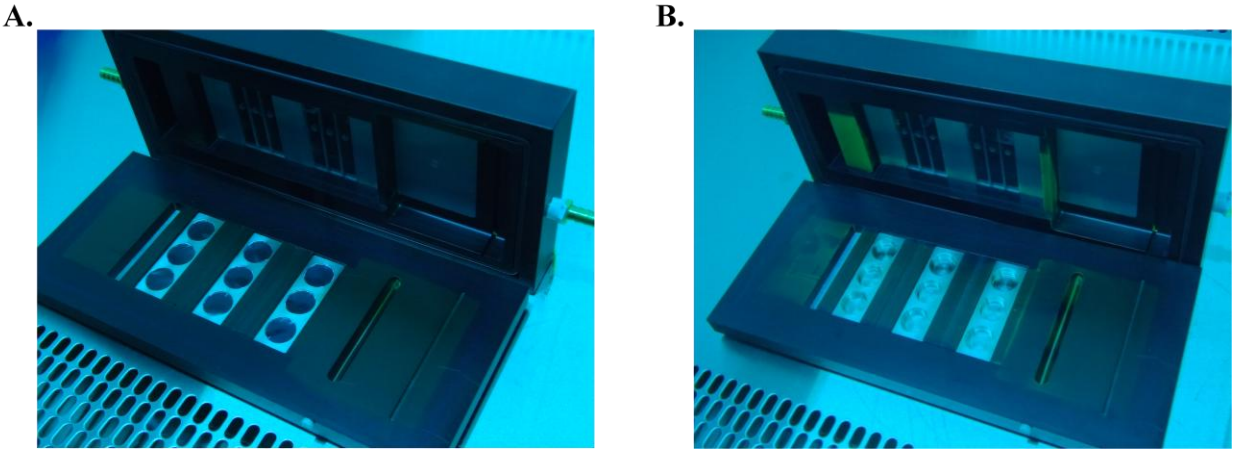

Figure D.9: Particle deposition profile inside SAIVES using a fluorescence indicator. A) No charge was applied to SAIVES, B) 5 KV was applied to both charging and electrostatic precipitation zones.

The following tests were conducted with the specific objective to determine the amount of particle deposition in the holes where the cell culture inserts (A, B, C) would be placed on the collection plates (1, 2, 3). The potential amount of particle mass deposition on the cell culture inserts could be predicted based on the collection efficiency. Cell culture inserts layout is shown

in **Figure D.10A**. For the first experiment, fluorescence indicator was collected for in water and was later analyzed using a fluorescence spectrophotometer (emission wavelength: 256 nm, excitation wavelength: 526 nm). To determine the mass concentration from absorbance data, 1 mg of the indicator was mixed in 1 ml of water and several dilutions were prepared (upto 0.0125 µg/ml) to create a standard curve. From the plot of absorbance versus concentration, the overall relationship between concentration and absorbance was best described by a straight line. Based on the linear regression equation, the mass concentration of the test samples were determined from the absorbance data. The experiment was repeated for four times.

Particle deposition percentage (η_2) in the cell culture inserts was calculated as:

$$\eta_2 = \frac{N_3}{N_1} X100\% \ldots\ldots\ldots\ldots\ldots\ldots(2)$$

where for condition N_1 particles were collected before SAIVES in deionized water (DIH_2O) or on Teflon filter. For condition N_3, 5 KV voltages were applied to CZ and ESZ and nine holes on the three collection plates (1, 2, and 3) were filled with DIH_2O.

Average particle deposition efficiency in the holes for nine inserts ranged from 1.2 to 3.5%. Total particle collection efficiency in all nine holes was 14.5 ± 3.9% and total mass collected was 0.45 ± 0.12 µg (mean ± SD) (**Figure D.10B**). Collection efficiency was higher for collection plate 1 followed by plate 2 and 3. In collection plate 1, the efficiency was the highest for A1 (3.5 ± 0.84%) and decreased gradually in B1 and C1. However, no such pattern was found in collection plate 2 and 3. Average mass deposited in each insert is presented in **Table D.2**.

Table D.2: Particle mass (µg) collection in each insert

Cell insert	Mean ± SD	Cell insert	Mean ± SD	Cell insert	Mean ± SD
A1	0.11 ± 0.026	A2	0.036 ± 0.017	A3	0.029 ± 0.012
B1	0.073 ± 0.025	B2	0.044 ± 0.009	B3	0.034 ± 0.007
C1	0.056 ± 0.019	C2	0.040 ± 0.017	C3	0.034 ± 0.013

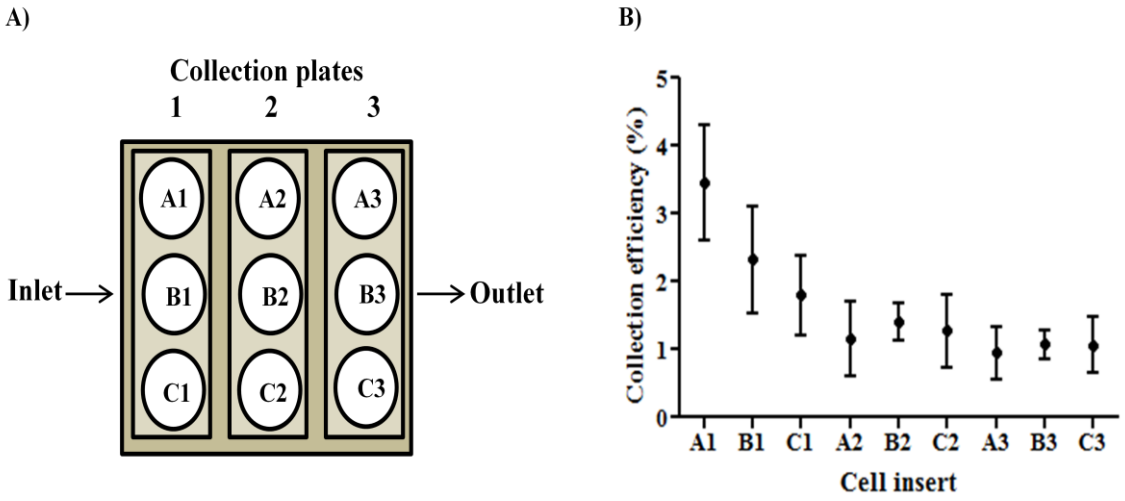

Figure D.10: A) Cell culture insert layout inside SAIVES. B) Collection efficiency of individual insert of SAIVES using fluorescence spectrophotometer. The experiment was repeated four times and results are presented as mean ± SD.

Particle collection efficiency was also determined by measuring the mass deposited on the insert area. Round shaped aluminum foil was placed in the holes where cell culture inserts would be placed and the same experimental procedure was followed. The mass of the foils was measured before and after the experiment. The difference in the mass would be the amount collected in the inserts. Two tests were performed using ammonium sulfate (Test 1 and 2) and one test using fluorescence indicator (Test 3). For condition N_1, particles were collected on a Teflon filter. Similar to the previous experiment, collection efficiency was higher in collection plate 1 (**Figure D.11**). Total particle collection efficiency in nine inserts was 6.04, 4.82 and 5.3% for Test 1, 2, and 3, respectively. Although total particle efficiency was lower (5.3% vs 14.5%), particle mass collection was higher in this test for fluorescence indicator (56.5 µg vs 0.45 µg). Total and individual particle mass collected on each insert hole are presented in **Table D.3**.

After the aluminum foils were weighted, they were examined using a Scanning Electron Microscope (SEM, Hitachi S2500) to check for any size-fractionated particle deposition profile. Here images for fluorescence indicator are presented only (images using ammonium sulfates particles were not clear) (**Figure D.12**). In accordance with previous tests, particle collection was

higher visually in all three inserts of collection plate 1 compared to other plates. Larger particle deposition (may be agglomerated particle) was also higher in that plate, especially in insert A1. Smaller particles were anticipated to travel far than bigger particles. However, deposition of smaller particles was observed in all three plates.

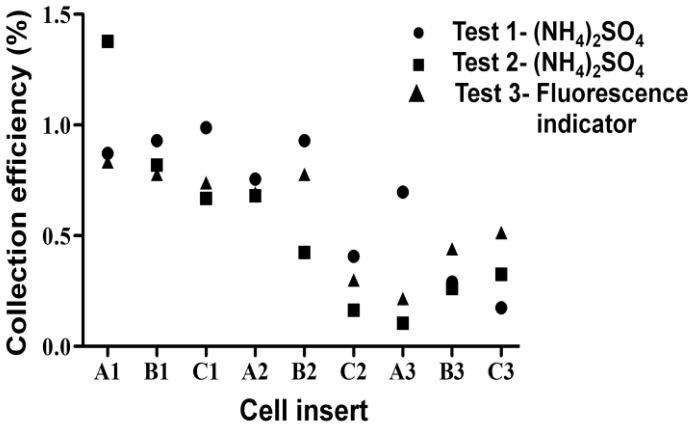

Figure D.11: Collection efficiency of individual insert determined by collecting particles on aluminum foil and measuring the collected mass.

Table D.3: Mass (µg) collection on each insert and total collected mass

Cell insert	**Test 1 ($(NH_4)_2SO_4$**	**Test 2 ($(NH_4)_2SO_4$**	**Test 3 Flu. indictor**
A1	15	23.7	8.9
B1	16	14.1	8.3
C1	17	11.5	7.9
A2	13	11.7	7.4
B2	16	7.3	8.3
C2	7	2.8	3.2
A3	12	1.8	2.3
B3	5	4.5	4.7
C3	3	5.6	5.5
Total	104	83	56.5

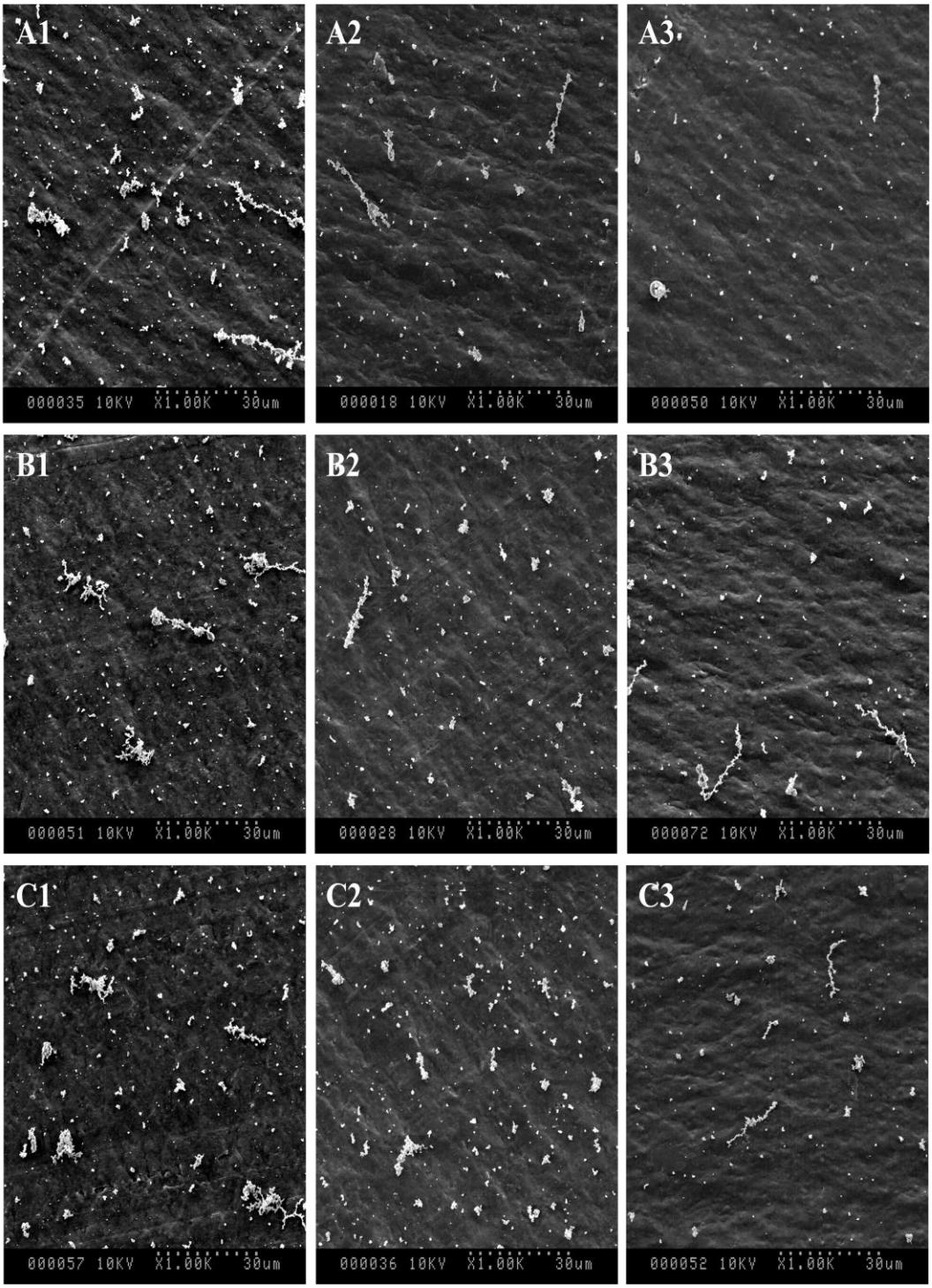

Figure D.12: Scanning Electron Microscope images of deposited fluorescence indicator in nine inserts of three collection plates.

The height of the repelling plates was adjusted by moving the plates vertically to check whether change in the distance of electric field results in different deposition profile. The location of both repelling and collection plates were also changed horizontally to improve size-fractionated particle deposition. However, no significant differences were observed after adjusting the height or location of the plates.

4.3 Effect of airflow on cell integrity

In addition to determining the collection efficiency of SAIVES, the maximum allowable flow rate without effecting cell integrity was also determined in this study. Calu-3 cells grown at ALI in Snapwell® inserts for 2 weeks. Later, the cells were placed in the SAIVES and exposed to filter air for 2 h for variable air flow rate of 0.5 to 3 L/min. Intercellular cell integrity was determined by measuring transepithelial electrical resistance (TEER) using a Epithelial Voltohmmeter (EVOM). Calu-3 cell line, an adenocarcinomic human tracheobronchial epithelial cell line, was used for all the ALI exposure experiments using SAIVES instead of A549 cells used in previous *in vitro* experiments. Calu-3 cells are preferred as a model for measuring airway epithelial barrier as they from tighter junctions and has similar epithelial morphology and electrical resistance as *in vivo* (Grainger et al., 2006). The change in TEER with respect to control was statistically significant for airflow rate of 1 L/min (**Figure D.13**). Therefore, the optimal airflow rate was found to be 0.5 L/min.

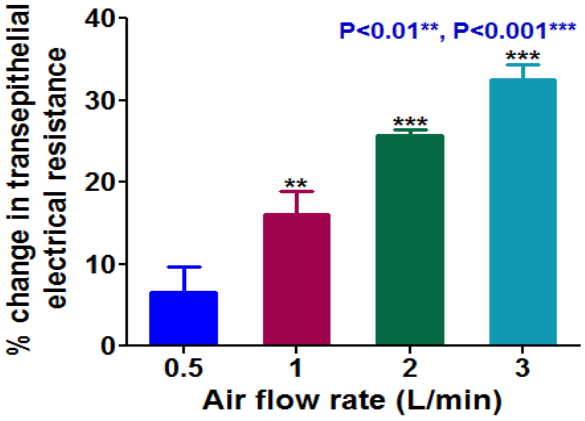

Figure D.13: Effect of airflow rate on cell integrity by measuring transepithelial electrical resistance (TEER) with respect to control.

4.4 Addition of physiological properties to the system

It is important to maintain a stable temperature (T) of 37ºC and 95% relative humidity (RH) in the SAIVES for optimal cell growth. A simple set-up was used to obtain the conditions (**Figure D.14**). Water was boiled to 100ºC and then added to the incoming air. Heating tape was also used to heat the incoming air. The moisture added air was passed through a tube to remove any extra moisture. The outlet temperature and RH were measured using a sensor. With this set-up, the RH obtained (92%) was close to the target value. However, with the addition of water vapor and heating tape, the outlet air was as high as 30ºC and was not stable. Therefore, this set-up was not suitable for achieving the optimal temperature.

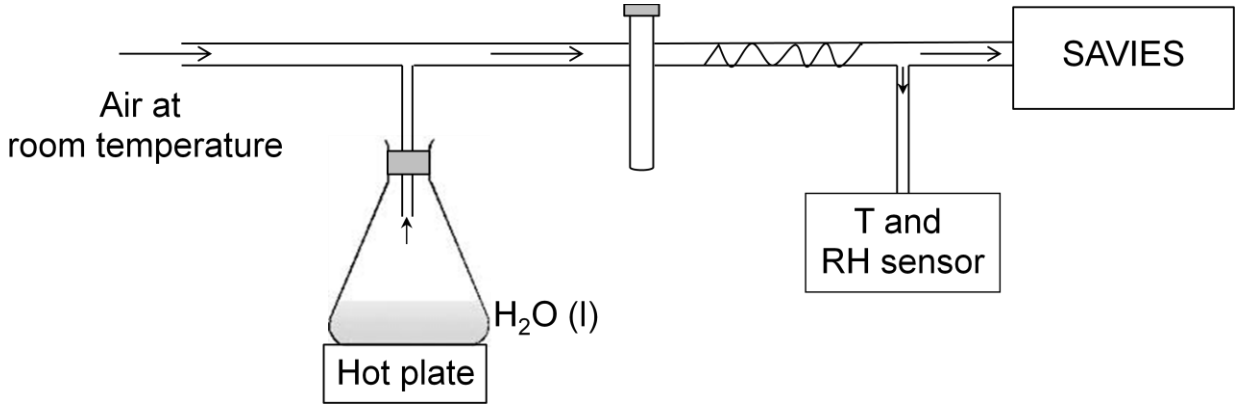

Figure D.14: A simple set-up for heating and adding relating humidity to the incoming air.

5. Conclusions

The main purpose of developing SAIVES was to achieve higher particle deposition in a reasonable time frame. Therefore, the system can be used for field studies for direct exposure of PM on cells, particularly for ultrafine particles. Application of a direct air-liquid interface system will limit the alteration of particle properties, allow realistic interaction between PM and cells, and improve dose-related information. In the current prototype of SAIVES, particle deposition profile was obtained by applying different methods. The findings from different methods appeared to be in agreement; higher particle collection was observed in collection plate 1 and deposition was higher in insert A1. Although overall particle deposition in the system ranged

from 40 to 57%, deposition efficiency in the insert areas were still very low (ranged from 0.3 to 3.5%). Application of high voltage to the CZ caused generation of ion wind that would travel from the corona wire to the electrode. Combination of air and ion wind velocities could have caused the directional change in the particles and lead to the increased deposition on the top plate, especially on the partition wall between CZ and EPZ.

Total particle mass collected in several cell insert areas was extremely low (<10 µg). A previous study showed that at least 10 µg/ml (equivalent to 4.5 .µg/cm^2 for a Snapwell plate) of ultrafine PM were required to induce HMOX-1 activation which is known as a sensitive biomarker (Chapter 4). In addition, allowable flow rate without effecting cell integrity was achieved as high as 0.5 L/min exposure duration. Due to low particle collection efficiency and allowable flow rate, it might not be possible to collect enough PM mass to induce any detectable biological responses in the cells. Therefore, prolonged exposure duration would be required to collect the desired PM mass. As the performance of the current prototype of SAIVES was not satisfactory, it was not used for *in vitro* study. However, with several design modifications it is expected that the efficiency will be increased.

6. Recommendations

Several design modifications are recommended here for improving particle deposition and overall performance of SAIVES:

1) Significant number of particles was lost on the partition wall, located next to the charging zone. If the wall is removed, more particles will be allowed to flow to the precipitation zone.

2) If the bottom collection plate is charged negatively instead of grounding, that may results in higher deposition.

3) It was hypothesized that particles would deposit in different plates with respect to their size; larger particles would deposit closer to the charging zone, whereas smaller particles would travel further. However, in the current design no significant particle segregated deposition pattern was observed. Therefore, instead of three collection plates design of EPZ with only one plate (with at

least three inserts) is recommended.

4) This system is aimed for using in field studies, if possible in a mobile laboratory. In the current design, addition of physiological parameters (37°C temperature, 95% relative humidity, 5% CO_2) requires a number of additional elements to the system which will be inconvenient in the field. If these design parameters could be combined in the system design, it would be easier to move around the system.

Appendix E

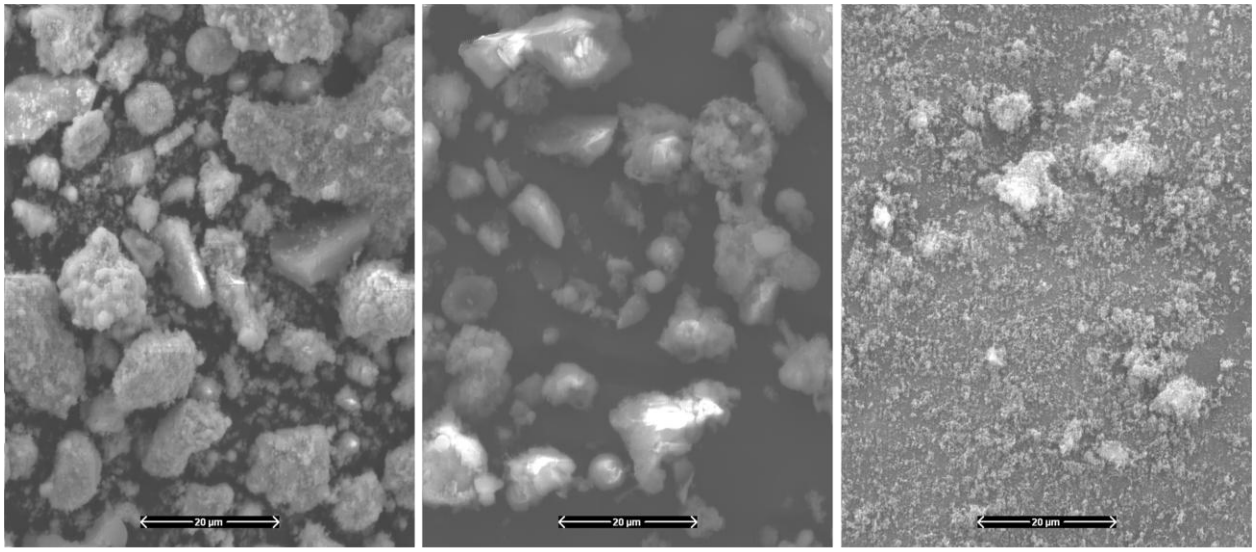

Figure E.1: Scanning electron microscope (SEM) images of different Standard Reference Materials (SRMs).

References

Adamkiewicz, G., Ebelt, S., Syring, M., Slater, J., Speizer, F.E., Schwartz, J., Suh, H. and Gold, D.R. 2004. Association between air pollution exposure and exhaled nitric oxide in an elderly population. Thorax 59, 204-209.

Ahlm, L., Liu, S., Day, D.A., Russell, L.M., Weber, R., Gentner, D.R., Goldstein, A.H., DiGangi, J.P., Henry, S.B., Keutsch, F.N., VandenBoer, T.C., Markovic, M.Z., Murphy, J.G., Ren, X. and Scheller, S. 2012. Formation and growth of ultrafine particles from secondary sources in Bakersfield, California. J. Geophys. Res-Atmos. 117, doi:10.1029/2011JD017144.

Akhtar, U.S., McWhinney, R.D., Rastogi, N., Abbatt, J.P.D., Evans, G.J. and Scott, J.A. 2010. Cytotoxic and proinflammatory effects of ambient and source-related particulate matter (PM) in relation to the production of reactive oxygen species (ROS) and cytokine adsorption by particles. Inhal. Toxicol. 22, 37-47.

Akhtar, U.S., Rastogi, N., McWhinney, R.D., Urch, B., Chow, C.W., Evans, G.J. and Scott, J.A. 2014. Comparative toxicity of size-fractionated ambient particulate matter in human airway epithelial cells. Toxicol. Rep. 1, 145-156, doi: 10.1016/j.toxrep.2014.05.002.

Alam, K., Blaschke, T., Madl, P., Mukhtar, A., Hussain, M., Trautmann, T. and Rahman, S. 2011. Aerosol size distribution and mass concentration measurements in various cities of Pakistan. J. Environ. Monitor. 13, 1944-1952.

Amatullah, H., North, M.L., Akhtar, U.S., Rastogi, N., Urch, B., Silverman, F.S., Chow, C. W., Evans, G.J. and Scott, J.A. 2012. Comparative cardiopulmonary effects of size-fractionated airborne particulate matter. Inhal. Toxicol. 24, 161-171.

Anderson, L. and Seilhamer, J. 1997. A comparison of selected mRNA and protein abundances in human liver. Electrophoresis 18, 533-537.

Araujo, J.A., Barajas, B., Kleinman, M., Wang, X.P., Bennett, B.J., Gong, K.W., Navab, M., Harkema, J., Sioutas, C., Lusis, A.J. and Nel, A.E. 2008. Ambient particulate pollutants in the

ultrafine range promote early atherosclerosis and systemic oxidative stress. Circ. Res. 102, 589-596.

Asgharian, B. and Yu, C. P. 1988. Deposition of inhaled fibrous particles in the human lung. J. Aerosol Med. 1, 37-50.

Atkinson, R.W., Fuller, G.W., Anderson, H.R., Harrison, R.M. and Armstrong, B. 2010. Urban ambient particle metrics and health: A time-series analysis. Epidemiology 21, 501-511.

Aufderheide, M. 2005. Direct exposure methods for testing native atmospheres. Exp. Toxicol. Pathol. 57, 213-226.

Aufderheide, M., Halter, B., Möhle, N. and Hochrainer, D. 2013. The CULTEX RFS: a comprehensive technical approach for the *in vitro* exposure of airway epithelial cells to the particulate matter at the air-liquid interface. BioMed Res. Int. Article ID 734137, http://dx.doi.org/10.1155/2013/734137.

Bai, Y.S., Suzuki, A.K. and Sagai, M. 2001. The cytotoxic effects of diesel exhaust particles on human pulmonary artery endothelial cells *in vitro*: Role of active oxygen species. Free Radic. Biol. Med. 30, 555-562.

Bakand, S., Winder, C., Khalil, C. and Hayes, A. 2006. An experimental *in vitro* model for dynamic direct exposure of human cells to airborne contaminants. Toxicol. Lett.165, 1-10.

Balakrishna, S., Lomnicki, S., McAvey, K.M., Cole, R.B., Dellinger, B., and Cormier S.A. 2009. Environmentally persistent free radicals amplify ultrafine particle mediated cellular oxidative stress and cytotoxicity. Part. Fibre Toxicol. 6.

Balashazy, I. and Hofmann, W. 2000. Quantification of local deposition patterns of inhaled radon decay products in human bronchial airway bifurcations. Health Phys. 78, 147-158.

Bartoli, C.R., Wellenius, G.A., Diaz, E.A., Lawrence, J., Coull, B.A., Akiyama, I., Lee, L.M., Okabe, K., Verrier, R.L. and Godleski, J.J. 2009. Mechanisms of inhaled fine particulate Air Pollution-induced Arterial Blood Pressure Changes. Environ. Health Persp. 117, 361-366.

Baulig, A., Sourdeval, M., Meyer, M., Marano, F. and Baeza-Squiban, A. 2003. Biological effects of atmospheric particles on human bronchial epithelial cells. Comparison with diesel exhaust particles. Toxicol. in Vitro 17, 567-573.

Becher, R., Hetland, R.B., Refsnes, M., Dahl, J.E., Dahlman, H.J. and Schwarze, P.E. 2001. Rat lung inflammatory responses after *in vivo* and *in vitro* exposure to various stone particles. Inhal. Toxicol. 13, 789-805.

Becker, S., Dailey, L.A., Soukup, J.M., Grambow, S.C., Devlin, R.B., and Huang, Y.C.T. 2005. Seasonal variations in air pollution particle-induced inflammatory mediator release and oxidative stress. Environ. Health. Persp. 113, 1032-1038.

Becker, S., Soukup, J.M., Sioutas, C. and Cassee, F.R. 2003. Response of human alveolar macrophages to ultrafine, fine, and coarse urban air pollution particles. Exp. Lung Res. 29, 29-44.

Beckett, W.S., Chalupa, D.F., Pauly-Brown, A., Speers, D.M., Stewart, J.C., Frampton, M.W., Utell, M.J., Huang, L.S., Cox, C., Zareba, W. and Oberdörster, G. 2005. Comparing inhaled ultrafine versus fine zinc oxide particles in healthy adults - A human inhalation study. Am. J. Respir. Crit. Care Med. 171, 1129-1135.

Beeson, W.L., Abbey, D.E. and Knutsen, S.F. 1998. Long-term concentrations of ambient air pollutants and incident lung cancer in California adults: Results from the AHSMOG study. Environ. Health Persp. 106, 813-822.

Behbod, B., Urch, B., Speck, M., Scott, J.A., Liu, L., Poon, R., Coull, B., Schwartz, J., Koutrakis, P., Silverman, F. and Gold, D.R. 2013. Endotoxin in concentrated coarse and fine ambient particles induces acute systemic inflammation in controlled human exposures. Occup. Environ. Med. 70, 761-767.

Bennett, W.D. and Zeman, K.L. 1998. Deposition of fine particles in children spontaneously breathing at rest. Inhal. Toxicol. 10, 831-842.

Bennett, W.D., Zeman, K.L., Kim, C. and Mascarella, J. 1997. Enhanced deposition of fine particles in COPD patients spontaneously breathing at rest. Inhal. Toxicol. 9, 1-14.

Birch, M.E. and Cary, R.A. 1996. Elemental carbon-based method for monitoring occupational exposures to particulate diesel exhaust. Aerosol Sci. Technol. 25, 221-241.

Boland, S., Baeza-Squiban, A., Bonvallot, V., Houcine, O., Pain, C., Meyer, M., Marano, F. 2001. Similar cellular effects induced by diesel exhaust particles from a representative diesel vehicle recovered from filters and Standard Reference Material 1650. Toxicol. in Vitro 15, 379-85.

Boland, S., Baeza-Squiban, A., Fournier, T., Houcine, O., Gendron, M.C., Chevrier, M., Jouvenot, G., Coste, A., Aubier, M. and Marano, F. 1999. Diesel exhaust particles are taken up by human airway epithelial cells *in vitro* and alter cytokine production. Am. J. Physiol. 276, L604-L613.

Bonetta, S., Gianotti, V., Gosetti, F., Oddone, M., Gennaro, M.C. and Carraro, E. 2009. DNA damage in A549 cells exposed to different extracts of $PM_{2.5}$ from industrial, urban and highway sites. Chemosphere 77, 1030-1034.

Brauer, M., Hoek, G., Van Vliet, P., Meliefste, K., Fischer, P.H., Wijga, A., Koopman, L.P., Neijens, H.J., Gerritsen, J., Kerkhof, M., Heinrich, J., Bellander, T., and Brunekreef, B. 2002. Air pollution from traffic and the development of respiratory infections and asthmatic and allergic symptoms in children. Am. J. Respir. Cell Mol. Biol. 166, 1092-8.

Brook, R.D. 2008. Cardiovascular effects of air pollution. Clin. Sci. 115, 175-187.

Brook, R.D., Brook, J.R. and Rajagopalan, S. 2003. Air pollution: The "heart" of the problem. Curr. Hypertens. Rep. 5, 32-39.

Brook, R.D., Brook, J.R., Urch, B., Vincent, R., Rajagopalan, S. and Silverman, F. 2002. Inhalation of fine particulate air pollution and ozone causes acute arterial vasoconstriction in healthy adults. Circulation 105, 1534-1536.

Brook, R.D., Franklin, B., Cascio, W., Hong, Y.L., Howard, G., Lipsett, M., Luepker, R., Mittleman, M., Samet, J., Smith, S.C. and Tager, I. 2004. Air pollution and cardiovascular disease - A statement for healthcare professionals from the expert panel on population and prevention science of the American Heart Association. Circulation 109, 2655-2671.

Brook, R.D., Urch, B., Dvonch, J.T., Bard, R.L., Speck, M., Keeler, G., Morishita, M., Marsik, F.J., Kamal, A.S., Kaciroti, N., Harkema, J., Corey, P., Silverman, F., Gold, D.R., Wellenius, G., Mittleman, M.A., Rajagopalan, S. and Brook, J.R. 2009. Insights into the mechanisms and mediators of the effects of air pollution exposure on blood pressure and vascular function in healthy humans. Hypertension 54, 659-667.

Brown, J.S., Zeman, K.L. and Bennett, W.D. 2002. Ultrafine particle deposition and clearance in the healthy and obstructed lung. Am. J. Respir. Crit. Care Med. 166, 1240-1247.

Bruijne, K., Ebersviller, S., Sexton, K.G., Lake, S., Leith, D., Goodman, R., Jetters, J., Walters, G.W., Doyle-Eisele, M., Woodside, R., Jeffries, H.E. and Jaspers, I. 2009. Design and testing of Electrostatic Aerosol *in Vitro* Exposure System (EAVES): An alternative exposure system for particles. Inhal. Toxicol. 21, 91-101.

Buist, A.S., McBurnie, M.A., Vollmer, W.M., Gillespie, S., Burney, P., Mannino, D.M., Menezes, A.M.B., Sullivan, S.D., Lee, T.A., Weiss, K.B., Jensen, R.L., Marks, G.B., Gulsvik, A., Nizankowska-Mogilnicka, E. and Grp, B.C.R. 2007. International variation in the prevalence of COPD (The BOLD Study): a population-based prevalence study. Lancet 370, 741-750.

Calderon-Garciduenas, L., Reed, W., Maronpot, R.R., Henriquez-Roldan, C., Delgado-Chavez, R., Calderon-Garciduenas, A., Dragustinovis, I., Franco-Lira, M., Aragon-Flores, M., Solt, A.C., Altenburg, M., Torres-Jordon, R. and Swenberg, J.A. 2004. Brain inflammation and Alzheimer's-like pathology in individuals exposed to severe air pollution. Toxicol. Pathol. 32, 650-658.

Camatini, M., Corvaja, V., Pezzolato, E., Mantecca, P. and Gualtieri, M. 2012. PM_{10}-biogenic fraction drives the seasonal variation of proinflammatory response in A549 cells. Environ.

Toxicol. 27, 63-73.

Camner, P., Anderson, M., Philipson, K., Bailey, A., Hashish, A., Jarvis, N., Bailey, M. and Svartengren, M. 1997. Human bronchiolar deposition and retention of 6-, 8- and 10-micrograms particles. Exp. Lung Res. 23(6), 517-535.

Canadian Certified Reference Materials Project (CCRMP). 2009. Non-ferrous dust (PD-1) certificate of analysis. http://www.nrcan.gc.ca/smm-mms/tect-tech/ccrmp/cer-cer/pd-1-eng.htm. (accessed on April 20, 2010)

Canadian Medical Association (CMA). 2008. No breathing room National illness costs of air pollution.http://www.cma.ca/multimedia/CMA/Content_Images/Inside_cma/Office_PublicHealth/ICAP/CMA_ICAP_sum_e.pdf. (accessed on May 17, 2010)

Carter, J.D., Ghio, A.J., Samet, J.M. and Devlin, R.B. 1997. Cytokine production by human airway epithelial cells after exposure to an air pollution particle is metal-dependent. Toxicol. Appl. Pharmacol. 146, 180-188.

Carter, J.M., Corson, N., Driscoll, K.E., Elder, A., Finkelstein, J.N., Harkema, J.N., Gelein, R., Wade-Mercer, P., Nguyen, K. and Oberdörster, G. 2006. A comparative dose-related response of several key pro- and antiinflammatory mediators in the lungs of rats, mice, and hamsters after subchronic inhalation of carbon black. J. Occup. Environ. Med. 48, 1265-1278.

Chalupa, D.C., Morrow, P.E., Oberdörster, G., Utell, M.J. and Frampton, M.W. 2004. Ultrafine particle deposition in subjects with asthma. Environ. Health Persp. 112, 879-882.

Chao, C., Tung, T.C.W. and Burnett, J. 1998. Influence of different indoor activities on the indoor particulate levels in residential buildings. Indoor Built Environ. 7, 110-121.

Cho, A.K., Sioutas, C., Miguel, A.H., Kumagai, Y., Schmitz, D.A., Singh, M., Eiguren-Fernandez, A. and Froines, J.R. 2005. Redox activity of airborne particulate matter at different sites in the Los Angeles Basin. Environ. Res. 99, 40-47.

Clark, N.A., Demers, P.A., Karr, C.J., Koehoorn, M., Lencar, C., Tamburic, L. and Brauer, M.

2010. Effect of early life exposure to air pollution on development of childhood asthma. Environ. Health Persp. 118, 284-290.

Cohen, A.J., Anderson, H.R., Ostro, B., Pandey, K.D., Krzyzanowski, M., Kuenzli, N., Gutschmidt, K., Pope, A., Romieu, I., Samet, J.M. and Smith, K. 2005. The global burden of disease due to outdoor air pollution. J. Toxicol. Environ. Health 68, 1301-1307.

Correia, A.W., Pope, C.A., III, Dockery, D.W., Wang, Y., Ezzati, M. and Dominici, F. 2013. Effect of air pollution control on life expectancy in the United States: An analysis of 545 US counties for the period from 2000 to 2007. Epidemiology 24, 23-31.

Daigle, C.C., Chalupa, D.C., Gibb, F.R., Morrow, P.E., Oberdörster, G., Utell, M.J. and Frampton, M.W. 2003. Ultrafine particle deposition in humans during rest and exercise. Inhal. Toxicol. 15, 539-552.

Delfino, R.J., Sioutas, C. and Malik, S. 2005. Potential role of ultrafine particles in associations between airborne particle mass and cardiovascular health. Environ. Health Persp. 113, 934-946.

Delfino, R.J., Staimer, N., Gillen, D., Tjoa, T., Sioutas, C., Fung, K., George, S.C. and Kleinman, M.T. 2006. Personal and ambient air pollution is associated with increased exhaled nitric oxide in children with asthma. J. Toxicol. Environ. Health 114, 1736-1743.

Devlin, R.B., Frampton, M.L. and Ghio, A.J. 2005. *In vitro* studies: What is their role in toxicology? Exper. Toxicol. Pathol. 57, 183-188.

Di Pietro, A., Visalli, G., Munao, F., Baluce, B., La Maestra, S., Primerano, P., Corigliano, F. and De Flora, S. 2009. Oxidative damage in human epithelial alveolar cells exposed *in vitro* to oil fly ash transition metals. Int. J. Hyg. Environ. Health 212, 196-208.

DiStefano, E., Eiguren-Fernandez, A., Delfino, R.J., Sioutas, C., Froines, J.R. and Cho, A.K. 2009. Determination of metal-based hydroxyl radical generating capacity of ambient and diesel exhaust particles. Inhal. Toxicol. 21, 731-738.

Dockery, D.W., Pope, C.A., Xu, X.P., Spengler, J.D., Ware, J.H., Fay, M.E., Ferris, B.G. and

Speizer, F.E. 1993. An association between air-pollution and mortality in 6 United-State cities. New Engl. J. Med. 329, 1753-1759.

Dominici, F., Peng, R.D., Bell, M.L., Pham, L., McDermott, A., Zeger, S.L. and Samet, J.M. 2006. Fine particulate air pollution and hospital admission for cardiovascular and respiratory diseases. J. Am. Med. Assoc. 295, 1127-1134.

Dormans, J., Steerenberg, P.A., Arts, J.H.E., van Bree, L., de Klerk, A., Verlaan, A.P.J., Bruijntjes, J.P., Beekhof, P., van Soolingen, D. and van Loveren, H. 1999. Pathological and immunological effects of respirable coal fly ash in male wistar rats. Inhal. Toxicol. 11, 51-69.

Dubowsky, S.D., Suh, H., Schwartz, J., Coull, B.A. and Gold, D.R. 2006. Diabetes, obesity, and hypertension may enhance associations between air pollution and markers of systemic inflammation. Environ. Health. Persp. 114, 992-998.

Duffin, R., Tran, C.L., Clouter, A., Brown, D.M., MacNee, W., Stone, V., and Donaldson, K. 2002. The importance of surface area and specific reactivity in the acute pulmonary inflammatory response to particles. Ann. Occup. Hyg. 46 (S1), 242–245.

Duvall, R.M., Norris, G.A., Dailey, L.A., Burke, J.M., McGee, J.K., Gilmour, M.I., Gordon, T. and Devlin, R.B. 2008. Source apportionment of particulate matter in the US and associations with lung inflammatory markers. Inhal. Toxicol. 20, 671-683.

Environment Canada, 2013. Peak ambient fine particulate matter concentrations at monitoring stations, Canada, 2011.
http://maps-cartes.ec.gc.ca/indicators-indicateurs/default.aspx?mapId=26&lang=en (accessed on June 12, 2014).

Fairley, D. 1999. Daily mortality and air pollution in Santa Clara County, California: 1989-1996. Environ. Health. Persp. 107, 637-641.

Fakhri, A.A., Ilic, L.M., Wellenius, G.A., Urch, B., Silverman, F., Gold, D.R. and Mittleman, M.A. 2009. Autonomic effects of controlled fine particulate exposure in young healthy adults:

Effect modification by ozone. Environ. Health. Persp. 117, 1287-1292.

Falk, R., Philipson, K., Svartengren, M., Bergmann, R., Hofmann, W., Jarvis, N., Bailey, M., and Camner, P. 1999. Assessment of long-term bronchiolar clearance of particles from measurements of lung retention and theoretical estimates of regional deposition. Exp. Lung Res. 25, 495-516.

Fine, P.M., Chakrabarti, B., Krudysz, M., Schauer, J.J. and Sioutas, C. 2004. Diurnal variations of individual organic compound constituents of ultrafine and accumulation mode particulate matter in the Los Angeles basin. Environ. Sci. Technol. 38, 1296-1304.

Fischer, H.C., Fournier-Bidoz S., Chan, W.C.W, and Pang, K.S. 2007. Quantitative detection of engineered nanoparticles in tissues and organs: An investigation of efficacy and linear dynamic ranges using ICP-AES. NanoBiotech. 3, 1646-1554.

Fleisher, B., Kulovich, M.V., Hallman, M., Gluck, L., 1985. Lung profile-sex differences in normal pregnancy. Obstet. Gynecol. 327-330.

Frampton, M.W., Ghio, A.J., Samet, J.M., Carson, J.L., Carter, J.D., and Devlin, R.B. 1999. Effects of aqueous extracts of PM_{10} filters from the Utah Valley on human airway epithelial cells. Am. J. Physiol. Lung Cell Mol. Physiol. 277, L960-7.

Fujii, T., Hayashi, S., Hogg, J.C., Vincent, R. and Van Eeden, S.F. 2001. Particulate matter induces cytokine expression in human bronchial epithelial cells. Am. J. Respir. Cell Mol. Biol. 25, 265-271.

Fukano, Y., Yoshimura, H. and Yoshida, T. 2006. Heme oxygenase-1 gene expression in human alveolar epithelial cells (A549) following exposure to whole cigarette smoke on a direct *in vitro* exposure system. Toxicol. Pathol. 57, 411-418.

Gangwal, S., Brown, J.S., Wang, A., Houck, K.A., Dix, D.J., Kavlock, R.J. and Hubal, E.A.C. 2011. Informing selection of nanomaterial concentrations for ToxCast *in vitro* testing based on occupational exposure potential. Environ. Health Persp. 119, 1539-1546.

Gauderman, W.J., Avol, E., Gilliland, F., Vora, H., Thomas, D., Berhane, K., McConnell, R.,

Kuenzli, N., Lurmann, F., Rappaport, E., Margolis, H., Bates, D. and Peters, J. 2004. The effect of air pollution on lung development from 10 to 18 years of age. New Engl. J. Med. 351, 1057-1067.

Gehring, U., Wijga, A.H., Brauer, M., Fischer, P., de Jongste, J.C., Kerkhof, M., Oldenwening, M., Smit, H.A. and Brunekreef, B. 2010. Traffic-related air pollution and the development of asthma and allergies during the first 8 years of life. Am. J. Resp. Criti. Care Med. 181, 596-603.

Ghio, A.J. 2004. Biological effects of Utah Valley ambient air particles in humans: A review. J. Aerosol Med. 17, 157-64.

Ghio, A.J. and Devlin, R.B. 2001. Inflammatory lung injury after bronchial instillation of air pollution particles. Am. J. Respir. Crit. Care Med. 164, 704-708.

Ghio, A.J., Kim, C. and Devlin, R.B. 2000. Concentrated ambient air particles induce mild pulmonary inflammation in healthy human volunteers. Am. J. Respir. Crit. Care Med. 162, 981-988.

Ghio, A.J., Stonehuerner, J., Dailey, L.A., and Carter, J.D. 1999. Metals associated with both the water-soluble and insoluble fractions of an ambient air pollution particle catalyze an oxidative stress. Inhal. Toxicol. 11, 37-49.

Giard, D.J., Aaronson, S.A., Todaro, G.J., Arnstein, P., Kersey, J.H., Dosik, H. and Parks, W.P. 1973. *In vitro* cultivation of human tumors: Establishment of cell lines derived from a series of solid tumors. J. Nat. Cancer Inst. 51, 1417-1423.

Gilmour, M.I., McGee, J., Duvall, R.M., Dailey, L., Daniels, M., Boykin, E., Cho, S.H., Doerfler, D., Gordon, T. and Devlin, R.B. 2007. Comparative toxicity of size-fractionated airborne particulate matter obtained from different cities in the United States. Inhal. Toxicol. 19, 7-16.

Gold, D.R., Litonjua, A., Schwartz, J., Lovett, E., Larson, A., Nearing, B., Allen, G., Verrier, M., Cherry, R. and Verrier, R. 2000. Ambient pollution and heart rate variability. Circulation 101,

1267-1273.

Goldberg, M.S., Bailar, J.C., 3rd, Burnett, R.T., Brook, J.R., Tamblyn, R., Bonvalot, Y., Ernst, P., Flegel, K.M., Singh, R.K. and Valois, M.F. 2000. Identifying subgroups of the general population that may be susceptible to short-term increases in particulate air pollution: a time-series study in Montreal, Quebec. Research report (Health Effects Institute), 7-113; Discussion 115-120.

Goldberg, M.S., Burnett, R.T., Yale, J.F.O., Valois, M.F. and Brook, J.R. 2006. Associations between ambient air pollution and daily mortality among persons with diabetes and cardiovascular disease. Environ. Res. 100, 255-267.

Gong, H., Linn, W.S., Clark, K.W., Anderson, K.R., Geller, M.D. and Sioutas, C. 2005. Respiratory responses to exposures with fine particulates and nitrogen dioxide in the elderly with and without COPD. Inhal. Toxicol. 17, 123-132.

Gong, H., Linn, W.S., Sioutas, C., Terrell, S.L., Clark, K.W., Anderson, K.R. and Terrell, L.L. 2003. Controlled exposures of healthy and asthmatic volunteers to concentrated ambient fine particles in Los Angeles. Inhal. Toxicol. 15, 305-325.

Graff, D.W., Cascio, W.E., Rappold, A., Zhou, H., Huang, Y.-C.T. and Devlin, R.B. 2009. Exposure to concentrated coarse air pollution particles causes mild cardiopulmonary effects in healthy young adults. Environ. Health Persp. 117, 1089-1094.

Grainger, C.I., Greenwell, L.L., Lockley, D.J., Martin, G.P. and Forbes, B. 2006. Culture of Calu-3 cells at the air interface provides a representative model of the airway epithelial barrier. Pharm. Res. 23, 1482-1490.

Gualtieri, M., Mantecca, P., Corvaja, V., Longhin, E., Perrone, M.G., Bolzacchini, E., and Camatini, M. 2009. Winter fine particulate matter from Milan induces morphological and functional alterations in human pulmonary epithelial cells (A549). Toxicol. Lett. 188, 52-62.

Guo, Y.F., Xiao, P., Lei, S.F., Deng, F.Y., Xiao, G.G., Liu, Y.Z., Chen, X.D., Li, L.M., Wu, S.,

Chen, Y., Jiang, H., Tan, L.J., Xie, J.Y., Zhu, X.Z., Liang, S.P. and Deng, H.W. 2008. How is mRNA expression predictive for protein expression? A correlation study on human circulating monocytes. Acta Bioch. Bioph. Sin. 40, 426-436.

Gupta, S., Siddiqui, S., Haldar, P., Raj, J.V., Entwisle, J.J., Wardlaw, A.J., Bradding, P., Pavord, I.D., Green, R.H. and Brightling, C.E. 2009. Qualitative analysis of high-resolution CT scans in severe asthma. Chest 136, 1521-1528.

Gurr, J.R., Wang, A.S.S., Chen, C.H. and Jan, K.Y. 2005. Ultrafine titanium dioxide particles in the absence of photoactivation can induce oxidative damage to human bronchial epithelial cells. Toxicology 213, 66-73.

Halliwell, B. and Gutteridge, J.M. 1999. Free Radicals in Biology and Medicine, 4th ed. Oxford University Press, Oxford, UK.

Halonen, J.I., Lanki, T., Yli-Tuomi, T., Tiittanen, P., Kulmala, M. and Pekkanen, J. 2009. Particulate air pollution and acute cardiorespiratory hospital admissions and mortality among the elderly. Epidemiology 20, 143-153.

Happo, M.S., Hirvonen, M.R., Hälinen, A.I., Jalava, P.I., Pennanen, A.S., Sillanpää, M., Hillamo, R. and Salonen R.O. 2010. Seasonal variation in chemical composition of size-segregated urban air particles and the inflammatory activity in the mouse lung. Inhal. Toxicol. 22(1), 17-32.

Hart, J.E., Laden, F., Eisen, E.A., Smith, T.J., Garshick, E., 2009. Chronic obstructive pulmonary disease mortality in railroad workers. Occup. Environ. Med. 66, 221-226.

Hatzis, C., Godleski, J.J., Gonzalez-Flecha, B., Wolfson, J.M. and Koutrakis, P. 2006. Ambient particulate matter exhibits direct inhibitory effects on oxidative stress enzymes. Environ. Sci. Technol. 40, 2805-2811.

Heinrich, U., Fuhst, R., Rittinghausen, S., Creutzenberg, O., Bellmann, B., Koch, W. and Levsen, K. 1995. Chronic inhalation exposure of wistar rats and two different strains of mice to

diesel engine exhaust, carbon black, and titanium dioxide. Inhal. Toxicol. 7, 533-556.

Herseth, J.I., Totlandsdal, A.I., Bytingsvik, S., Kaur, J., Noer, M. and Bolling, A.K. 2013. The challenge of obtaining correct data for cellular release of inflammatory mediators after *in vitro* exposure to particulate matter. Toxicol. Lett. 221, 110-117.

Hetland, R.B., Cassee, F.R., Refsnes, M., Schwarze, P.E., Lag, M., Boere, A.J.F. and Dybing, E. 2004. Release of inflammatory cytokines, cell toxicity and apoptosis in epithelial lung cells after exposure to ambient air particles of different size fractions. Toxicol. in Vitro 18, 203-212.

Hetland, R.B., Schwarze, P.E., Johansen, B.V., Myran, T., Uthus, N. and Refsnes, M. 2001. Silica-induced cytokine release from A549 cells: Importance of surface area versus size. Hum. Exp. Toxicol. 20, 46-55.

Hinds W.C. 1999. Aerosol Technology: Properties, Behaviour, and Measurement of Airborne Particles, 2nd edition, John Wiley & Sonc, INC., New York, USA.

Hofmann, W. 2009. Modeling particle deposition in human lungs: modeling concepts and comparison with experimental data. Biomarkers 14, 59-62.

Hofmann, W. and Koblinger, L. 1990. Monte Carlo modeling of aerosol deposition in human lungs. Part II: Deposition fractions and their sensitivity to parameter variations. J. Aerosol Sci. 21, 675-688.

Hofmann, W., Martonen, T.B. and Graham R.C. 1989. Predicted deposition of nonhygroscopic aerosols in the human lung as a function of subject age. J. Aerosol Med. 2, 49-68.

Holder, A.L., Lucas, D., Goth-Goldstein, R. and Koshland, C.P. 2008. Cellular response to diesel exhaust particles strongly depends on the exposure method. Toxicol. Sci. 103, 108-115.

Horemans, B., Van Holsbeke, C., Vos, W., Darchuk, L., Novakovic, V., Fontan, A.C., De Backer, J., Van Grieken, R., De Backer, W. and De Wael, K. 2012. Particle deposition in airways of chronic respiratory patients exposed to an urban aerosol. Environ. Sci. Technol. 46, 12162-12169.

Huang, Y.C.T., Karoly, E.D., Dailey, L.A., Schmitt, M.T., Silbajoris, R., Graff, D.W. and Devlin, R.B. 2011. Comparison of gene expression profiles induced by coarse, fine and ultrafine particulate matter. J. Toxicol. Environ. Health-Part a, 74, 296-312.

Huang, Y.C.T., Li, Z.W., Harder, S.D., and Soukup, J.M. 2004. Apoptotic and inflammatory effects induced by different particles in human alveolar macrophages. Inhal. Toxicol. 16, 863-878.

Hussain, M., Renate, W.-H. and Werner, H. 2011. Effect of intersubject variability of extrathoracic morphometry, lung airways dimensions and respiratory parameters on particle deposition. J. Thorac. Dis. 3, 156-170.

Hutt, J.A., Vuillemenot, B.R., Barr, E.B., Grimes, M.J., Hahn, F.F., Hobbs, C.H., March, T.H., Gigliotti, A.P., Seilkop, S.K., Finch, G.L., Mauderly, J.L. and Belinsky, S.A. 2005. Life-span inhalation exposure to mainstream cigarette smoke induces lung cancer in B6C3F1 mice through genetic and epigenetic pathways. Carcinogenesis 26, 1999-2009.

International Agency for Research on Cancer (IARC), 2013. IARC Scientific Publication No. 161. Air Pollution and Cancer. Editors: Kurt Straif, Aaron Cohen, and Jonathan Samet. http://www.iarc.fr/en/publications/books/sp161/index.php (accessed April 8, 2014).

International Commission on Radiological Protection (ICRP), 1975. Report of the Tas Group on Reference Man, ICRP Publication 23, Pergamon, Oxford.

International Commission on Radiological Protection (ICRP), 1982. Limits for intakes of radionuclides by workers**.** Publication 30. Elsevier Science, Oxford.

International Commission on Radiological Protection (ICRP), 1994. Human respiratory tract model for radiological protection. Publication 66. Annals of the ICRP 24(1-3). Elsevier Science Ltd., Oxford.

Jakober, C.A., Riddle, S.G., Robert, M.A., Destaillats, H., Charles, M.J., Green, P.G. and Kleeman, M.J. 2007. Quinone emissions from gasoline and diesel motor vehicles. Environ. Sci.

Technol. 41, 4548-4554.

Jalava, P.I., Hirvonen, M.R., Sillanpää, M., Pennanen, A.S., Happo, M.S., Hillamo, R., Cassee, F.R., Gerlofs-Nijland, M., Borm, P.J.A., Schins, R.P.F., Janssen, N.A.H. and Salonen, R.O. 2009. Associations of urban air particulate composition with inflammatory and cytotoxic responses in RAW 246.7 cell line. Inhal. Toxicol. 21, 994-1006.

Jeong, C. H., McGuire, M.L., Herod, D., Dann, T., Dabek-Zlotorzynska, E., Wang, D., Ding, L., Celo, V., Mathieu, D. and Evans, G. 2011. Receptor model based identification of $PM_{2.5}$ sources in Canadian cities. Atmos. Pollut. Res. 2, 158-171.

Karlsson, H.L., Nygren, J. and Moller, L. 2004. Genotoxicity of airborne particulate matter: the role of cell-particle interaction and of substances with adduct-forming and oxidizing capacity. Mutat. Res-Gen Tox En. 565, 1-10.

Karoly, E.D., Li, Z., Dailey, L.A., Hyseni, X. and Huang, Y.-C.T. 2007. Up-regulation of tissue factor in human pulmonary artery endothelial cells after ultrafine particle exposure. Environ. Health Persp. 115, 535-540.

Katsouyanni, K., Touloumi, G., Samoli E., Petasakis, Y., Analitis, A., Le Tertre, A., Rossi, G., Zmirou, D., Ballester, F., Boumghar, A., Anderson, H.R., Wojtyniak, B., Paldy, A., Braunstein, R., Pekkanen, J., Schindler, C. and Schwartz, J. 2003. Sensitivity analysis of various models of short-term effects of ambient particles on total mortality in 29 cities in APHEA2. In: Revised analyses of time-series of Air Pollution and Health. Special Report, Health Effects Institute, Boston, 157-164.

Katsouyanni, K., Touloumi, G., Samoli, E., Gryparis, A., Le Tertre, A., Monopolis, Y., Rossi, G., Zmirou, D., Ballester, F., Boumghar, A., Anderson, H.R., Wojtyniak, B., Paldy, A., Braunstein, R., Pekkanen, J., Schindler, C. and Schwartz, J. 2001. Confounding and effect modification in the short-term effects of ambient particles on total mortality: Results from 29 European cities within the APHEA2 project. Epidemiology 12, 521-531.

Kelly, F.J. 2003. Oxidative stress: Its role in air pollution and adverse health effects. J. Occup. Environ. Med. 60, 612-616.

Kim, C.S. and Hu, S.C. 1998. Regional deposition of inhaled particles in human lungs: comparison between men and women. J. Appl. Physiol. 84, 1834-44.

Kim, C.S. and Kang, T.C. 1997. Comparative measurement of lung deposition of inhaled fine particles in normal subjects and patients with obstructive airway disease. Am. J. Respir. Crit. Care Med. 155, 899-905.

Kirby, M., Mathew, L., Wheatley, A., Santyr, G.E., McCormack, D.G. and Parraga, G. 2010. Chronic obstructive pulmonary disease: Longitudinal hyperpolarized He-3 MR imaging. Radiology 256, 280-289.

Knaapen, A.M., Shi, T.M., Borm, P.J.A., and Schins, R.P.F. 2002. Soluble metals as well as the insoluble particle fraction are involved in cellular DNA damage induced by particulate matter. Mol. Cell. Biochem. 234, 317-326.

Knebel, J.W., Ritter, D. and Aufderheide, M. 2002. Exposure of human lung cells to native diesel motor exhaust - development of an optimized in vitro test strategy. Toxicol. in Vitro 16, 185-192.

Koblinger, L. and Hofmann, W. 1985. Analysis of human lung morphometric data for stochastic aerosol deposition calculations. Phys. Med. Biol. 30, 541-556.

Koblinger, L. and Hofmann, W. 1990. Monte Carlo modeling of aerosol deposition in human lungs. Part I: Simulation of particle transport in stochastic lung structure. J. Aerosol Sci. 21, 661-674.

Kocbach, A., Todandsdal, A.I., Lag, M., Refsnes, A., and Schwarze, P.E. 2008. Differential binding of cytokines to environmentally relevant particles: A possible source for misinterpretation of *in vitro* results? Toxicol. Lett. 176, 131-137.

Kok T.M.C.M., Driece H.A.L. and Hogervorst J.G.F. 2006. Toxicological assessment of ambient and traffic-related particulate matter: A review of recent studies. Mutat. Res. 613:103-122.

Kosciuch, J., Krenke, R., Gorska, K., Zukowska, M., Maskey-Warzechowska, M. and Chazan, R. 2013. Airway dimensions in asthma and COPD in high resolution computed tomography: Can we see the difference? Respir. Care 58, 1335-1342.

Kuenzli, N., Jerrett, M., Mack, W.J., Beckerman, B., LaBree, L., Gilliland, F., Thomas, D., Peters, J. and Hodis, H.N. 2005. Ambient air pollution and atherosclerosis in Los Angeles. Environ. Health Persp. 113, 201-206.

Kumagai, Y., Koide, S., Taguchi, K., Endo, A., Nakai, Y., Yoshikawa, T. and Shimojo, N. 2002. Oxidation of proximal protein sulfhydryls by phenanthraquinone, a component of diesel exhaust particles. Chem. Res. Toxicol. 15, 483-489.

Kunkel, S.L., Standiford, T., Kasahara, K., and Strieter, R.M. 1991. Interleukin-8 (IL-8) – the major neutrophils chemotactic factor in the lung. Exp. Lung Res. 17, 17-23.

La Rovere, M.T., Pinna, G.D., Maestri, R., Mortara, A., Capomolla, S., Febo, O., Ferrari, R., Franchini, M., Gnemmi, M., Opasich, C., Riccardi, P.G., Traversi, E. and Cobelli, F. 2003. Short-term heart rate variability strongly predicts sudden cardiac death in chronic heart failure patients. Circulation 107, 565-570.

Laden, F., Neas, L.M., Dockery, D.W., and Schwartz, J. 2000. Association of fine particulate matter from different sources with daily mortality in six US cities. Environ. Health Persp. 108, 941-947.

Laden, F., Schwartz, J., Speizer, F.E. and Dockery, D.W. 2006. Reduction in fine particulate air pollution and mortality - Extended follow-up of the Harvard six cities study. Am. J. Resp. Crit. Care Med. 173, 667-672.

Lauer, F.T., Mitchell, L.A., Bedrick, E., McDonald, J.D., Lee, W.Y., Li, W.W., Olvera, H., Amaya, M.A., Berwick, M., Gonzales, M., Currey, R., Pingitore, N.E. and Burchiel, S.W. 2009.

Temporal-spatial analysis of US-Mexico border environmental fine and coarse PM air sample extract activity in human bronchial epithelial cells. Toxicol. Appl. Pharmacol. 238, 1-10.

Lawrence, S., Sokhi, R., Ravindra, K., Mao, H., Prain, H.D. and Bull, I.D. 2013. Source apportionment of traffic emissions of particulate matter using tunnel measurements. Atmos. Environ. 77, 548-557.

LeFevre, M.E., Green, F.H.Y., Joel, D.D. and Laqueur, W. 1982. Frequency of black pigment in livers and spleens of coal workers: correlation with pulmonary pathology and occupational information. Hum. Pathol. 13, 1121-1126.

Lestari, F., Green, A.R., Chattopadhyay, G. and Hayes, A.J. 2006. An alternative method for fire smoke toxicity assessment using human lung cells. Fire Safety J. 41, 605-615.

Li, N., Hao, M.Q., Phalen, R.F., Hinds, W.C. and Nel, A.E. 2003a. Particulate air pollutants and asthma- A paradigm for the role of oxidative stress in PM-induced adverse health effects. Clin. Immunol. 109, 250-265.

Li, N., Kim, S., Wang, M., Froines, J., Sioutas, C. and Nel, A. 2002. Use of a stratified oxidative stress model to study the biological effects of ambient concentrated and diesel exhaust particulate matter. Inhal. Toxicol. 14, 459-486.

Li, N., Sioutas, C., Cho, A., Schmitz, D., Misra, C., Sempf, J., Wang, M.Y., Oberley, T., Froines, J., and Nel, A. 2003b. Ultrafine particulate pollutants induce oxidative stress and mitochondrial damage. Environ Health Persp, 111, 455-460.

Li, N., Venkatesan, M.I., Miguel, A., Kaplan, R., Gujuluva, C., Alam, J. and Nel, A. 2000. Induction of heme oxygenase-1 expression in macrophages by diesel exhaust particle chemicals and quinones via the antioxidant-responsive element. J. Immunol. 165, 3393-3401.

Li, N., Xia, T., and Nel, A.E. 2008. The role of oxidative stress in ambient particulate matter-induced lung diseases and its implications in the toxicity of engineered nanoparticles. Free Radic. Biol. Med. 44, 1689-1699.

Li, R., Ning, Z., Majumdar, R., Cui, J., Takabe, W., Jen, N., Sioutas, C. and Hsiai, T. 2010. Ultrafine particles from diesel vehicle emissions at different driving cycles induce differential vascular pro-inflammatory responses: Implication of chemical components and NF-kappa B signaling. Part. Fibre Toxicol. 7.

Li, S., Li, H., Xin, H. and Burns, R.T. 2011. Particulate matter concentrations and emissions of a high-rise layer house in Iowa. T. Asabe, 54, 1093-1101.

Li, X.Y., Gilmour, P.S., Donaldson, K. and MacNee, W. 1997. *In vivo* and *in vitro* proinflammatory effects of particulate air pollution (PM_{10}). Environ. Health Persp. 105, 1279-1283.

Löndahl, J., Swietlicki, E., Rissler, J., Bengtsson, A., Boman, C., Blomberg, A., and Sandstrom, T. 2012. Experimental determination of the respiratory tract deposition of diesel combustion articles in patients with chronic obstructive pulmonary disease. Part. Fibre Toxicol. 9, 30.

Löndahl, J., Pagels, J., Boman, C., Swietlicki, E., Massling, A., Rissler, J., Blomberg, A., Bohgard, M. and Sandstrom, T. 2008. Deposition of biomass combustion aerosol particles in the human respiratory tract. Inhal. Toxicol. 20, 923-933.

Long, W.Q., Tate, R.B., Neuman, M., Manfreda, J., Becker, A.B. and Anthonisen, N.R. 1998. Respiratory symptoms in a susceptible population due to burning of agricultural residue. Chest 113, 351-357.

Loomis, D., Grosse, Y., Lauby-Secretan, B., El Ghissassi, F., Bouvard, V., Benbrahim-Tallaa, L., Guha, N., Baan, R., Mattock, H., Straif, K. and Iarc. 2013. The carcinogenicity of outdoor air pollution. Lancet Oncol. 14, 1262-1263.

Lu, S., Duffin, R., Poland, C., Daly, P., Murphy, F., Drost, E., MacNee, W., Stone, V. and Donaldson, K. 2009. Efficacy of simple short-term *in vitro* assays for predicting the potential of metal oxide nanoparticles to cause pulmonary inflammation. Environ. Health Persp. 117, 241-247.

MacNee, W. 2006. ABC of chronic obstructive pulmonary disease - Pathology, pathogenesis, and pathophysiology. Brit. Med. J. 332, 1202-1204.

Maier, K.L., Alessandrini, F., Beck-Speier, I., Hofer, T.P.J., Diabate, S., Bitterle, E., Stoeger, T., Jakob, T., Behrendt, H., Horsch, M., Beckers, J., Ziesenis, A., Hueltner, L. and Frankenberger, M. 2008. Health effects of ambient particulate matter - Biological mechanisms and inflammatory responses to *in vitro* and *in vivo* particle exposures. Inhal. Toxicol. 20, 319-337.

Mantecca, P., Farina, F., Moschini, E., Gallinotti, D., Gualtieri, M., Rohr, A., Sancini, G., Palestini, P. and Camatini, M. 2010. Comparative acute lung inflammation induced by atmospheric PM and size-fractionated tire particles. Toxicol. Lett. 198, 244-254.

Mar, T.F., Norris, G.A., Koenig, J.Q. and Larson, T.V. 2000. Associations between air pollution and mortality in Phoenix, 1995-1997. Environ. Health Persp. 108, 347-353.

Martin, T.R., Castile, R.G., Fredberg, J.J., Wohl, M.E., Mead, J. 1987. Airway size is related to sex but not lung size in normal adults. J. Appl. Physiol. 63, 2042–204.

Mauad, T., Rodriguez Ferreira Rivero, D.H., de Oliveira, R.C., de Faria Coimbra Lichtenfels, A.J., Guimaraes, E.T., de Andre, P.A., Kasahara, D.I., de Siqueira Bueno, H.M. and Nascimento Saldiva, P.H. 2008. Chronic exposure to ambient levels of urban particles affects mouse lung development. Am. J. Respir. Crit. Care Med. 178, 721-728.

Mazzarella, G., Ferraraccio, F., Prati, M.V., Annunziata, S., Bianco, A., Mezzogiorno, A., Liguori, G., Angelillo, I.F. and Cazzola, M. 2007. Effects of diesel exhaust particles on human lung epithelial cells: An *in vitro* study. Respir. Med. 101, 1155-1162.

McClellan, R.O. 2000. Particle interactions with the respiratory tract. In Gehr P, Heyder J (eds) Particle-lung interactions, 1st edn. Marcel Dekker Inc., New York.

McCreanor, J., Cullinan, P., Nieuwenhuijsen, M.J., Stewart-Evans, J., Malliarou, E., Jarup, L., Harrington, R., Svartengren, M., Han, I., Ohman-Strickland, P., Chung, K.F. and Zhang, J.F. 2007. Respiratory effects of exposure to diesel traffic in persons with asthma. New Engl. J. Med.

357, 2348-2358.

McWhinney, R.D., Rastogi, N., Urch, B., Silverman, F., Brook, J.R., Evans, G.J. and Abbatt, J.P.D. 2012. Characterization of the University of Toronto Concentrated Aerosol Particle Exposure Facility (CAPEF)-effects on fine and ultrafine nonrefractory aerosol composition. Aerosol Sci. Technol. 46, 697-707.

Medalia, A.I., Rivin, D., and Sanders, D.R. 1983. A comparison of carbon-black with soot. Sci. Total Environ. 31, 1-22.

Miller, K.A., Siscovick, D.S., Sheppard, L., Shepherd, K., Sullivan, J.H., Anderson, G.L. and Kaufman, J.D. 2007. Long-term exposure to air pollution and incidence of cardiovascular events in women. New Engl. J. Med. 356, 447-458.

Mills, N.L., Robinson, S.D., Fokkens, P.H.B., Leseman, D.L.A.C., Miller, M.R., Anderson, D., Freney, E.J., Heal, M.R., Donovan, R.J., Blomberg, A., Sandström, T., MacNee, W., Boon, N.A., Donaldson, K., Newby, D.E. and Cassee, F.R. 2008. Exposure to concentrated ambient particles does not affect vascular function in patients with coronary heart disease. Environ. Health Persp. 116, 709-715.

Mills, N.L., Toernqvist, H., Gonzalez, M.C., Vink, E., Robinson, S.D., Soederberg, S., Boon, N.A., Donaldson, K., Sandstroem, T., Blomberg, A. and Newby, D.E. 2007. Ischemic and thrombotic effects of dilute diesel-exhaust inhalation in men with coronary heart disease. New Engl. J. Med. 357, 1075-1082.

Mitschik, S., Schierl, R., Nowak, D. and Joerres, R.A. 2008. Effects of particulate matter on cytokine production *in vitro*: A comparative analysis of published studies. Inhal. Toxicol. 20, 399-414.

Möller, W., Felten, K., Sommerer, K., Scheuch, G., Meyer, G., Meyer, P., Haussinger, K. and Kreyling, W.G. 2008. Deposition, retention, and translocation of ultrafine particles from the central airways and lung periphery. Am. J. Respir. Crit. Care Med. 177, 426-432.

Monn, C. and Becker, S. 1999. Cytotoxicity and induction of proinflammatory cytokines from human monocytes exposed to fine ($PM_{2.5}$) and coarse particles ($PM_{10-2.5}$) in outdoor and indoor air. Toxicol. Appl. Pharmacol. 155, 245-252.

Murray, C. D. 1926. The physiological principle of minimum work applied to the angle of branching of arteries. J. Gen. Physiol. 9(6), 835–841.

Murray, J.F. 1976. The normal lung: The basis for diagnosis and treatment of pulmonary disease. W. B. Saunders Company, Philadelphia.

Musante, C. J. and Martonen, T. B. 1999. Predicted deposition patterns of ambient particulate air pollutants in children's lungs under resting conditions. In: Proceedings of the third colloquium on particulate air pollution and human health; June; Durham, NC. Irvine, CA: University of California, Air Pollution Health Effects Laboratory, p. 7-15 - 7-20.

Narciso, S.P., Nadziejko, E., Chen, L.C., Gordon, T. and Nadziejko, C. 2003. Adaptation to stress induced by restraining rats and mice in nose-only inhalation holders. Inhal. Toxicol. 15, 1133-1143.

National Institute of Standards and Technology (NIST), 2009. . http://ts.nist.gov/measurementservices/ referencematerials/index.cfm. (accessed September 17, 2009)

National Institute of Standards Technology (NIST), 2010a. Material details SRM1648a- Urban particulate matter. https://www-s.nist.gov/srmors/view_detail.cfm?srm=1648A. (accessed on April 20, 2010)

National Institute of Standards Technology (NIST), 2010b. Material details SRM2975- Diesel particulate matter. https://www-s.nist.gov/srmors/view_detail.cfmsrm=2975. (accessed on April 20, 2010)

Nemmar, A., Hoet, P.H.M., Vanquickenborne, B., Dinsdale, D., Thomeer, M., Hoylaerts, M.F., Vanbilloen, H., Mortelmans, L. and Nemery, B. 2002. Passage of inhaled particles into the blood

circulation in humans. Circulation 105, 411-414.

Nemmar, A., Hoylaerts, M.F., Hoet, P.H.M. and Nemery, B. 2004. Possible mechanisms of the cardiovascular effects of inhaled particles: systemic translocation and prothrombotic effects. Toxicol. Lett. 149, 243-253.

Ni, T., Li, P., Han, B., Bai, Z., Ding, X., Wang, Q., Huo, J. and Lu, B. 2013. Spatial and temporal variation of chemical composition and mass closure of ambient PM_{10} in Tianjin, China. Aerosol Air Qual. Res. 13, 1832-1846.

North, M.L., Grasemann, H., Khanna, N., Inman, M.D., Gauvreau, G.M. and Scott, J.A. 2013. Increased ornithine-derived polyamines cause airway hyperresponsiveness in a mouse model of asthma. Am. J. Respir. Cell Mol. Biol. 48, 694-702.

Ntziachristos, L., Froines, J.R., Cho, A.K., and Sioutas, C. 2007. Relationship between redox activity and chemical speciation of size-fractionated particulate matter. Part. Fibre Toxicol. 4, 5.

Oberdörster, G. 1996. Significance of particle parameters in the evaluation of exposure-dose-response relationships of inhaled particles. Particul. Sci. Technol. 14, 135-151.

Oberdörster, G. 2001. Pulmonary effects of inhaled ultrafine particles. Int. Arch. Occup. Environ. Health 74, 1-8.

Oberdörster, G., Gelein, R.M., Ferin, J. and Weiss, B. 1995. Association of particulate air-pollution and acute mortality: involvement of ultrafine particles? Inhal. Toxicol. 7, 111-124.

Oberdörster, G., Sharp, Z., Atudorei, V., Elder, A., Gelein, R., Kreyling, W. and Cox, C. 2004. Translocation of inhaled ultrafine particles to the brain. Inhal. Toxicol.16, 437-445.

Oglesby, S. and Nichols, G. B. 1978. Electrostatic Precipitation, 1st edition, Marcel Dekker Inc., New York, USA.

Ostro, B., Lipsett, M., Reynolds, P., Goldberg, D., Hertz, A., Garcia, C., Henderson, K.D. and Bernstein, L. 2010. Long-term exposure to constituents of fine particulate air pollution and

mortality: Results from the California teachers study. Environ. Health Persp. 118, 363-369.

Parker, K. 2003. Electrical Operation of electrostatic precipitators. The Institution of Electrical Engineers, London, UK.

Peng, R.D., Chang, H.H., Bell, M.L., McDermott, A., Zeger, S.L., Samet, J.M. and Dominici, F. 2008. Coarse particulate matter air pollution and hospital admissions for cardiovascular and respiratory diseases among medicare patients. J. Am. Med. Assoc. 299, 2172-2179.

Penton, P.C., Wang, X., Amatullah, H., Cooper, J., Godri, K., North, M.L., Khanna, N., Scott, J.A. and Chow, C.-W. 2013. Spleen tyrosine kinase inhibition attenuates airway hyperresponsiveness and pollution-induced enhanced airway response in a chronic mouse model of asthma. J. Allergy Clin. Immun. 131, 512-520.

Peretz, A., Sullivan, J.H., Leotta, D.F., Trenga, C.A., Sands, F.N., Allen, J., Carlsten, C., Wilkinson, C.W., Gill, E.A. and Kaufman, J.D. 2008. Diesel exhaust inhalation elicits acute vasoconstriction *in vivo*. Environ. Health Persp. 116, 937-942.

Perrone, M.G., Gualtieri, M., Consonni, V., Ferrero, L., Sangiorgi, G., Longhin, E., Ballabio, D., Bolzacchini, E. and Camatini, M. 2013. Particle size, chemical composition, seasons of the year and urban, rural or remote site origins as determinants of biological effects of particulate matter on pulmonary cells. Environ. Pollution 176, 215-227.

Peters, A., Dockery, D.W., Muller, J.E. and Mittleman, M.A. 2001. Increased particulate air pollution and the triggering of myocardial infarction. Circulation 103, 2810-2815.

Peters, A., Liu, E., Verrier, R.L., Schwartz, J., Gold, D.R., Mittleman, M., Baliff, J., Oh, J.A., Allen, G., Monahan, K. and Dockery, D.W. 2000. Air pollution and incidence of cardiac arrhythmia. Epidemiology 11, 11-17.

Peters, A., Wichmann, H.E., Tuch, T., Heinrich, J. and Heyder, J. 1997. Respiratory effects are associated with the number of ultrafine particles. Am. J. Respir. Crit. Care Med. 155, 1376-1383.

Politis M., Pilinis C., Lekkas T.D. 2008. Ultrafine particles (UFP) and health effects. Dangerous. like no other PM? Review and analysis. Glob. NEST J. 10:439-452.

Phalen, R.F. and Oldham, M.J. 2001. Methods for modeling particle deposition as a function of age. Respir. Physiol. 128, 119-130.

Pope, C.A. 1991. Respiratory hospital admissions associate with PM_{10} pollution in Utah, Salt – lake, and Cache Valleys. Arch. Environ. Health, 46, 90-97.

Pope, C.A., Burnett, R.T., Thun, M.J., Calle, E.E., Krewski, D., Ito, K. and Thurston, G.D. 2002. Lung cancer, cardiopulmonary mortality, and long-term exposure to fine particulate air pollution. J. Am. Med. Assoc. 287, 1132-1141.

Pope, C.A., Burnett, R.T., Thurston, G.D., Thun, M.J., Calle, E.E., Krewski, D. and Godleski, J.J. 2004. Cardiovascular mortality and long-term exposure to particulate air pollution - Epidemiological evidence of general pathophysiological pathways of disease. Circulation 109, 71-77.

Pope, C.A., Ezzati, M. and Dockery, D.W. 2009. Fine-particulate air pollution and life expectancy in the United States. New Engl. J. Med. 360, 376-386.

Pope, C.A., Renlund, D.G., Kfoury, A.G., May, H.T. and Horne, B.D. 2008. Relation of heart failure hospitalization to exposure to fine particulate air pollution. Am. J.Cardiol. 102, 1230-1234.

Pope, C.A., Schwartz, J., and Ransom, M.R. 1992. Daily mortality and PM_{10} pollution in Utah Valley. Arch. Environ. Health, 47, 211-217.

Pope, C.A., Thun, M.J., Namboodiri, M.M., Dockery, D.W., Evans, J.S., Speizer, F.E. and Heath, C.W. 1995. Particulate air pollution as a predictor of mortality in a prospective study of U.S. adults. Am. J. Respir. Crit. Care Med. 151, 669-674.

Pritchard, J.N., Jefferies, S.J. and Black, A. 1986. Sex-differences in the regional deposition of inhaled particles in the 2.5-7.5 μm size range. J. Aerosol Sci. 17, 385-389.

Quinlan, G.J., Evans, T.W., and Gutteridge, J.M.C. 2002. Iron and the redox status of the lungs. Free Radic. Biol. Med. 33, 1306-1313.

Quinlan, T., Spivack, S. and Mossman, B.T. 1994. Regulation of entioxidant enzymes in lung after oxidant injury. Environ. Health Persp. 102 Suppl 2, 79-86.

Raabe, O.G., Yeh, H.C., Schum, G.M., and Phalen, R.F. 1976. Tracheobronchial geometry: Human, dog, rat, hamster (Report LF-53). Lovelace Foundation, Albuquerque, NM.

Raaschou-Nielsen, O., Andersen, Z.J., Beelen, R., Samoli, E., Stafoggia, M., Weinmayr, G., Hoffmann, B., Fischer, P., Nieuwenhuijsen, M.J., Brunekreef, B., Xun, W.W., Katsouyanni, K., Dimakopoulou, K., Sommar, J., Forsberg, B., Modig, L., Oudin, A., Oftedal, B., Schwarze, P.E., Nafstad, P., De Faire, U., Pedersen, N.L., Ostenson, C.-G., Fratiglioni, L., Penell, J., Korek, M., Pershagen, G., Eriksen, K.T., Sorensen, M., Tjonneland, A., Ellermann, T., Eeftens, M., Peeters, P.H., Meliefste, K., Wang, M., Bueno-de-Mesquita, B., Key, T.J., de Hoogh, K., Concin, H., Nagel, G., Vilier, A., Grioni, S., Krogh, V., Tsai, M.-Y., Ricceri, F., Sacerdote, C., Galassi, C., Migliore, E., Ranzi, A., Cesaroni, G., Badaloni, C., Forastiere, F., Tamayo, I., Amiano, P., Dorronsoro, M., Trichopoulou, A., Bamia, C., Vineis, P. and Hoek, G. 2013. Air pollution and lung cancer incidence in 17 European cohorts: prospective analyses from the European Study of Cohorts for Air Pollution Effects (ESCAPE). Lancet Oncol. 14, 813-822.

Ramgolam, K., Chevaillier, S., Marano, F., Baeza-Squiban, A. and Martinon, L. 2008. Proinflammatory effect of fine and ultrafine particulate matter using size-resolved urban aerosols from Paris. Chemosphere 72, 1340-1346.

Ramgolam, K., Favez, O., Cachier, H., Gaudichet, A., Marano, F., Martinon, L., Baeza-Squiban, A. 2009. Size-partitioning of an urban aerosol to identify particle determinants involved in the proinflammatory response induced in airway epithelial cells. Part Fibre Toxicol. 6, 10.

Rastogi, N., McWhinney, R.D., Akhtar, U.S., Urch, B., Fila, M., Abbatt, J.P.D., Scott, J.A., Silverman, F.S., Brook, J.R. and Evans, G.J. 2012. Physical characterization of the University of

Toronto coarse, fine, and ultrafine high-volume particle concentrator systems. Aerosol Sci. Technol. 46, 1015-1024.

Rehbein, P.J.G., Jeong, C.H., McGuire, M.L. and Evans, G.J. 2012. Strategies to enhance the interpretation of single-particle ambient aerosol data. Aerosol Sci. Technol. 46, 584-595.

Reiss, R., Anderson, E.L., Cross, C.E., Hidy, G., Hoel, D., McClellan, R., and Moolgavkar, S. 2007. Evidence of health impacts of sulfate- and nitrate-containing particles in ambient air. Inhal. Toxicol. 19, 419-449.

Reymao, M.S.F., Cury, P.M., Lichtenfels, A., Lemos, M., Battlehner, C.N., Conceicao, G.M.S., Capelozzi, V.L., Montes, G.S., Junior, M.F., Martins, M.A., Bohm, G.M. and Saldiva, P.H.N. 1997. Urban air pollution enhances the formation of urethane-induced lung tumors in mice. Environ. Res. 74, 150-158.

Riley, M.R., Boesewetter, D.E., Kim, A.M., and Sirvent, F.P. 2003. Effects of metals Cu, Fe, Ni, V, and Zn on rat lung epithelial cells. Toxicology 190, 171-184.

Risom, L., Moller, P. and Loft, S. 2005. Oxidative stress-induced DNA damage by particulate air pollution. Mutat. Res-Fund. Mol. M. 592, 119-137.

Rissler, J., Swietlicki, E., Bengtsson, A., Boman, C., Pagels, J., Sandstrom, T., Blomberg, A. and Löndahl, J. 2012. Experimental determination of deposition of diesel exhaust particles in the human respiratory tract. J. Aerosol Sci. 48, 18-33.

Ritter, D., Knebel, J.W. and Aufderheide, M. 2001. *In vitro* exposure of isolated cells to native gaseous compounds - Development and validation of an optimized system for human lung cells. Exp. Toxicol. Pathol. 53, 373-386.

Rossner, P., Jr., Topinka, J., Hovorka, J., Milcova, A., Schmuczerova, J., Krouzek, J. and Sram, R.J. 2010. An acellular assay to assess the genotoxicity of complex mixtures of organic pollutants bound on size segregated aerosol. Part II: Oxidative damage to DNA. Toxicol. Lett. 198, 312-316.

Rostami, A.A. 2009. Computational modeling of aerosol deposition in respiratory tract: A review. Inhal. Toxicol. 21, 262-290.

Rothen-Rutishauser, B. M., Blank, F., Muehlfeld, C. and Gehr, P. 2008. *In vitro* models of the human epithelial airway barrier to study the toxic potential of particulate matter. Expert. Opin. Drug Metab. Toxicol. 4, 1075-1089.

Rothen-Rutishauser, B.M., Kiama, S.G. and Gehr, P. 2005. A three-dimensional cellular model of the human respiratory tract to study the interaction with particles. Am. J. Respir. Cell Mol. Biol. 32, 281-289.

Rundell, K.W., Hoffman, J.R., Caviston, R., Bulbulian, R. and Hollenbach, A.M. 2007. Inhalation of ultrafine and fine particulate matter disrupts systemic vascular function. Inhal. Toxicol. 19, 133-140.

Sacks, J.D., Stanek, L.W., Luben, T.J., Johns, D.O., Buckley, B.J., Brown, J.S. and Ross, M. 2011. Particulate matter-induced health effects: Who is susceptible? Environ. Health Persp. 119, 446-454.

Saldiva, P.H.N., Clarke, R.W., Coull, B.A., Stearns, R.C., Lawrence, J., Murthy, G.G.K., Diaz, E., Koutrakis, P., Suh, H., Tsuda, A., and Godleski, J.J. 2002. Lung inflammation induced by concentrated ambient air particles is related to particle composition. Am. J. Respir. Crit. Care Med. 165, 1610-1617.

Sánchez-Pérez, Y., Chirino, Y.I., Osornio-Vargas, A.R., Morales-Barcenas, R., Gutierrez-Ruiz, C., Vazquez-Lopez, I., and Garcia-Cuellar, C.M. 2009. DNA damage response of A549 cells treated with particulate matter (PM_{10}) of urban air pollutants. Cancer Lett. 278, 192-200.

Sasaki, J., Aschmann, S.M., Kwok, E.S.C., Atkinson, R. and Arey, J. 1997. Products of the gas-phase OH and NO_3 radical-initiated reactions of naphthalene. Environ. Sci. Technol. 31, 3173-3179.

Savi, M., Kalberer, M., Lang, D., Ryser, M., Fierz, M., Gaschen, A., Ricka, J. and Geiser, M.

2008. A novel exposure system for the efficient and controlled deposition of aerosol particles onto cell cultures. Environ. Sci. Technol. 42, 5667-5674.

Sawyer, K., Mundandhara, S., Ghio, A. J., and Madden, M. C. 2010. The effects of ambient particulate matter on human alveolar macrophage oxidative and inflammatory responses. J. Toxicol. Environ. Health-Part a**,** 73 (1), 41-57.

Sayes, C.M., Reed, K.L. and Warheit, D.B. 2007. Assessing toxicity of fine and nanoparticles: Comparing *in vitro* measurements to *in vivo* pulmonary toxicity profiles. Toxicol. Sci. 97, 163-180.

Schikowski, T., Sugiri, D., Ranft, U., Gehring, U., Heinrich, J., Wichmann, H.E. and Kramer, U. 2005. Long-term air pollution exposure and living close to busy roads are associated with COPD in women. Respir. Res. 6.

Schiller-Scotland, C. F., Hlawa, R., Gebhart, J., Wönne, R., and Heyder, J. 1992. Total deposition of aerosol particles in the respiratory tract of children during spontaneous and controlled mouth breathing. J. Aerosol Sci. 23 Suppl. 1, S457-S460.

Schins, R.P.F. and Hei, T.K. 2007. Genotoxic effects of particles. In: Donaldson K, Borm P (eds) Particle toxicology, 1st edn. CRC Press, New York.

Schlesinger, R.B. 1995. Deposition and clearance of inhaled particles. In McClellan, R.O. and Henderson, R.F. (eds) Concepts in Inhal. Toxicol., 2nd edn. Taylor & Francis, Washington.

Schlesinger, R.B. 2007. The health impact of common inorganic components of fine particulate matter ($PM_{2.5}$) in ambient air: A critical review. Inhal. Toxicol. 19, 811-832.

Schulz, H., Brand, P., and Heyder, J. 2000. Particle deposition in the respiratory tract. In Gehr P, Heyder J (eds) Particle-lung interactions, 1st edn. Marcel Dekker, Inc., New York.

Schwartz J. 1994. Air pollution and daily mortality: A review and meta analysis. Environ. Res. 64: 36-52.

Schwarze, P.E., Ovrevik, J., Lag, M., Refsnes, M., Nafstad, P., Hetland, R.B., and Dybing, E. 2006. Particulate matter properties and health effects: consistency of epidemiological and toxicological studies. Hum. Exp. Toxicol. 25, 559-579.

Seagrave, J. 2008. Mechanisms and implications of air pollution particle associations with chemokines. Toxicol. Appl. Pharmacol. 232, 469-477.

Seagrave, J., Knall, C., McDonald, J.D., and Mauderly, J.L. 2004. Diesel particulate material-binds and concentrates a proinflammatory cytokine that causes neutrophil migration. Inhal. Toxicol. 16, 93-98.

Seagrave, J., McDonald, J.D. and Mauderly, J.L. 2005. *In vitro* versus *in vivo* exposure to combustion emissions. Exp. Toxicol. Pathol. 57, 233-238.

Seagrave, J., McDonald, J.D., Bedrick, E., Edgerton, E.S., Gigliotti, A.P., Jansen, J.J., Ke, L., Naeher, L.P., Seilkop, S.K., Zheng, M. and Mauderly, J.L. 2006. Lung toxicity of ambient particulate matter from southeastern US sites with different contributing sources: Relationships between composition and effects. Environ. Health Persp. 114, 1387-1393.

Semmler, M., Seitz, J., Erbe, F., Mayer, P., Heyder, J., Oberdörster, G. and Kreyling, W.G. 2004. Long-term clearance kinetics of inhaled ultrafine insoluble iridium particles from the rat lung, including transient translocation into secondary organs. Inhal. Toxicol. 16, 453-459.

Shebl, F.M., Pinto, L.A., Garcia-Pineres, A., Lempicki, R., Williams, M., Harro, C. and Hildesheim, A. 2010. Comparison of mRNA and protein measures of cytokines following caccination with human papillomavirus-16 L1 virus-like particles. CancEpider em. Biomar. Prevention 19, 978-981.

Shi, T.M., Schins, R.P.F., Knaapen, A.M., Kuhlbusch, T., Pitz, M., Heinrich, J. and Borm, P.J.A. 2003. Hydroxyl radical generation by electron paramagnetic resonance as a new method to monitor ambient particulate matter composition. J. Environ. Monitor. 5, 550-556.

Shinyashiki, M., Eiguren-Fernandez, A., Schmitz, D.A., Di Stefano, E., Li, N., Linak, W.P., Cho,

S.H., Froines, J.R., and Cho, A.K. 2009. Electrophilic and redox properties of diesel exhaust particles. Environ. Res. 109, 239-244.

Sillanpää, M., Geller, M.D., Phuleria, H.C. and Sioutas, C. 2008. High collection efficiency electrostatic precipitator for *in vitro* cell exposure to concentrated ambient particulate matter (PM). J. Aerosol Sci. 39, 335-347.

Singh, P., DeMarini, D.M., Dick, C.A.J., Tabor, D.G., Ryan, J.V., Linak, W.P., Kobayashi, T. and Gilmour, M.I. 2004. Sample characterization of automobile and forklift diesel exhaust particles and comparative pulmonary toxicity in mice. Environ. Health Persp. 112, 820-825

Sint, T., Donohue, J.F. and Ghio, A.J. 2008. Ambient air pollution particles and the acute exacerbation of chronic obstructive pulmonary disease. Inhal. Toxicol. 20, 25-29.

Sioutas, C., Delfino, R.J. and Singh, M. 2005. Exposure assessment for atmospheric ultrafine particles (UFPs) and implications in epidemiologic research. Environ. Health Persp. 113, 947-955.

Sioutas, C., Koutrakis, P. and Burton, R.M. 1995. A technique to expose animals to concentrated fine ambient aerosols. Environ. Health Persp. 103, 172-177.

Soukup, J.M. and Becker, S. 2001. Human alveolar macrophage responses to air pollution particulates are associated with insoluble components of coarse material, including particulate endotoxin. Toxicol. Appl. Pharm. 171, 20-26.

Southern Ontario Centre for Atmospheric Aerosol Research (SOCAAR), 2007. Facilities-Concentrated Ambient Particle Exposure Facility (CAPEF). http://www.socaar.utoronto.ca/fac-inst/Facilities.htm. (accessed September 21, 2009).

Squadrito, G.L., Cueto, R., Dellinger, B. and Pryor, W.A. 2001. Quinoid redox cycling as a mechanism for sustained free radical generation by inhaled airborne particulate matter. Free Radic. Biol. Med. 31, 1132-1138.

Steenhof, M., Gosens, I., Strak, M., Godri, K.J., Hoek, G., Cassee, F.R., Mudway, I.S., Kelly, F.J., Harrison, R.M., Lebret, E., Brunekreef, B., Janssen, N.A.H. and Pieters, R.H.H. 2011. *In vitro* toxicity of particulate matter (PM) collected at different sites in the Netherlands is associated with PM composition, size fraction and oxidative potential - the RAPTES project. Part. Fibre Toxicol. 8.

Steerenberg, P.A., van Amelsvoort, L., Lovik, M., Hetland, R.B., Alberg, T., Halatek, T., Bloemen, H.J.T., Rydzynski, K., Swaen, G., Schwarze, P., Dybing, E. and Cassee, F.R. 2006. Relation between sources of particulate air pollution and biological effect parameters in samples from four European cities: An exploratory study. Inhal. Toxicol. 18, 333-346.

Stoelzel, M., Breitner, S., Cyrys, J., Pitz, M., Woelke, G., Kreyling, W., Heinrich, J., Wichmann, H.E. and Peters, A. 2007. Daily mortality and particulate matter in different size classes in Erfurt, Germany. J. Expo. Sci. Env. Epidem. 17, 458-467.

Suwa, T., Hogg, J.C., Quinlan, K.B., Ohgami, A., Vincent, R. and van Eeden, S.F. 2002. Particulate air pollution induces progression of atherosclerosis. J. Am. Coll. Cardiol. 39, 935-942.

Svenningsen, S., Kirby, M., Starr, D., Coxson, H.O., Paterson, N.A.M., McCormack, D.G. and Parraga, G. 2014. What are ventilation defects in asthma? Thorax 69, 63-71.

Tan, P.V., Fila, M.S., Evans, G.J. and Jervis, R.E. 2002. Aerosol laser ablation mass spectrometry of suspended powders from PM sources and its implications to receptor modeling. J. Air Waste Manage. Assoc. 52, 27-40.

Thomson, E.M., Williams, A., Yauk, C.L. and Vincent, R. 2009. Impact of nose-only exposure system on pulmonary gene expression. Inhal. Toxicol. 21 Suppl 1, 74-82.

Thorpe, A. and Harrison, R.M. 2008. Sources and properties of non-exhaust particulate matter from road traffic: A review. Sci. Total Environ. 400, 270-282.

Thurlbeck, W.M. 1982. Postnatal human lung growth. Thorax 37, 564-571.

Törnqvist, H., Mills, N.L., Gonzalez, M., Miller, M.R., Robinson, S.D., Megson, I.L., MacNee, W., Donaldson, K., Soderberg, S., Newby, D.E., Sandstrom, T. and Blomberg, A. 2007. Persistent endothelial dysfunction in humans after diesel exhaust inhalation. Am. J. Respir. Crit. Care Med.176, 395-400.

Turner, M.C., Krewski, D., Pope, C.A., III, Chen, Y., Gapstur, S.M. and Thun, M.J. 2011. Long-term ambient fine particulate matter air pollution and lung cancer in a large cohort of never-smokers. Am. J. Resp. Crit. Care Med. 184, 1374-1381.

Ulrich, M.M.W., Alink, G.M., Kumarathasan, P., Vincent, R., Boere, A.J.F. and Cassee, F.R. 2002. Health effects and time course of particulate matter on the cardiopulmonary system in rats with lung inflammation. J. Toxicol. Environ. Health A 65, 1571-1595.

United States Environmental Protection Agency (USEPA), 1996. Air quality criteria for particulate matter. Volume II. Research Triangle Park, NC: National Certre for Environmental Assessment-RTP Office; report nos. EPA/600/P-95/001bF.

United States Environmental Protection Agency (USEPA), 2012. Six common air pollutants. http://www.epa.gov/air/urbanair/ (accessed April 8, 2014).

United States Environmental Protection Agency (USEPA), 1993. Provisional guidance for hydrocarbons. EPA/600/R-93/089, July 1993.
http://epa-prgs.ornl.gov/chemicals/help/documents/600R93089.pdf. (accessed on May 2, 2010).

United States Environmental Protection Agency (USEPA), 2004. Air quality criteria for particulate matter Volume II. Research Triangle Park, NC: National Certre for Environmental Assessment-RTP Office, report nos. EPA/600/P-99/002bF.

Urch, B., Silverman, F., Corey, P., Brook, J.R., Lukic, K.Z., Rajagopalan, S., and Brook, R.D. 2005. Acute blood pressure responses in healthy adults during controlled air pollution exposures. Environ. Health Persp. 113, 1052-1055.

Urch, B., Speck, M., Corey, P., Wasserstein, D., Manno, M., Lukic, K.Z., Brook, J.R., Liu, L., Coull, B., Schwartz, J., Gold, D.R. and Silverman, F. 2010. Concentrated ambient fine particles and not ozone induce a systemic interleukin-6 response in humans. Inhal. Toxicol. 22, 210-218.

Utah Bureau of Air Quality, 1990. Draft Utah State Implementation Plan, Utah State Department of Health, Salt Lake City.

Utell, M.J. and Frampton, M.W. 2000. Toxicologic methods: Controlled human exposures. Environ. Health Persp. 108, 605-613.

Valavanidis, A., Fiotakis, K. and Vlachogianni, T. 2008. Airborne particulate matter and human health: Toxicological assessment and importance of size and composition of particles for oxidative damage and carcinogenic mechanisms. J. Environ. Sci. Health C 26, 339-362.

Valentine, R., and Kennedy, G.L. 2008. Inhalation toxicology. In Hayes AW (ed) Principles and methods of toxicology, 5th edn. CRC Press, New York.

Veranth, J.M., Moss, T.A., Chow, J.C., Labban, R., Nichols, W.K., Walton, J.C., Watson, J.G., and Yost, G.S. 2006. Correlation of *in vitro* cytokine responses with the chemical composition of soil-derived particulate matter. Environ. Health Persp. 114, 341-349.

Verma, V., Shafer, M.M., Schauer, J.J. and Sioutas, C. 2010. Contribution of transition metals in the reactive oxygen species activity of PM emissions from retrofitted heavy-duty vehicles. Atmos. Environ. 44, 5165-5173.

Vincent, R., Kumarathasan, P., Goegan, P., Bjarnason, S.G., Guenette, J., Berube, D., Adamson, I.Y., Desjardins, S., Burnett, R.T., Miller, F.J. and Battistini, B. 2001. Inhalation toxicology of urban ambient particulate matter: acute cardiovascular effects in rats. Res. Rep. Health Effects Inst. 5-54; Discussion 55-62.

Volckens, J., Dailey, L., Walters, G. and Devlin, R.B. 2009. Direct particle-to-cell deposition of coarse ambient particulate matter increases the production of inflammatory mediators from cultured human airway epithelial cells. Environ. Sci. Technol., 43, 4595-4599.

Wang, B., Li, K., Jin, W., Lu, Y., Zhang, Y., Shen, G., Wang, R., Shen, H., Li, W., Huang, Y., Zhang, Y., Wang, X., Li, X., Liu, W., Cao, H. and Tao, S. 2013. Properties and inflammatory effects of various size fractions of ambient particulate matter from Beijing on A549 and J774A.1 cells. Environ. Sci. Technol. 47, 10583-10590.

Wang, L., Atkinson, R. and Arey, J. 2007. Formation of 9, 10-phenanthrenequinone by atmospheric gas-phase reactions of phenanthrene. Atmos. Environ. 41, 2025-2035.

Watterson, T.L., Sorensen, J., Martin, R. and Coulombe, R.A. 2007. Effects of $PM_{2.5}$ collected from Cache Valley Utah on genes associated with the inflammatory response in human lung cells. J. Toxicol. Environ. Health A 70, 1731-1744.

Weibel, E. R. 1963. Morphometry of human lung. NewYork, Academic Press.

Weiss, S.T., Utell, M.J. and Samet, J.M. 1999. Environmental tobacco smoke exposure and asthma in adults. Environ. Health Persp. 107, 891-895.

Wellenius, G.A., Coull, B.A., Godleski, J.J., Koutrakis, P., Okabe, K., Savage, S.T., Lawrence, J.E., Murthy, G.G.K. and Verrier, R.L. 2003. Inhalation of concentrated ambient air particles exacerbates myocardial ischemia in conscious dogs. Environ. Health Persp. 111, 402-408.

Wessels, A., Birmili, W., Albrecht, C., Hellack, B., Jermann, E., Wick, G., Harrison, R.M. and Schins, R.P.F. 2010. Oxidant generation and toxicity of size-fractionated ambient particles in human lung epithelial cells. Environ. Sci. Technol. 44, 3539-3545.

Wittmaack, K. 2007. In search of the most relevant parameter for quantifying lung inflammatory response to nanoparticle exposure: Particle number, surface area, or what? Environ. Health Persp. 115, 187-194.

Wolz, L., Krause, G., Scherer, G., Aufderheide, M. and Mohr, U. 2002. *In vitro* genotoxicity assay of sidestream smoke using a human bronchial epithelial cell line. Food Chem. Toxicol. 40, 845-850.

World Health Organization (WHO), 2006. Air quality guidelines global update 2005. Available at**:** www.cepis.org.pe/bvsea/fulltext/guidelines05.pdf. (accessed on July 2, 2009).

Xiao, G.G., Wang, M.Y., Li, N., Loo, J.A. and Nel, A.E. 2003. Use of proteomics to demonstrate a hierarchical oxidative stress response to diesel exhaust particle chemicals in a macrophage cell line. J. Biol. Chem. 278, 50781-50790.

Yeh, H.C. and Schum, G.M. 1980. Models of human lung airways and their application to inhaled particle deposition. Bull. Math. Biol. 42, 461-80.

Yeh, HC. 1980. Respiratory tract deposition models. Report, Inhalation Tox. Res. Inst. LF-72, UC-48.

Yilmaz, S., Ekici, A., Ekici, M. and Keles, H. 2006. High-resolution computed tomography findings in elderly patients with asthma. Eur. J. Radiol. 59, 238-243.

Zanobetti, A. and Schwartz, J. 2005. The effect of particulate air pollution on emergency admissions for myocardial infarction: A multicity case-crossover analysis. Environ. Health Persp. 113, 978-982.

Zanobetti, A., Schwartz, J. and Dockery, D.W. 2000. Airborne particles are a risk factor for hospital admissions for heart and lung diseases. Environ. Health Persp. 108, 1071-1077.

Zhang, H. and Papadakis, G. 2010. Computational analysis of flow structure and particle deposition in a single asthmatic human airway bifurcation. J. Biomech. 43, 2453-2459.